Candidate markers of Olaparib sensitivity and resistance from genomic data analyses of human cancer cell lines

Setor Amuzu, MSc

Department of Human Genetics
Faculty of Medicine
McGill University, Montreal, Quebec, Canada
August 2020

A thesis submitted to McGill University in partial fulfillment of the requirements of the degree of Doctor of Philosophy

DEDICATION

To my family, who are the foundation of my support and encouragement.

ABSTRACT

Olaparib is an oral inhibitor of poly(ADP-ribose) polymerase (PARP) manufactured by AstraZeneca under the brand name Lynparza®. It was first clinically approved as monotherapy for the maintenance treatment of *BRCA1/2*-mutated (germline or somatic) high-grade serous ovarian, fallopian tube or primary peritoneal cancers who were sensitive to platinum-based chemotherapy. The antitumor activity of olaparib is based on the synthetic lethality relationship between PARP and BRCA1/2 where loss of BRCA1/2 function or PARP inhibition alone is compatible with cell survival, but the combination of BRCA1/2 inactivation and PARP inhibition leads to cell death. Olaparib treatment has been most successful in minimizing tumor growth and delaying tumor recurrence in high-grade serous ovarian carcinoma (HGSOC) where 50% of cases are estimated to be HR-deficient primarily through genomic inactivation of *BRCA1/2*. Genomic and molecular alterations in HR repair genes and genes in other DNA repair pathways and cell cycle regulation have been associated with olaparib sensitivity and resistance mainly through *in vitro* analysis of human cancer cell lines. The aim of this study is to identify new genomic markers of olaparib response in genes involved in DNA repair, cell cycle regulation or other pathways and biological processes to contribute to improved understanding of olaparib sensitivity and resistance and provide candidate markers for further preclinical and clinical evaluation that may ultimately help identify patients most likely to respond to treatment with olaparib or inform alternative strategies for treatment of patients with tumors possessing more resistant genomic features.

*In vitro o*laparib response and genomic data from two independent groups of human cancer cell lines were investigated in this thesis. The analysis of 18 HGSOC cell lines

focussed on characterizing mutational signatures unique to sensitive and resistant cell lines, and identifying functional genomic variations in DNA repair and cell cycle genes comprising sequence variants, copy number variations (CNVs), and differential gene expression between sensitive and resistant cell lines. This analysis identified *CDK2* p.Thr14Lys, *MPG* deletion associated with low mRNA expression, and *PARP1* p.Val762Ala as candidate markers of olaparib sensitivity. Conversely, *RIF1* amplification and *SMAD4* nonsense mutations (p.Gln83*, p.Arg445*) were identified as candidate markers of olaparib resistance. In the analyses of the pan-cancer cell lines (n=896) from the Genomics of Drug Sensitivity in Cancer (GDSC) database, multivariate and univariate linear regression methods were used to identify significant gene predictors of olaparib response based on mRNA expression. Some of the significant gene predictors successfully validated in the HGSOC cell lines through identification of SNVs, CNVs, or differential gene expression include *PUM3, EEF1A1,* and *ELP4.* Altogether, these analyses identified novel candidate genes and known markers of olaparib sensitivity and resistance through investigation of protein-coding sequence variants, CNVs, and mRNA gene expression in two independent groups of human cancer cell lines.

RÉSUMÉ

L'olaparib est un inhibiteur oral de la poly(ADP-ribose) polymérase (PARP) fabriqué par AstraZeneca sous le nom de marque Lynparza®. Il a d'abord été cliniquement approuvé en monothérapie pour le traitement d'entretien des cancers à mutation *BRCA1/2* (germinale ou somatique) sensibles à la chimiothérapie à base de platine de type séreux de haut grade de l'ovaire, de la trompe de Fallope ou de cancers primitifs du péritonéal. L'activité antitumorale de l'olaparib est basée sur la relation de létalité synthétique entre PARP et BRCA1/2, où la perte de la fonction BRCA1/2 ou l'inhibition de PARP seule est compatible avec la survie cellulaire mais la combinaison de l'inactivation de BRCA1/2 et de l'inhibition de PARP conduit à la mort cellulaire. Le traitement à l'olaparib a été le plus efficace pour minimiser la croissance tumorale et retarder la récidive tumorale dans le carcinome séreux de l'ovaire de haut grade (HGSOC), où 50% des cas sont estimés déficitaires en RH principalement par l'inactivation génomique de *BRCA1/2*. Les altérations génomiques et moléculaires des gènes de réparation RH et des gènes d'autres voies de réparation de l'ADN et de la régulation du cycle cellulaire, ont été associées à la sensibilité et à la résistance à l'olaparib principalement par l'analyse *in vitro* de lignées cellulaires de cancer humain. Le but de cette étude est d'identifier de nouveaux marqueurs génomiques de la réponse à l'olaparib dans les gènes impliqués dans la réparation de l'ADN, la régulation du cycle cellulaire ou d'autres voies et processus biologiques, afin de contribuer à une meilleure compréhension de la sensibilité et de la résistance à l'olaparib et de fournir des marqueurs candidats pour une évaluation préclinique et clinique plus poussée. Ceci pourrait aider à identifier les patients les plus susceptibles de répondre au traitement

par l'olaparib ou informer sur des stratégies alternatives pour le traitement des patients atteints de tumeurs possédant des caractéristiques génomiques plus résistantes.
La réponse olaparib *in vitro* et les données génomiques de deux groupes indépendants de lignées cellulaires cancéreuses humaines ont été étudiées dans cette thèse. L'analyse de 18 lignées cellulaires HGSOC s'est concentrée sur la caractérisation des signatures mutationnelles uniques aux lignées cellulaires sensibles et résistantes, et l'identification des variations génomiques fonctionnelles dans la réparation de l'ADN et les gènes du cycle cellulaire comprenant des variantes de séquence (SNV), des variations du nombre de copies (CNV) et l'expression différentielle des gènes entre les gènes sensibles et lignées cellulaires résistantes. Cette analyse a identifié *CDK2* p.Thr14Lys, la délétion *MPG* associée à une faible expression de l'ARNm ainsi que *PARP1* p.Val762Ala comme marqueurs candidats de la sensibilité à l'olaparib. À l'inverse, l'amplification *RIF1* et les mutations non-sens *SMAD4* (p.Gln83*, p.Arg445*) ont été identifiées comme des marqueurs candidats de la résistance à l'olaparib. Dans les analyses des lignées cellulaires pan-cancéreuses (n = 896) de la base de données Genomics of Drug Sensitivity in Cancer (GDSC), des méthodes de régression linéaire multivariée et univariée ont été utilisées pour identifier des prédicteurs géniques significatifs de la réponse de l'olaparib sur la base de l'expression de l'ARNm. Certains des prédicteurs géniques significatifs validés avec succès dans les lignées cellulaires HGSOC grâce à l'identification des SNV, des CNV ou de l'expression génique différentielle comprennent *PUM3*, *EEF1A1* et *ELP4.* Dans l'ensemble, ces analyses ont identifié de nouveaux gènes candidats et des marqueurs connus de la sensibilité et de la résistance à l'olaparib grâce à l'étude des variantes de séquence codant pour les

protéines, des CNV et de la variation de l'expression des gènes de l'ARNm dans deux groupes indépendants de lignées cellulaires cancéreuses humaines.

TABLE OF CONTENTS

List of Abbreviations

3-MeA	3-methyladenine
ACC	Adrenocortical carcinoma
ALL	Acute lymphoblastic leukemia
ARF	Alternate reading frame
ART	ADP-ribosyltransferase
ARTD	Diptheria-toxin-like ADP-ribosyltransferase
BAM	Binary alignment Map
BLCA	Bladder urothelial carcinoma
BRCA	Breast invasive carcinoma
CA125	Cancer antigen 125
CCLE	Cancer cell line encyclopedia
CDDP	Cis-diamminedichloroplatinum(II) or cisplatin
CESC	Cervical squamous cell carcinoma and endocervical adenocarcinoma
CLL	Chronic lymphocytic leukemia
CNV	Copy number variation
COREAD	Colon adenocarcinoma and Rectum adenocarcinoma
COSMIC	Catalogue of Somatic Mutations in Cancer
DLBC	Lymphoid Neoplasm Diffuse Large B-cell Lymphoma
DSB	Double strand break
EOC	Epithelial ovarian cancer
ESCA	Esophageal carcinoma
ExAC	Exome aggregation consortium
FA	Fanconi anemia
FDR	False discovery rate
GBM	Glioblastoma multiforme
GDSC	Genomics of Drug Sensitivity in Cancer
gnomAD	Genome aggregation database
HER2	Human epidermal growth factor receptor 2
HGSOC	High grade serous epithelial ovarian cancer

HNSC	Head and Neck squamous cell carcinoma
HR	Homologous recombination
HRD	Homologous recombination deficiency
IC_{50}	Half maximal inhibitory concentration
ICL	Interstrand crosslink
IDL	Insertion-deletion loop
IGV	Integrative genomics viewer
KIRC	Kidney renal clear cell carcinoma
LAML	Acute myeloid leukemia
LCML	Chronic myelogenous leukemia
LGG	Brain lower grade glioma
LIHC	Liver hepatocellular carcinoma
LUAD	Lung adenocarcinoma
LUSC	Lung squamous cell carcinoma
MAE	Mean absolute error
MB	Medulloblastoma
MESO	Mesothelioma
MM	Multiple myeloma
MMEJ	Microhomology mediated end-joining
MMR	Mismatch repair
NACT	Neoadjuvant chemotherapy
NB	Neuroblastoma
NHEJ	Non-homologous end joining
OV	Ovarian serous cystadenocarcinoma
PAAD	Pancreatic adenocarcinoma
PAR	Poly ADP-ribose
PFS	Progression free survival
PRAD	Prostate adenocarcinoma
RMSE	Root mean-squared error
SBS	Single base substitution
SCLC	Small cell lung cancer

SD	Standard deviation
siRNA	Short-interfering RNA
SKCM	Skin cutaneous melanoma
SNP	Single nucleotide polymorphism
SNV	Single nucleotide variant
SSB	Single strand break
STAD	Stomach adenocarcinoma
STICs	Serous tubal intraepithelial carcinomas
STR	Short tandem repeats
THCA	Thyroid carcinoma
UCEC	Uterine corpus endometrial carcinoma
US FDA	United States Food and Drug Administration
VAF	Variant allele frequency
WES	Whole exome sequencing

List of Figures

List of Tables

Acknowledgements

I am sincerely grateful to my supervisor Dr. Ioannis Ragoussis, first, for the opportunity to pursue a PhD in his lab and for his immense guidance and support throughout my studies. My PhD studies was supported with funding from the Canadian Queen Elizabeth II (QEII) Diamond Jubilee scholarship through the Quantitative Biology and Medical Genetics for the World program. I am very grateful to Dr. Mark Lathrop, Dr. Ioannis Ragoussis, and Dr. Simon Gravel and for setting up this scholarship program that provided critical financial support for my PhD studies. I am also thankful to all my lab mates (past and present) who helped me settle into the lab, taught me a lot about genomic technologies and analyses, provided useful feedback and encouragement especially Timothée Revil, Spyridon Oikonomoplous, Dunarel Badescu, Somayyeh Fahiminiya, Yu Chang Wang, Suzanna Arcand, Corinne Darmond, Melissa Zwaig, Charles Meunier, and Javad Nadaf. I am also grateful for the companionship of Anthony Bayega who also began his PhD studies in the lab at the same time as I did. We learned a lot together. I would like to express my gratitude to the members of my supervisory committee, Dr. Patrica N. Tonin and Dr. Celia Greenwood, for their valuable guidance and feedback that helped shape my PhD research project. I am thankful to Dr. Greenwood for her guidance regarding statistical approaches for my project. I am particularly grateful to Dr. Tonin and her lab for welcoming me into their lab meetings where I learned a lot about ovarian cancer heredity, biology, and treatment. I had many positive and beneficial discussions with fellow PhD candidates in her lab, Wejdan Alenezi and Caitlin Fierheller, who were also working on projects related to ovarian cancer. Dr. Tonin was also instrumental for our collaboration with Dr. Anne-Marie Mes-Masson of Université de Montreal who provided *in vitro* olaparib response and genomic

data of ovarian cancer cell lines developed in her lab. This was a key collaboration that facilitated my PhD research project and I am very grateful to Dr. Anne-Marie Mes-Masson and her lab. I also appreciate the support of Ross MacKay, Tania Abou Younes, Ksenia Egorova for processing my tuition and stipend payments, and reimbursements for conference and workshop costs.

Most importantly, I am grateful to my family. To my wife, Theresa, for her constant support and encouragement especially during the most challenging times of my studies. I thank my son, Nathan Keli, who has brought so much joy into our lives. Thank you to my parents, Dr. and Mrs. Kwasi Amuzu, for everything they have taught me, always believing in me, and for their many sacrifices that have enabled me to advance my career. Special thanks to my siblings (Kafui, Elorm and Yayra) for always supporting me. To my friends, especially fellow QEII scholar Chief Ben-Eghan, who have supported me during my studies I am grateful. As a Christian, I thank God for grace that has sustained me throughout my studies and I pray for His blessings for all who have supported me.

Contribution to Original Knowledge

The work presented in this thesis constitutes an original contribution to genomic markers of response to the PARP inhibitor olaparib. The results presented in this thesis are derived from extensive investigations of functional genomic variations and *in vitro* olaparib response in two groups (GDSC and HGSOC) of human cancer cell lines. Through linear regression analyses of olaparib response on mRNA gene expression in pan-cancer GDSC cell lines, I propose expression of *PUM3*, *EEF1A1*, and *ELP4* as novel candidate markers of sensitivity to olaparib. I validate these findings in the HGSOC cell lines by identifying CNVs, single nucleotide variants (SNVs), or differential gene expression of these genes in sensitive or resistant cell lines. I also formulate hypotheses on how these novel candidates may mediate olaparib sensitivity based on existing knowledge of the functions of these genes, and suggest that genes (*PUM3*, *EEF1A1*) encoding proteins that interact with PARP1 may contribute to olaparib sensitivity. From independent analyses of the HGSOC cell lines, this thesis also presents low expression of *MPG* and *CDK2* missense variant p.Thr14Lys as potential novel sources of base excision repair deficiency and HR repair deficiency respectively that contribute to sensitivity to olaparib.

Format of the Thesis

This thesis is written in the traditional format and consists of 6 chapters. Chapter 1 contains the Introduction and provides a review of relevant literature including an overview of ovarian cancer, ovarian cancer treatment, development of PARP inhibitors, DNA repair pathways, known genomic markers of PARP inhibitor response, utility of cancer cell lines in identifying drug biomarkers, hypotheses, and objectives. Portions of chapter 1 are modified from a literature review article that I co-first authored and has been accepted for publication in the journal Seminars in Cancer Biology (PubMed ID: 32827632). Chapter 2 describes the materials and methods used in this thesis. It contains details about the two groups of cell lines and the analyses that were done. Chapter 3 contains all the results of this thesis which are under preparation for publication. It has been divided into four main sections. Chapter 4 contains a discussion of all the results in thesis. Chapter 5 contains conclusions and future directions. Chapter 6 is a list of all references cited in this thesis. Finally, the Appendices contain permissions relevant for chapter 1, one table of genes investigated in chapter 2, and two supplementary tables of results described in chapter 3.

Contributions of Authors

The work presented in this thesis was done while I was a PhD candidate in the Department of Human Genetics under the supervision and support of Dr. Ioannis Ragoussis and his lab.

I wrote Chapter 1 (Introduction) after reviewing scientific literature covering ovarian cancer, ovarian cancer treatment, olaparib and other PARP inhibitors, DNA repair pathways, genomic markers of PARP inhibitor response, and utility of cancer cell lines in identifying drug biomarkers in order to provide the background and frame the hypotheses and objectives of this thesis. This was guided by Dr. Patricia Tonin, and Dr. Ioannis Ragoussis.

For Chapter 2 (Materials and Methods), raw whole exome sequencing (WES) data, normalized mRNA gene expression data, and *in vitro* olaparib response data for 18 HGSOC cell was provided by Dr. Anne-Marie Mes-Masson's lab. Timothée Revil did initial quality control and generated reference-aligned binary alignment map (BAM) files from WES data for 10 of the HGSOC cell lines. I performed the remaining bioinformatic analyses of WES data for the cell lines – quality control and generating remaining BAM files, variant calling (SNVs and indels), CNV calling, mutational signature analysis, variant annotation, filtering and prioritization, visualizations and interpretation of results. I performed the differential gene expression analysis, interpreted and visualized the results. Dr. Ioannis Ragoussis oversaw all aspects of the analysis and interpretation of results. I identified the publicly available GDSC data as a valuable resource to complement my analysis of the HGSOC cell lines and obtained *in vitro* olaparib response and mRNA gene expression data. Dr. Celia Greenwood provided guidance on

statistical analysis of this data. I performed linear regression analyses of olaparib response on mRNA gene expression for these cell lines, visualized and interpreted the results.

For Chapters 3 (Results), 4 (Discussion), and 5 (Conclusions and Future Directions), I investigated the functional implications of alterations in candidate genes to develop hypotheses on how they might contribute to olaparib response. This was guided by Dr. Ioannis Ragoussis and Dr. Patricia Tonin.

Chapter 1: Introduction

1.1 Ovarian cancer: epidemiology, genetic risk factors, pathogenesis, genomic and molecular features

Ovarian cancer is the most lethal cancer of the female reproductive system. In 2016 an estimated 254,000 new cases and 165,000 deaths occurred worldwide [1]. Estimates for new ovarian cancer cases and deaths in 2019 are 3,000 and 1,900 respectively, according to the Canadian Cancer Society [2]. Ovarian cancer is the fifth most common cause of cancer death among females in Canada, accounting for 4.9% of all cancer deaths. Ovarian cancer is a heterogenous disease and can be broadly classified into three groups: epithelial, germ cell, and specialized stromal cell tumors. The majority of ovarian cancers are epithelial ovarian cancers (EOC), also referred to as ovarian carcinomas. There are five main histological subtypes of epithelial origin, namely: high-grade serous, low-grade serous, endometroid, clear cell, and mucinous. Altogether, these subtypes represent about 90% of ovarian cancer cases [3]. Several risk factors are associated with ovarian cancer. Genetic risk factors are among the most significant although personal, lifestyle and environmental factors including age, ethnic background, and hormonal and reproductive factors also influence ovarian cancer risk. A family history of early adulthood ovarian cancer, particularly among first-degree relatives, is an important genetic risk factor. Rare high-penetrant pathogenic variants in *BRCA1* and *BRCA2* genes account for most hereditary cases, and 10%‑15% of all ovarian cases [4,5]. These genes are involved in homologous recombination (HR) DNA repair, a critical pathway for high fidelity repair of DNA double-strand breaks. High grade serous ovarian carcinoma (HGSOC) cases are predominantly associated with germline

BRCA1/2 pathogenic variants. However, mutations in other HR genes including *RAD51C*, *RAD51D*, *BRIP1*, *BARD1*, and *PALB2* have also been found to increase ovarian cancer risk [6,7].

Table 1.1.1. Features of the five major histological subtypes of EOC. Sources - Hollis & Gourley, 2016 [8], Matulonis et al., 2016 [9], Jayson et al., 2014 [10].

	High-grade serous	**Endometrioid**	**Clear cell**	**Mucinous**	**Low-grade serous**
Estimated proportion of EOC cases (%)	70	10	10	<5	<5
Overall prognosis	Poor	Favourable	Intermediate	Intermediate	Intermediate
Tissue of origin or precursor lesion	Distal fallopian epithelium	Endometriosis	Endometriosis	Poorly defined	Serous borderline tumor
Intrinsic chemosensitivity	High	High	Low	Low	Low
Associated hereditary syndromes	Germline BRCA1/2	Lynch syndrome	Lynch syndrome		
Frequent genetic mutations or molecular abnormalities	*BRCA1, BRCA2, TP53, NF1, RB1, CDK12, CCNE1* amplification	*PTEN, PIK3CA, ARID1A, CTNNB1*	*PTEN, PIK3CA, ARID1A*	*KRAS*, *HER2* amplification	*KRAS, BRAF*

Furthermore, germline mutations in additional genes involved in DNA repair such as *CHEK2*, *MRE11A*, *RAD50*, *ATM* and *TP53* may also increase ovarian cancer risk [6,11]. Collectively, these genes are described as having low penetrance or moderate

penetrance because mutations in each of these genes appear to add a small or moderate contribution to overall ovarian cancer risk relative to *BRCA1* or *BRCA2*. Hereditary ovarian cancers tend to develop earlier in life compared to non-inherited (sporadic) cases.

An increased risk of ovarian cancer, especially endometroid or clear cell subtypes, is also associated with rare genetic syndromes, such as Lynch syndrome. Lynch syndrome is commonly associated with mutations in DNA mismatch repair (MMR) genes *MLH1*, *MSH2*, *PMS2*, or *MSH6* [12,13]. Mutations in any of these genes can allow cells to grow and divide unchecked, leading to the development of cancerous tumors. However, most cases of ovarian cancer are sporadic, where the associated genetic alterations are somatic – not inherited – but acquired during a person's lifetime. Mutations in *TP53* are the single most commonly identified mutations in aggressive sporadic high-grade serous ovarian carcinomas, present in more than 90% of these tumors [14].

While the cellular origin and pathogenesis of ovarian cancer remains an active area of research, current evidence suggests that high-grade serous neoplasms originate from epithelium of the fallopian tube. Tumor lesions within the fimbriated end of the fallopian tube (known as serous tubal intraepithelial carcinomas or STICs) have been found to have similar morphology and *TP53* mutations and expression as HGSOC tumors, suggesting that neoplastic transformation begins at these tubal lesions and spreads aggressively onto the ovary [15]. *TP53* mutations are ubiquitous in HGSOC tumors and

have been proposed as driver mutations of HGSOC pathogenesis [14,16]. Cancer may also develop from epithelial cells lining the abdomen (peritoneum). Primary peritoneal cancer resembles EOC and can often spread to the ovaries and fallopian tubes. Collectively, these cancers are similar in their symptoms, progression, and treatment. Ovarian cancer is diagnosed at advanced stages (III-IV) in about 70%-80% [8,17] of cases due to the lack of unique symptoms at early stages. Treatment is largely ineffective at advanced stage and contributes to poor 5-year survival rate of about 45% [2]. Ovarian cancer symptoms such as bloating, constipation, and abdominal pain can be mistaken for largely benign gastrointestinal problems. Screening in high risk groups (for example carriers of *BRCA1* or *BRCA2* mutations) involves measuring CA 125 (Cancer Antigen 125 or mucin 16) levels and the use of transvaginal ultrasonography. The CA 125 blood test is not reliable alone and is often used in the clinic in combination with radiographic imaging. Elevated CA 125 levels are common in HGSOC cases, compared to other non-serous subtypes, [18] but are also elevated in non-cancerous disorders such as ovarian cysts, uterine fibroids, and endometriosis [19,20]. Staging of ovarian cancer is based on guidelines by the International Federation of Gynecology and Obstetrics (FIGO) [21]. Stage I disease is limited to the ovaries only - both ovaries may be affected. Stage II disease extends to the pelvis affecting tubes or uterus or both. At Stage III, disease has spread within the abdomen or affected lymph nodes or both. Stage IV is characterized by distant metastases, beyond the pelvis and abdomen, involving pleural effusions and spread of cancer to inside the liver and other organs. HGSOC is the most common and most lethal histological subtype of ovarian cancer, accounting for most advanced-stage disease and mortality.

1.2 Ovarian cancer treatment

Standard first line treatment involves platinum-based chemotherapy and cytoreductive surgery. Treatment plans for first-line management of newly diagnosed ovarian cancer include either primary surgical cytoreduction (to debulk tumors) followed by combination platinum-based chemotherapy, or neoadjuvant chemotherapy (NACT) – where chemotherapy is administered before surgery – followed by interval surgical cytoreduction and further chemotherapy after surgery. Primary cytoreductive surgery is performed to achieve maximum macroscopic resection of disseminated carcinomatosis. The results of surgical cytoreduction are often described as suboptimal (any tumor focus is 1 cm or greater in size; R2 resection), optimal (residual cancer is less than 1 cm; R1 resection) or no evidence of residual macroscopic cancer; R0 resection). As expected, patients with R0 resection have much better outcomes in terms of overall survival and progression-free survival compared to patients with visible disease post surgery [22,23]. The use of platinum-based chemotherapy post surgery depends on the stage, grade, and histology of cancer. Higher grades (II or above), HGSOC, and clear cell carcinoma typically receive platinum-based chemotherapy. Different strategies are available to improve overall survival of advanced-stage ovarian cancer patients. These include the use of intraperitoneal-delivered cisplatin in patients with R1 resection (optimally cytoreduced cancer) and inclusion of dose-dense weekly paclitaxel treatment instead of 3-week cycles [24–26].

Typically, the combination of a platinum analogue (either cisplatin or carboplatin), and a taxane (either paclitaxel or docetaxel) are administered intravenously as chemotherapy.

Cisplatin (also known as cis-diamminedichloroplatinum(II) or CDDP) is the first of its class to be used as a chemotherapeutic agent. It was first approved by the United States Food and Drug Administration (US FDA) in 1978 for the treatment of testicular, and bladder cancers [27]. It has since been widely used in the clinic against a variety of additional solid tumors, including ovarian, colorectal, lung, and head and neck cancers. Cisplatin has been especially effective for patients with testicular or ovarian cancer. Cisplatin covalently binds to DNA bases, after activation with water molecules, to form DNA adducts. It preferentially binds platinum to the N7 position of the imidazole ring of purine bases (adenine and guanine) producing distortions in DNA, including inter- and intra-strand adducts, as well as protein-DNA complexes [28,29]. These platinum–DNA adducts disrupt cellular process like DNA replication and transcription ultimately leading to apoptotic cell death. The most severe safety issue with cisplatin is its nephrotoxicity (kidney damage), although it is also neurotoxic (peripheral nerves) and ototoxic (inner ear) [30–32]. This motivated the development of carboplatin which is as effective as cisplatin but usually has fewer and less severe side effects [33,34]. Indeed, similar survival rates have been reported for ovarian cancer patients treated with carboplatin or cisplatin [35]. Carboplatin is the most common choice of platinum chemotherapeutic in many countries. It was approved by the US FDA for ovarian cancer treatment in 1989. Carboplatin (cis-diammine-[1,1-cyclobutanedicarboxylato] platinum(II)) forms the same platinum-DNA adducts as cisplatin. It is not nephrotoxic or neurotoxic but is principally associated with thrombocytopenia, a decrease in the number of platelet cells in the blood [36].

Paclitaxel is an antineoplastic compound originally extracted from the bark of the Pacific yew tree *Taxus brevifolia.* It was approved for treatment of ovarian cancer in 1992, and then breast cancer in 1994 by the US FDA. Prior to first approval, a phase II clinical trial found that twelve patients (30%) with platinum-resistant ovarian cancer responded to paclitaxel treatment, either completely or partially, for periods ranging from three to five months [37]. Paclitaxel binds to microtubules, which are important for the formation of mitotic spindle during cell division. Microtubule disassembly is important for normal separation of sister chromatids during anaphase of mitosis. Paclitaxel prevents cell division by inhibiting the disassembly of microtubules leading to G2/M cell cycle arrest [38] and subsequently apoptosis. Docetaxel is a taxane derived by a semi-synthetic process from the European Yew tree *Taxus baccata* [39]. It was reported to have greater *in vitro* cytotoxicity, about 1.2 to 2.6 times, than paclitaxel in ovarian carcinoma cell lines [40,41]. Docetaxel, like paclitaxel, blocks microtubule disassembly leading to cell cycle arrest [42]. Similar progression-free survival (PFS) has been reported in a phase III clinical trial comparing carboplatin and paclitaxel to carboplatin and docetaxel as first-line chemotherapy in EOCs or primary peritoneal cancers [43]. However, carboplatin-docetaxel was associated with substantially lower neurotoxicity than carboplatin-paclitaxel.

The combination of carboplatin and paclitaxel has long been the accepted standard for first-line chemotherapy of EOC [44–47], producing high response rates of at least 6 months without evidence of cancer progression. However, recurrence of cancer after

initial platinum-based chemotherapy is very common for women diagnosed with advanced-stage cancer.

Alterations in several genes have been linked to resistance to standard platinum-taxane chemotherapy. Inactivation of the tumor suppressors genes *RB1, NF1, RAD51B* and *PTEN,* by disruption of transcriptional units due to structural rearrangement (gene breakage), has been found in HGSOC cases with acquired resistance [48]. Patch et al. [48] also found amplification of the *CCNE1* locus (chromosome 19q12) to be enriched in primary platinum-resistant and refractory HGSOC cases. This is consistent with a prior study linking *CCNE1* amplification with poor survival in ovarian cancer [49]. *CCNE1* encodes cyclin E1 which is a co-factor for cyclin-dependent kinases 1 and 2 (CDK1/2) and activates transcription of HR genes *BRCA1* and *BRCA2* mediated by E2F transcription factors [50]. *CCNE1* amplification rarely co-occurs with inactivation of BRCA1 or BRCA2 [51]. Most cases with germline or somatic mutations in *BRCA1* or *BRCA2* have favourable response to treatment. However, reversion mutations which, restore the wildtype reading frame, lead to development of resistance to platinum-based chemotherapy [48,52]. Upregulation of *ABCB1* and subsequent overexpression of the drug efflux pump multidrug resistance protein 1 (MDR1) is another mechanism of platinum resistance in EOC. The activity of this cell surface protein minimizes the accumulation of anti-cancer agent in tumor cells. It transports a variety of chemotherapy agents including cisplatin, paclitaxel and docetaxel and plays a major role in cellular detoxification [53–55].

More than 80% of patients relapse after initial response to first line treatment [9] at a median of 15 months after initial diagnosis. Subsequent chemotherapy treatments are linked to chemoresistance with longer treatment-free periods associated with higher response rates. Poly (ADP-ribose) polymerase inhibitors (PARPi) have shown promise as maintenance therapy for relapsed patients with BRCA-mutated high-grade serous ovarian carcinoma who were initially sensitive to platinum-based chemotherapy.

1.3 PARP inhibitors as maintenance treatment for ovarian cancer

The first poly (ADP-ribose) polymerase (PARP1) was discovered in 1964 [56]. PARP1 belongs to a family of 17 enzymes with a common catalytic motif ‑ ADP-ribosyltransferase (ART) also known as ARTD (diptheria-toxin-like ADP-ribosyltransferase). The majority of ARTDs add a single ADP-ribose but PARP1, PARP2, PARP5a, and PARP5b are the only ARTDs capable of building PAR chains [57,58]. PARP1 and PARP2 are involved in DNA damage repair. PARP1 repairs both single and double strand DNA breaks while PARP2 is required to repair single strand breaks of DNA.

Major clinical PARP inhibitors (PARPis), approved for use in the clinic or involved in clinical trials, include olaparib, talazoparib, niraparib, rucaparib and veliparib. These PARPis inhibit both PARP1 and PARP2. PARP1 is expressed ubiquitously and generates the majority of PAR polymers. PARylation is a common reversible post-translational modification important for DNA repair and epigenetic marking. PARP inhibition is in two parts – catalytic inhibition, and PARP trapping. PARPis bind to the

NAD^+-binding site of PARP, thereby blocking NAD^+ binding and PARylation. The major clinical PARP inhibitors structurally mimic nicotinamide, allowing them to compete for the NAD^+ binding site of PARP1 or PARP2. When PARP is inhibited while bound to a single strand break site it is said to be trapped. The side chain attached to the nicotinamide moiety confers differential PARP-trapping potential to PARPis (Figure 1.3.1). After talazoparib, niraparib is the strongest PARP trapper, followed by olaparib and rucaparib which have equivalent PARP-trapping potential, and veliparib is the weakest PARP trapper [59,60]. PARP trapping is considered the major source of cytotoxicity of PARP inhibitors. This is because trapped PARP1 stalls the progress of DNA replication forks. In normal cells, removal of this replication stress involves HR pathway proteins, such as BRCA1 and BRCA2. However, tumor cells defective in the HR pathway succumb to this stress and die by apoptosis.

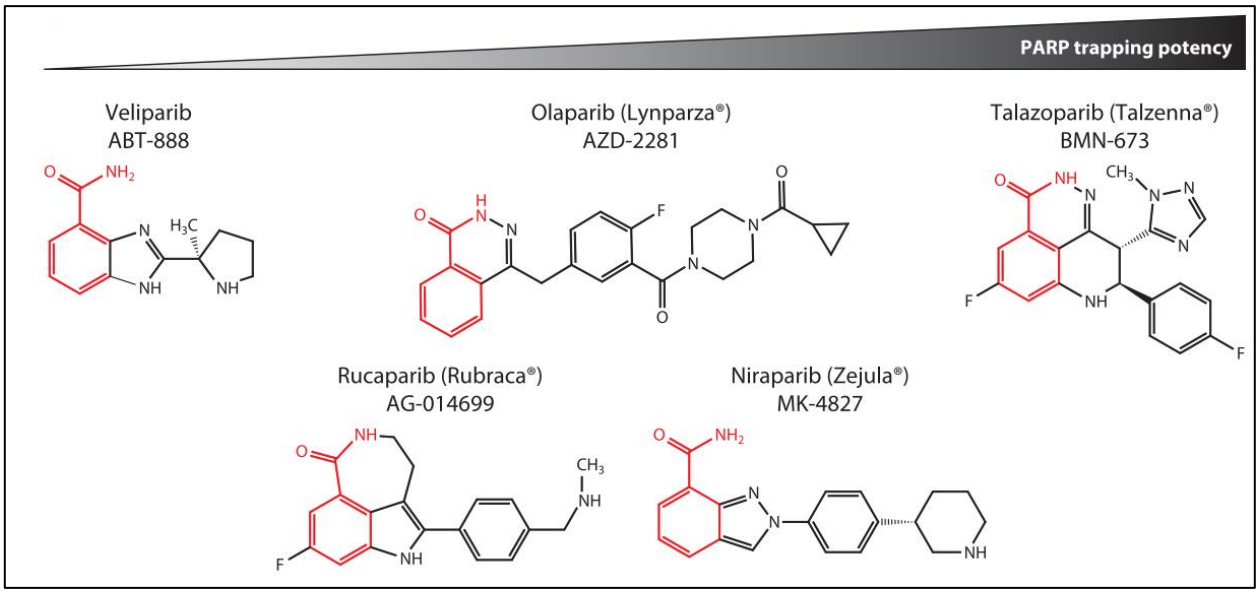

Figure 1.3.1. Molecular structures of major PARP inhibitors active in the clinic or in clinical trials. The nicotinamide moiety is shown in red. PARPis are ranked in order of

PARP trapping potency. Veliparib has low PARP trapping, olaparib, rucaparib and niraparib are medium PARP trappers, while talazoparib has high PARP trapping potency. Figure is from Murai and Pommier (2019) [61]. Permission was obtained from the journal to reuse this figure. The license to reuse this figure is in Appendix B.

The clinical application of PARP inhibitors as monotherapy is based on synthetic lethality induced by a combination of BRCA1/2 deficiency and PARP inhibition. The evidence for this is derived from various studies including *in vitro* studies [62,63], and *in vivo* studies using BRCA1 and BRCA2 knockout mice models [64,65]. Silencing *PARP1* expression by short-interfering RNA (siRNA) significantly diminished cell survival in *BRCA1*- and *BRCA2*-deficient embryonic stem cells [62]. Down-regulation of *BRCA2* by siRNA was also found to sensitize breast cancer cell lines to PARP inhibition and increase single-strand breaks leading to collapsed replication forks which triggers homologous recombination DNA repair [63]. In *BRCA1*-deficient mammary tumor models, PARP inhibition with AZD2281 (also known as olaparib) inhibited tumor growth and increased survival [64]. This study also demonstrated that combination of AZD2281 with cisplatin or carboplatin increased recurrence interval and overall survival. Hay *et al*. [65] reported significant regression of tumor growth in 46 out of 52 *BRCA2*-deficient mammary tumors. Additionally, they report significantly increased time to tumor relapse and death in these mice for the combination of AZD2281 and carboplatin, supporting prior work by Rottenberg *et al.* [64].

Olaparib is an inhibitor of PARP1 and PARP2, and the first PARPi to be evaluated as monotherapy [66]. The primary clinical trial that led to US FDA approval of olaparib (referred to as *study 19,* ClinicalTrials.gov number - NCT00753545) involved 265 high-grade serous EOC patients with platinum sensitive-relapsed disease [67]. It was a randomized, double-blind, placebo-controlled, phase 2 study with 136 patients assigned to olaparib group and 129 patients to the placebo group. The primary endpoint was progression-free survival (PFS) based on the RECIST (Response Evaluation Criteria in Solid Tumors) guidelines. This study reported significantly improved PFS with olaparib than placebo (median PFS of 8.4 months versus 4.8 months, Hazard Ratio of progression or death [HR] = 0.35, 95% confidence interval [CI] = 0.25 – 0.49, $p<0.0001$). This was even more pronounced in patients with germline or somatic BRCA1/2 mutations (median PFS of 11.2 months versus 4.3 months, HR = 0.18, 95% CI = 0.10 – 0.31, $p<0.0001$) [67,68].

Subsequently, olaparib (Lynparza®) has been approved, with similar conditions, in many countries including Canada, where it is indicated for use as monotherapy for maintenance treatment of platinum-sensitive, relapsed *BRCA1/2*-mutated (germline or somatic) ovarian, fallopian tube or primary peritoneal cancer that was partially or fully responsive to platinum-based chemotherapy. It is administered orally. Approval has also been extended to include all platinum sensitive patients, regardless of *BRCA1/2* mutation status supported by results from the SOLO-2 phase III trial (ClinicalTrials.gov number -NCT01874353) [69]. Olaparib is also approved in the US, Canada and elsewhere as the first-line maintenance therapy for *BRCA1/2*-mutated (germline or somatic) HGSOC, as well as fallopian tube or primary peritoneal cancer. This approval

was based on the phase III SOLO1 trial (ClinicalTrials.gov number - NCT01844986) which demonstrated significant benefit of olaparib compared to placebo (HR = 0.30, 95% CI = 0.23 – 0.41, P<0.001) as maintenance treatment following first-line platinum-based chemotherapy in advanced (stage III/IV) HGSOC [70]. Olaparib is also approved for treatment of germline *BRCA1/2*-mutated advanced ovarian cancer previously treated with three or more lines of chemotherapy. In 2017, AstraZeneca and Merck formed an alliance to co-develop and co-commercialize Lynparza and other drugs. Olaparib is currently approved as first-line maintenance treatment in *BRCA1/2*-mutated advanced ovarian cancer, maintenance treatment of recurrent ovarian cancer, and treatment of advanced germline *BRCA1/2*-mutated ovarian cancer.

Apart from ovarian cancer, olaparib is also approved for the treatment of germline *BRCA1/2*-mutated, human epidermal growth factor receptor 2 (HER2)-negative metastatic breast cancer previously treated with chemotherapy in the neoadjuvant, adjuvant, or metastatic setting. The randomized OlympiAD phase III trial provided evidence to support this approval, reporting longer PFS in olaparib group compared to standard therapy group (median PFS 7.0 months versus 4.2 months; HR = 0.58, 95% CI = 0.43 – 0.80, P<0.0001) [71]. Underscoring its importance for BRCA1/2-mutated cancers, olaparib was also approved, by the US FDA, for first-line maintenance therapy of germline *BRCA1/2*-mutated metastatic pancreatic cancer. This approval was based on results of the phase III POLO trial which reported significant improvement in PFS of olaparib users versus placebo (median PFS 7.4 months versus 3.8 months, HR = 0.53, 95% CI = 0.35 to 0.82; P = 0.004) in germline *BRCA1/2*-mutated metastatic pancreatic

cancer patients [72]. Clinical trials of PARP inhibitors in prostate cancer are underway – 16 trials spanning phase 1 to phase 3 are recruiting or yet to recruit (based on a search of ClinicalTrials.gov, February 11, 2020). Given that 8%-12% of metastatic prostate cancer have *BRCA2* mutations or homozygous deletions [73,74] this subpopulation may be the next to benefit from PARPi treatment.

Other PARP inhibitors have been approved to treat ovarian cancer patients. Niraparib (Zejula® by GlaxoSmithKline) was approved as maintenance treatment for platinum-sensitive ovarian, fallopian tube or primary peritoneal cancer regardless of *BRCA1/2* mutation status. Rucaparib (Rubraca® by Clovis Oncology), like olaparib and niraparib, was also approved as maintenance treatment for platinum-sensitive ovarian, fallopian tube or primary peritoneal cancer regardless of *BRCA1/2* mutation status. Additionally, it is approved for treatment of advanced disease *BRCA1/2*-mutated (germline or somatic) previously treated with 2 or more lines of chemotherapy [75]. Talazoparib (Talzenna® by Pfizer) is approved for treatment of germline *BRCA1/2*-mutated, HER2-negative, locally advanced or metastatic breast cancer [76].

1.4 Overview of DNA repair pathways

An important hallmark of HGSOC and indeed other types of cancer is genomic instability. DNA repair pathways are important for maintaining genomic stability and defects in one or more DNA repair pathways are characteristic of multiple cancer types. Loss of DNA repair genes influences cancer risk, progression, and therapeutic response. DNA repair proteins work together in functional pathways to repair specific

types of DNA damage originating from endogenous and exogenous sources. Base DNA damage, multiple and bulky base DNA damage, and DNA strand breaks are three main types of DNA damage, as reviewed by Chatterjee and Walker (2017) [77].

Table 1.4.1. Overview of DNA repair pathways and types of damage they repair. Core DNA repair genes per pathway are sourced from Knijnenburg *et al*. (2018) [78].

Class of DNA damage	**DNA repair pathway**	**Examples of DNA damage**	**Core DNA repair genes**
Base DNA damage 	Direct reversal	Alkylation Ultraviolet (UV) photolesions	*MGMT, ALKBH2, ALKBH3*
	Base excision repair	Alkylation Base deamination	*PARP1, POLB, APEX1, APEX2, FEN1, TDG, TDP1, UNG*
Multiple and bulky base DNA damage   	Nucleotide excision repair	Bulky UV photolesions, DNA adducts from chemotherapeutics	*CUL5*, *ERCC1, ERCC2, ERCC4, ERCC5, ERCC6, ERCC8, POLE, POLE3, XPA, XPC*
	Mismatch repair	Mismatches Insertion-deletion loops	*MSH2, MSH3, MSH6, MLH1, MLH3, PMS1, PMS2, EXO1*
	Interstrand crosslink repair/Fanconi anemia pathway	Interstrand crosslinks	*FANCA, FANCB, FANCC, FANCD2, FANCI, FANCL, FANCM, UBE2T*
	Translesion DNA synthesis	Bulky lesions or adducts impeding replication	*POLN, POLQ, REV1, REV3L, SHPRH*
DNA breaks  	Single strand break repair (SSBR)	Single strand breaks	*PARP1, XRCC1*
	Homologous recombination (HR)	Double strand breaks	*BRCA1, BRCA2, MRE11A, NBN, RAD50, TP53BP1, XRCC2, XRCC3, BARD1, BLM, BRIP1, EME1, GEN1, MUS81, PALB2, RAD51, RAD52, RBBP8, SHFM1, SLX1A, TOP3A*
	Non-homologous end joining (NHEJ)	Double strand breaks	*LIG4, NHEJ1, POLL, POLM, PRKDC, XRCC4, XRCC5, XRCC6*

1.4.1 Direct Reversal

Some DNA lesions, such as alkylated bases, can be reversed. Reversal of alkylated bases is achieved by two different classes of enzymes. The enzyme AGT (O^6-alkylguanine-DNA alkyltransferase), also known as MGMT (O^6-methylguanine DNA methyltransferase), specializes in reversing O-alkylated DNA adducts including methyl, ethyl, 2-chloroethyl, benzyl and aliphatic groups. AGT transfers the alkyl group from the oxygen of the DNA base to the cysteine residue in its catalytic pocket in a single reaction [79].

AlkB-related α-ketoglutarate-dependent dioxygenases (AlkB) specialize in reversing N-alkylated base adducts. There are nine members of this class of enzymes in human cells: ALKBH1 to ALKBH8, and FTO (Fat Mass and Obesity associated) alpha-ketoglutarate dependent dioxygenase. To remove methyl groups, the AlkB proteins add a hydroxyl group to the alkyl group in the presence of α-ketoglutarate and iron(II). This releases the methyl group as formaldehyde and reverts the methylated base to its original form [80,81].

1.4.2 Base Excision Repair

Thousands of single base modifications or nucleotide damage occur each day through spontaneous deamination of bases, activity of reactive oxygen species and other metabolites.

The base excision repair (BER) pathway corrects single base damage including oxidation, alkylation, deamination, and loss of a DNA base (abasic site). The damaged or lost base is removed and replaced. In BER, chromatin remodelling at site of DNA damage occurs prior to recognition of a lesion by a DNA glycosylase [82]. These enzymes are the major family of enzymes involved in BER, and may be either monofunctional or bifunctional. Monofunctional DNA glycosylases remove damaged bases by cleavage of the N-glycosidic bond leaving the sugar-phospate backbone intact. Examples of monofunctional DNA glycosylases are the uracil glycosylases N-methylpurine DNA Glycosylase (MPG) and MutY Homolog (MUTYH). Bifunctional DNA glycosylases have lyase activity in addition to glycosylase activity, allowing them to cleave the phosphodiester bond of DNA to create a single-strand break. These include Nei-like DNA glycosylase 1 (NEIL1), Nei-like DNA glycosylase 2 (NEIL2), Nth-like DNA glycosylase 1 (NTHL1). Specific lesions are recognized by specific DNA glycosylases. For example, MPG targets 3-methyladenine, 7-methylguanine, and 3-methylguanine [83]. There are two types of BER, short patch repair and long patch repair.

Monofunctional glycosylases create abasic sites that are repaired by the short patch pathway. Apurinic/apyrimidinic (AP) endonuclease 1 (APE1) then cleaves the

phosphodiester bond 5’ to the abasic site and creates a hydroxyl residue at the 3’ end and deoxyribose phosphate (dRP) at the 5′-end. This. This gap is filled with a nucleotide by DNA polymerase β (POL β) and ligated by DNA ligase 1 (LIG1) or a complex of DNA ligase 3 (LIG3) and XRCC1 (X-ray repair cross-complementing protein 1) [84]. In long patch repair, 2-13 nucleotides may be replaced. After excision of bases by a bifunctional glycosylase, the resulting gap is also processed by APE1. Nucleotides are then replaced by POL β or POL δ/ε. This involves strand displacement and is then followed by removal of 5’ flap by the flap endonuclease (FEN1) and completed with LIG1-mediated ligation [85].

1.4.3 Nucleotide Excision Repair

Photolesions induced by ultraviolet (UV) light such as pyrimidine-pyrimidone (6–4) photoproducts (6–4PPs) and cyclobutane pyrimidine dimers (CPDs) are repaired by the nucleotide excision repair (NER) pathway. There are two main forms of NER: global genome NER (GG−NER) and transcription−coupled NER (TC −NER). In GG-NER, xeroderma pigmentosum group C protein (XPC) in complex with RAD23B and CETN2 function as DNA damage sensor by scanning for the presence of transient single-stranded DNA (ssDNA) formed by impaired base pairing due to a lesion within DNA. To repair CPDs, another complex (UV-DDB; UV DNA damage binding protein) comprising of DDB1 and DDB2 binds to the lesion and stimulates binding of XPC [86,87], and subsequently to transcription initiation factor II H (TFIIH). Next, structure specific endonucleases XPF-ERCC1 and XPG make 5’ and 3’ incisions, a few nucleotides from the lesion, respectively. The resulting gap is then filled with nucleotides by replication

proteins PCNA, RFC, and POL δ, ε, or κ. To complete the repair, ligation is carried out by XRCC1-LIG3 or LIG1.

Transcription-coupled NER occurs when a DNA lesion stalls the progress of RNA polymerase II during transcription. It begins with the recruitment of ERCC8 and ERCC6, which stimulates the assembly of additional proteins including UVSSA, USP7, XAB2, HMGN1, and TFIIH to facilitate removal of the lesion from the transcribed strand. The ERCC8-ERCC6 complex moves RNA polymerase II in a backwards direction to expose the lesion site. The subsequent steps of double incision, gap filling, and ligation are the same as global-genome nucleotide excision repair [88]. Notably, platinum–DNA adducts formed by cisplatin block RNA polymerase II during transcription and can be repaired by transcription-coupled NER [89,90].

1.4.4 Mismatch Repair

The mismatch repair (MMR) pathway repairs base mismatches that occur during DNA replication, and insertion-deletion loops (IDLs) which are usually found in repetitive DNA sequences [91]. Key proteins MSH2 and MSH6 form a heterodimer (MSH2/MSH6 also known as MutSα complex) to recognize base mismatches and short (one or two nucleotides) IDLs, while the MSH2/MSH3 (or MutSβ) heterodimer detects long IDLs up to 13 nucleotides [92,93]. MutS forms a sliding clamp and interacts with proliferating cell nuclear antigen (PCNA) to recognize mismatches and IDLs. PCNA is also important for DNA synthesis that occurs later in the repair process. MutLα, a heterodimer comprised of MLH1 and PMS2, is also recruited to the damage site. It interacts with exonuclease

(EXO1) to excise the mismatch. The resulting gap is stabilized by RPA. DNA synthesis is then carried out by POL δ, RFC, and high mobility group box 1 protein (HMGB1). Finally, LIG1 ligates the strands to complete the repair.

1.4.5 Fanconi Anemia Pathway

Interstrand crosslinks (ICLs) occur when two bases from complementary strands become covalently linked. This damage can be induced by platinum compounds, such as cisplatin and carboplatin, as well as alkylating agents. These lesions are repaired by Fanconi anemia proteins (FANCA to FANCT) and associated proteins [94]. Hence interstrand crosslink repair is also known as the Fanconi anemia (FA) pathway. FA is an autosomal recessive disorder caused by mutations in the genes encoding FA proteins. The disorder is characterized by a predisposition to certain cancers, congenital anomalies, and bone marrow failure [95].

Fanconi anemia pathway is engaged with the recruitment of FANCM, FAAP24, and MFH (histone fold protein complex) proteins to the site of DNA damage. FANCM promotes the activation of multiple FA proteins through phosphorylation by ATR (ataxia telangiectasia and RAD3-related). This is followed by monoubiquitylation of the FANCD2-FANCI heterodimer by FANCL and ubiquitin-conjugating enzyme E2 T (UBE2T). This is the key activation step of the FA pathway. Next the DNA strand with the lesion is excised by structure specific endonucleases such as XPF-ERCC1 (also involved in NER), MUS8-EME1, SLX4-SLX1, FAN1, and SNM1A/SNM1B which make

incisions 5’ and 3’ to the lesion [96]. ICLs stall replication forks. In replicating cells, the leading strand with the lesion is bypassed by translesion synthesis coordinated by REV1, followed by ligation to create an intact DNA molecule. This molecule becomes the template for homologous recombination-mediated repair of the double strand break involving the lagging strand of the original DNA molecule. The ends of the leftover strand are processed by nucleases such as CtBP-interacting protein (CtIP), MRN (MRE11–RAD50–NBS1), and EXO1. Strand invasion mediated by RAD51 and BRCA2 facilitates homologous recombination, followed by polymerase extension, resolution, and ligation [97]. The NER pathway ultimately removes the remaining ICL hook from the leading strand.

1.4.6 Translesion DNA Synthesis

Translesion DNA synthesis (TLS) is a DNA damage tolerance pathway. It is accomplished by specialized DNA polymerases that can replicate opposite or past DNA lesions, but with lower fidelity compared to replicative DNA polymerases, making this pathway a source of mutagenesis. Notably, TLS polymerases lack a 3’-5’ exonuclease domain, present in replicative DNA polymerases, that is important for proofreading repaired lesions [98].

In the polymerase switch model of translesion synthesis, polymerases assemble in two steps to bypass a lesion at a stalled replication fork. To begin, POL η, POL ι, or POL κ inserts a nucleotide opposite the DNA lesion. This enzyme is referred to as the *inserter.* An *extender* enzyme, either POL ζ or POL κ [99], then extends the primer template.

Both steps are coordinated by REV1 which acts as a scaffold and interacts with insertion and extension polymerases [100]. REV1 and the TLS pathway have been reported to promote acquired resistance to cisplatin and cyclophosphamide by generating resistance-inducing mutations [101,102].

1.4.7 Single Strand Break Repair

Unrepaired single strand breaks (SSB) can collapse DNA replication forks and stall transcription. PARP1 is required for detecting single strand breaks and recruiting XRCC1 (X-ray repair cross-complementing protein 1) through transient formation of poly(ADP-ribose) [PAR] chains on its auto-modification domain using NAD^+. PAR chains are degraded by PAR glycohydrolase (PARG) [103,104]. XRCC1 provides a scaffold for recruiting additional proteins polynucleotide kinase 3´- phosphatase (PNKP), aprataxin (APTX) and (LIG3) to process the SSB. The next step also involves PARP1 which promotes 5' endonuclease activity of FEN1. DNA polymerases δ, ε, β fill the resulting gap with nucleotides which are then ligated by LIG1.

1.4.8 Double Strand Break Repair

Double strand breaks (DSBs) are the most toxic form of DNA damage. These lesions cause cell death if unrepaired, and misrepaired DSBs may produce chromosomal translocations relevant for tumorigenesis [105]. Two pathways that have evolved to repair DSBs are homologous recombination and non-homologous end joining (NHEJ). While NHEJ repair occurs throughout the cell cycle, homologous recombination is

restricted to the late S and G2 phases where sister chromatids are available to be used as templates for repair.

Chromatin modification is the first event to occur at the DSB site. PARP1 PARylates chromatin at the DSB site and recruits chromatin remodelers such as ALC1 (amplified in liver cancer 1) and NuRD (nucleosome remodeling and deacetylase) complex to facilitate access to the DSB by additional proteins [106,107]. Highlighting the importance of PARP1 for initiating DSB repair, inactivation of NuRD or ALC1 leads to defects in DSB repair and increased sensitivity to DNA damage. Chromatin modification is followed by a series of events including activation of ATM, phosphorylation of histone H2AX, recruitment of MDC1, and subsequently recruitment of 53BP1 and BRCA1. PARP1 is also involved in recruiting BRCA1 to DSBs through its interaction with BARD1 (BRCA1-associated RING domain protein 1) which forms a dimer with BRCA1 [108]. BRCA1 and 53BP1 are antagonistic partners. While 53BP1 negatively regulates DNA end resection in the G1 phase of the cell cycle [109], BRCA1 promotes resection in the S phase and exclusion of 53BP1 from DSB site [110,111]. Thereby, BRCA1 promotes HR while 53BP1 promotes NHEJ repair.

In classic NHEJ repair, the Ku70-Ku80 heterodimer binds to DSB ends and provides a scaffold to recruit other NHEJ proteins. This is followed by recruitment and activation of DNA-dependent protein kinase catalytic subunit (DNA-PKcs) which keep the broken ends close to each other. DNA-PKcs further recruit additional proteins such as Artemis, PNKP (polynucleotide kinase/phostase), and APTX to prepare the ends for ligation [112–114]. XRCC4 (X-ray repair cross-complementing protein 4), XRCC4-like factor

(XLF), and DNA ligase 4 (LIG4) are also recruited and form a complex to join the ends and complete the process.

HR is initiated by the MRN (MRE11-RAD50-NBS1) complex which recognises and binds DSBs and recruits ATM and TIP60. ATM is activated by TIP60 and then phosphorylates histone H2AX. This recruits MDC1 which is also phosphorylated by ATM before it serves as a scaffold for RNF8 and RNF168. These E3 ubiquitin-protein ligases catalyze the ubiquitination of H2AX which provides a docking site for 53BP1 and BRCA1. In the S/G2 phase of the cell cycle, BRCA1 initiates ubiquitination of CtIP which signals the recruitment of RPA and RAD51 proteins. MRN then cooperates with CtIP, DNA2, EXO1 and BLM to resect the DSB ends. This involves 5’ to 3’ nucleolytic degradation to create 3’ single stranded DNA (ssDNA) overhangs [115,116]. DNA end resection commits the DSB to HR repair. These overhangs are protected by RPA (replicating protein A) which forms a coat on each overhang. RAD51 then displaces RPA to form RAD51-single strand DNA (RAD51-ssDNA) nucleofilaments. Formation of these filaments require the help of BRCA1, BRCA2, PALB2 and the RAD51 homologues [117,118]. The RAD51-ssDNA nucleofilament then search for homologous sequences in the template DNA duplex and invades it to form a D-loop. For strand invasion to occur, RAD54 and RAD54B remove RAD51, allowing the 3’ hydroxyl group to prime synthesis by DNA polymerase δ in the presence of PCNA [119]. The D-loop may be resolved by synthesis-displacement strand annealing (SDSA) where the extended strand dissociates and anneals with the second end of the broken DNA molecule. Further synthesis and ligation occur to complete the repair. Alternatively, the extended strand may invade the second end of the break forming a double Holliday

junction intermediate that is processed by protein complexes BLM-TOPOIII-RMI1-RMI2 complex, and specialized nucleases MUS81-EME1 complex, SLX1-SLX4 complex and GEN1 endonuclease [120,121]. SDSA is the predominant mode of resolving HR D-loops in somatic human cells [122].

1.5 Known markers of sensitivity to PARP inhibitors

Although *BRCA1* and *BRCA2* mutations leading to defective BRCA1 and BRCA2 proteins that compromise HR repair are key markers of olaparib sensitivity, they are not the only markers of sensitivity. *BRCA1* and *BRCA2* mutations are also markers of sensitivity to platinum-based chemotherapy [123,124] given that repair of ICLs generated by platinum adducts requires BRCA1 and BRCA2 [97,125]. Loss of other tumor suppressor DNA repair proteins have been found to increase sensitivity to PARP inhibition *in vitro*. The majority of these proteins are also involved in HR or related DNA repair pathways and include ATM, ATR, RAD51, RAD54, DSS1, RPA1, CHK1, CHK2, FANCD2, FANCA, or FANCC [126].

HR deficiency is a fundamental vulnerability of HGSOC. About 50% of HGSOCs have some form of HR defect involving genetic or epigenetic alterations to HR pathway genes [51,127]. These include germline or somatic mutations in *BRCA1/2* (19%), promoter methylation of *BRCA1* (10%) and *RAD51C* (2%), mutations of core RAD genes (1.5%), FA genes (2%), other HR genes (2%), and *CDK12* (3%), a positive regulator of *BRCA1* expression [128,129]. Silencing of *CDK12* expression by RNA interference was shown

to confer sensitivity to PARP inhibition in HGSOC cell lines [128]. Additionally, homozygous copy number deletion of *PTEN* (7%) and copy number amplification of *EMSY* (6%) are also potential sources of HR deficiency in EOCs.

Apart from HR defects, BER and SSBR defects also sensitize cells to PARP inhibition. *XRCC1* and *POLB* deficiency increased sensitivity of cells PARPis potentially through increased PARP trapping [130,131]. PARP1 recruits XRCC1 and Pol β (POLB) to the site of single strand break generated by BER, for example, following cleavage of abasic sites by APEX1. Excess PARP activation in *XRCC1*- and *POLB*-deficient cells, in an attempt recruit the encoded proteins, makes more PARP1 available to be trapped by a PARPi.

MMR and NER pathways are also involved in the repair of DSB and their loss of function has been reported to reduce DSB repair. These roles are reviewed by Zhang et al., (2009) [132]. Subsequently, defects in MMR and NER have been linked to olaparib sensitivity based on gene expression analysis and experimental validation of 18 HGSOC cell lines by Fleury *et al*., (2017) [133]. Down-regulation of key HR, MMR and NER genes (*MRE11A*, *MLH1* and *ERCC8*, respectively) by siRNA increased sensitivity of cells to olaparib. The authors of this study propose a model for PARP inhibitor sensitivity where defective MMR and NER pathways, in addition to deficient HR, is associated with highest sensitivity. The 18 HGSOC cell lines investigated by the Fleury *et al*., (2017) [133] study are also important for my genomic analyses for markers of

olaparib sensitivity and resistance and are further described in subsequent chapters of this thesis.

Beyond individual genes, genomic scars or signatures indicative of defective HR repair may also be evident in tumor DNA even when there are no obvious alterations in genes of HR repair pathway. Tumors with HR repair deficiency depend on the NHEJ repair pathway to repair double strand breaks, essentially, by ligating broken chromosome ends. These tumors accumulate errors in the form of mutations, small insertions and deletions [134], and exhibit loss-of-heterozygosity (LOH) of extensive parental chromosomal regions [135]. A mutational signature of homologous recombination repair deficiency (HRD), designated signature 3, has been associated with the presence of *BRCA1* and *BRCA2* mutations in breast, ovarian and pancreatic cancer cases [134].

Two companion diagnostics aimed at identifying such signatures have recently been approved by the US FDA for use of PARPis in EOC patients. The FoundationFocus™ CDx $_{\text{BRCA LOH}}$ assay detects *BRCA1* and *BRCA2* sequence alterations and the frequency of genomic LOH events from formalin-fixed, paraffin-embedded (FFPE) ovarian tumor tissue using next-generation sequencing (NGS) technology. This assay was approved to aid the identification of ovarian cancer patients eligible for treatment with PARPi, Rubraca® (rucaparib). Myriad's myChoice® HRD (homologous recombination deficiency) [136] uses a combination of single nucleotide variants (SNVs), insertions and deletions (indels), and large rearrangement variants in protein coding regions and intron/exon boundaries of the *BRCA1* and *BRCA2* and the determination of a genomic

instability score (GIS) based on LOH, telomeric allelic imbalance (TAI) [137], and large-scale state transitions (LST)[138] events to diagnose HR defect . It was approved to help identify patients eligible for Lynparza® (olaparib) and Zejula® (niraparib), also PARPi.

1.6 Known mechanisms of resistance to PARP inhibitors

Multiple mechanisms have been proposed to account for resistance to PARPis. These can be grouped into three main classes, as reviewed by Mateo *et al*., (2019) [139], namely: restoration of HR repair function, mitigation of replication stress, and other mechanisms not related to HR repair and replication stress such as decreased PARP trapping and drug export. Resistance to PARP inhibition can occur through the restoration of HR function. Secondary mutations are mutations that reverse the effect of the primary loss-of-function mutation and restore full or partial function. These mutations may restore the open reading frame of *BRCA1/2, RAD51C/D,* and *PALB2* in tumors that originally harbored frameshift or nonsense mutations in these HR genes [140,141]. Secondary mutations in *BRCA1/2* are also associated with resistance to chemotherapy in EOC [142]. Hypomorphic variants, which produce partial loss of function, in BRCA1 protein are also linked to PARPi resistance. For example, *BRCA1* p.Glu23fs variant (also known as *BRCA1* 185delAG) and mutations in exon 11 of *BRCA1* produce a *BRCA1-Δ11q* splice variant lacking the majority of exon 11 [143,144]. Restoration of HR repair function may also occur through demethylation of *BRCA1* and *RAD51C* promoter regions leading to resistance [145,146]. Methylation of promoter region occurs

on cytosines that precede a guanine nucleotide (also known as CpG sites) and represses gene expression, by inhibiting binding of transcription factors and recruiting repressive proteins. Demethylation restores gene expression and subsequent function of encoded protein. Additionally, loss of function of 53BP1, RIF1, REV7 or proteins in the Shieldin complex that suppress nucleolytic resection of DSB termini has also been found to restore BRCA1 function and confer PARPi resistance in *BRCA1*-deficient cells [147–151].

Another class of PARPi resistance factors are involved in mitigating replication stress by protecting or stabilizing the replication fork [152]. Stalled replication forks are susceptible to excessive nuclease activity at exposed nascent DNA ends by MRE11 leading replication fork collapse and cell death. PARP1 and BRCA2 regulate MRE11 activity at stalled replication forks [153]. In BRCA1/2-deficient cells, loss of PTIP (Pax-interacting protein 1), KMT2B/C (Lysine methyltransferase B and C, or MLL3/4) complex protein, or CHD4 (Chromodomain Helicase DNA Binding Protein 4) function can also restore the stability of replication forks in *BRCA1/2*-deficient cells through reduced recruitment of MRE11 thereby protecting the replication fork [154]. This renders cells resistant to PARPis as well as cisplatin and topotecan (a topoisomerase I inhibitor). EZH2 activity can also influence stalled replication forks generated by PARP inhibition. It encodes the enzymatic subunit of polycomb repressive complex 2 (PRC2) where it catalyzes histone 3 (H3) lysine 27 mono-, di-, or trimethylation. In BRCA2-deficient tumors, EZH2 localizes at stalled replication forks, methylates Lys27of H3 (H3K27me3) and recruits MUS81 nuclease which, like MRE11, degrades the replication

fork leading to PARPi sensitivity [155]. On the other hand, low expression of EZH2 results in low methylation of H3 and prevents recruitment of MUS81 leading to fork stabilization and PARPi resistance. RADX antagonizes RAD51 activity at replication forks. Deletion of RADX restores stability of replication fork and results in resistance to PARPi and other chemotherapeutic agents [156]. This is attributed to enhanced association of RAD51 with stalled forks. RAD51 is important for protection and repair of damaged replication forks [157]. Inactivation of SMARCAL1 also induces resistance to olaparib and cisplatin by preventing replication fork reversal and subsequent MRE11-mediated degradation [158].

Mutations in the DNA-binding zinc-finger domains of *PARP1* can result in PARPi resistance by reducing PARP trapping [159]. Loss of PARG leads to increased PARylation and sustained PARP1 signalling that can lead to PARPi resistance [160]. Increased expression of P-glycoprotein efflux pump encoded by *ABCB1* is also known to reduce the efficacy of PARP inhibition [64].

1.7 Cancer cell lines as models for drug development and understanding mechanisms of drug response

Human cancer cell lines are the oldest and most popular biological models for investigating cancer biology and potential efficacy of anticancer drugs. Indeed, breast cancer cell lines were used in a key, highly-cited, study in the preclinical development of PARP inhibitors [63]. Bryant *et al*., (2005) [63] depleted *BRCA2* expression, using

siRNAs, in MCF7 and MDA-MB-231 breast cancer cells and showed poor survival of these cells following PARP inhibition.

Several publicly available databases have catalogued the genomic alterations of cancer cell lines and their *in vitro* response to hundreds of drugs and compounds including PARPis. The first database based on the NCI-60 panel was generated by measuring pharmacologic profiles of 60 human-derived cancer cell lines from nine tissues including ovary and breast [161]. It was subsequently updated with genomic features such as mRNA gene expression, sequence variants from whole exome sequencing, and copy number variants from SNP arrays in the CellMiner database [162]. Some of the drug developments enabled by the genomic, molecular, and pharmacologic characterization of the NCI-60 panel cell lines are oxaliplatin (a cisplatin analogue) for colon cancer [163], eribulin (non-taxane microtubule inhibitor) for metastatic breast cancer [164], and bortezomib (proteasome inhibitor) for treatment of multiple myeloma [165]. Later databases such as Genomics of Drug Sensitivity in Cancer (GDSC) [166], Cancer Cell Line Encyclopedia (CCLE) [167] are larger with over 1,000 cell lines spanning about 30 cancer types but substantially overlap the NCI-60 panel cell lines. These resources have enhanced the utility of cancer cell lines, facilitating the selection of cell lines with specific genomic features for more targeted experiments to investigate the mechanism of action of anti-cancer agents and supported the development of precision treatments in cancer.

Cell lines have also become important for the discovery and evaluation of potential biomarkers of PARP inhibitor response and resistance. The combination of genomic characterization and *in vitro* drug response in cell lines in multiple cancer types has increased the potential to identify and study pharmacogenomic associations. For example, Murai et al., (2016) [168] discovered that *SLFN11* mRNA expression in the NCI-60 panel correlates with PARPi sensitivity, and experimentally validated this association using isogenic *SLFN11*-expressing and *SLFN11*-deficient cell lines. This study also reported that *SLFN11* was downregulated in about 45% of cancer cell lines, as shown in the CCLE database which contains over 1,000 cell lines. Recently, downregulation of *SLFN11* was reported in 7% of HGSOC patients with disease progression after treatment with PARPi [169]. Demonstrating that publicly available cell line databases can yield clinically relevant biomarkers.

Despite the utility of cell lines for drug development and biomarker discovery there are some limitations to these models. These include acquisition of additional genomic abnormalities *in vitro* that lead to poor recapitulation of patients' genomic and molecular microenvironment, and contamination by other cell lines. To address cross-contamination, quality control measures such as fingerprinting using single nucleotide polymorphisms (SNPs) and short tandem repeats (STR) profiles have been used to help uniquely identify cell lines. The availability of large genomic datasets characterizing patient tumors across diverse cancer types, such as The Cancer Genome Atlas (TCGA) [170], facilitates the evaluation of genomic similarities and differences between cancer cell lines and patient tumors. This provides a way to address the limitation of genomic

and molecular differences between patients' tumors and cell lines whereby only genomic variations in cell lines that have been reported in clinical samples are prioritized over those that have not been reported before or rarely found in clinical samples.

Other preclinical models more accurately represent genomic and molecular features of clinical tumor samples. These include patient-derived organoids (three-dimensional cell cultures generated from a patient's tumor), patient-derived xenografts developed from implants of patients' tumor cells in immunodeficient mice, and genetically engineered mouse models. Cell lines are typically the first models evaluated for anticancer drug activity, before other preclinical models are evaluated, and subsequently clinical trials are conducted after successful preclinical evaluations. This is reflected in the development of olaparib, which began with evaluations in cell lines [62,63] followed by mouse models [64,65], and clinical trials [67,68,70].

This thesis is based on genomic analyses of olaparib-screened pan-cancer cell lines from the GDSC database [166] and HGSOC cell lines from Fleury *et al*., (2017) [133]. The HGSOC cell lines are derived from tumor tissue or ascites cells of patients who were either treated with platinum-based chemotherapy or chemotherapy-naïve at sample collection. The cell lines were established after long-term passages and were considered spontaneously immortalized after over 50 passages [171–173]. The GDSC [166] human cancer cell lines comprise adult and childhood cancers of epithelial, mesenchymal and haematopoietic origin sourced from academic laboratories and commercial vendors. These cell lines have been categorized according to tissue of origin and TCGA tumor type descriptions.

1.8 Rationale, Hypotheses & Objectives

PARP inhibitors were the first approved class of drugs to target a vulnerability of *BRCA1/2*-mutated breast, ovarian, and pancreatic cancers. Olaparib is the leading PARP inhibitor, with the most indications for clinical use. However, not all *BRCA1/2*-mutated cases respond to olaparib treatment, while some responders do not harbor *BRCA1/2* mutations or other known markers of PARPi response. The efficacy of a targeted treatment may depend on several factors in addition to the alteration targeted by the treatment. These mediators can promote sensitivity or resistance to the targeted treatment. Given that PARP inhibitors induce DNA damage (such as single strand breaks and double strand breaks) and replication stress, most genes known to mediate olaparib sensitivity and resistance are involved in DNA repair and cell cycle regulation pathways. Additional genes in these pathways may also contribute to olaparib response. While genes in other pathways could also contribute to olaparib response via novel mechanisms that are yet to be characterized. I hypothesize that genomic and molecular characterization of a collection of HGSOC cell lines with known *in vitro* olaparib response can reveal novel candidate genomic markers. Interrogation of existing publicly available genomic data in pan-cancer cell lines with known *in vitro* olaparib response from large pharmacogenomic databases can further increase the potential to discover novel candidates.

The aim of my thesis is to identify new candidate genomic markers of olaparib sensitivity and resistance through pharmacogenomic data analysis of two independent groups of human-derived cancer cell lines. The first group comprises 18 HGSOC cell

lines classified as sensitive, intermediate or resistant based on *in vitro* olaparib response by Fleury et al., (2017) [133]. The second group consists of 896 cell lines from 30 cancer types with mRNA gene expression and *in vitro* olaparib response data from the GDSC database [166]. My objectives are to:

1. Characterize exome sequencing variation (in terms of SNVs, indels, CNVs, and mutational signatures), find differentially expressed genes based on mRNA levels, and identify variations unique to olaparib-sensitive and -resistant cell lines focusing on DNA repair and cell cycle genes in the HGSOC cell lines;
2. Identify all genes whose expression based on mRNA is statistically associated with *in vitro* olaparib sensitivity or resistance in the GDSC pan-cancer cell lines; and
3. Integrate candidate markers from HGSOC and GDSC analyses to prioritize and validate novel candidate markers of olaparib response.

The results of this study comprise known and novel associations between specific genomic or gene alterations and olaparib sensitivity or resistance from human cancer cell lines. These associations can be experimentally validated and then potentially included, with other known markers, into assays to be evaluated as predictive biomarkers in clinical trials. Ultimately, these findings can improve our understanding of PARP inhibitor sensitivity and resistance and contribute to enhanced selection of patients most likely to respond from PARPi treatment or inform alternative strategies for treating patients with more resistant genomic features.

Chapter 2: Materials and Methods

2.1 Exome characterization and differential gene expression analysis of 18 HGSOC cell lines previously screened for *in vitro* olaparib response

HGSOC cell lines were derived from tumor or ascites (Table 2.1.1). For cell lines derived from solid tumor, tumor tissue was scraped into a 100 mm plate with complete ovarian surface epithelial (OSE) medium and maintained for 40 days with weekly replacements of the culture medium [173,174]. Cell lines derived from ascites were established from cells collected after centrifugation and maintained in the same conditions as tumor-derived cells. Cells were considered spontaneously immortalized after more than 50 passages. *In vitro* olaparib response of these HGSOC cell lines was determined by clonogenic survival assay and expressed as half-maximal inhibitory concentration (IC_{50}) [133].

Table 2.1.1 Features of 18 HGSOC cell lines. The cell lines were derived from tissue samples from 12 HGSOC patients – 14 from primary cancer cases and four derived from cases with recurrent disease. All cases had advanced stage (III-IV) disease at the time of tissue procurement. Cell lines follow the naming convention TOV- or OV- for tumor-derived and ascites-derived cells respectively, followed by a unique case (patient) number, and may followed by G (Gauche; meaning left ovary) or D (Droite; right ovary), or R (recurrence). OV866(2) was derived from ascites cells from HGSOC in patient 866 at second recurrence of disease.

	Chemo-status at sample collection	
	Pre-chemo (10)	**Post-chemo (8)**
Tumor (9)	TOV2978G TOV3291G TOV1946 TOV2223G TOV3133G TOV1369	TOV3041G TOV2295(R) TOV3133D
Ascites (9)	OV90 OV4453 OV1946 OV2295	OV866(2) OV4485 OV3133(R) OV2295(R2) OV1369(R2)

IC_{50} values were determined for each cell line and used to classify cell lines into sensitive, intermediate, and resistant response groups (Figure 2.1.1).

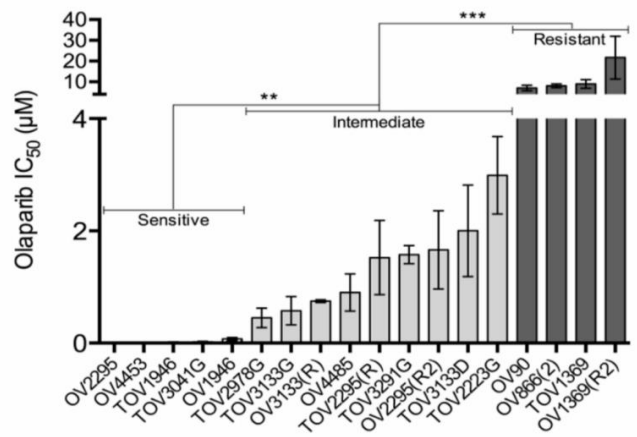

Figure 2.1.1. *In vitro o*laparib response of 18 HGSOC cell lines. Bars represent mean±SEM (Standard Error of Mean) of IC_{50} (μM) values generated from clonogenic assays performed in triplicate and repeated three times. Student's t-test analysis of IC_{50} values comparing a cell line with each of the other cell lines was performed, and the shifts of significant (p-value < 0.05) to not significant (p-value > 0.05) difference between individual cell lines was used to define three groups of olaparib response. Sensitive cell lines had mean IC_{50} of $4x10^{-4}$ μM or less, intermediate cell lines had mean IC_{50} between 0.45 μM and 1.20 μM, and resistant cell lines had mean IC_{50} greater or equal to 7.04 μM. This figure is derived from Figure 1C of Fleury *et al*., 2017 [133] published in the journal Oncotarget (https://www.oncotarget.com/article/10308/text/) and licensed under a Creative Commons Attribution 3.0 License (http://creativecommons.org/licenses/by/3.0/). The figure is used in this thesis in accordance with this license and has not been modified.

These cell lines have been previously characterized at genetic and molecular levels [173–176]. All but one (TOV3041G) of the 18 cell lines harbor somatic mutations in *TP53*, which is the most common somatically mutated gene in HGSOC cases. However, TOV3041G does not express TP53 at protein level. Two cell lines were

derived from patients that carry germline pathogenic variants in *BRCA1* (OV4485) or *BRCA2* (OV4453) [173]. In this thesis, the 18 HGSOC cell lines were characterized in terms of sequence and copy number variations using whole exome sequencing data and analysed for differentially expressed genes between sensitive and resistant cell lines using microarray mRNA gene expression data (Figure 2.1.2).

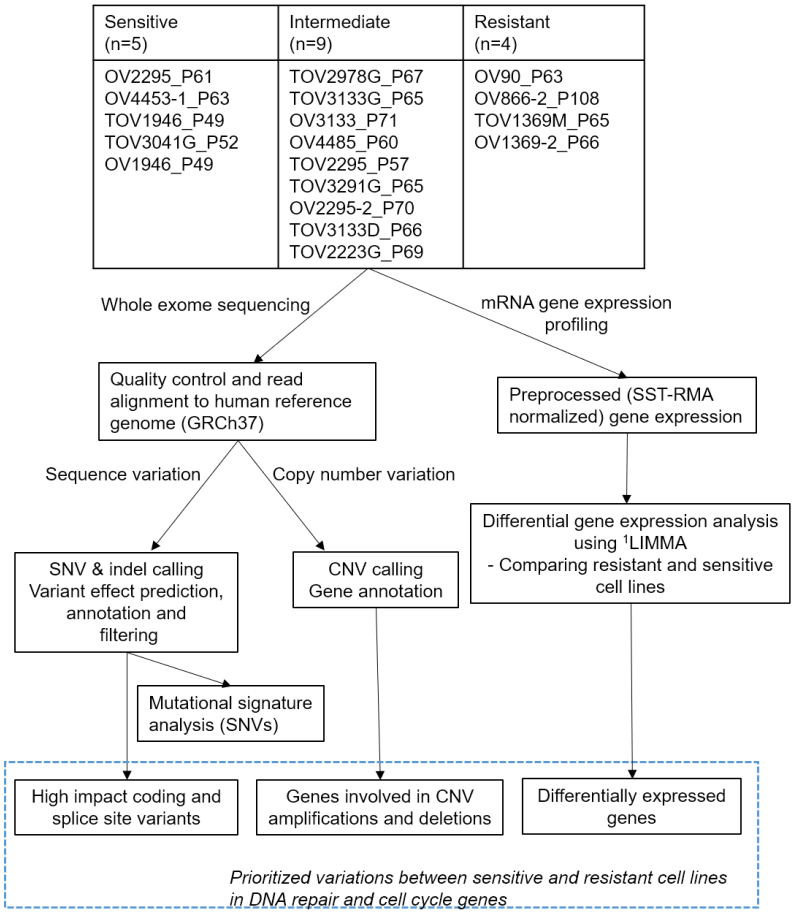

Figure 2.1.2. Overview of analyses of HGSOC cell lines. Cell lines were screened for *in vitro* olaparib response as reported by Fleury *et al*., (2017) [133]. Cell line names used here also indicate the passage (P) number for individual cell lines, and correspond to the abbreviated versions reported by Fleury *et al*., (2017) [133]. The first part of the full names, before the underscore, matches the short names used in the Fleury *et al*., (2017) study. [1]Linear models for microarray data.

2.1.1 Exome sequencing, read mapping and variant calling

A workflow highlighting the analysis steps used to process SNVs and small (50 bp or less) insertions and deletions (indels) is shown below (Figure 2.1.1.1).

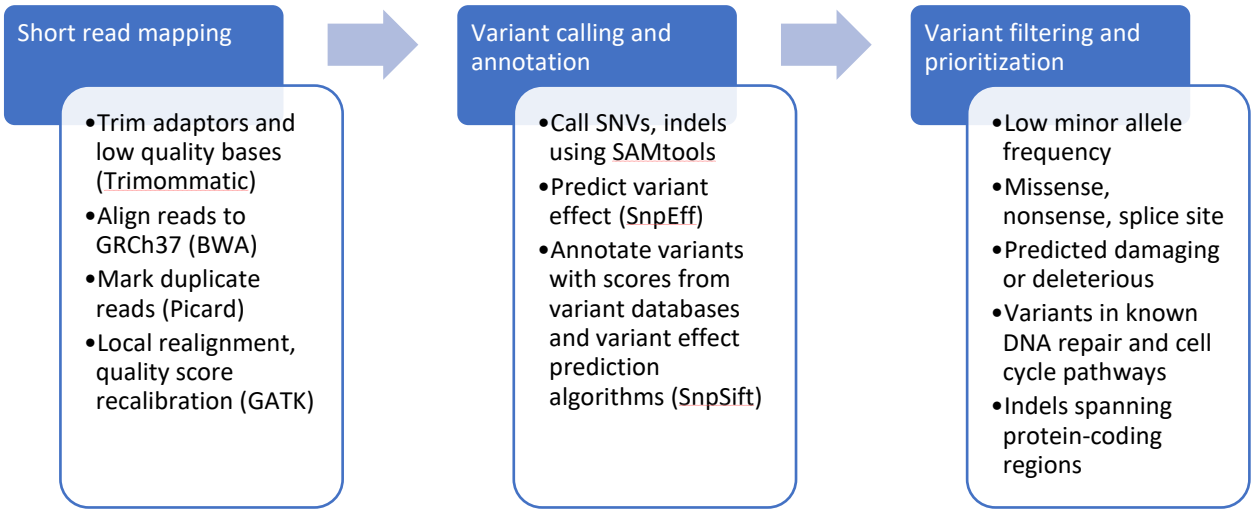

Figure 2.1.1.1 Workflow for SNV and indel identification and analysis from whole exome sequencing data of 18 HGSOC cell lines.

Exome sequencing of the cell lines was done using the Illumina HiSeq 2000 platform, following target enrichment with the Roche Nimblegen SeqCap EZ exome v3 kit, at the McGill University and Genome Quebec Innovation Centre (now called McGill Genome Centre). Sequencing was paired-end with average read length of 100 bases. Sequencing adapters were trimmed and trailing low quality (Phred33 score >= Q30) bases were removed using Trimmomatic [177] (version 0.36). Reads were then aligned to human reference genome build GRCh37 using BWA (Burrows Wheeler Aligner) [178]. Picard [179] (version 2.9.0) was used to mark duplicate reads. Local realignment around indels, and base quality score recalibration was done using GATK (Genome Analysis Toolkit) [180] (version 3.5). SAMtools/BCFtools [181] (version 1.3.1) was used

for variant calling. Variant effects were then predicted with SnpEff [182], and annotated with dbSNP [183] and COSMIC [184] identifiers using SnpSift [185]. Variant scores and predictions from variant effect prediction algorithms were obtained from the dbNSFP (database of non-synonymous functional predictions) [186] and dbscSNV (database of splice-altering SNVs) [187] databases. These scores and predictions were also annotated using SnpSift. Annotated variants were then exported into R [188] for further filtering and prioritization.

2.1.2 Filtering and prioritization of SNVs and indels

Read depth of 10 or greater and variant allele frequency of at least 30% were used as confidence filtering criteria for variants. Since PARP inhibition causes impaired DNA repair and replication stress leading to cell death, mutations in DNA repair and cell cycle genes were first investigated for potential markers. In total, 533 DNA repair and cell cycle genes were queried for mutations. This gene list is provided in Appendix C. Genes were derived from a curated list of genes for a pan-cancer survey of DNA damage repair deficiency in TCGA (The Cancer Genome Atlas) [78], and a merged list of cell cycle genes from KEGG (Kyoto Encyclopedia of Genes and Genomes) [189] and Qiagen's cell cycle gene expression array [190]. Additional genes previously associated with resistance mechanisms to PARP inhibitors, such as *SLFN11* [168] and *ABCB1* [64] are were also investigated for mutations. High impact variants in all genes, across the entire exome, were then investigated. Nonsynonymous SNVs were considered damaging or deleterious based on the consensus prediction of at least four (out of seven) variant effect prediction algorithms; SIFT (Sorting Intolerant From Tolerant) [191], PolyPhen2 (Polymorphism Phenotyping v2) [192], FATHMM-MKL [193],

Mutation Assessor [194], Mutation Taster [195], REVEL [196], and MetaSVM [197]. Since damaging variants are rare in the general population an additional criterion for selecting potentially damaging SNVs is that they must be present at 0.1% minor allele frequency (MAF) or lower in the Genome Aggregation Database (gnomAD) [198] database version 2.1, or not reported in this database. The gnomAD database contains short variant data (SNVs and indels) from 141,456 unrelated individuals (125,748 exomes and 15,708 genomes) in non-disease groups sequenced as part of various disease-specific and population genetic studies. Potential splice altering variants were selected based on consensus scores (0.6 or greater) of ADA (adaptive boost) and RF (random forest) in the database of single nucleotide variants within splicing consensus regions (dbscSNV) [187]. Since calling indels from repetitive regions using short read sequencing data are error-prone, indels called by SAMtools that overlap repeats were filtered out using repeatmasker [199] in rtracklayer [200] package in R. Sequence variants that met filtering and prioritization criteria were manually verified using Integrative Genomics Viewer (IGV) [201].

2.1.3 Mutational signature analysis

Somatic single nucleotide variants (SNVs) were selected for mutational signature analysis. SNVs that pass confidence filtering and are present at MAF of 0.1% or less in gnomAD database, or confirmed somatic in COSMIC (Catalogue of Somatic Mutations in Cancer) were considered somatic variants. Since whole exome sequencing data from blood or normal tissue was not available for the cell lines this strategy was used to select likely somatic variants. Mutational signatures [202] were derived from the frequencies of all six types of single-base somatic substitutions of pyrimindine bases

within a trinucleotide context (including the bases 5' and 3' of the mutated base). Mutational signatures of DNA repair deficiencies are of particular interest – these include signatures 6, 15, 20, and 26 which have been associated with defective MMR, and signature 3 which is indicative of HR repair deficiencies [134]. The R package deconstructSigs [203] was used to determine the contributions of known mutational signatures within individual cell lines using COSMIC single base substitution (SBS) mutational signatures version 2 as reference.

2.1.4 Copy number variation analysis

CNVkit [204] version 0.9 was used to call CNVs using GRCh37-aligned sequence reads in BAM (Binary Alignment Map) format, genomic coordinates of exome capture target regions in a BED (Browser Extensible Data) file, and GRCh37 reference sequence in FASTA format as inputs. Regions of poor mapping based on GRCh37, containing centromeres, telomeres, and highly repetitive sequences were excluded from the analysis using precomputed BED file included in the software package (https://github.com/etal/cnvkit/blob/master/data/access-5k-mappable.grch37.bed). Target regions were grouped into bins of 267 bp size, on average, according to default settings and read depth for these bins were computed. CNVkit uses targeted reads and off-target reads to infer copy number. Therefore, off-target coverage (number of reads mapping to regions outside the exome capture targets) was also determined for each cell line. Read depth for each sample is median-centered, across bins, and corrected for GC content and repetitive sequence biases. Corrected bin-level coverage was compared to a neutral (or flat) reference which assumes all target and off-target regions are equally covered and diploid. Bin-level copy number ratios were aggregated

into segments using the default circular binary segmentation algorithm with low-coverage and outlier bins filtered out. Genes involved in CNV segments were selected using the *genemetrics* command with minimum absolute log2 copy ratio threshold (-t) of 0.4 (gain >= 0.4, loss <= -0.4) and minimum number of bins (-m) per gene of 5. Amplifications and deletions were defined by log2 copy ratio thresholds of 1 and -1 respectively.

2.1.5 Differential Gene expression analysis

Normalized mRNA gene expression data were provided by Dr. Anne-Marie Mes-Masson's group at Université de Montréal. Gene expression profiling was done for all 18 cell lines using the Clariom™ S human array. Normalization was done using Signal Space Transformation-Robust Multi array Average (SST-RMA). Normalized expression values per gene were converted to z-scores (mean-centred expression divided by standard deviation). Differential gene expression analysis was done using the linear models for microarray data (LIMMA [205]) package in R. In total, 17,403 protein coding genes were analysed. For each gene, mean expression level in the sensitive cell lines (n=5) was compared to the mean expression level in resistant cell lines (n=4). The lmFit function was used to fit robust linear models to the data and calculate mean expression. A moderated t-test was used to compare the expression between resistant and sensitive groups using the eBayes function. Resulting p-values were adjusted for multiple testing using false discovery rate (FDR). Significant differentially expressed genes are defined by FDR-adjusted p-value <=0.05, and absolute log2 fold change>=1.5.

2.2 Olaparib response and mRNA gene expression association analyses

Statistical methods were used to identify significant gene predictors of olaparib response based on mRNA expression (Figure 2.2.1).

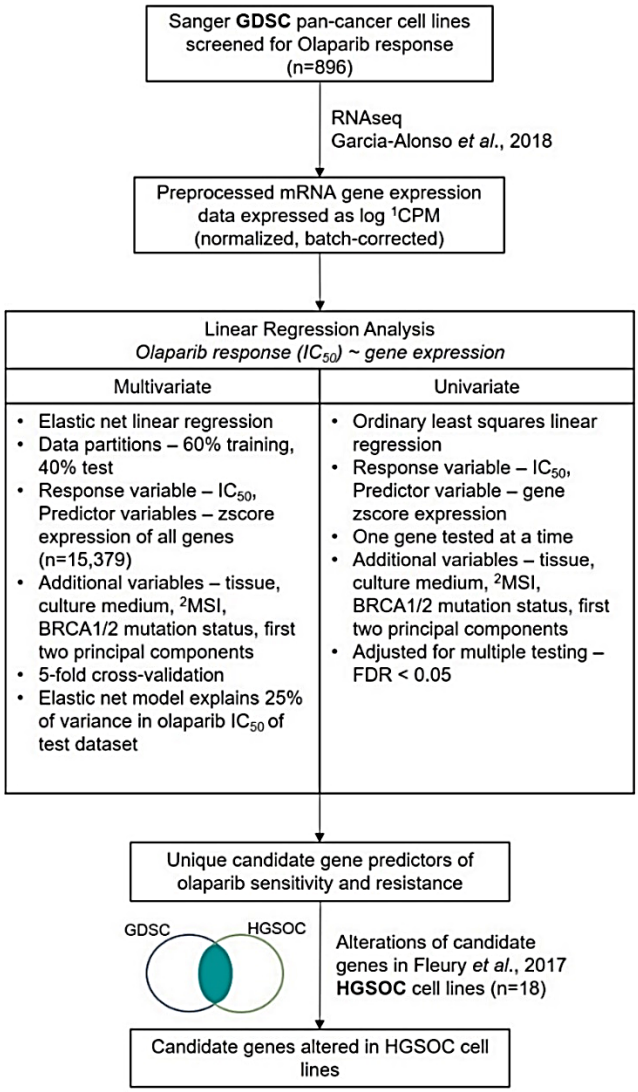

Figure 2.2.1. Overview of analyses of GDSC pan-cancer cell lines. Candidate gene predictors of olaparib sensitivity and resistance derived from multivariate and univariate linear regression methods are validated in HGSOC cell lines.

2.2.1 Data description and linear regression analyses

GDSC is a pharmacogenomic database providing genomic data (exome sequencing, gene expression, methylation, CNVs) for over 1,000 cell lines derived from human

cancers, and drug response (IC_{50}) data for over 300 drugs and compounds [166]. Drug response data were from GDSC1 release 7.0 (March 2018). This includes pharmacogenomic data from ovarian and breast cancers (Table 2.2.1.1).

Gene expression data were merged RNAseq data derived from GDSC, CCLE [206], and Genentech [207] which were used to investigate transcription factor-drug interactions and reported by Garcia-Alonso *et al*., 2018 [208]. Data were preprocessed, normalized, batch-corrected, and filtered to remove low expressed genes and samples. These data are available at the following link: https://www.synapse.org/#!Synapse:syn10463688/wiki/463140. In total, 896 Olaparib-screened cell lines with mRNA expression data for 15,379 genes were available for analysis (Figure 2.2.1.1). This formed the working dataset. This dataset was analysed using multivariate and univariate linear regression approaches.

Table 2.2.1.1. Frequency and types of GDSC cancer cell lines with mRNA gene expression data analysed in this thesis project.

Cancer type (TCGA classification)	**Abbreviation**	**Number of cell lines**
Adrenocortical carcinoma	ACC	1
Acute lymphoblastic leukemia	ALL	22
Bladder Urothelial Carcinoma	BLCA	17
Breast invasive carcinoma	BRCA	45
Cervical squamous cell carcinoma and endocervical adenocarcinoma	CESC	13
Chronic Lymphocytic Leukemia	CLL	3
Colon adenocarcinoma and Rectum adenocarcinoma	COAD/READ	46
Lymphoid Neoplasm Diffuse Large B-cell Lymphoma	DLBC	30
Esophageal carcinoma	ESCA	32
Glioblastoma multiforme	GBM	34
Head and Neck squamous cell carcinoma	HNSC	39
Kidney renal clear cell carcinoma	KIRC	30
Acute Myeloid Leukemia	LAML	25
Chronic Myelogenous Leukemia	LCML	10
Brain Lower Grade Glioma	LGG	17
Liver hepatocellular carcinoma	LIHC	16
Lung adenocarcinoma	LUAD	57
Lung squamous cell carcinoma	LUSC	15
Medulloblastoma	MB	3
Mesothelioma	MESO	19
Multiple Myeloma	MM	16
Neuroblastoma	NB	25
Ovarian serous cystadenocarcinoma	OV	32
Pancreatic adenocarcinoma	PAAD	25
Prostate adenocarcinoma	PRAD	6
Small Cell Lung Cancer	SCLC	51
Skin Cutaneous Melanoma	SKCM	50
Stomach adenocarcinoma	STAD	20
Thyroid carcinoma	THCA	16
Uterine Corpus Endometrial Carcinoma	UCEC	9
Unknown	-	172

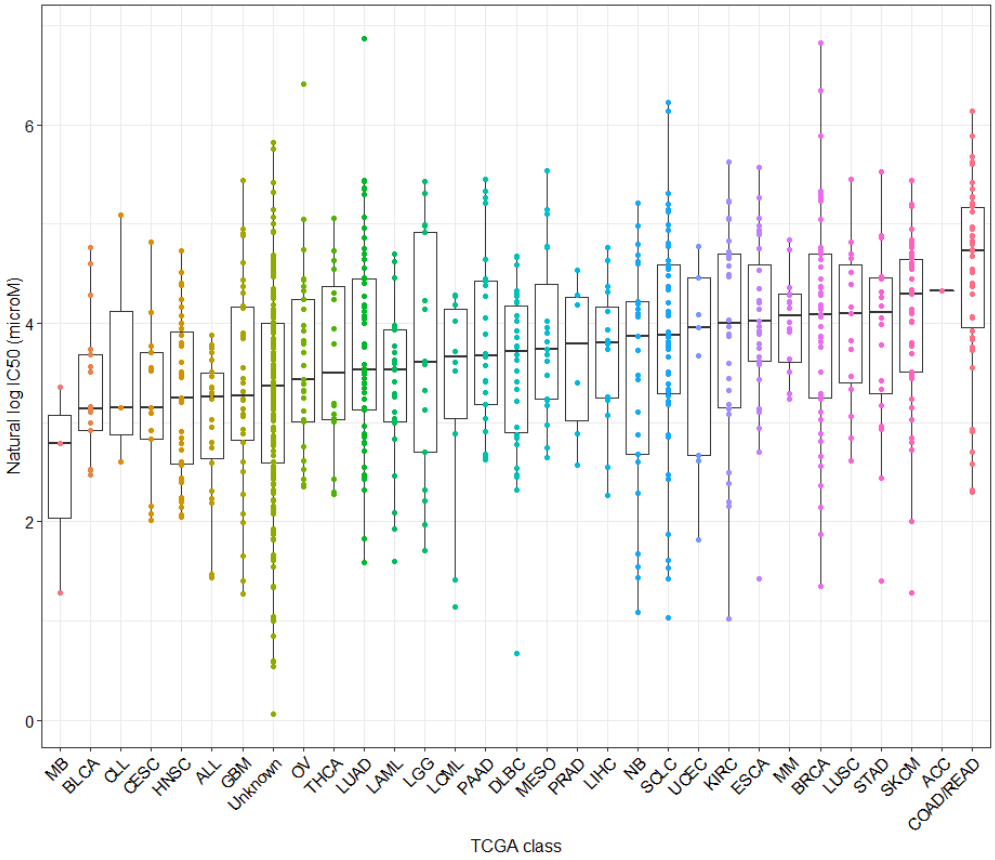

Figure 2.2.1.1. Distribution of Olaparib response (IC_{50}) across cell lines of multiple cancer types using TCGA classifications. Dots represent individual cell lines. Boxplots represent cell lines in TCGA classes. Boxplots are ordered according to median IC_{50}. Full meaning of TCGA class abbreviations are provided in the List of Abbreviations section.

Data was randomly partitioned into training (60%) and test (40%) sets, ensuring that these partitions were balanced to have similar proportions of cell lines from each tissue type. A linear regression model with elastic net regularization was fit using log-transformed IC_{50} as response and z-score expression for all genes as predictors with tissue of origin, microsatellite instability (MSI) status (MSI-high: MSI-H, microsatellite

stable: MSS), *BRCA1/2* mutation status (encoded as 1 for mutation in either *BRCA1* or *BRCA2,* and 0 for cell line without mutation in either *BRCA1* or *BRCA2*), first two principal components of gene expression principal component analysis, culture medium as covariates. Five-fold cross-validation was performed on the training set over a range of tuning parameters (alpha ranges from 0, 0.5 or 1 and lambda ranges from 0 to 1 with 0.01 increment). The optimum model (alpha=0.5, lambda=0.14) was selected based on lowest root mean-squared error (RMSE).

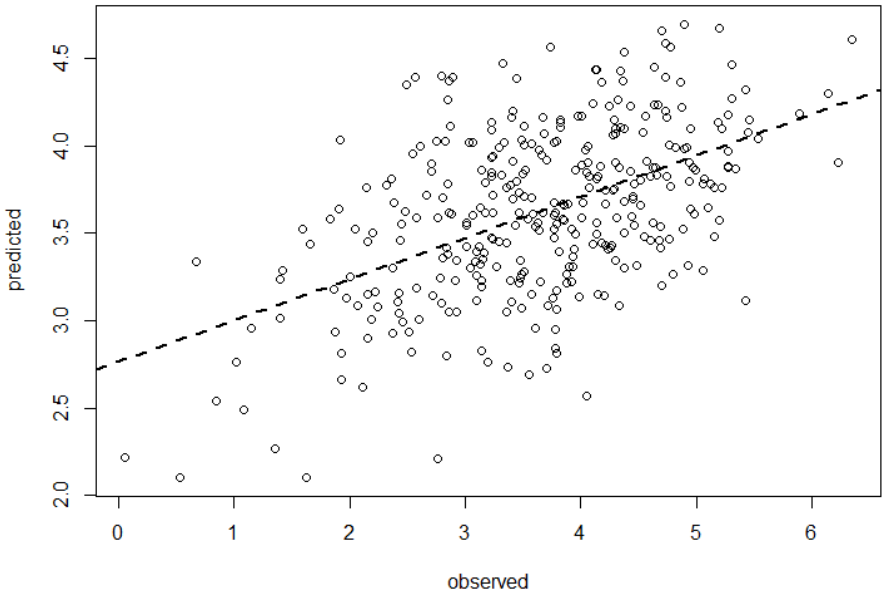

Figure 2.2.1.2. Performance of elastic net multivariate linear regression model on prediction of IC_{50} in test data. Observed or actual IC_{50} values (horizontal axis) in test dataset plotted against predicted IC_{50} values (vertical axis) using elastic net model developed from training dataset. Points along the dashed line show agreement between observed and predicted values.

The performance of the elastic net multivariate model was evaluated on the test data partition. This model explained 25.2% (R^2) of the variation in log-transformed IC50 with RMSE=0.898 and mean absolute error (MAE)=0.734. Genes with coefficients greater or equal to zero were considered significant gene predictors. Data partitioning, model fitting and evaluation, and visualization were done in R using *caret* [209], *glmnet*, and *ggplot2* packages.

Multiple ordinary least squares (OLS) linear regression models, for one gene at a time, were also done with IC_{50} as response and gene expression as a predictor, keeping the same covariates as the multivariate approach. Correction for multiple testing was done using False Discovery Rate (FDR), genes with FDR-adjusted p-values less than 0.05 were considered significant gene predictors. This was done in R using functions *lm* and *p.adjust* from *stats* package.

2.3 Summary

The methods described above represent the systematic application of diverse software tools and databases to gain insights into genomic alterations and their functional molecular consequences in cancer models that may explain or provide clues for understanding drug response, and assess the frequency of these alterations in clinical tumor cases. This thesis used genomic, transcriptomic and molecular data shared by our collaborator Dr. Anne-Marie Mes-Masson's laboratory at Université de Montréal, and additional genomic and molecular data shared by the Genomics of Drug Sensitivity in Cancer project, an international collaboration between the Cancer Genome Project at the Wellcome Sanger Institute (UK) and the Center for Molecular Therapeutics of Massachusetts General Hospital Cancer Center (USA). TCGA data accessed through the cBioPortal for Cancer Genomics was also used in this thesis. The results generated from analyzing these data highlight some of the benefits of data sharing with documentation in promoting the discovery of candidate genomic markers for cancer therapeutics. Free and open source software tools were used to analyze data in this thesis, illustrating how unrestricted access by the research community at-large to such resources can more readily advance genomics studies.

Chapter 3: Results

3.1 Exome characterization of 18 HGSOC cell lines with varying response to olaparib yields potential genomic markers of olaparib response

Eighteen HGSOC cell lines were sequenced to average read depth per target ranging from 82x – 152x (Table 3.1.1).

Table 3.1.1. Summary of exome sequencing statistics for 18 HGSOC cell lines

Cell line	Total number of reads	Percentage mapped reads	Average read depth
OV1369-2_P66	97,402,090	99.95%	97.63
OV1946_P49	114,685,864	100.00%	124.51
OV2295-2_P70	98,339,734	99.93%	93.72
OV2295_P61	85,975,628	99.93%	83.97
OV3133_P71	99,610,462	99.94%	94.58
OV4453-1_P63	134,127,961	100.00%	147.10
OV4485_P60	140,329,278	100.00%	152.71
OV866-2_P108	75,971,021	100.00%	83.82
OV90_P63	118,620,667	99.69%	82.53
TOV1369M_P65	95,852,954	99.92%	96.61
TOV1946_P49	111,899,217	100.00%	122.00
TOV2223G_P69	112,178,967	100.00%	121.67
TOV2295_P57	93,053,413	99.91%	88.15
TOV2978G_P67	112,205,120	100.00%	123.22
TOV3041G_P52	86,702,356	100.00%	95.43
TOV3133D_P66	99,257,617	99.92%	95.38
TOV3133G_P65	92,355,924	99.93%	89.17
TOV3291G_P65	92,028,434	100.00%	101.63

More than 99% of reads per cell line mapped to reference genome. Across cell lines, at least 70% of target sequence is sequenced to 30x read depth or greater.

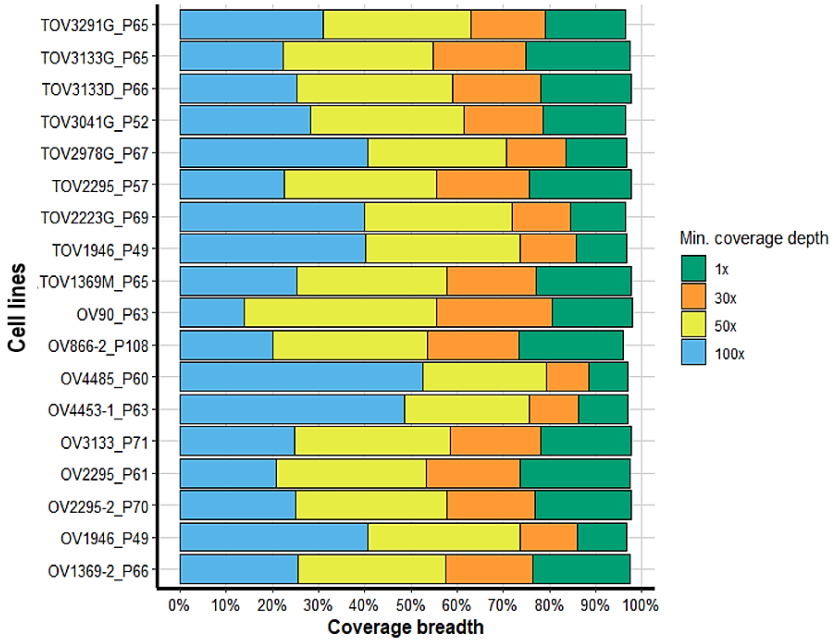

Figure 3.1.1. Mean percentage of target regions (coverage breadth) sequenced to 1x, 30x, 50x, and 100x read depth thresholds for each cell line.

Protein-coding and splice-site sequence variants were analysed for all cell lines. The frequencies of rare (less than 0.1% allele frequency in gnomAD or not reported in this database) variants predicted functionally damaging or deleterious variants per cell line are presented in Figure 3.1.2. No cell line is significantly enriched for a particular type of variant. On average, there are 498 functionally relevant variants per cell line ranging from 453 to 567.

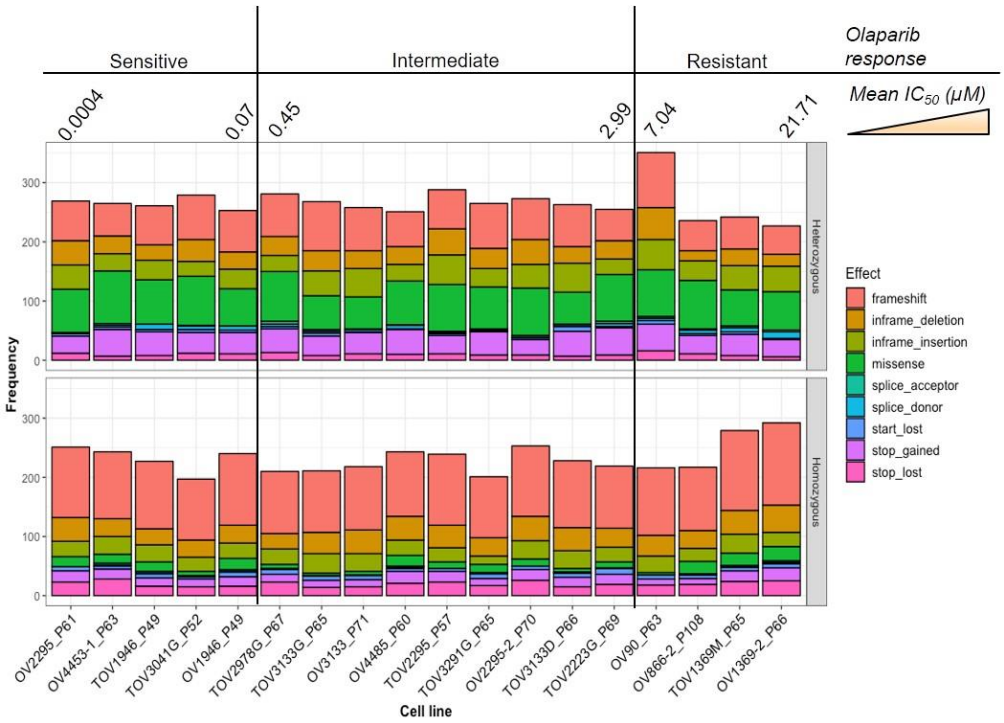

Figure 3.1.2. Frequency of rare protein-coding and splice-site DNA sequence variants predicted to be functionally damaging or deleterious. Predictions are based on the consensus of at least four out of seven functional prediction algorithms. Cell lines arranged, left to right, in order of increasing resistance. OV2295_P61 and OV1369-2_P66 are most sensitive and resistant cell lines respectively. Sensitive, Intermediate and Resistant are *in vitro* olaparib response groups previously defined by IC_{50} values as reported in Fleury et al., (2017) [133]. Mean IC_{50} track shows the minimum and maximum of mean IC_{50} of cell lines per olaparib response group.

3.1.1 COSMIC mutational signatures 1 and 3 are common in HGSOC cell lines

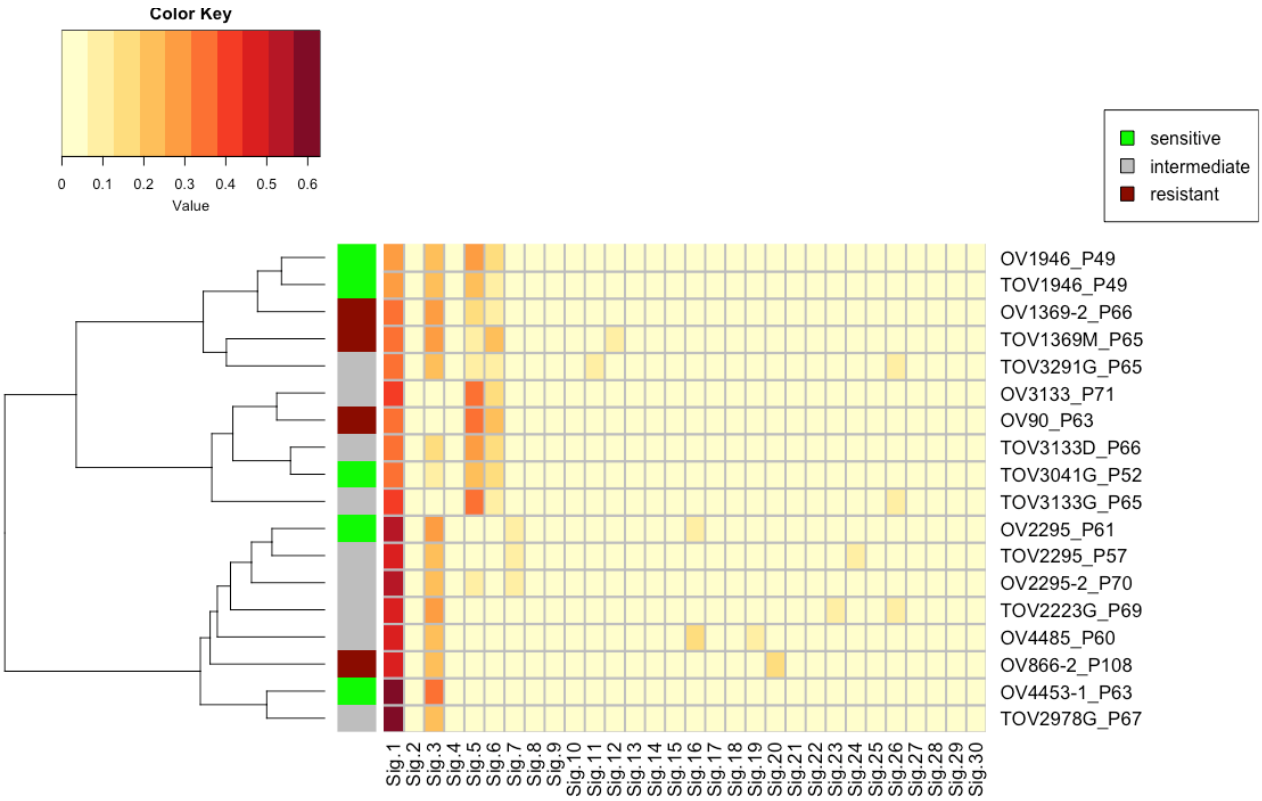

Figure 3.1.1.1. Hierarchical clustering of cell lines by COSMIC single base substitution mutational signatures based on Euclidean distance and complete linkage.

Analysis of single base substitution (SBS) mutational signatures in 18 HGSOC cell lines reveals that cell lines exhibit multiple mutational signatures. The dominant signatures are 1 and 3, which are associated with aging and HR repair deficiency, respectively (Figure 3.1.1.1). These are also the dominant signatures that have been reported in EOC cases [134] and show that cell lines are similar to patient tumors, based on mutational signatures. Signature 1 is observed in all 18 cell lines while signature 3 is seen in 15 cell lines including BRCA1/2-mutated OV4485_P60 and OV4453-1_P63. However, no mutational signature is unique to a specific olaparib response group.

Sensitive (n=5), intermediate (n=7), and resistant (n=3) cell lines have mutational signature 3 which is associated with HR defect. COSMIC signature 3 is attributed to defective DNA double-strand break-repair by homologous recombination and is strongly associated with germline and somatic *BRCA1* and *BRCA2* mutations in breast, pancreatic, and ovarian cancers. Signature 3 is also with *RAD51C* and *PALB2* in breast cancer [210]. Among the cell lines, only OV4485_P60 (intermediate) and OV4453 (sensitive) have *BRCA1* and *BRCA2* mutations respectively, both have mutational signature 3. OV4453 has a truncating *BRCA2* mutation (p.Glu1953*) and was found to have most similar mutation spectrum to COSMIC mutational signature 3 among the HGSOC cell lines (based on the signature 3 weight calculated using deconstructsigs) . OV4485_P60 (c.4548-1G>T) has a deleterious splice acceptor mutation but has a truncating mutation in *SMAD4* which may partly explain why it has intermediate response. This is described in section 3.1.3. For the remaining cell lines with signature 3, no potentially damaging mutations in *BRCA1/2* or HR repair were found. However, sensitive cell lines with signature 3 but no *BRCA1/2* mutations, such as TOV3041G_P52, were found to have other alterations (described in sections 3.1.2 and 3.1.3) that could explain their sensitive response.

3.1.2 Common *PARP1* variant linked to low PARylation is present in sensitive and intermediate cell lines without *BRCA1/2* mutations

The *PARP1* missense variant p.Val762Ala (rs1136410) occurs in sensitive cell line TOV3041G_P52 and intermediate cell line TOV2978G_P67. The variant occurs in homozygous state in TOV3041G and heterozygous state in TOV2978G. PARP1 p.Val762Ala occurs in the catalytic domain of PARP1 and is the most common missense variant in the catalytic domain of PARP1 (based on investigation of dbSNP version 150). The variant is present at overall frequency of 20.7% in the gnomAD database and is most common among East Asians with a frequency of 44.7%. This variant has been extensively investigated as a potential cancer predisposing variant and has been linked to increased risk of breast of cancer in a Saudi Arabian population [211], and increased risk of colorectal cancer in a Chinese population [212]. Interestingly, *PARP1* p.Val762Ala has been found to reduce PARP1 activity by about 40% with or without PARP inhibition leading to reduced PARylation [213]. The observation of sensitivity to olaparib in cell lines harboring this *PARP1* variant is consistent with this finding.

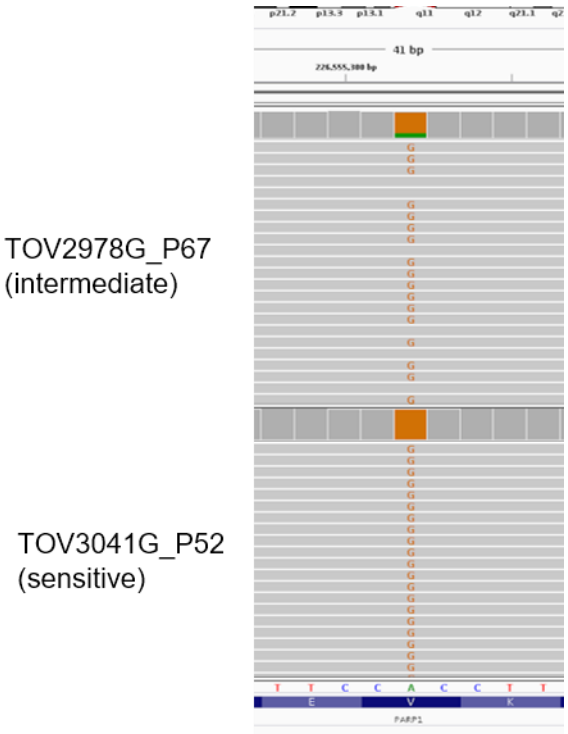

Figure 3.1.2.1. Integrative Genomics Viewer (IGV) screenshot showing read depth of *PARP1* p.Val762Ala variant in two HGSOC cell lines. The genomic base substitution (1:g.226555302A>G) associated with this variant is shown for sensitive cell line TOV3041G_P52 (bottom) and intermediate cell line TOV2978G_P67 (top). Read depth and variant allele frequency are 73 and 100% for TOV3041G_P52 and 64 and 80% for TOV2978G_P67 respectively.

3.1.3 Rare, potentially deleterious variants in DNA repair and cell cycle control genes

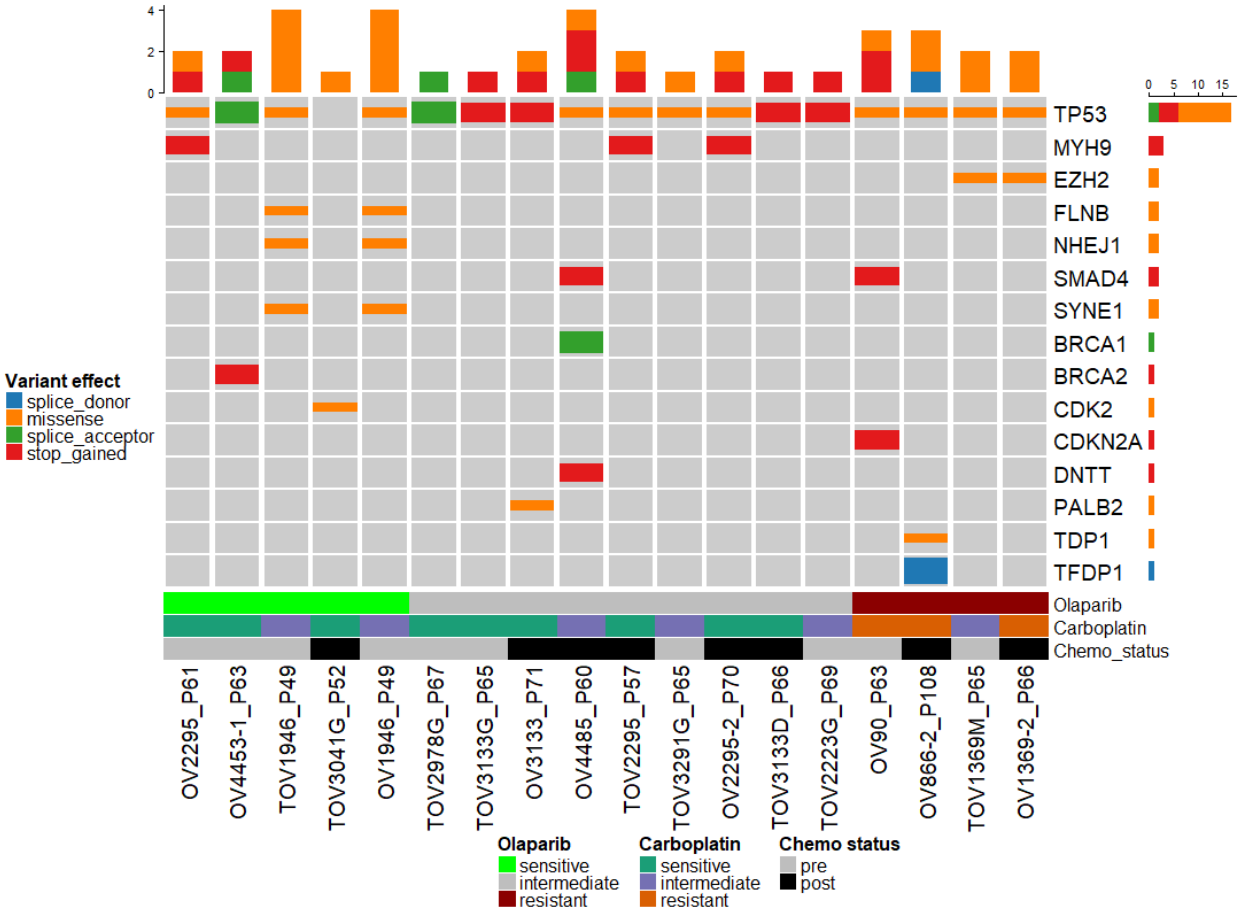

Figure 3.1.3.1. Rare, potentially deleterious, homozygous variants in DNA repair and cell cycle genes for 18 HGSOC cell lines. Cell lines arranged, left to right, in order of increasing resistance. OV2295_P61 and OV1369-2_P66 are most sensitive and resistant cell lines respectively.

Given that alterations in genes of DNA repair and cell cycle pathways have been shown to drive cell line response to olaparib [126,129,131,133,168,214], sequence variants (Figure 3.1.3.1) and copy number variation (Tables 3.1.3.1 and 3.1.3.2) in these genes were first analyzed for potential candidate markers. *TP53* is the most

common somatically mutated gene in HGSOC [14,16]. Consistent with previous reports [172–174,176], all but one (TOV3041G_P52) of the cell lines is mutated in *TP53*. All 17 *TP53* mutations (2 splice acceptor, 4 stop-gained, 11 missense) are classified as pathogenic in the ClinVar database [215]. While TOV3041G_P52 does not have a *TP53* mutation, it has been shown to not express p53 protein [173]. Majority (n=11) of *TP53* mutations were found with copy number loss but the splice acceptor mutation in OV4453-1_P63 occurs with amplification of *TP53* locus.

Table 3.1.3.1. *TP53* mutations and *TP53* CNVs in HGSOC cell lines

Cell line	**Olaparib response**	***TP53* Mutation**	**Effect**	***TP53* CNV**
OV2295_P61	sensitive	p.Ile195Thr	missense	loss
OV4453-1_P63	sensitive	c.376-1G>A	splice_acceptor	amplification
TOV1946_P49	sensitive	p.Arg273Cys	missense	diploid
OV1946_P49	sensitive	p.Arg273Cys	missense	loss
TOV3041G_P52	sensitive	None	-	loss
TOV2978G_P67	sensitive	c.920-2A>G	splice_acceptor	loss
TOV3133G_P65	intermediate	p.Gln192*	stop_gained	loss
OV3133_P71	intermediate	p.Gln192*	stop_gained	loss
OV4485_P60	intermediate	p.Arg273His	missense	loss
TOV2295_P57	intermediate	p.Ile195Thr	missense	loss
TOV3291G_P65	intermediate	p.Arg249Trp	missense	gain
OV2295-2_P70	intermediate	p.Ile195Thr	missense	loss
TOV3133D_P66	intermediate	p.Gln192*	stop_gained	loss
TOV2223G_P69	intermediate	p.Trp53*	stop_gained	gain
OV90_P63	resistant	p.Ser215Arg	missense	diploid
OV866-2_P108	resistant	p.Arg249Trp	missense	diploid
TOV1369M_P65	resistant	p.Gly244Cys	missense	loss
OV1369-2_P66	resistant	p.Gly244Cys	missense	loss

Pathogenic variants in *BRCA1* (c.4548-1G>T, splice acceptor) and *BRCA2* (p.Glu1953*, stop-gained) were rediscovered in OV4485_P60 and OV4453-1_P63, respectively, and in this study found to be associated with copy number loss.

OV4485_P60 and OV4453-1_P63 are the only cell lines that were derived from HGSOC patients with germline mutations in *BRCA1* or *BRCA2* [173].

Table 3.1.3.2. CNVs of DNA repair and cell cycle genes (apart from *TP53)* with rare, deleterious, homozygous variants in HGSOC cell lines. [1]Alternate reading frame.

Cell line	Olaparib Response	Variant	Gene	Effect	CNV
OV1369-2_P66	resistant	p.Ile55Met	*EZH2*	Missense	gain
OV1946_P49	sensitive	p.Glu5Gly	*FLNB*	Missense	loss
OV1946_P49	sensitive	p.Ala172Pro	*NHEJ1*	Missense	loss
OV1946_P49	sensitive	p.Leu4502Phe	*SYNE1*	Missense	loss
OV2295_P61	sensitive	p.Tyr124*	*MYH9*	Stop-gained	loss
OV2295-2_P70	intermediate	p.Tyr124*	*MYH9*	Stop-gained	gain
OV3133_P71	intermediate	p.Leu939Trp	*PALB2*	Missense	loss
OV4453-1_P63	sensitive	p.Glu1953*	*BRCA2*	Stop-gained	loss
OV4485_P60	intermediate	p.Gln83*	*SMAD4*	Stop-gained	loss
OV4485_P60	intermediate	c.4548-1G>T	*BRCA1*	Splice_acceptor	loss
OV4485_P60	intermediate	p.Arg287*	*DNTT*	Stop-gained	loss
OV866-2_P108	resistant	p.Pro545Ala	*TDP1*	Missense	diploid
OV866-2_P108	resistant	c.12+2T>C	*TFDP1*	Splice_donor	diploid
OV90_P63	resistant	p.Arg445*	*SMAD4*	Stop-gained	loss
OV90_P63	resistant	p.Cys141*(p16) p.Cys100*(p14 [1]ARF)	*CDKN2A*	Stop-gained	loss
TOV1369M_P65	resistant	p.Ile55Met	*EZH2*	Missense	diploid
TOV1946_P49	sensitive	p.Glu5Gly	*FLNB*	Missense	loss
TOV1946_P49	sensitive	p.Ala172Pro	*NHEJ1*	Missense	loss
TOV1946_P49	sensitive	p.Leu4502Phe	*SYNE1*	Missense	diploid
TOV2295_P57	intermediate	p.Tyr124*	*MYH9*	Stop-gained	loss
TOV3041G_P52	sensitive	p.Thr14Lys	*CDK2*	Missense	loss

Additional variants (Table 3.1.3.2) identified through this analysis includes potential markers of olaparib response and resistance. The *CDK2* missense (p.Thr14Lys) variant in TOV3041G_P52 (Figure 3.1.3.2) occurs in the ATP-binding protein kinase domain and is predicted to be deleterious. The variant occurs with copy number loss. *CDK2* p.Thr14Lys variant is rare and was not found in gnomAD or dbSNP databases. *CDK2* is

mutated in 0.4% (2/523) of tumors of EOC cases, according to the TCGA PanCancer Atlas [216,217]. CDK2 is a serine/threonine protein kinase. The *CDK2* p.Thr14Lys variant may impair CDK2 function since activation and deactivation of CDK2 kinase activity is dependent on dephosphorylation and phosphorylation of CDK2 amino acid residues Thr14, Tyr15, and Thr160 [218,219]. CDK2-mediated phosphorylation of CtIP is required for interaction of CtIP with BRCA1 to promote HR repair [220].

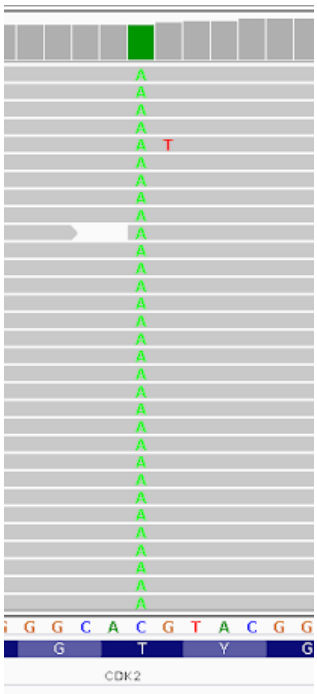

Figure 3.1.3.2. IGV screenshot showing reads supporting CDK2 p.Thr14Lys variant in a sensitive HGSOC cell line. The genomic base substitution (g.12: 56360833C>A) of *CDK2* missense variant p.Thr14Lys is shown for sensitive cell line TOV3041G_P52. Read depth – 46, Variant allele frequency (VAF) – 100%.

SMAD4 is involved in the transforming growth factor (TGF)-beta pathway where it activates other SMAD proteins (receptor-regulated Smads, R-Smads) after TGF-beta stimulation at cell membrane [221]. It forms heterotrimeric complexes with R-Smads and then moves to the nucleus where it associates with other transcription factors to regulate expression of target genes that in turn regulate cell growth and proliferation [222]. SMAD4 acts as mediator for TGF-beta signaling, and influences tumorigenesis through several mechanisms, such as cell cycle arrest, apoptosis, and epithelial-mesenchymal transition. The *SMAD4* truncating mutation in BRCA1-mutated OV4485_P60 (intermediate) occurs, upstream from the one in OV90_P63 (resistant) at p.Gln83* (exon 2), in the N-terminal MH1 domain (DNA-binding) and is predicted to trigger nonsense-mediated mRNA decay, a process that degrades mRNAs with premature stop codons. The SMAD4 mutation (p.Arg445*) in OV90_P63 (resistant) occurs in the middle of the polypeptide-binding C-terminal Mad homology 2 (MH2) domain and likely disrupts formation of SMAD2/3:SMAD4 heterotrimeric complex leading to loss of function. SMAD4 is mutated in 0.8% (4/523) EOC cases in the TCGA PanCancer Atlas [216,217].

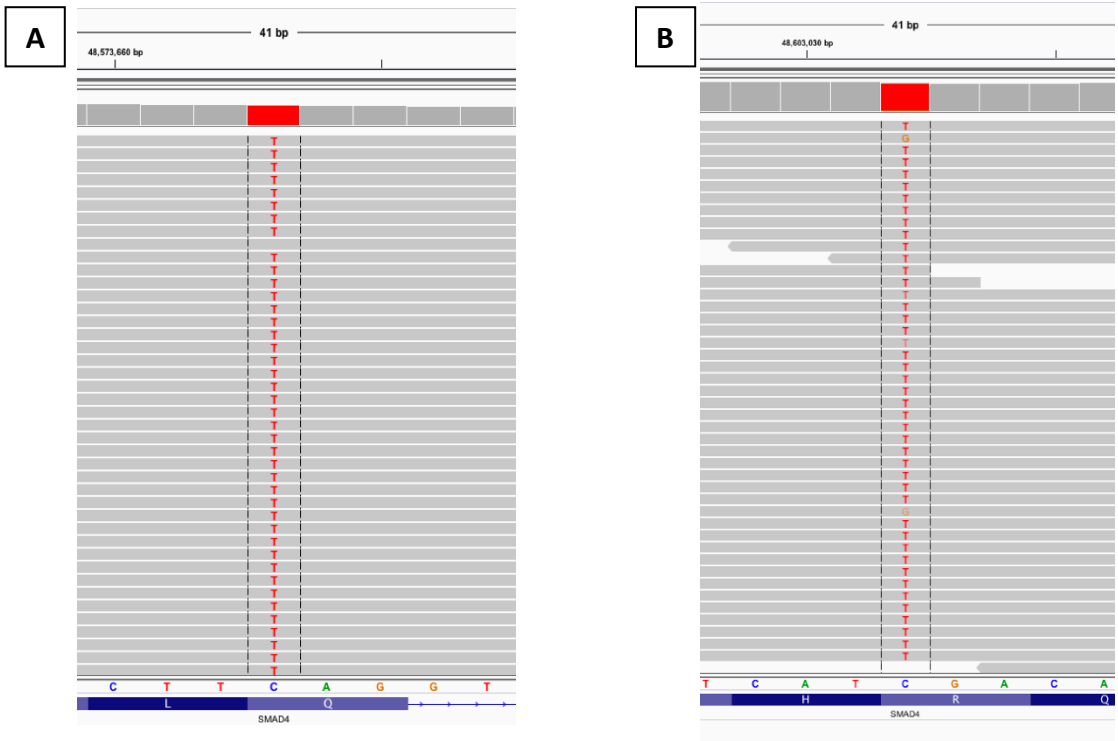

Figure 3.1.3.3. Truncating mutations of *SMAD4* in resistant and intermediate HGSOC cell lines. **A**. Intermediate cell line OV4485_P60 (g.18:48573663C>T, p.Gln83*), read depth – 61, VAF – 98%, **B.** Resistant cell line OV90_P63 (g.18:48603032C>T, p.Arg445*, rs377767360), read depth – 42, VAF – 96%.

3.1.4 Copy number variations linked to differentially expressed genes

CNVs are prevalent in HGSOC cell lines. On average, 989 genes are amplified, and 201 genes are deleted per cell line (Figure 3.1.4.1). The total number of genes that are amplified or deleted in the cell lines are 4,581 (67%) and 2,258 (33%) respectively. Similarly, more genes are amplified than deleted among EOC cases in the TCGA PanCancer Atlas 2018 (n=572) – 22,235 (58%) and 16,419 (42%) respectively.

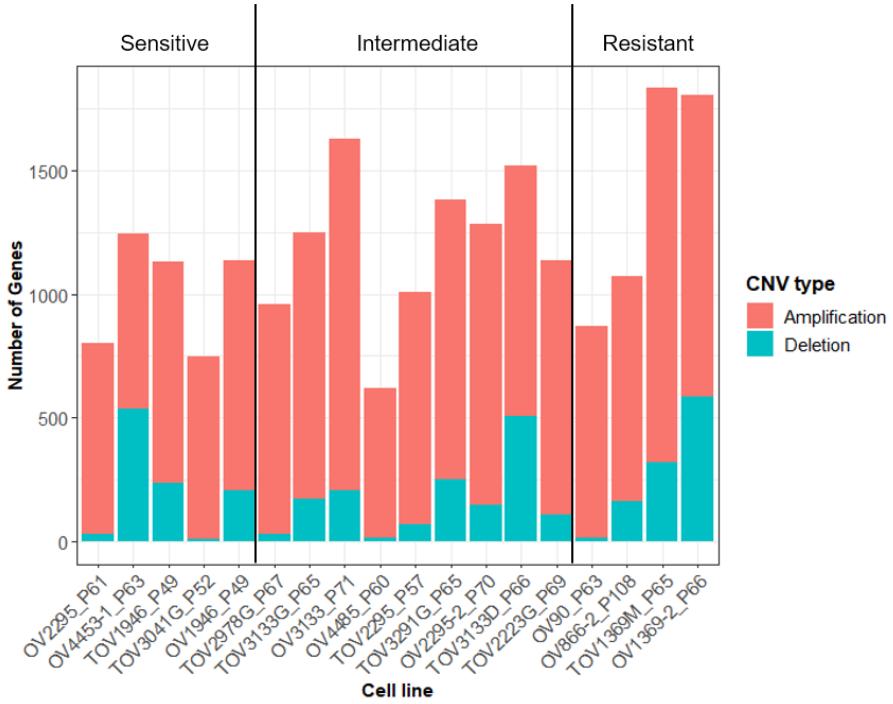

Figure 3.1.4.1. Number of genes involved in copy number amplifications and deletions per HGSOC cell line. From left to right, cell lines are arranged from most sensitive (OV2295_P61) to most resistant (OV1369-2_P66).

Copy number amplification of *CCNE1* locus is observed in OV866-2_P108 (resistant) and TOV3291G_P65 (intermediate) as previously reported [173]. *CCNE1* is amplified in approximately 20% of HGSOC cases [51] and has been associated with poor survival. *MYC* is amplified in intermediate cell lines TOV2295_P57 and TOV2978G_P67. Other

oncogenes, *MECOM* and *KRAS* are amplified in intermediate (OV2295-2_P70, OV3133_P71, TOV223G_P69, TOV3133D_P66, TOV3133G_P65) and resistant (OV866-2_P108, OV1369-2_P66, TOV1369M_P65) cell lines respectively. Similarly, *MYC* (33.2%), *MECOM* (27.8%), and *KRAS* (9.4%) are amplified in EOC cases of the TCGA PanCancer Atlas [216,217] dataset.

In total 162 genes are significantly differentially expressed between resistant and sensitive cell lines with 45 (27.8%) of these genes involved in CNVs through amplifications and deletions.

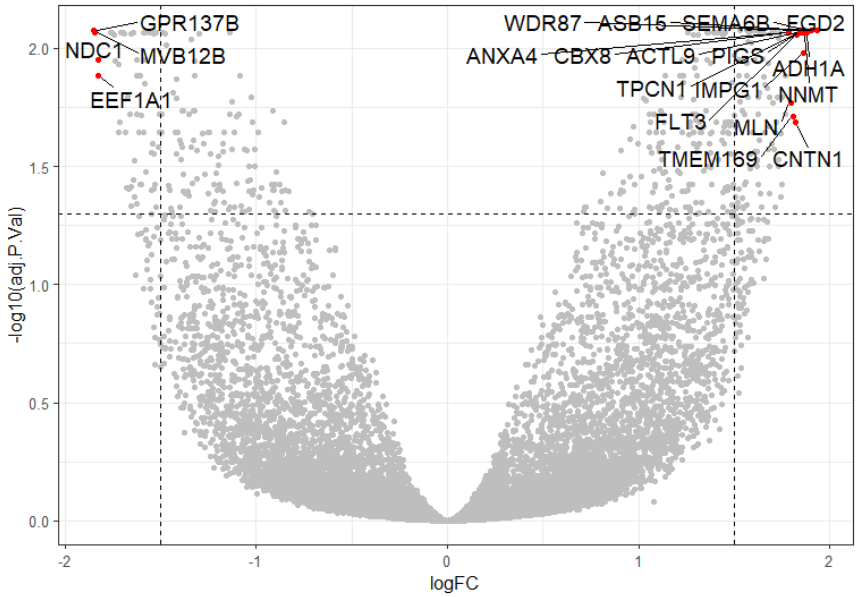

Figure 3.1.4.2. Volcano plot showing differentially expressed genes between sensitive and resistant HGSOC cell lines. Top 20 significant differentially expressed genes are labelled and annotated with red dots. Significant genes are defined by FDR-adjusted p-value <= 0.05 (represented by dashed horizontal line) and absolute log2 fold change >=1.5 (dashed vertical lines). On the left side of the plot (logFC < 0) are genes that are highly expressed in sensitive cell lines, on the right side (logFC >0) are genes that are highly expressed in resistant cell lines.

Notably, the BER glycosylase *MPG* is significantly highly expressed in resistant cell lines compared to sensitive cell lines. This observation is supported by copy number gain in resistant cell lines (OV1369-2_P66, TOV1369M_P65) and copy number deletions in sensitive cell lines (OV1946_P49, TOV1946_P49). Copy number profile of the *MPG* locus across the 18 HGSOC cell lines is shown in Figure 3.1.4.3. *MPG* is amplified or deleted in 1.7% and 1.2% of EOC tumors in the TCGA PanCancer Atlas (n=572) respectively [216,217].

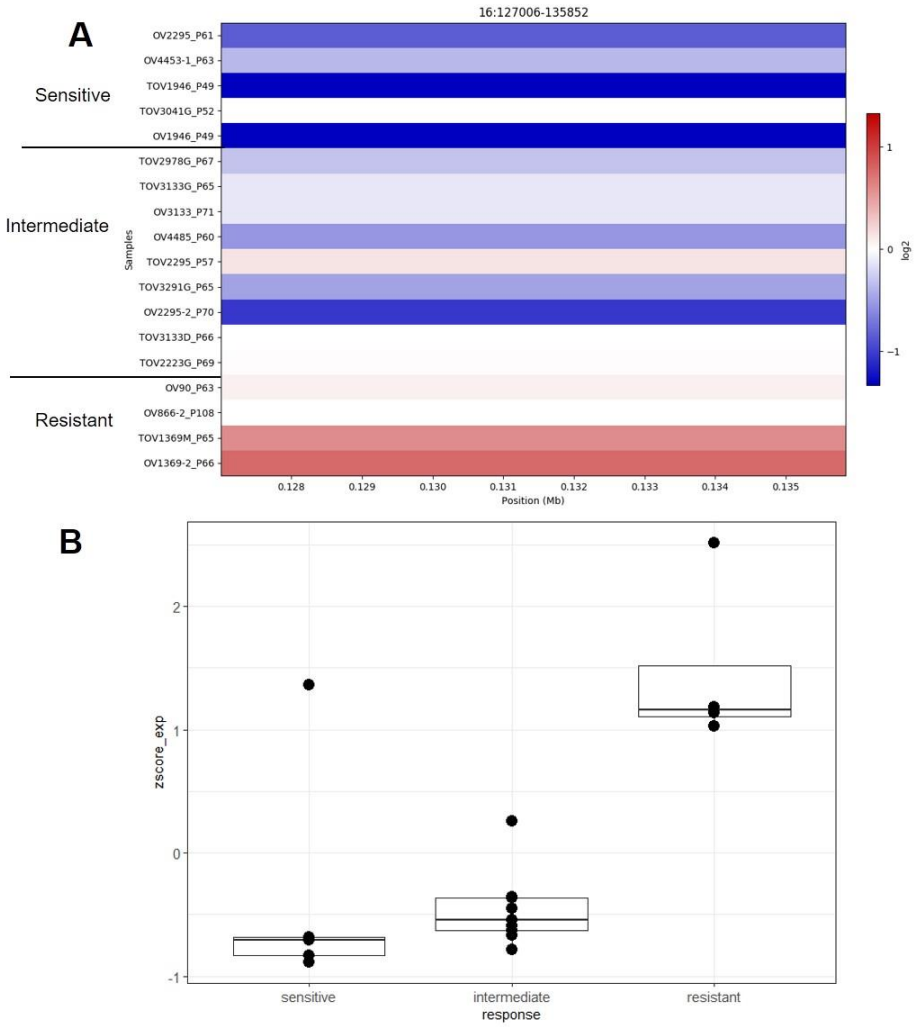

Figure 3.1.4.3. CNV profile of *MPG* across 18 HGSOC cell lines and *MPG* mRNA expression. **A**. Heatmap of copy number status expressed as log2 copy number ratio for *MPG* locus in 18 HGSOC cell lines. On vertical axis, samples are arranged from top to bottom in order of increasing olaparib resistance with OV2295_P61 the most sensitive and OV1369-2_P66 the most resistant. Copy number of *MPG* shows a trend of copy number loss or deletions in sensitive cell lines to copy number gains in resistant cell lines, from top to bottom. **B**. Boxplots showing *MPG* expression in cell lines in sensitive, intermediate and resistant olaparib response groups. *MPG* mRNA is highly expressed in resistant cell lines compared to sensitive cell lines.

Additionally, CNVs also occur in the NHEJ repair gene *RIF1* (Replication timing regulatory factor 1) in cell lines from different olaparib response groups. *RIF1* is deleted in OV4453-1_P63 (sensitive) but amplified in OV1369-2_P66 (resistant). RIF1 cooperates with 53BP1 to promote NHEJ over HR for the repair of DNA double strand breaks [223].

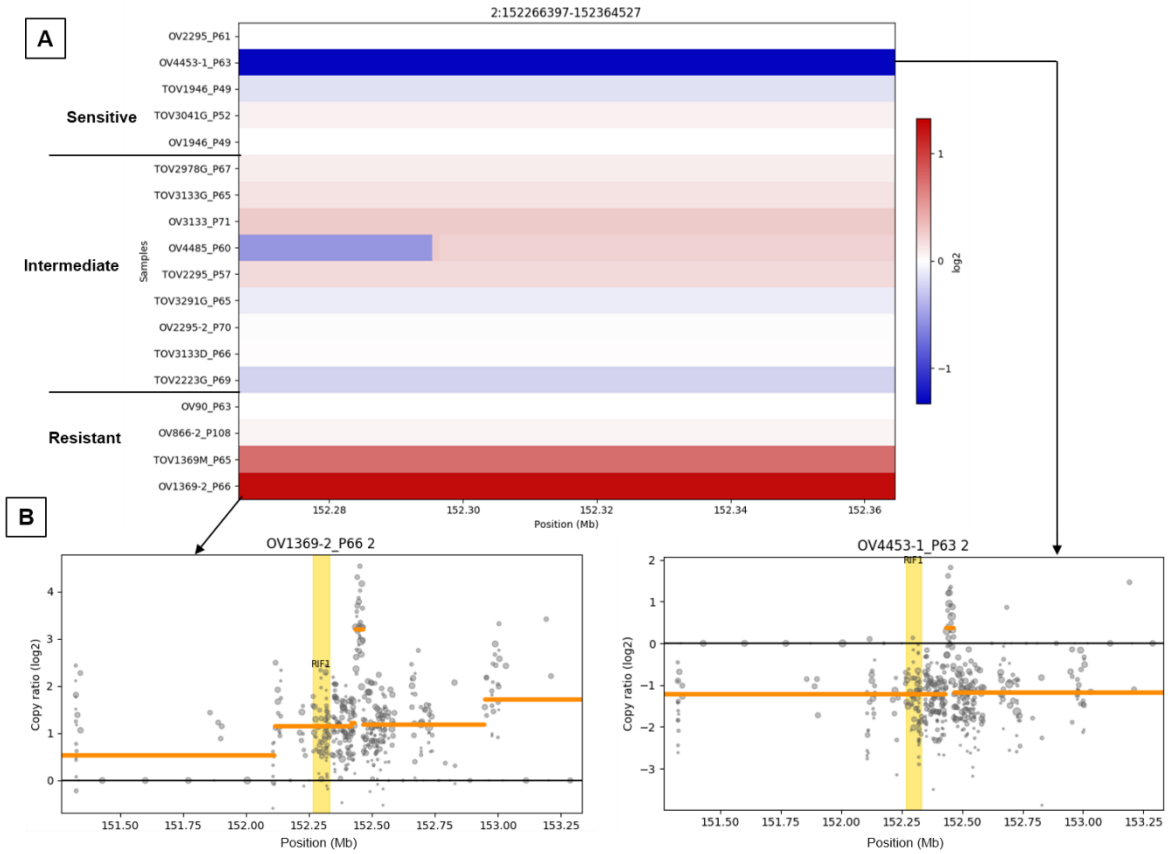

Figure 3.1.4.4. *RIF1* copy number profile across 18 HGSOC cell lines and amplified or deleted CNV segments in respective cell lines. **A.** *RIF1* copy number profile in HGSOC cell lines. On vertical axis, samples are arranged from top to bottom in order of increasing olaparib resistance with OV2295_P61 the most sensitive and OV1369-2_P66 the most resistant. Amplification – log2 copy number ratio >= 1 (deep red), deletion – log2 copy number ratio <= -1 (deep blue). **B.** Scatter plot of bin-level coverage showing

amplified segments for *RIF1* in OV1369-2_P66 (left) and deleted segment in OV4453-1_P63 (right).

Consistent with this observation, *RIF1* mRNA expression is low in OV4453-1_P63 but high in OV1369-2_P66 (Figure 3.1.4.5). In the TCGA PanCancer Atlas EOC cases, *RIF1* is amplified in 0.7% (4/572) of tumors while no *RIF1* deletions are reported [216,217]. In one of the cases with *RIF1* amplification, *RIF1* mRNA is also highly expressed.

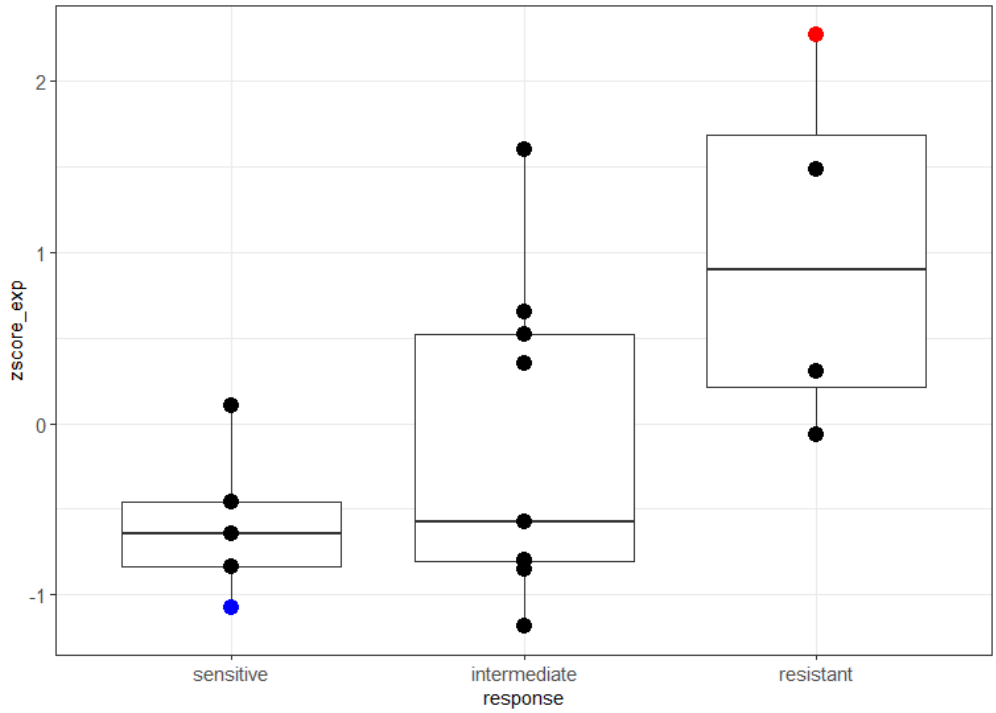

Figure 3.1.4.5. *RIF1* mRNA expression in HGSOC cell lines in sensitive, intermediate, and resistant olaparib response groups. Resistant and sensitive cell lines with copy number amplification (OV1369-2_P66) and deletion (OV4453-1_P63) involving *RIF1* are shown in red and blue dots respectively.

3.2 Olaparib response and mRNA gene expression association analysis using publicly available pan-cancer cell lines identifies candidate olaparib response genes

Univariate and multivariate linear regression methods were used to estimate the relationships between mRNA gene expression and olaparib response (IC_{50}) in 896 human-derived cell lines from diverse types of cancer. This approach reveals 83 significant gene predictors in common from 121 multivariate and 1,176 univariate significant gene predictors. The complete list of candidate genes from both analyses are in Appendix D (multivariate) and Appendix E (univariate). In total, there are 1,214 unique, significant gene predictors. These genes are either associated with increased sensitivity or increased resistance to olaparib from these analyses. Among the candidate genes, 32 are known to be involved in DNA repair or cell cycle regulation pathways (Table 3.2.1). This includes *APTX* which is involved in single strand break repair and operates downstream of PARP1-mediated recruitment of XRCC1. Basal mRNA expression of *APTX* is associated with increased sensitivity to olaparib. Interestingly cyclin dependent kinase inhibitors *CDKN2A*, *CDKN2B*, and *CDKN2C* are associated with resistance. Expression of *TP53 – a* key regulator of genomic stability, cell proliferation and death – is also associated with expression of sensitivity. Basal mRNA expression of *FANCE, XRCC5,* and *PMS1* which are involved in Fanconi anemia, non-homologous end-joining and mismatch DNA repair pathways respectively is associated with increased sensitivity to olaparib.

Table 3.2.1 Candidate olaparib sensitivity and resistance genes derived from analyses of GDSC cell lines in known DNA repair and cell cycle pathways

Gene symbol	Ensembl ID	Analysis	Association
APTX	ENSG00000137074	Multivariate, univariate	sensitivity
AURKB	ENSG00000178999	univariate	sensitivity
CCNA1	ENSG00000133101	univariate	sensitivity
CDC20	ENSG00000117399	univariate	sensitivity
CDKN2A	ENSG00000147889	univariate	resistance
CDKN2B	ENSG00000147883	multivariate	resistance
CDKN2C	ENSG00000123080	univariate	resistance
CKAP5	ENSG00000175216	univariate	sensitivity
E2F1	ENSG00000101412	Multivariate, univariate	resistance
EBP	ENSG00000147155	univariate	resistance
FANCE	ENSG00000112039	Multivariate, univariate	sensitivity
FXYD5	ENSG00000089327	univariate	sensitivity
GADD45G	ENSG00000130222	univariate	resistance
HMGA2	ENSG00000149948	univariate	sensitivity
IPO7	ENSG00000205339	univariate	sensitivity
KIF18A	ENSG00000121621	univariate	sensitivity
LLGL1	ENSG00000131899	univariate	sensitivity
MELK	ENSG00000165304	univariate	sensitivity
MNAT1	ENSG00000020426	univariate	sensitivity
ORC2	ENSG00000115942	univariate	sensitivity
PER1	ENSG00000179094	multivariate	sensitivity
PFN1	ENSG00000108518	univariate	sensitivity
PLK3	ENSG00000173846	univariate	sensitivity
PMS1	ENSG00000064933	univariate	sensitivity
PSMB6	ENSG00000142507	univariate	sensitivity
SLFN11	ENSG00000172716	Multivariate, univariate	sensitivity
STAG1	ENSG00000118007	univariate	sensitivity
TP53	ENSG00000141510	univariate	sensitivity
TUBA1C	ENSG00000167553	univariate	sensitivity
TUBA4A	ENSG00000127824	univariate	resistance
VAMP8	ENSG00000118640	univariate	resistance
XRCC5	ENSG00000079246	univariate	sensitivity
YWHAE	ENSG00000108953	Multivariate, univariate	sensitivity

The top 10 genes associated with sensitivity or resistance to olaparib among the common predictors are shown in Figure 3.2.1.

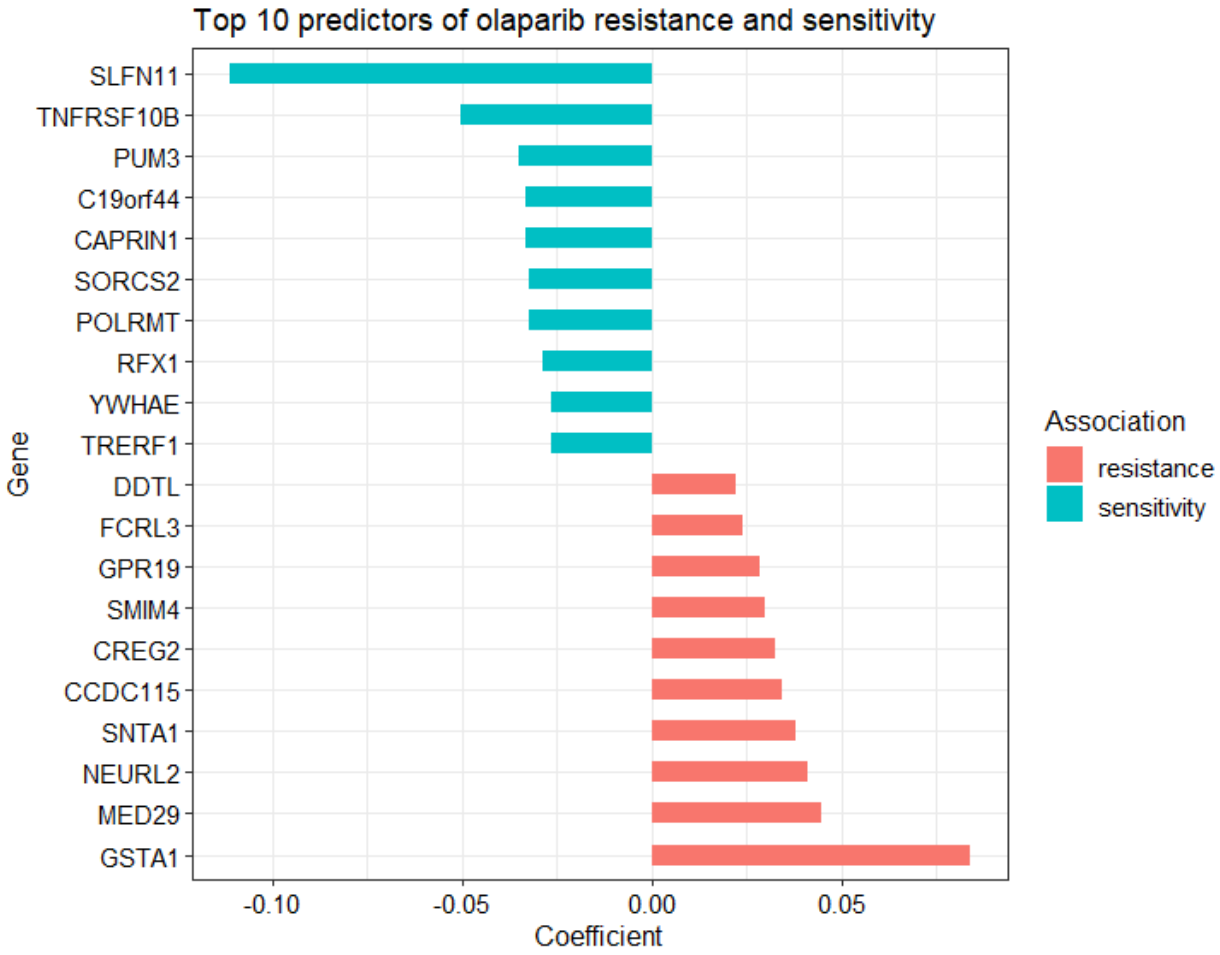

Figure 3.2.1. Top 10 gene predictors of olaparib resistance and sensitivity from linear regression analyses of GDSC pan-cancer cell lines. Coefficients from elastic net multivariate linear regression are shown on the horizontal axis and gene symbols on the vertical axis. Genes associated with resistance have coefficients greater than zero (increased IC_{50}), while genes associated with sensitivity have coefficients less than zero (decreased IC_{50}).

3.2.1 Known markers of olaparib response are among candidate olaparib sensitivity and resistance genes

SLFN11 mRNA expression is most strongly associated with increased sensitivity to olaparib. *SLFN11* expression was found to be correlated to PARP inhibitor response, especially talazoparib, in the NCI-60 panel of human cancer cell lines which includes breast, ovarian, and prostate cancer cell lines and was experimentally shown to sensitize cancer cells to PARP inhibitors including olaparib [168]. Second among the top predictors of sensitivity, *TNFRSF10B* also known as Death Receptor 5 has also been previously associated with PARPi response and is highly expressed in sensitive cells [224]. On the other hand, among resistance candidate genes, *GSTA1* mRNA expression is the top predictor of resistance to olaparib and has been found to be involved in cisplatin resistance [225]. Outside of the top candidates above, other genes from these analyses have also been reported to be associated with olaparib response. For example, ATP Binding Cassette Subfamily B Member 1 (*ABCB1*), associated with resistance from univariate analysis, encodes MDR1 a P-glycoprotein drug efflux pump that has been linked to resistance to olaparib and chemotherapeutic agent paclitaxel [64,226]. Additionally, Ubiquitin Conjugating Enzyme E2 R2 (*UBE2R2*) is associated with sensitivity to olaparib from both univariate and multivariate analyses and was previously identified as a candidate olaparib sensitivity gene in complementary RNA interference screens [227].

3.2.2 Novel candidate markers of olaparib response

Although both analyses rediscover several known markers of olaparib response, there are also many novel candidates that have not been previously linked, statistically or experimentally, to olaparib response. Pumilio RNA Binding Family Member 3 (*PUM3*) is one of these candidates. *PUM3* is one of the top 10 predictors of olaparib sensitivity (3rd in Figure 3.2.1) and was identified by both multivariate and univariate analysis (Table 3.2.2.1). *PUM3* mRNA expression is negatively correlated with olaparib IC50 in 20 cancer types (Figure 3.2.2.1) with Pearson's r ranging from -0.63 to -0.11. PUM3 is known to interact with PARP1 by binding to its catalytic domain and inhibiting its poly ADP-ribosylation activity [228]. This is particularly interesting because olaparib also binds to the catalytic domain of PARP1 to inhibit its function. Suggesting that PUM3 may compete with olaparib to inhibit PARP1 activity, at least in some context, and thereby act as a potential endogenous inhibitor of PARP1.

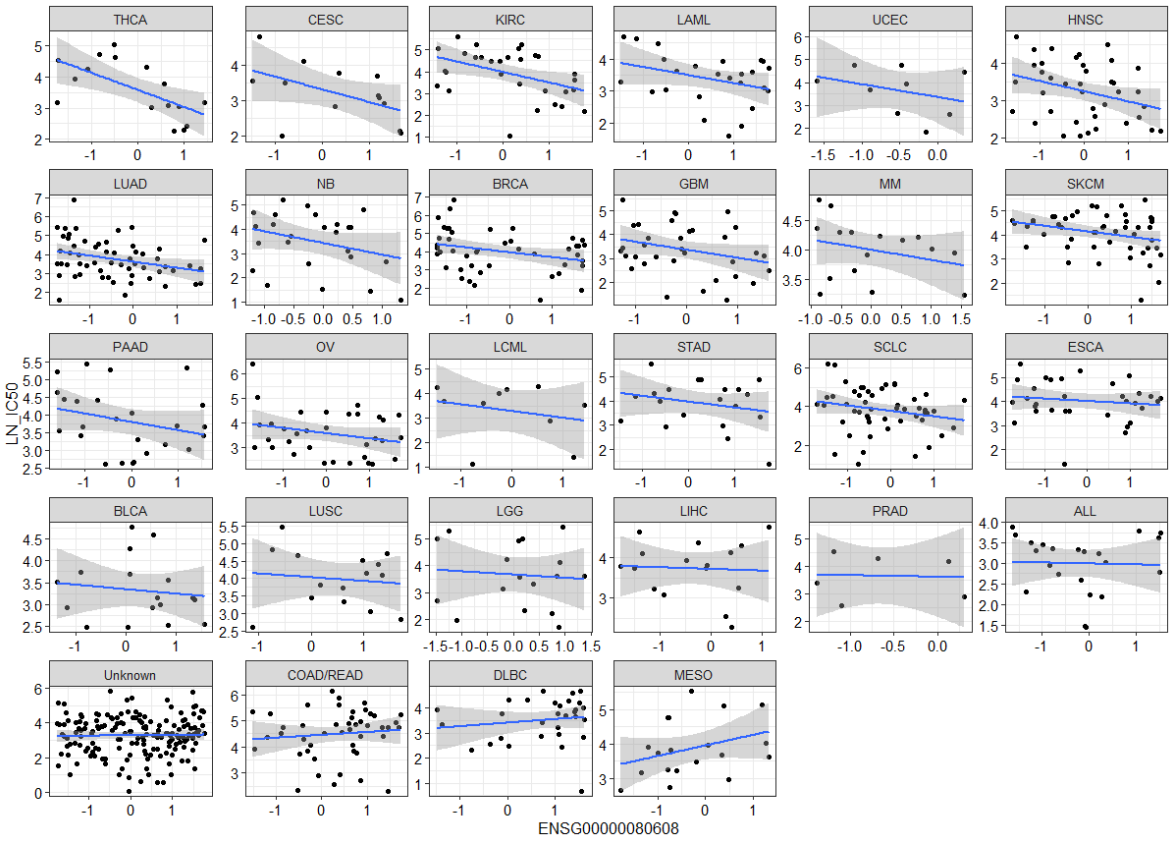

Figure 3.2.2.1. Correlations between *PUM3* mRNA expression and Olaparib IC_{50} GDSC cell lines of multiple cancer types. Each plot shows *PUM3* z-score expression (horizontal axis) plotted against natural log of olaparib IC_{50} (vertical axis) in a specific cancer type (in the title) based on TCGA classes. Plots are arranged from top left (THCA: Thyroid carcinoma) to bottom right (MESO: Mesothelioma) in order of increasing Pearson correlation coefficient. Cell lines of unknown cancer type are also shown in the plot titled Unknown. Complete list of abbreviation meanings is in List of Abbreviations section. Cancer types where olaparib treatment is approved – OV (Ovarian serous cystadenocarcinoma), BRCA (Breast invasive carcinoma), PAAD (Pancreatic adenocarcinoma). Blue lines in each plot are linear regression lines. Shaded region around blue lines represent 95% confidence region. Only cancer types with at least five cell lines are shown.

Elongator Acetyltransferase Complex Subunit 4*, ELP4,* is another interesting candidate olaparib sensitivity gene that emerged as a significant predictor from the univariate analysis. From this analysis, *ELP4* and *ELP5* mRNA expression is significantly associated with increased sensitivity to olaparib (Table 3.2.2.1). *ELP4* and *ELP5* are subunits of the elongator complex (comprised of ELP1, ELP2, ELP3, ELP4, ELP5, ELP6) whose functions include transcriptional elongation [229], and tRNA modification [230]. Interestingly, *ELP4* was recently found to be a novel HR repair pathway gene [231].

Table 3.2.2.1. Summary results from univariate analysis of GDSC cell lines for key candidate olaparib sensitivity genes.

Gene	**Coefficient**	**95% confidence interval**	**FDR-adjusted p value**
PUM3	-0.180	-0.247 – -0.114	1.66×10^{-4}
ELP4	-0.118	-0.191 – -0.044	0.0311
ELP5	-0.131	-0.200 – -0.063	0.00925
EEF1A1	-0.132	-0.210 – -0.054	0.0211

Apart from *PUM3, EEF1A1,* another gene encoding a protein that interacts with PARP1 emerged as a significant predictor of olaparib sensitivity. *EEF1A1* encodes eukaryotic translation elongation factor 1 alpha 1 which is a subunit of elongation factor complex 1 and is involved in protein synthesis where it promotes binding of aminoacyl-tRNA to ribosomes in a guanosine triphosphate (GTP)-dependent manner [232]. It also forms a complex with PARP1 and tyrosine protein kinase TXK to function as a T-helper 1 (Th1)

cell-specific transcription factor, that binds to the promoter of interferon gamma (*IFNG*) and is therefore involved in Th1 cytokine production [233]. From the univariate analysis, expression of *EEF1A1* is associated with increased sensitivity to olaparib. Although EEF1A1 interacts with PARP1 it has also not been previously linked to PARP inhibitor response. Upregulation of *EEF1A1* has been reported to have pro-apoptotic effect [234]. *EEF1A1* is also known to be involved in cytoskeletal organization and cell morphology through interaction with actin [235,236].

3.3 Novel candidate olaparib response genes linked to genomic alterations in independent HGSOC cell lines

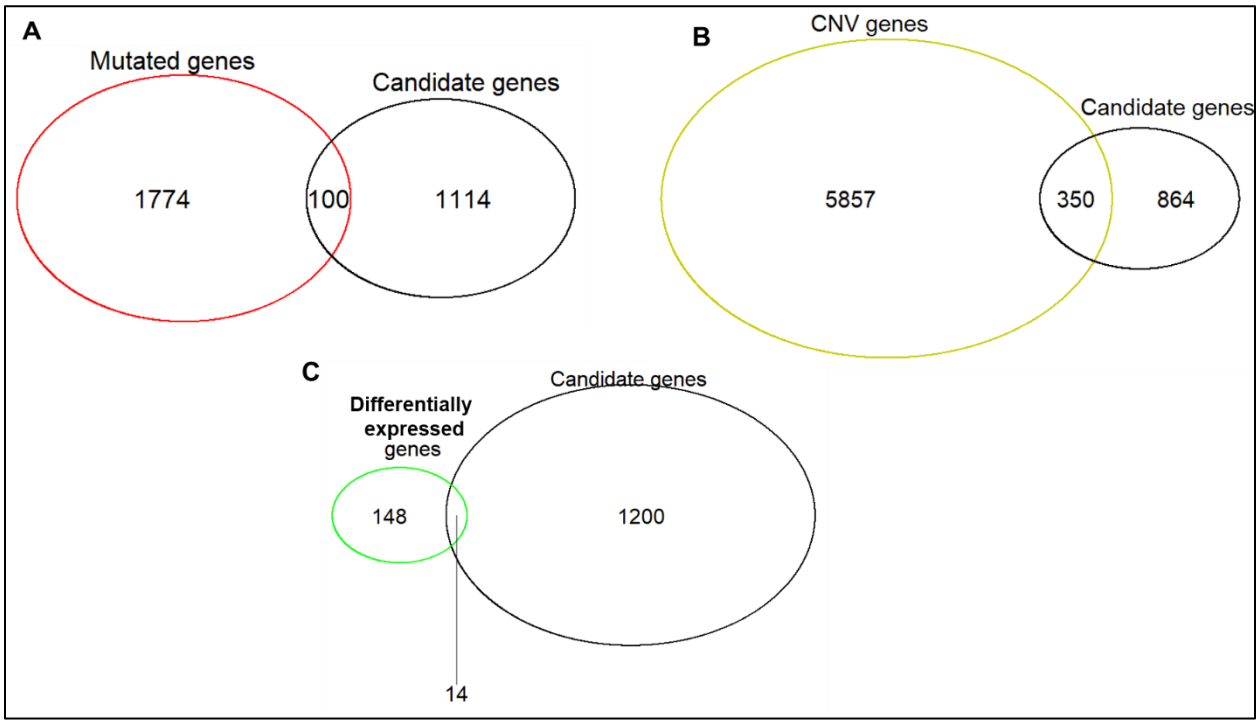

Figure 3.3.1. Candidate olaparib response genes derived from GDSC cell lines that are validated in HGSOC cell lines. Number of candidate olaparib sensitivity and resistance genes identified from multivariate and univariate linear regression analyses that are **(A)** Heterozygous or homozygous for rare functionally relevant sequence variants, **(B)** Involved in CNVs (amplifications and deletions), and **(C)** Significantly differentially expressed between resistant and sensitive HGSOC cell lines.

To validate the findings from GDSC pan-cancer cell lines in HGSOC cell lines, all 1,214 candidate genes, from both univariate and multivariate analyses, were investigated for mutations, CNVs, or whether they were differentially expressed between sensitive and resistant HGSOC cell lines. CNVs are abundant in HGSOC cases and can affect mRNA

gene expression, where deletions can lead low expression and amplifications may promote high expression. Therefore, candidate olaparib response genes from GDSC pan-cancer analysis were also investigated for CNV alterations in the HGSOC cell lines. Other mechanisms for regulating gene expression that were not investigated in the HGSOC cell lines include promoter methylation, histone modification, and microRNA activity. Candidate olaparib response genes that are altered by these mechanisms in HGSOC cell lines were not captured. To maximize the use of the genomic variation data (mutations, CNVs, gene expression) generated from the HGSOC cell lines and increase the potential to find candidate genes that may also contribute to olaparib response in HGSOC cell lines all candidate genes were investigated for mutations, CNVs, and differential expression. A total of 431 (35.5%) unique genes were altered in at least one of these ways. These genes were further prioritized based on whether they were known to be functionally linked to PARP by searching peer-reviewed literature. Genomic alterations involving candidate olaparib response genes identified in sensitive or resistant HGSOC cell lines would suggest a role for these candidate genes in olaparib response. Known functions of these validated candidate genes could provide clues for plausible mechanisms by which they mediate olaparib sensitivity or resistance. Key candidate genes with relevant functions and altered in the HGSOC cell lines are presented below.

Copy number deletions of *PUM3* were found in two resistant and one intermediate HGSOC cell lines (Figure 3.3.2A). Consistent with these copy number deletions, these resistant (TOV1369M_P65, OV1369-2_P66) and intermediate (TOV3133D_P66) cell

lines were also found to express low levels of *PUM3* mRNA compared to sensitive and intermediate cell lines (Figure 3.3.2B). Taken together these findings implicate *PUM3* mRNA expression in olaparib response with high expression associated with increased sensitivity (from GDSC cell lines) and low expression associated with increased resistance (from HGSOC cell lines).

Investigating the HGSOC cell lines for genomic alterations involving *ELP4* revealed rare (< 0.1% minor allele frequency in gnomAD) potentially deleterious, heterozygous, missense variants of *ELP4* (p.Arg317Cys) as well as *ELP6* (p.Gln151Arg) in TOV2978G_P67 (Figure 3.3.3). This cell line is in the intermediate response group, it is on the boundary of sensitive and intermediate groups (Figure 2.1.1) and is sensitive to carboplatin *in vitro* [173]. It does not have a *BRCA1/2* mutation, or mutations in other canonical HR repair genes but has mutational signature 3. While *ELP4* and *ELP5* mRNA expression are associated with olaparib sensitivity from univariate analysis of GDSC pan-cancer cell lines, *ELP4* and *ELP6* missense variants may contribute to sensitivity to PARPi in the HGSOC cell line TOV2978G_P67.

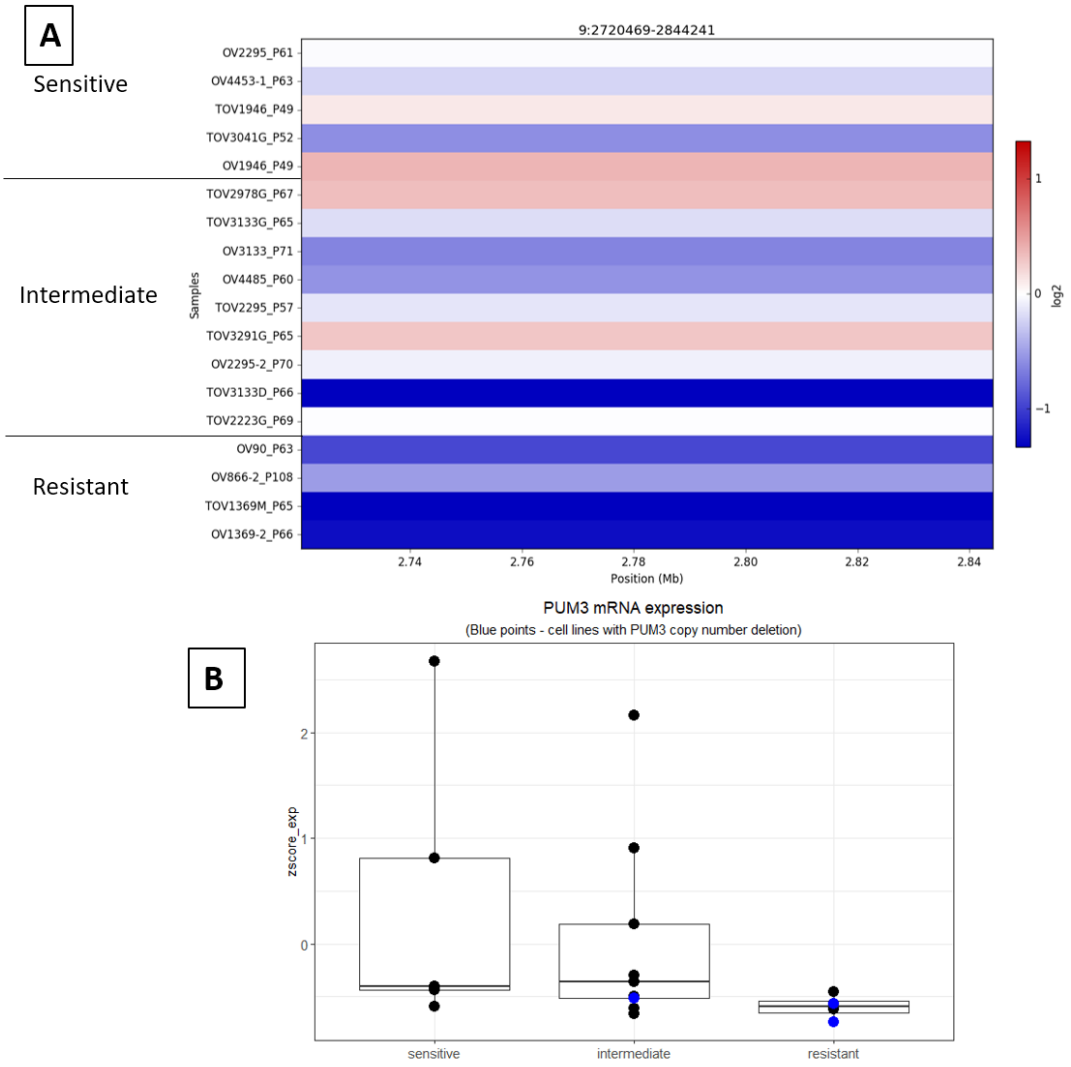

Figure 3.3.2 *PUM3* copy number profile and mRNA expression in HGSOC cell lines. **A.** Log2 copy number ratio for copy number segments spanning *PUM3* gene locus for 18 HGSOC cell lines. **B.** Boxplots of z-score *PUM3* mRNA expression in sensitive, intermediate, and resistant HGSOC cell line groups.

Thus far, ELP4 is the only subunit of the elongator complex that has been implicated in HR repair [231]. However, ELP5, and ELP6 may also have roles in HR repair since all three proteins (ELP4, ELP5, and ELP6) share a RecA ATPase-like protein domain that

is also found in RAD51 which plays an important role in homology search and strand exchange in HR and form a discrete subcomplex by dimerization of ELP4/5/6 heterotrimer into a hexameric ring [237,238].

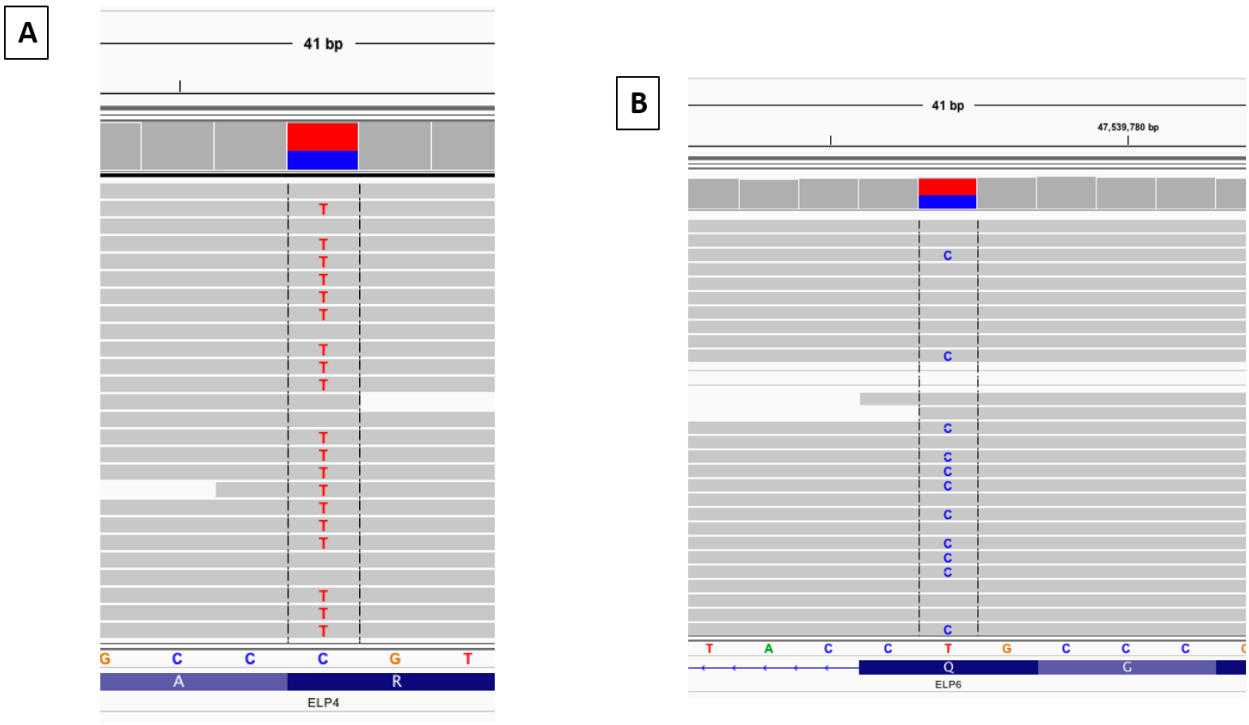

Figure 3.3.3. Missense variants in *ELP4* and *ELP5* genes in intermediate HGSOC cell line TOV2978G_P67. **A**. *ELP4* missense variant (p.Arg317Cys, rs764805051, 11:g.31669307C>T) in HGSOC cell line TOV2978G_P67. Read depth – 310, VAF – 59% (T). **B**. *ELP6* missense variant (p.Gln151Arg, 3:g.47539777C>T) in TOV2978G_P67. Read depth – 45, VAF – 44% (C).

EEF1A1 is significantly differentially expressed between olaparib-sensitive and -resistant HGSOC cell lines (Figure 3.3.4). It is highly expressed in sensitive cell lines compared to resistant cell lines. This is consistent with the observation that increased

expression of *EEF1A1* is associated with sensitivity to olaparib in the independent GDSC pan-cancer cell lines.

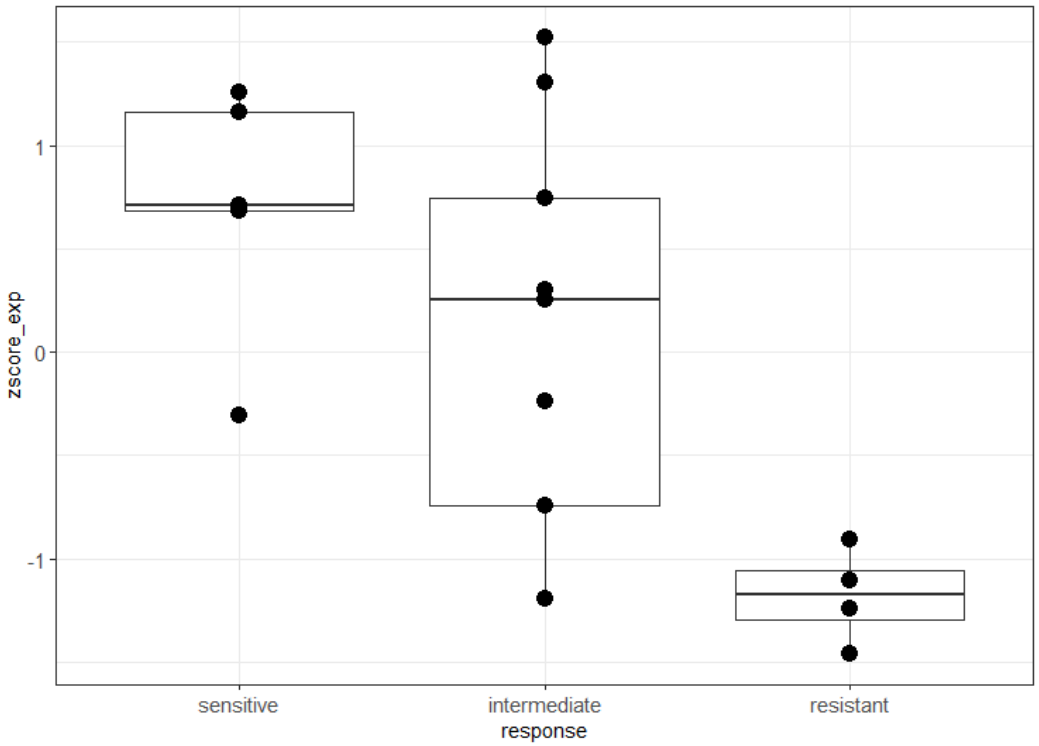

Figure 3.3.4. *EEF1A1* mRNA expression in HGSOC cell lines in sensitive, intermediate, and resistant olaparib response groups.

3.4. Frequency of genomic alterations involving candidate olaparib response genes in the TCGA EOC cases

The key candidate genes described above were investigated for mutations, copy number variation, and mRNA expression in tumor samples where this data for these types of alterations were available (Figure 3.4.1). In total, 201 samples from EOC cases in the TCGA PanCancer Atlas dataset were investigated using cBioPortal [216,217]. Notably, high mRNA expression is the most common alteration of *PUM3* in EOC cases and is supported by amplification of *PUM3* in some cases. *PUM3* alterations are also mutually exclusive of pathogenic variants in *BRCA1* and *BRCA2*. This suggests that a subset of *PUM3*-expressing EOC cases, distinct from *BRCA1/2* mutation carriers, may benefit from olaparib treatment.

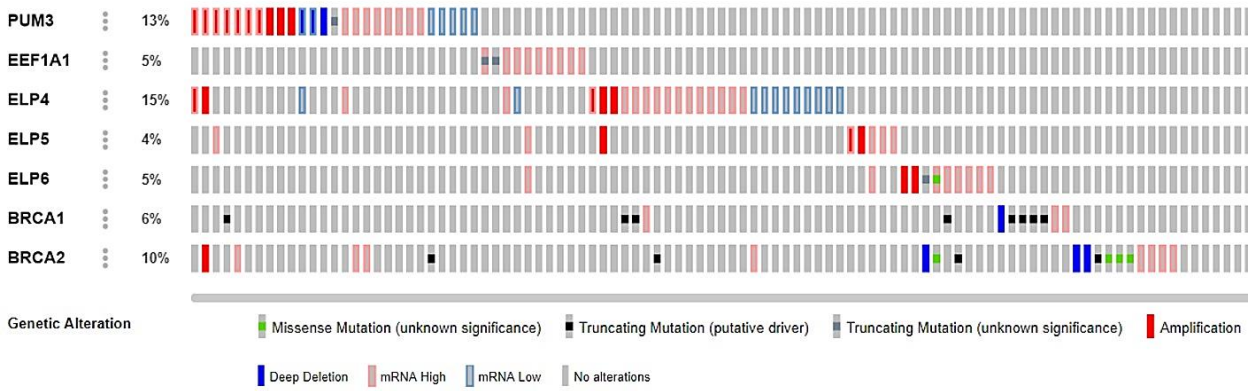

Figure 3.4.1. Frequency and types of alterations of key candidate olaparib response genes in TCGA ovarian cancer cases. Mutations, CNVs, and gene expression variation in *PUM3, EEF1A1, ELP4, ELP5, ELP6* compared to *BRCA1* and *BRCA2* in tumor samples (n=201) with complete data from EOC cases in the TCGA PanCancer Atlas study derived from cBioPortal [216,217].

3.5 Summary

Analyses of sequence, copy number, and gene expression variations of DNA repair and cell cycle genes in HGSOC cell lines with distinct olaparib response groups revealed potential variations that may explain olaparib sensitivity or resistance in specific cell lines. Additionally, candidate genes in diverse pathways, beyond DNA repair and cell cycle, were found from statistical analysis using linear regression models to predict olaparib response from mRNA gene expression of pan-cancer cell lines in the GDSC database. Linking HGSOC and pan-cancer analyses, some novel candidate olaparib response genes derived from the pan-cancer analysis were found to harbor sequence or copy number alterations, or differential expression that may contribute to olaparib response in the HGSOC cell lines.

Chapter 4: Discussion

4.1 Overview of thesis findings

PARP inhibitors are important treatment options for *BRCA1/2*-associated cancers especially HGSOC. Mounting evidence indicates that additional factors beyond *BRCA1/2* mutation status and HRD contribute to sensitivity and resistance to PARPis [64,130,131,133,155,158,168]. In this thesis, functional genomic variations and gene expression from two independent groups of human cancer cell lines with varying *in vitro* response to olaparib were independently analysed and then integrated to identify potential variants and genes associated with olaparib sensitivity and resistance, as summarized in Figure 4.1.1. The investigation of 18 HGSOC cell lines identified sequence variants, CNVs, and gene expression variation associated with olaparib response in DNA repair and cell cycle regulation genes that have not been previously reported in these cell lines. The analysis of the pan-cancer GDSC cell lines, reveals that basal mRNA expression of specific genes is significantly associated with olaparib response (IC_{50}). While some of these genes have been reported to promote olaparib sensitivity or resistance, several others have not been previously reported. Of particular interest, are novel candidate genes that encode proteins that are known to interact with PARP1 and an emerging HR repair pathway gene. Interestingly, these novel candidate genes with relevant functions are also altered in terms of SNVs, CNVs, or differentially expressed between sensitive and resistant HGSOC cell lines, suggesting that they may also affect olaparib response in those cell lines harboring them.

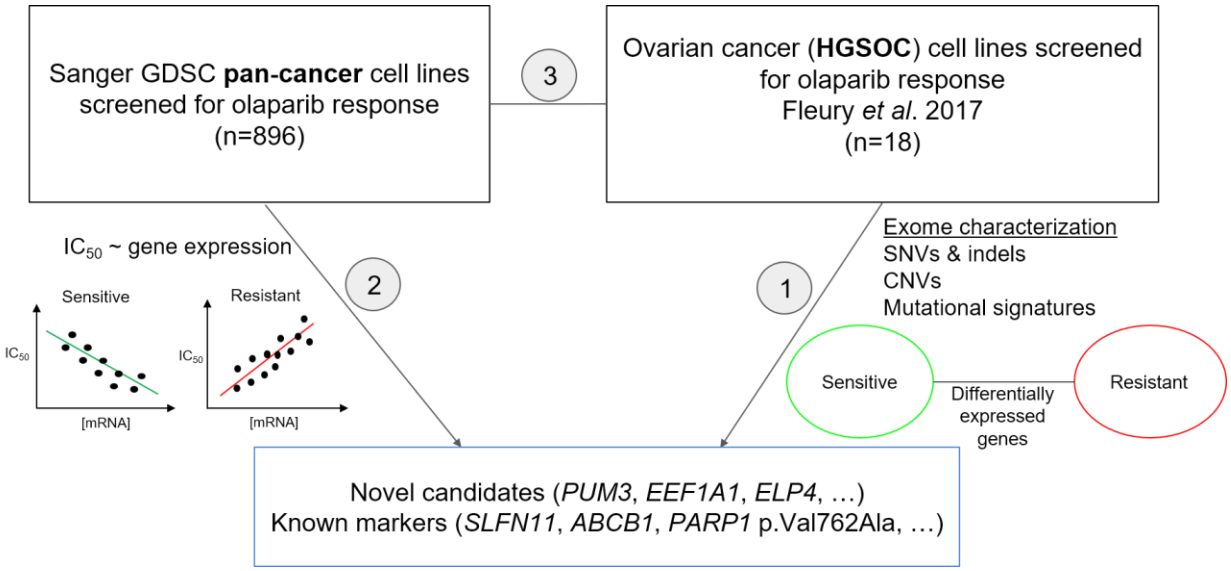

Figure 4.1.1 Overview of thesis project analyses and findings. **1.** Exome characterization and differential gene expression analyses of 18 HGSOC cell lines with distinct olaparib response groups links SNVs, CNVs, and differential expression of DNA repair and cell cycle genes to olaparib response. **2.** Olaparib response and gene expression association analysis using pan-cancer cell lines from the publicly available GDSC database identifies known and novel candidate olaparib response genes. **3.** Key novel candidate olaparib sensitivity genes identified in GDSC cell lines are validated in HGSOC cell lines. Independent analyses of GDSC and HGSOC cell lines finds known markers of PARPi response.

4.2 Potential genomic markers of olaparib response in known DNA repair and cell cycle genes

Cancer cell lines are important models for studying *in vitro* drug response to discover pharmacogenomic associations. Relevant cell lines that capture the genomic and molecular features of the specific cancer of interest are important for finding reliable biomarkers. The 18 HGSOC cell lines investigated in this thesis project harbor important molecular genetic features consistent with those found in patients' tumors: *TP53* mutations (n=17), *BRCA1/2* mutations (n=2), *CCNE1* amplification (n=2). Through this project we revealed that COSMIC mutational signature 3 which is associated with HR repair defect and common in ovarian, breast, and pancreatic cancers is present in 15 of these cell lines [134]. However, our results show that this mutational signature did not distinguish olaparib-sensitive and -resistant HGSOC cell lines.

Olaparib targets PARP1 and PARP2. PARP1 is the major PARP enzyme, accounting for about 85% of PARP activity [239]. Therefore, defective PARP1 activity combined with PARP inhibition by olaparib could render cells olaparib-sensitive. A missense variant in *PARP1* (p.Val762Ala, rs1136410) found in TOV3041G_P52 (sensitive) and TOV2978G_P67 (intermediate) cell lines could contribute to defective PARP1 and olaparib sensitivity. Notably the HGSOC cell lines with this variant do not have *BRCA1/2* mutations but were shown to have COSMIC mutational signature 3. The *PARP1* p.Val762Ala variant occurs in the catalytic domain of PARP1 and has been shown to reduce PARylation activity of PARP1 by approximately 40% with or without PARP inhibition by 3-aminobenzamide [213]. However, it is not clear whether *PARP1* p.Val762Ala diminishes PARP trapping as has been reported for another *PARP1* variant

p.Arg591Cys [240]. Although the variant has been linked to increased cancer susceptibility, it is common in the population based on data from the gnomAD database which reported an overall minor allele frequency of 20.7%. The high frequency of this variant in the general population makes it attractive as a potential biomarker of olaparib sensitivity: genotyping cancer patients may help identify those most likely to benefit from olaparib treatment. The high allele frequency of *PARP1* p.Val762Ala is also attractive in relation to carriers of *BRCA1/2* pathogenic variants due to the lower frequency of the latter. Sensitivity to olaparib has been based on synthetic lethality of HR deficiency primarily caused by BRCA1/2 mutations and BER deficiency from PARP inhibition. The *PARP1* p.Val762Ala missense variant is another potential source of BER deficiency present in TOV3041G_P52 and TOV2978G_P67 cell lines that contributes to sensitivity to olaparib.

MPG is significantly differentially expressed between olaparib-sensitive and -resistant HGSOC cell lines. *MPG* mRNA expression is low in sensitive cell lines with copy number deletions while it is high in resistant cell lines with copy number amplifications (Figure 3.1.4.2). MPG is a DNA glycosylase involved in the BER pathway. It specializes in the removal of alkylated purine bases 3-methyladenine (3-MeA) and 7-methylguanine which occur approximately 600 and 4,000 times daily per human genome respectively [241]. These are among the most common types of endogenous DNA lesions. Importantly, the 3-MeA lesion is especially cytotoxic as it blocks DNA replication and MPG is the only known glycosylase specialized in removing it. Consistent with its known function, knockdown of *MPG* in the cervical carcinoma HeLa cell line increased

sensitivity to DNA alkylating agents temozolomide and carmustine [242]. Deficiency of other BER proteins (XRCC1 and Pol β) have been reported to sensitize mouse embryonic fibroblast cells to PARP inhibition [131]. However, MPG knockdown or inhibition has not been shown to sensitize cells to PARPis. MPG downregulation could represent another mechanism resulting in of BER deficiency that promotes sensitivity to PARP inhibition.

Another missense variant found in TOV3041G_P52 that potentially contributes to olaparib sensitivity occurs in *CDK2*. The *CDK2* p.Thr14Lys missense variant occurs in the ATP-binding catalytic domain of CDK2 and is predicted to be deleterious based on *in silico* variant effect prediction algorithms. CDK2 is required to activate the endonuclease CtIP (encoded by retinoblastoma binding protein 8, RBBP8) which cooperates with BRCA1 and MRE11-RAD50-NBN (MRN) complex in DNA-end resection step of HR repair [115,220]. CDK2 also cooperates with ATM to phosphorylate ERCC6 (also known as Cockayne Syndrome Group B Protein, CSB) which is important for chromatin remodeling at DNA double-strand breaks by removal of histones [243]. Loss of CtIP function has been shown to disrupt HR and increase sensitivity to PARP inhibitors olaparib and veliparib in breast cancer cell lines [244]. The rare, deleterious missense variant in *CDK2* (p.Thr14Lys) may result in HR deficiency in TOV3041G_P52 through impaired activation of key HR protein CtIP and ERCC6, partly accounting for this cell line's sensitivity to olaparib.

Analysis of the HGSOC cell lines also reveals potential markers of resistance to olaparib. Resistant HGSOC cell lines have been shown to be more proficient at HR

repair than intermediate and sensitive cell lines [133]. However additional alterations in DNA repair and cell cycle control genes may also contribute to resistance. *RIF1* amplification and high expression in resistant cell line OV1369-2_P66 could be important for mitigating DNA replication damage triggered by olaparib. RIF1 has been shown to protect stalled replication forks from degradation by DNA2 (DNA replicaton helicase/nuclease 2), independent of its role in NHEJ [245]. In contrast, RIF1 is deleted and has low expression in sensitive cell line OV4453-1_63 which is HR-deficient through a *BRCA2* protein truncating mutation (p.Glu1953*). BRCA2 is also involved in protecting stalled replication forks by blocking MRE11 [246]. *CDKN2A* is a tumor suppressor gene that encodes p16 protein which inhibits phosphorylation of retinoblastoma (RB) protein, by interacting with CDK4 and CDK6, and blocks cell cycle progression [247,248]. Inactivation of CDKN2A in OV90_P63 through a protein truncating mutation (p.Cys141*, p16) may promote rapid entry into mitosis and increased cell division. Protein truncating mutations of another tumor suppressor gene *SMAD4* in *BRCA1*-mutated OV4485_P60 (intermediate) and OV90_P63 (resistant) are particularly interesting. The *SMAD4* mutation (p.Arg445*) in OV90_P63 occurs in the MH2 domain which has been shown to be important for binding of SMAD4 to SMAD2 and SMAD3 to form a heterotrimer that is then translocated to the nucleus where it ultimately regulates transcription of target genes [222]. *SMAD4* mutations have been linked to carboplatin resistance in ovarian cancer cell lines. A *SMAD4* mutation (p.Ser344Ile) within the MH2 domain was reported in ovarian cancer cell lines that acquired resistance to carboplatin [249]. The *SMAD4* mutation in OV4485_P60 may

dampen its sensitivity to olaparib even though this cell line is HR repair deficient through a *BRCA1* mutation (c.4548-1G>T).

4.3 Novel candidate olaparib sensitivity genes

The analyses of pan-cancer cell lines in the GDSC database to identify genes whose mRNA expression is significantly associated with sensitivity or resistance to olaparib revealed novel candidate genes with relevant functions. The major findings from this analysis that were successfully replicated in the HGSOC cell lines can be classified into two groups of genes: PARP1 interactors (*PUM3*, *EEF1A1*) and emerging HR factors (*ELP4*, *ELP5*, *ELP6*).

PARP1 is the most active target of olaparib [239]. Therefore, any underlying factors that influence PARP1 levels or activity can also affect PARP inhibitor response. *PUM3* mRNA expression was ranked the third strongest predictor of olaparib sensitivity, among common significant predictors from the combined multivariate and univariate analyses, with increased expression correlated with increased sensitivity in multiple cancer types (Figure 3.2.1). PUM3 (KIAA0020 or human Puf-A, hPuf-A) binds to mRNA and regulates translation using its highly conserved PuF domains. A Puf domain consists of 35 to 39 amino acids capable of associating with the 3'-untranslated region (3'-UTR) of target mRNAs and interacts with other regulatory proteins to promote mRNA degradation and repression of translation [250,251]. Puf proteins are highly conserved among most eukaryotic organisms and are involved in stem cell maintenance, cell development and differentiation. Deletion of PUF-8 in the roundworm, *Caenorhabditis*

elegans, led to the development of germ cell tumors [252]. PUM3 is one of the newly discovered members of the human Puf protein family [253]. It shares 63% amino acid homology with zebrafish Puf-A. Unlike classical PUF proteins, which are localized to the cytoplasm PUM3 is predominantly found in the nucleolus. PUM3 has been linked with tumor development. *PUM3* expression has been reported to be positively associated breast cancer progression. High expression of *PUM3* was observed in 70% (n=185) of breast cancer biopsies comprising diverse histological subtypes compared to normal breast tissues, ductal carcinoma *in situ*, and adjacent noncancerous tissues [254]. Downregulation of PUM3 by siRNA sensitizes cells to the DNA topoisomerase I (TOP1) inhibitor camptothecin and UV treatment while cells constitutively overexpressing PUM3 are rendered resistant to genotoxic exposure [228]. However, neither of these DNA damage-inducing agents specifically binds to PARP1 to inhibit PARylation. Cytotoxicity of TOP1 inhibitors is based on interference of DNA replication and transcription by trapped TOP1-DNA cleavage complexes [255–257]. UV light can also generate TOP1-DNA cleavage complexes and pyrimidine dimers that impede DNA replication [258,259]. PUM3 interacts with the catalytic domain of PARP1 and inhibits poly(ADP-ribosyl)ation activity of PARP1 *in vitro* [228]. The effect of depleting PUM3 expression or deleting the gene and effect of response to treatment with PARP inhibitor has not been reported. Results presented in this thesis reveal that *PUM3* mRNA expression is associated with increased sensitivity to olaparib. This supports the hypothesis that PUM3-mediated inhibition of PARylation by PARP1 may support olaparib-mediated catalytic inhibition of PARP1 and sensitize cells. However, it is not known if PUM3 can contribute to PARP trapping which is considered the major part of PARPi cytotoxicity.

EEF1A1 mRNA expression is associated with increased sensitivity to olaparib in the GDSC pan-cancer cell lines and is highly expressed in olaparib-sensitive HGSOC cell lines, including BRCA2-mutated OV4453-1_P63, compared to resistant cell lines. The interaction of EEF1A1 with PARP1 is different from that of PUM3 as it does not involve inhibition of PARylation. EEF1A1 is a subunit of a complex also comprised of PARP1 and tyrosine kinase TXK that functions as a transcription factor for IFNG in T-helper 1 cells [233]. IFNG expression has been found to be a predictive marker of sensitivity to immune checkpoint inhibitors nivolumab and pembrolizumab in non-small cell lung cancer and melanoma cases respectively [260]. While it is unclear how *EEF1A1* expression may contribute to olaparib sensitivity, through its interaction with PARP1, EEF1A1 could link PARP inhibition to immunotherapy and may also be a potential marker of sensitivity to immunotherapy or combination of immunotherapy and PARPi. There is interest to combine immunotherapy with PARPis. A phase 2 clinical trial (NCT02734004) of olaparib and programmed cell death ligand 1 (PDL-1) inhibitor durvalumab (Imfinzi) in platinum-sensitive relapsed germline *BRCA1/2*-mutated ovarian cancer is ongoing [261]. *BRCA1/2*-mutated, HR-deficient HGSOC is associated with increased neoantigens, tumor-infiltrating lymphocytes (TILs) and favorable prognosis than HR-proficient HGSOC [262].

Expression of *ELP4 and ELP5* at mRNA level is associated with increased sensitivity to olaparib in GDSC pan-cancer cell lines. An intermediate HGSOC cell line (TOV2978G_P67) has rare, potentially damaging heterozygous variants in *ELP4* (p.Arg317Cys) and *ELP6* (p.Gln151Arg). ELP4, ELP5, and ELP6 are subunits of the

RNA polymerase II elongator complex [263]. TOV2978G_P67 does not have *BRCA1/2* mutations although we find that it exhibits mutational signature 3, associated with HR deficiency, and has been previously shown to be sensitive to carboplatin [173]. ELP4 was discovered as a novel HR repair gene through coevolution analysis of 600 species and functional experiments and was found to have coevolved with *BRCA1* and *BARD1* in plants and mammals [231]. ELP4 was experimentally associated with the HR repair pathway using two systems. Knockdown of *ELP4* function led to a significant reduction in brood size of *C. elegans* following exposure to ionizing radiation. Defective HR repair pathway can cause germline radiation sensitivity [264]. Using the Direct Repeat-Green Fluorescence Protein (DR-GFP) assay, knockdown of *ELP4* significantly reduced HR efficiency in the osteosarcoma cell line U2OS [231]. However, the specific role of ELP4 in HR is not known. Since ELP4/5/6 form a discrete subcomplex and share a RecA ATPase-like protein domain [237,238] that is also found in key HR protein RAD51, ELP5 and ELP6 may cooperate ELP4 in a HR repair role.

4.4 Summary

Response to olaparib is multifactorial and is potentially influenced by genomic alterations in different genes (Table 4.4.1). This thesis identified candidate genomic markers of olaparib response in known DNA repair and cell cycle control pathways associated with the molecular mechanism of olaparib. The key findings from this part of the thesis, involving analysis of genomic variation in HGSOC cell lines with distinct olaparib response groups are *PARP1* p.Val762Ala, *MPG* mRNA low expression mediated by copy number deletions, and *CDK2* p.Thr14Lys. In particular, low expression of *MPG* and deleterious missense variant of *CDK2* (p.Thr14Lys) represent novel sources of BER deficiency and HR repair deficiency respectively consistent with the concept of synthetic lethality of these pathways required for cytotoxicity of PARP inhibition. However, *PARP1* p.Val762Ala could be the more useful marker of olaparib sensitivity as it occurs in PARP1 (a direct target of olaparib), is known to reduce PARylation, and is more common in the general population (~20%). Fleury *et al*., (2017) [133] used 18 HGSOC cell lines to experimentally demonstrate that knockdown of key MMR and NER genes increased sensitivity to olaparib, and proposed that a combination of HR and MMR or NER deficiency promotes the highest sensitivity to olaparib. My findings from genomic analysis of these cell lines identified alterations in other genes of DNA repair pathways such as BER, and cell cycle genes such as *CDK2* that potentially contribute to olaparib sensitivity or resistance.

Importantly, this thesis also reveals novel candidate markers of olaparib response through basal mRNA gene expression and olaparib response association analysis of

pan-cancer cell lines that are replicated in the HGSOC cell lines. These candidates include PUM3 whose mRNA expression is strongly associated with increased sensitivity to olaparib and is known to interact with PARP1 by binding to its catalytic domain to reduce PARylation. *ELP4* and *EEF1A1* are also associated with olaparib sensitivity. ELP4 is an emerging HR repair factor that is known to form a complex with ELP5 and ELP6 which are also associated with olaparib sensitivity in pan-cancer cell lines and mutated in a borderline-sensitive HGSOC cell line respectively. Interestingly, ELP4, ELP5, and ELP6 share a RecA ATPase-like protein domain that is also found in the HR recombinase RAD51. EEF1A1 interacts with PARP1 and TXK to form a transcription factor that is specific for T helper 1 cells and promotes expression of IFNG. EEF1A1 is highly expressed in sensitive HGSOC cell lines but has low expression in resistant cell lines. Taken together, these candidates represent gene and variant level associations with *in vitro* olaparib response phenotype in model human cancer cell lines that bring new plausible mechanisms of sensitivity into focus and provide additional sources of sensitivity under the current concept of synthetic lethality.

Table 4.4.1. Candidate genomic markers of olaparib response derived from analyses of HGSOC cell lines and GDSC pan-cancer cell lines. Listed are the HGSOC cell lines that harbor resistance and sensitivity markers from both sources. Cell lines are arranged in order of increasing resistance from top to bottom. Cell lines above green line are sensitive, those below red line are resistant, and those between red and green lines are intermediate. [1]*BRCA2*-mutated (p.Glu1953*), [2]*BRCA1*-mutated (c.4548-1G>T), [3]CDKN2A p.Cys100*(p16).

Source	**HGSOC cell lines**					**GDSC pan-cancer cell lines**		
Association	**Sensitivity**			**Resistance**		**Sensitivity**		**Resistance**
Candidate marker	*PARP1* p.Val762Ala	*CDK2* p.Thr14Lys	*MPG* deletion or low expression	*RIF1* amplification	*SMAD4* p.Gln83* or p.Arg445*	*EEF1A1* high expression	*ELP4* p.Arg317Cys & *ELP6* p.Gln151Arg	*PUM3* deletion and low expression
Cell line								
OV2295_P61			+			+		
[1]OV4453-1_P63			+			+		
TOV1946_P49			+			+		
TOV3041G_P52	+	+						
OV1946_P49			+			+		
TOV2978G_P67	+						+	
TOV3133G_P65								
OV3133_P71								
[2]OV4485_P60					+			
TOV2295_P57								
TOV3291G_P65								
OV2295-2_P70								
TOV3133D_P66								
TOV2223G_P69								+
[3]OV90_P63					+			
OV866-2_P108								
TOV1369M_P65								+
OV1369-2_P66				+				+

Chapter 5: Conclusions and Future Directions

These results implicate new genes as potential biomarkers of olaparib response from genomic data analysis of two independent groups of cancer cell lines.

The candidate genes and variants presented in this thesis require further investigations to assess their value in predicting olaparib sensitivity and resistance. These candidates alone do not constitute all the genomic markers required for olaparib sensitivity or resistance. They must be integrated with other known markers such as *BRCA1/2* mutation and methylation status, HRD assays, *ABCB1* upregulation, 53BP1 inactivation, and *SLFN11* downregulation to help define the genomic and molecular profiles of olaparib responders and non-responders. Ultimately, therapeutic biomarkers are useful for selecting patients most likely to benefit from a treatment. To determine the potential utility of novel candidate markers presented in this thesis functional molecular characterization is required. Prior to the COVID-19 outbreak and subsequent decrease in research activity, we had started a collaboration with Dr. Alexandre Orthwein (Department of Oncology, McGill University) regarding experiments to investigate the effect of knockout of *ELP4* on *in vitro* olaparib response using cancer cell lines. Dr. Orthwein's lab were involved in the discovery of *ELP4* as a novel HR gene. Similarly, Dr. Jean Yves-Masson's lab (CHU de Québec, Université Laval) was interested in performing similar experiments targeting *PUM3*. However, no results have emerged from these collaborations yet to include in this thesis. The results of such investigations can inform the next steps for these candidates. Demonstrated effect of gene silencing on *in vitro* olaparib response can lead to further experiments to understand the mechanism of *PUM3*- or *ELP4* -mediation of olaparib response.

Additionally, genomic and clinical data analyses could provide information on the potential usefulness of these candidates. Investigation of pre- and post- olaparib treatment genomic data from patients' tumors for alterations in the candidate genes can help determine whether these findings may be relevant in clinical settings. This analysis can reveal whether candidate genes are differentially expressed or mutated between responsive and non-responsive patients especially those without *BRCA1/2* mutations, and whether candidate genes may be involved in acquired resistance. However, such genomic and clinical data for olaparib-treated patients are not publicly available like the TCGA data which were investigated in this thesis, as PARP inhibitors have only recently been introduced in the clinic.

Ultimately, the published results of this thesis can stimulate further research into olaparib, and other PARPi response, focusing on genomic and molecular alterations of *PUM3*, *EEF1A1* and *ELP4*.

Chapter 6: References

1. Fitzmaurice C, Akinyemiju TF, Al Lami FH, Alam T, Alizadeh-Navaei R, Allen C, Alsharif U, Alvis-Guzman N, Amini E, Anderson BO, Aremu O, Artaman A, Asgedom SW, et al. Global, Regional, and National Cancer Incidence, Mortality, Years of Life Lost, Years Lived With Disability, and Disability-Adjusted Life-Years for 29 Cancer Groups, 1990 to 2016. JAMA Oncol. American Medical Association; 2018; 4: 1553. doi: 10.1001/jamaoncol.2018.2706.
2. Canadian Cancer Statistics Advisory Committee. Canadian Cancer Statistics 2019 [Internet]. Toronto, ON; 2019. Available from https://www.cancer.ca/~/media/cancer.ca/CW/cancer information/cancer 101/Canadian cancer statistics/Canadian-Cancer-Statistics-2019-EN.pdf?la=en
3. Prat J. Ovarian carcinomas: five distinct diseases with different origins, genetic alterations, and clinicopathological features. Virchows Arch. Springer-Verlag; 2012; 460: 237–49. doi: 10.1007/s00428-012-1203-5.
4. Pal T, Permuth-Wey J, Betts JA, Krischer JP, Fiorica J, Arango H, LaPolla J, Hoffman M, Martino MA, Wakeley K, Wilbanks G, Nicosia S, Cantor A, et al. *BRCA1* and *BRCA2* mutations account for a large proportion of ovarian carcinoma cases. Cancer. John Wiley & Sons, Ltd; 2005; 104: 2807–16. doi: 10.1002/cncr.21536.
5. Zhang S, Royer R, Li S, McLaughlin JR, Rosen B, Risch HA, Fan I, Bradley L, Shaw PA, Narod SA. Frequencies of BRCA1 and BRCA2 mutations among 1,342 unselected patients with invasive ovarian cancer. Gynecol Oncol. Academic Press; 2011; 121: 353–7. doi: 10.1016/J.YGYNO.2011.01.020.
6. Walsh T, Casadei S, Lee MK, Pennil CC, Nord AS, Thornton AM, Roeb W, Agnew KJ, Stray SM, Wickramanayake A, Norquist B, Pennington KP, Garcia RL, et al. Mutations in 12 genes for inherited ovarian, fallopian tube, and peritoneal carcinoma identified by massively parallel sequencing. Proc Natl Acad Sci U S A. National Academy of Sciences; 2011; 108: 18032–7. doi: 10.1073/pnas.1115052108.
7. Pennington KP, Swisher EM. Hereditary ovarian cancer: Beyond the usual suspects. Gynecol Oncol. Academic Press; 2012; 124: 347–53. doi:

10.1016/J.YGYNO.2011.12.415.

8. Hollis RL, Gourley C. Genetic and molecular changes in ovarian cancer. Cancer Biol Med. Chinese Anti-Cancer Association; 2016; 13: 236–47. doi: 10.20892/j.issn.2095-3941.2016.0024.
9. Matulonis UA, Sood AK, Fallowfield L, Howitt BE, Sehouli J, Karlan BY. Ovarian cancer. Nat Rev Dis Prim. Nature Publishing Group; 2016; 2: 16061. doi: 10.1038/nrdp.2016.61.
10. Jayson GC, Kohn EC, Kitchener HC, Ledermann JA. Ovarian cancer. Lancet (London, England). Elsevier; 2014; 384: 1376–88. doi: 10.1016/S0140-6736(13)62146-7.
11. Thorstenson YR, Roxas A, Kroiss R, Jenkins MA, Yu KM, Bachrich T, Muhr D, Wayne TL, Chu G, Davis RW, Wagner TMU, Oefner PJ. Contributions of ATM mutations to familial breast and ovarian cancer. Cancer Res. American Association for Cancer Research; 2003; 63: 3325–33. Available from http://www.ncbi.nlm.nih.gov/pubmed/12810666
12. Engel C, Loeffler M, Steinke V, Rahner N, Holinski-Feder E, Dietmaier W, Schackert HK, Goergens H, von Knebel Doeberitz M, Goecke TO, Schmiegel W, Buettner R, Moeslein G, et al. Risks of less common cancers in proven mutation carriers with lynch syndrome. J Clin Oncol. American Society of Clinical Oncology; 2012; 30: 4409–15. doi: 10.1200/JCO.2012.43.2278.
13. Crispens MA. Endometrial and ovarian cancer in lynch syndrome. Clin Colon Rectal Surg. Thieme Medical Publishers; 2012; 25: 97–102. doi: 10.1055/s-0032-1313780.
14. Cancer Genome Atlas Research Network TCGAR. Integrated genomic analyses of ovarian carcinoma. Nature. NIH Public Access; 2011; 474: 609–15. doi: 10.1038/nature10166.
15. Kuhn E, Kurman RJ, Vang R, Sehdev AS, Han G, Soslow R, Wang T-L, Shih I-M. TP53 mutations in serous tubal intraepithelial carcinoma and concurrent pelvic high-grade serous carcinoma--evidence supporting the clonal relationship of the two lesions. J Pathol. NIH Public Access; 2012; 226: 421–6. doi: 10.1002/path.3023.

16. Ahmed AA, Etemadmoghadam D, Temple J, Lynch AG, Riad M, Sharma R, Stewart C, Fereday S, Caldas C, Defazio A, Bowtell D, Brenton JD. Driver mutations in TP53 are ubiquitous in high grade serous carcinoma of the ovary. J Pathol. Wiley-Blackwell; 2010; 221: 49–56. doi: 10.1002/path.2696.
17. Bowtell DD, Böhm S, Ahmed AA, Aspuria P-J, Bast RC, Beral V, Berek JS, Birrer MJ, Blagden S, Bookman MA, Brenton JD, Chiappinelli KB, Martins FC, et al. Rethinking ovarian cancer II: reducing mortality from high-grade serous ovarian cancer. Nat Rev Cancer. Nature Publishing Group; 2015; 15: 668–79. doi: 10.1038/nrc4019.
18. Tian C, Markman M, Zaino R, Ozols RF, McGuire WP, Muggia FM, Rose PG, Spriggs D, Armstrong DK. CA-125 change after chemotherapy in prediction of treatment outcome among advanced mucinous and clear cell epithelial ovarian cancers: a Gynecologic Oncology Group study. Cancer. NIH Public Access; 2009; 115: 1395–403. doi: 10.1002/cncr.24152.
19. Kobayashi H, Yamada Y, Sado T, Sakata M, Yoshida S, Kawaguchi R, Kanayama S, Shigetomi H, Haruta S, Tsuji Y, Ueda S, Kitanaka T. A randomized study of screening for ovarian cancer: a multicenter study in Japan. Int J Gynecol Cancer. BMJ Specialist Journals; 2008; 18: 414–20. doi: 10.1111/j.1525-1438.2007.01035.x.
20. Jacobs IJ, Skates SJ, MacDonald N, Menon U, Rosenthal AN, Davies AP, Woolas R, Jeyarajah AR, Sibley K, Lowe DG, Oram DH. Screening for ovarian cancer: a pilot randomised controlled trial. Lancet. Elsevier; 1999; 353: 1207–10. doi: 10.1016/S0140-6736(98)10261-1.
21. Prat J. Staging classification for cancer of the ovary, fallopian tube, and peritoneum. Int J Gynecol Obstet. John Wiley & Sons, Ltd; 2014; 124: 1–5. doi: 10.1016/j.ijgo.2013.10.001.
22. Horowitz NS, Miller A, Rungruang B, Richard SD, Rodriguez N, Bookman MA, Hamilton CA, Krivak TC, Maxwell GL. Does Aggressive Surgery Improve Outcomes? Interaction Between Preoperative Disease Burden and Complex Surgery in Patients With Advanced-Stage Ovarian Cancer: An Analysis of GOG 182. J Clin Oncol. American Society of Clinical Oncology; 2015; 33: 937. doi:

10.1200/JCO.2014.56.3106.

23. Chang S-J, Hodeib M, Chang J, Bristow RE. Survival impact of complete cytoreduction to no gross residual disease for advanced-stage ovarian cancer: a meta-analysis. Gynecol Oncol. Elsevier; 2013; 130: 493–8. doi: 10.1016/j.ygyno.2013.05.040.
24. Armstrong DK, Bundy B, Wenzel L, Huang HQ, Baergen R, Lele S, Copeland LJ, Walker JL, Burger RA. Intraperitoneal Cisplatin and Paclitaxel in Ovarian Cancer. N Engl J Med. Massachusetts Medical Society; 2006; 354: 34–43. doi: 10.1056/NEJMoa052985.
25. Katsumata N, Yasuda M, Takahashi F, Isonishi S, Jobo T, Aoki D, Tsuda H, Sugiyama T, Kodama S, Kimura E, Ochiai K, Noda K. Dose-dense paclitaxel once a week in combination with carboplatin every 3 weeks for advanced ovarian cancer: a phase 3, open-label, randomised controlled trial. Lancet. Elsevier; 2009; 374: 1331–8. doi: 10.1016/S0140-6736(09)61157-0.
26. Katsumata N, Yasuda M, Isonishi S, Takahashi F, Michimae H, Kimura E, Aoki D, Jobo T, Kodama S, Terauchi F, Sugiyama T, Ochiai K. Long-term results of dose-dense paclitaxel and carboplatin versus conventional paclitaxel and carboplatin for treatment of advanced epithelial ovarian, fallopian tube, or primary peritoneal cancer (JGOG 3016): a randomised, controlled, open-label trial. Lancet Oncol. Elsevier; 2013; 14: 1020–6. doi: 10.1016/S1470-2045(13)70363-2.
27. Kelland L. The resurgence of platinum-based cancer chemotherapy. Nat Rev Cancer. Nature Publishing Group; 2007; 7: 573–84. doi: 10.1038/nrc2167.
28. Fichtinger-Schepman AMJ, Van der Veer JL, Den Hartog JHJ, Lohman PHM, Reedijk J. Adducts of the antitumor drug cis-diamminedichloroplatinum(II) with DNA: formation, identification, and quantitation. Biochemistry. American Chemical Society; 1985; 24: 707–13. doi: 10.1021/bi00324a025.
29. Chaney SG, Campbell SL, Temple B, Bassett E, Wu Y, Faldu M. Protein interactions with platinum–DNA adducts: from structure to function. J Inorg Biochem. Elsevier; 2004; 98: 1551–9. doi: 10.1016/J.JINORGBIO.2004.04.024.
30. Schaeppi U, Heyman IA, Fleischman RW, Rosenkrantz H, Ilievski V, Phelan R, Cooney DA, Davis RD. cis-Dichlorodiammineplatinum(II) (NSC-119 875):

Preclinical toxicologic evaluation of intravenous injection in dogs, monkeys and mice. Toxicol Appl Pharmacol. Academic Press; 1973; 25: 230–41. doi: 10.1016/S0041-008X(73)80009-2.

31. DeConti RC, Toftness BR, Lange RC, Creasey WA. Clinical and Pharmacological Studies with cis-Diamminedichloroplatinum (II). Cancer Res. 1973; 33: 1310–5. Available from https://cancerres.aacrjournals.org/content/33/6/1310.full-text.pdf
32. Cvitkovic E, Spaulding J, Bethune V, Martin J, Whitmore WF. Improvement of Cis-dichlorodiammineplatinum (NSC 119875): Therapeutic index in an animal model. Cancer. 1977; 39: 1357–61. doi: 10.1002/1097-0142(197704)39:4<1357::AID-CNCR2820390402>3.0.CO;2-C.
33. Harrap KR. Preclinical studies identifying carboplatin as a viable cisplatin alternative. Cancer Treat Rev. Elsevier; 1985; 12 Suppl A: 21–33. doi: 10.1016/0305-7372(85)90015-5.
34. Knox RJ, Friedlos F, Lydall DA, Roberts JJ. Mechanism of cytotoxicity of anticancer platinum drugs: evidence that cis-diamminedichloroplatinum(II) and cis-diammine-(1,1-cyclobutanedicarboxylato)platinum(II) differ only in the kinetics of their interaction with DNA. Cancer Res. American Association for Cancer Research; 1986; 46: 1972–9. Available from http://www.ncbi.nlm.nih.gov/pubmed/3512077
35. Aabo K, Adams M, Adnitt P, Alberts D, Athanazziou A, Barley V, Bell D, Bianchi U, Bolis G, Brady M, Brodovsky H, Bruckner H, Buyse M, et al. Chemotherapy in advanced ovarian cancer: four systematic meta-analyses of individual patient data from 37 randomized trials. Br J Cancer. Nature Publishing Group; 1998; 78: 1479–87. doi: 10.1038/bjc.1998.710.
36. Galluzzi L, Senovilla L, Vitale I, Michels J, Martins I, Kepp O, Castedo M, Kroemer G. Molecular mechanisms of cisplatin resistance. Oncogene. Nature Publishing Group; 2012; 31: 1869–83. doi: 10.1038/onc.2011.384.
37. McGuire WP, Rowinsky EK, Rosenhein NB, Grumbine FC, Ettinger DS, Armstrong DK, Donehower RC. Taxol: A unique antineoplastic agent with significant activity in advanced ovarian epithelial neoplasms. Ann Intern Med. 1989; 111: 273–9. doi: 10.7326/0003-4819-111-4-273.

38. Schiff PB, Horwitz SB. Taxol stabilizes microtubules in mouse fibroblast cells. Proc Natl Acad Sci U S A. National Academy of Sciences; 1980; 77: 1561–5. doi: 10.1073/pnas.77.3.1561.
39. Denis JN, Correa A, Greene AE. An improved synthesis of the taxol side chain and of RP 56976. J Org Chem. American Chemical Society; 1990; 55: 1957–9. doi: 10.1021/jo00293a052.
40. Kelland LR, Abel G. Comparative in vitro cytotoxicity of taxol and Taxotere against cisplatin-sensitive and-resistant human ovarian carcinoma cell lines. Cancer Chemother Pharmacol. Springer; 1992; 30: 444–50. doi: 10.1007/BF00685595.
41. Engblom P, Rantanen V, Kulmala J, Heiskanen J, Grenman S. Taxane sensitivity of ovarian carcinoma in vitro. Anticancer Res. 1997; 17: 2475–9. Available from http://www.ncbi.nlm.nih.gov/pubmed/9252666
42. Ringel I, Horwitz SB. Studies With RP 56976 (Taxotere): A Semisynthetic Analogue of Taxol. J Natl Cancer Inst. Narnia; 1991; 83: 288–91. doi: 10.1093/jnci/83.4.288.
43. Vasey PA, Jayson GC, Gordon A, Gabra H, Coleman R, Atkinson R, Parkin D, Paul J, Hay A, Kaye SB. Phase III Randomized Trial of Docetaxel-Carboplatin Versus Paclitaxel-Carboplatin as First-line Chemotherapy for Ovarian Carcinoma. J Natl Cancer Inst. Narnia; 2004; 96: 1682–91. doi: 10.1093/jnci/djh323.
44. du Bois A, Lück H-J, Meier W, Adams H-P, Möbus V, Costa S, Bauknecht T, Richter B, Warm M, Schröder W, Olbricht S, Nitz U, Jackisch C, et al. A Randomized Clinical Trial of Cisplatin/Paclitaxel Versus Carboplatin/Paclitaxel as First-Line Treatment of Ovarian Cancer. J Natl Cancer Inst. Narnia; 2003; 95: 1320–9. doi: 10.1093/jnci/djg036.
45. Ozols RF, Bundy BN, Greer BE, Fowler JM, Clarke-Pearson D, Burger RA, Mannel RS, DeGeest K, Hartenbach EM, Baergen R. Phase III Trial of Carboplatin and Paclitaxel Compared With Cisplatin and Paclitaxel in Patients With Optimally Resected Stage III Ovarian Cancer: A Gynecologic Oncology Group Study. J Clin Oncol. American Society of Clinical Oncology; 2003; 21: 3194–200. doi: 10.1200/JCO.2003.02.153.
46. McGuire WP, Hoskins WJ, Brady MF, Kucera PR, Partridge EE, Look KY, Clarke-

Pearson DL, Davidson M. Cyclophosphamide and cisplatin versus paclitaxel and cisplatin: a phase III randomized trial in patients with suboptimal stage III/IV ovarian cancer (from the Gynecologic Oncology Group). Semin Oncol. 1996; 23: 40–7. Available from http://www.ncbi.nlm.nih.gov/pubmed/8941409

47. Piccart MJ, Bertelsen K, James K, Cassidy J, Mangioni C, Simonsen E, Stuart G, Kaye S, Vergote I, Blom R, Grimshaw R, Atkinson RJ, Swenerton KD, et al. Randomized Intergroup Trial of Cisplatin-Paclitaxel Versus Cisplatin-Cyclophosphamide in Women With Advanced Epithelial Ovarian Cancer: Three-Year Results. J Natl Cancer Inst. Narnia; 2000; 92: 699–708. doi: 10.1093/jnci/92.9.699.
48. Patch A-M, Christie EL, Etemadmoghadam D, Garsed DW, George J, Fereday S, Nones K, Cowin P, Alsop K, Bailey PJ, Kassahn KS, Newell F, Quinn MCJ, et al. Whole–genome characterization of chemoresistant ovarian cancer. Nature. Nature Publishing Group; 2015; 521: 489–94. doi: 10.1038/nature14410.
49. Nakayama N, Nakayama K, Shamima Y, Ishikawa M, Katagiri A, Iida K, Miyazaki K. Gene amplification CCNE1 is related to poor survival and potential therapeutic target in ovarian cancer. Cancer. 2010; 116: 2621–34. doi: 10.1002/cncr.24987.
50. Bracken AP, Ciro M, Cocito A, Helin K. E2F target genes: unraveling the biology. Trends Biochem Sci. Elsevier Current Trends; 2004; 29: 409–17. doi: 10.1016/J.TIBS.2004.06.006.
51. Network TCGAR. Integrated genomic analyses of ovarian carcinoma. Nature. 2012; 474: 609–15. doi: 10.1038/nature10166.
52. Sakai W, Swisher EM, Karlan BY, Agarwal MK, Higgins J, Friedman C, Villegas E, Jacquemont C, Farrugia DJ, Couch FJ, Urban N, Taniguchi T. Secondary mutations as a mechanism of cisplatin resistance in BRCA2-mutated cancers. Nature. NIH Public Access; 2008; 451: 1116–20. doi: 10.1038/nature06633.
53. Stordal B, Hamon M, McEneaney V, Roche S, Gillet J-P, O'Leary JJ, Gottesman M, Clynes M. Resistance to paclitaxel in a cisplatin-resistant ovarian cancer cell line is mediated by P-glycoprotein. PLoS One. Public Library of Science; 2012; 7: e40717. doi: 10.1371/journal.pone.0040717.
54. Wils P, Phung-Ba V, Warnery A, Lechardeur D, Raeissi S, Hidalgo IJ, Scherman

D. Polarized transport of docetaxel and vinblastine mediated by P-glycoprotein in human intestinal epithelial cell monolayers. Biochem Pharmacol. Elsevier; 1994; 48: 1528–30. doi: 10.1016/0006-2952(94)90580-0.

55. Dalton WS, Durie BG, Alberts DS, Gerlach JH, Cress AE. Characterization of a new drug-resistant human myeloma cell line that expresses P-glycoprotein. Cancer Res. American Association for Cancer Research; 1986; 46: 5125–30. Available from http://www.ncbi.nlm.nih.gov/pubmed/2875788
56. Chambon P, Weill JD, Doly J, Strosser MT, Mandel P. On the formation of a novel adenylic compound by enzymatic extracts of liver nuclei. Biochem Biophys Res Commun. Academic Press; 1966; 25: 638–43. doi: 10.1016/0006-291X(66)90502-X.
57. de Murcia G, de Murcia JM. Poly(ADP-ribose) polymerase: a molecular nick-sensor [Internet]. Trends in Biochemical Sciences. Trends Biochem Sci; 1994. p. 172–6. doi: 10.1016/0968-0004(94)90280-1.
58. d'AMOURS D, DESNOYERS S, d'SILVA I, POIRIER GG. Poly(ADP-ribosyl)ation reactions in the regulation of nuclear functions. Biochem J. Portland Press Ltd.; 1999; 342: 249–68. doi: 10.1042/bj3420249.
59. Murai J, Huang SN, Das BB, Renaud A, Zhang Y, Doroshow JH, Ji J, Takeda S, Pommier Y. Trapping of PARP1 and PARP2 by Clinical PARP Inhibitors. Cancer Res. NIH Public Access; 2012; 72: 5588–99. doi: 10.1158/0008-5472.CAN-12-2753.
60. Murai J, Huang S-YN, Renaud A, Zhang Y, Ji J, Takeda S, Morris J, Teicher B, Doroshow JH, Pommier Y. Stereospecific PARP trapping by BMN 673 and comparison with olaparib and rucaparib. Mol Cancer Ther. NIH Public Access; 2014; 13: 433–43. doi: 10.1158/1535-7163.MCT-13-0803.
61. Murai J, Pommier Y. PARP Trapping Beyond Homologous Recombination and Platinum Sensitivity in Cancers. Annu Rev Cancer Biol. Annual Reviews ; 2019; 3: 131–50. doi: 10.1146/annurev-cancerbio-030518-055914.
62. Farmer H, McCabe N, Lord CJ, Tutt ANJ, Johnson DA, Richardson TB, Santarosa M, Dillon KJ, Hickson I, Knights C, Martin NMB, Jackson SP, Smith GCM, et al. Targeting the DNA repair defect in BRCA mutant cells as a therapeutic strategy.

Nature. Nature Publishing Group; 2005; 434: 917–21. doi: 10.1038/nature03445.

63. Bryant HE, Schultz N, Thomas HD, Parker KM, Flower D, Lopez E, Kyle S, Meuth M, Curtin NJ, Helleday T. Specific killing of BRCA2-deficient tumours with inhibitors of poly(ADP-ribose) polymerase. Nature. 2005; 434: 913–7. doi: 10.1038/nature03443.
64. Rottenberg S, Jaspers JE, Kersbergen A, van der Burg E, Nygren AOH, Zander SAL, Derksen PWB, de Bruin M, Zevenhoven J, Lau A, Boulter R, Cranston A, O'Connor MJ, et al. High sensitivity of BRCA1-deficient mammary tumors to the PARP inhibitor AZD2281 alone and in combination with platinum drugs. Proc Natl Acad Sci U S A. National Academy of Sciences; 2008; 105: 17079–84. doi: 10.1073/pnas.0806092105.
65. Hay T, Matthews JR, Pietzka L, Lau A, Cranston A, Nygren AOH, Douglas-Jones A, Smith GCM, Martin NMB, O'connor M, Clarke AR. Poly(ADP-ribose) polymerase-1 inhibitor treatment regresses autochthonous brca2/p53-mutant mammary tumors in vivo and delays tumor relapse in combination with carboplatin. Cancer Res. 2009; 69: 3850–5. doi: 10.1158/0008-5472.CAN-08-2388.
66. Fong PC, Boss DS, Yap TA, Tutt A, Wu P, Mergui-Roelvink M, Mortimer P, Swaisland H, Lau A, O'Connor MJ, Ashworth A, Carmichael J, Kaye SB, et al. Inhibition of Poly(ADP-Ribose) Polymerase in Tumors from *BRCA* Mutation Carriers. N Engl J Med. Massachusetts Medical Society ; 2009; 361: 123–34. doi: 10.1056/NEJMoa0900212.
67. Ledermann J, Harter P, Gourley C, Friedlander M, Vergote I, Rustin G, Scott C, Meier W, Shapira-Frommer R, Safra T, Matei D, Macpherson E, Watkins C, et al. Olaparib Maintenance Therapy in Platinum-Sensitive Relapsed Ovarian Cancer. N Engl J Med. Massachusetts Medical Society ; 2012; 366: 1382–92. doi: 10.1056/NEJMoa1105535.
68. Ledermann J, Harter P, Gourley C, Friedlander M, Vergote I, Rustin G, Scott CL, Meier W, Shapira-Frommer R, Safra T, Matei D, Fielding A, Spencer S, et al. Olaparib maintenance therapy in patients with platinum-sensitive relapsed serous ovarian cancer: a preplanned retrospective analysis of outcomes by BRCA status

in a randomised phase 2 trial. Lancet Oncol. Elsevier; 2014; 15: 852–61. doi: 10.1016/S1470-2045(14)70228-1.

69. Pujade-Lauraine E, Ledermann JA, Selle F, Gebski V, Penson RT, Oza AM, Korach J, Huzarski T, Poveda A, Pignata S, Friedlander M, Colombo N, Harter P, et al. Olaparib tablets as maintenance therapy in patients with platinum-sensitive, relapsed ovarian cancer and a BRCA1/2 mutation (SOLO2/ENGOT-Ov21): a double-blind, randomised, placebo-controlled, phase 3 trial. Lancet Oncol. Elsevier; 2017; 18: 1274–84. doi: 10.1016/S1470-2045(17)30469-2.
70. Moore K, Colombo N, Scambia G, Kim B-G, Oaknin A, Friedlander M, Lisyanskaya A, Floquet A, Leary A, Sonke GS, Gourley C, Banerjee S, Oza A, et al. Maintenance Olaparib in Patients with Newly Diagnosed Advanced Ovarian Cancer. N Engl J Med. Massachusetts Medical Society; 2018; 379: 2495–505. doi: 10.1056/NEJMoa1810858.
71. Robson M, Im S-A, Senkus E, Xu B, Domchek SM, Masuda N, Delaloge S, Li W, Tung N, Armstrong A, Wu W, Goessl C, Runswick S, et al. Olaparib for Metastatic Breast Cancer in Patients with a Germline *BRCA* Mutation. N Engl J Med. Massachusetts Medical Society; 2017; 377: 523–33. doi: 10.1056/NEJMoa1706450.
72. Golan T, Hammel P, Reni M, Van Cutsem E, Macarulla T, Hall MJ, Park J-O, Hochhauser D, Arnold D, Oh D-Y, Reinacher-Schick A, Tortora G, Algül H, et al. Maintenance Olaparib for Germline *BRCA* -Mutated Metastatic Pancreatic Cancer. N Engl J Med. Massachusetts Medical Society; 2019; 381: 317–27. doi: 10.1056/NEJMoa1903387.
73. Robinson D, Van Allen EM, Wu Y-M, Schultz N, Lonigro RJ, Mosquera J-M, Montgomery B, Taplin M-E, Pritchard CC, Attard G, Beltran H, Abida W, Bradley RK, et al. Integrative clinical genomics of advanced prostate cancer. Cell. NIH Public Access; 2015; 161: 1215–28. doi: 10.1016/j.cell.2015.05.001.
74. Pritchard CC, Mateo J, Walsh MF, De Sarkar N, Abida W, Beltran H, Garofalo A, Gulati R, Carreira S, Eeles R, Elemento O, Rubin MA, Robinson D, et al. Inherited DNA-Repair Gene Mutations in Men with Metastatic Prostate Cancer. N Engl J Med. Massachusetts Medical Society; 2016; 375: 443–53. doi:

10.1056/NEJMoa1603144.

75. Oza AM, Tinker A V., Oaknin A, Shapira-Frommer R, McNeish IA, Swisher EM, Ray-Coquard I, Bell-McGuinn K, Coleman RL, O'Malley DM, Leary A, Chen L, Provencher D, et al. Antitumor activity and safety of the PARP inhibitor rucaparib in patients with high-grade ovarian carcinoma and a germline or somatic BRCA1 or BRCA2 mutation: Integrated analysis of data from Study 10 and ARIEL2. Gynecol Oncol. Academic Press; 2017; 147: 267–75. doi: 10.1016/J.YGYNO.2017.08.022.
76. Learn About TALZENNA® (talazoparib) | Safety Info [Internet]. Available 2020 Aug 14, from https://www.talzenna.com/about-talzenna
77. Chatterjee N, Walker GC. Mechanisms of DNA damage, repair, and mutagenesis. Environ Mol Mutagen. NIH Public Access; 2017; 58: 235–63. doi: 10.1002/em.22087.
78. Knijnenburg TA, Wang L, Zimmermann MT, Chambwe N, Gao GF, Cherniack AD, Fan H, Shen H, Way GP, Greene CS, Liu Y, Akbani R, Feng B, et al. Genomic and Molecular Landscape of DNA Damage Repair Deficiency across The Cancer Genome Atlas. Cell Rep. Elsevier; 2018; 23: 239-254.e6. doi: 10.1016/j.celrep.2018.03.076.
79. Kaina B, Christmann M, Naumann S, Roos WP. MGMT: Key node in the battle against genotoxicity, carcinogenicity and apoptosis induced by alkylating agents. DNA Repair (Amst). 2007; . doi: 10.1016/j.dnarep.2007.03.008.
80. Drabløs F, Feyzi E, Aas PA, Vaagbø CB, Kavli B, Bratlie MS, Peña-Diaz J, Otterlei M, Slupphaug G, Krokan HE. Alkylation damage in DNA and RNA—repair mechanisms and medical significance. DNA Repair (Amst). Elsevier; 2004; 3: 1389–407. doi: 10.1016/J.DNAREP.2004.05.004.
81. Falnes PØ, Klungland A, Alseth I. Repair of methyl lesions in DNA and RNA by oxidative demethylation. Neuroscience. Pergamon; 2007; 145: 1222–32. doi: 10.1016/J.NEUROSCIENCE.2006.11.018.
82. Odell ID, Wallace SS, Pederson DS. Rules of engagement for base excision repair in chromatin. J Cell Physiol. John Wiley & Sons, Ltd; 2013; 228: 258–66. doi: 10.1002/jcp.24134.

83. Chakravarti D, Ibeanu GC, Tano K, Mitra S. Cloning and expression in Escherichia coli of a human cDNA encoding the DNA repair protein N-methylpurine-DNA glycosylase. J Biol Chem. 1991; 266: 15710–5. Available from http://www.ncbi.nlm.nih.gov/pubmed/1874728
84. Almeida KH, Sobol RW. A unified view of base excision repair: lesion-dependent protein complexes regulated by post-translational modification. DNA Repair (Amst). NIH Public Access; 2007; 6: 695–711. doi: 10.1016/j.dnarep.2007.01.009.
85. Svilar D, Goellner EM, Almeida KH, Sobol RW. Base excision repair and lesion-dependent subpathways for repair of oxidative DNA damage. Antioxid Redox Signal. Mary Ann Liebert, Inc.; 2011; 14: 2491–507. doi: 10.1089/ars.2010.3466.
86. Wakasugi M, Kawashima A, Morioka H, Linn S, Sancar A, Mori T, Nikaido O, Matsunaga T. DDB Accumulates at DNA Damage Sites Immediately after UV Irradiation and Directly Stimulates Nucleotide Excision Repair. J Biol Chem. American Society for Biochemistry and Molecular Biology; 2002; 277: 1637–40. doi: 10.1074/JBC.C100610200.
87. Scrima A, Konícková R, Czyzewski BK, Kawasaki Y, Jeffrey PD, Groisman R, Nakatani Y, Iwai S, Pavletich NP, Thomä NH. Structural basis of UV DNA-damage recognition by the DDB1-DDB2 complex. Cell. Howard Hughes Medical Institute; 2008; 135: 1213–23. doi: 10.1016/j.cell.2008.10.045.
88. Marteijn JA, Lans H, Vermeulen W, Hoeijmakers JHJ. Understanding nucleotide excision repair and its roles in cancer and ageing. Nat Rev Mol Cell Biol. Nature Publishing Group; 2014; 15: 465–81. doi: 10.1038/nrm3822.
89. Jung Y, Lippard SJ. Direct Cellular Responses to Platinum-Induced DNA Damage. Chem Rev. American Chemical Society; 2007; 107: 1387–407. doi: 10.1021/CR068207J.
90. Jamieson ER, Lippard SJ. Structure, Recognition, and Processing of Cisplatin−DNA Adducts. Chem Rev. American Chemical Society; 1999; 99: 2467–98. doi: 10.1021/CR980421N.
91. Jiricny J. The multifaceted mismatch-repair system. Nat Rev Mol Cell Biol. Nature Publishing Group; 2006; 7: 335–46. doi: 10.1038/nrm1907.
92. Palombo F, Iaccarino I, Nakajima E, Ikejima M, Shimada T, Jiricny J. hMutSβ, a

heterodimer of hMSH2 and hMSH3, binds to insertion/deletion loops in DNA. Curr Biol. Cell Press; 1996; 6: 1181–4. doi: 10.1016/S0960-9822(02)70685-4.

93. Marra G, Iaccarino I, Lettieri T, Roscilli G, Delmastro P, Jiricny J. Mismatch repair deficiency associated with overexpression of the MSH3 gene. Proc Natl Acad Sci U S A. National Academy of Sciences; 1998; 95: 8568–73. doi: 10.1073/pnas.95.15.8568.
94. Ceccaldi R, Sarangi P, D'Andrea AD. The Fanconi anaemia pathway: new players and new functions. Nat Rev Mol Cell Biol. Nature Publishing Group; 2016; 17: 337–49. doi: 10.1038/nrm.2016.48.
95. Kee Y, D'Andrea AD. Molecular pathogenesis and clinical management of Fanconi anemia. J Clin Invest. American Society for Clinical Investigation; 2012; 122: 3799–806. doi: 10.1172/JCI58321.
96. Clauson C, Schärer OD, Niedernhofer L. Advances in understanding the complex mechanisms of DNA interstrand cross-link repair. Cold Spring Harb Perspect Biol. Cold Spring Harbor Laboratory Press; 2013; 5: a012732. doi: 10.1101/cshperspect.a012732.
97. Long DT, Räschle M, Joukov V, Walter JC. Mechanism of RAD51-dependent DNA interstrand cross-link repair. Science. American Association for the Advancement of Science; 2011; 333: 84–7. doi: 10.1126/science.1204258.
98. Zhou B-L, Pata JD, Steitz TA. Crystal Structure of a DinB Lesion Bypass DNA Polymerase Catalytic Fragment Reveals a Classic Polymerase Catalytic Domain. Mol Cell. Cell Press; 2001; 8: 427–37. doi: 10.1016/S1097-2765(01)00310-0.
99. Washington MT, Johnson RE, Prakash L, Prakash S. Human DINB1-encoded DNA polymerase kappa is a promiscuous extender of mispaired primer termini. Proc Natl Acad Sci U S A. National Academy of Sciences; 2002; 99: 1910–4. doi: 10.1073/pnas.032594399.
100. Wojtaszek J, Lee C-J, D'Souza S, Minesinger B, Kim H, D'Andrea AD, Walker GC, Zhou P. Structural basis of Rev1-mediated assembly of a quaternary vertebrate translesion polymerase complex consisting of Rev1, heterodimeric polymerase (Pol) ζ, and Pol κ. J Biol Chem. American Society for Biochemistry and Molecular Biology; 2012; 287: 33836–46. doi: 10.1074/jbc.M112.394841.

101. Xie K, Doles J, Hemann MT, Walker GC. Error-prone translesion synthesis mediates acquired chemoresistance. Proc Natl Acad Sci U S A. National Academy of Sciences; 2010; 107: 20792–7. doi: 10.1073/pnas.1011412107.
102. Okuda T, Lin X, Trang J, Howell SB. Suppression of hREV1 expression reduces the rate at which human ovarian carcinoma cells acquire resistance to cisplatin. Mol Pharmacol. American Society for Pharmacology and Experimental Therapeutics; 2005; 67: 1852–60. doi: 10.1124/mol.104.010579.
103. Braun SA, Panzeter PL, Collinge MA, Althaus FR. Endoglycosidic cleavage of branched polymers by poly(ADP-ribose) glycohydrolase. Eur J Biochem. 1994; 220: 369–75. doi: 10.1111/j.1432-1033.1994.tb18633.x.
104. Brochu G, Duchaine C, Thibeault L, Lagueux J, Shah GM, Poirier GG. Mode of action of poly(ADP-ribose) glycohydrolase. Biochim Biophys Acta - Gene Struct Expr. Elsevier; 1994; 1219: 342–50. doi: 10.1016/0167-4781(94)90058-2.
105. Zhu C, Mills KD, Ferguson DO, Lee C, Manis J, Fleming J, Gao Y, Morton CC, Alt FW. Unrepaired DNA Breaks in p53-Deficient Cells Lead to Oncogenic Gene Amplification Subsequent to Translocations. Cell. Cell Press; 2002; 109: 811–21. doi: 10.1016/S0092-8674(02)00770-5.
106. Chou DM, Adamson B, Dephoure NE, Tan X, Nottke AC, Hurov KE, Gygi SP, Colaiácovo MP, Elledge SJ. A chromatin localization screen reveals poly (ADP ribose)-regulated recruitment of the repressive polycomb and NuRD complexes to sites of DNA damage. Proc Natl Acad Sci U S A. National Academy of Sciences; 2010; 107: 18475–80. doi: 10.1073/pnas.1012946107.
107. Ahel D, Hořejší Z, Wiechens N, Polo SE, Garcia-Wilson E, Ahel I, Flynn H, Skehel M, West SC, Jackson SP, Owen-Hughes T, Boulton SJ. Poly(ADP-ribose)-dependent regulation of DNA repair by the chromatin remodelling enzyme ALC1. Science. Europe PMC Funders; 2009; 325: 1240. doi: 10.1126/SCIENCE.1177321.
108. Li M, Yu X. Function of BRCA1 in the DNA damage response is mediated by ADP-ribosylation. Cancer Cell. Elsevier; 2013; 23: 693–704. doi: 10.1016/j.ccr.2013.03.025.
109. Bothmer A, Robbiani DF, Feldhahn N, Gazumyan A, Nussenzweig A,

Nussenzweig MC. 53BP1 regulates DNA resection and the choice between classical and alternative end joining during class switch recombination. J Exp Med. The Rockefeller University Press; 2010; 207: 855–65. doi: 10.1084/jem.20100244.

110. Bunting SF, Callén E, Wong N, Chen H-T, Polato F, Gunn A, Bothmer A, Feldhahn N, Fernandez-Capetillo O, Cao L, Xu X, Deng C-X, Finkel T, et al. 53BP1 inhibits homologous recombination in Brca1-deficient cells by blocking resection of DNA breaks. Cell. NIH Public Access; 2010; 141: 243–54. doi: 10.1016/j.cell.2010.03.012.
111. Chapman JR, Sossick AJ, Boulton SJ, Jackson SP. BRCA1-associated exclusion of 53BP1 from DNA damage sites underlies temporal control of DNA repair. J Cell Sci. 2012; 125: 3529–34. doi: 10.1242/jcs.105353.
112. Ma Y, Pannicke U, Schwarz K, Lieber MR. Hairpin opening and overhang processing by an Artemis/DNA-dependent protein kinase complex in nonhomologous end joining and V(D)J recombination. Cell. Elsevier; 2002; 108: 781–94. doi: 10.1016/s0092-8674(02)00671-2.
113. Bernstein NK, Williams RS, Rakovszky ML, Cui D, Green R, Karimi-Busheri F, Mani RS, Galicia S, Koch CA, Cass CE, Durocher D, Weinfeld M, Glover JNM. The Molecular Architecture of the Mammalian DNA Repair Enzyme, Polynucleotide Kinase. Mol Cell. Cell Press; 2005; 17: 657–70. doi: 10.1016/J.MOLCEL.2005.02.012.
114. Ahel I, Rass U, El-Khamisy SF, Katyal S, Clements PM, McKinnon PJ, Caldecott KW, West SC. The neurodegenerative disease protein aprataxin resolves abortive DNA ligation intermediates. Nature. Nature Publishing Group; 2006; 443: 713–6. doi: 10.1038/nature05164.
115. Chen L, Nievera CJ, Lee AY-L, Wu X. Cell cycle-dependent complex formation of BRCA1.CtIP.MRN is important for DNA double-strand break repair. J Biol Chem. American Society for Biochemistry and Molecular Biology; 2008; 283: 7713–20. doi: 10.1074/jbc.M710245200.
116. Nimonkar A V., Genschel J, Kinoshita E, Polaczek P, Campbell JL, Wyman C, Modrich P, Kowalczykowski SC. BLM–DNA2–RPA–MRN and EXO1–BLM–RPA–

MRN constitute two DNA end resection machineries for human DNA break repair. Genes Dev. Cold Spring Harbor Laboratory Press; 2011; 25: 350–62. doi: 10.1101/GAD.2003811.

117. Zhang F, Fan Q, Ren K, Andreassen PR. PALB2 Functionally Connects the Breast Cancer Susceptibility Proteins BRCA1 and BRCA2. Mol Cancer Res. American Association for Cancer Research; 2009; 7: 1110–8. doi: 10.1158/1541-7786.MCR-09-0123.
118. Taylor MRG, Špírek M, Chaurasiya KR, Ward JD, Carzaniga R, Yu X, Egelman EH, Collinson LM, Rueda D, Krejci L, Boulton SJ. Rad51 Paralogs Remodel Pre-synaptic Rad51 Filaments to Stimulate Homologous Recombination. Cell. Elsevier; 2015; 162: 271–86. doi: 10.1016/j.cell.2015.06.015.
119. Li X, Stith CM, Burgers PM, Heyer W-D. PCNA is required for initiation of recombination-associated DNA synthesis by DNA polymerase delta. Mol Cell. Elsevier; 2009; 36: 704–13. doi: 10.1016/j.molcel.2009.09.036.
120. Rass U, Compton SA, Matos J, Singleton MR, Ip SCY, Blanco MG, Griffith JD, West SC. Mechanism of Holliday junction resolution by the human GEN1 protein. Genes Dev. Cold Spring Harbor Laboratory Press; 2010; 24: 1559–69. doi: 10.1101/gad.585310.
121. Fekairi S, Scaglione S, Chahwan C, Taylor ER, Tissier A, Coulon S, Dong M-Q, Ruse C, Yates JR, Russell P, Fuchs RP, McGowan CH, Gaillard P-HL, et al. Human SLX4 is a Holliday junction resolvase subunit that binds multiple DNA repair/recombination endonucleases. Cell. NIH Public Access; 2009; 138: 78–89. doi: 10.1016/j.cell.2009.06.029.
122. Zapotoczny G, Sekelsky J. Human Cell Assays for Synthesis-Dependent Strand Annealing and Crossing over During Double-Strand Break Repair. G3 Genes, Genomes, Genet. G3: Genes, Genomes, Genetics; 2017; 7: 1191–9. doi: 10.1534/G3.116.037390.
123. Pennington KP, Walsh T, Harrell MI, Lee MK, Pennil CC, Rendi MH, Thornton A, Norquist BM, Casadei S, Nord AS, Agnew KJ, Pritchard CC, Scroggins S, et al. Germline and somatic mutations in homologous recombination genes predict platinum response and survival in ovarian, fallopian tube, and peritoneal

carcinomas. Clin cancer Res. American Association for Cancer Research; 2014; 20: 764–75. doi: 10.1158/1078-0432.CCR-13-2287.

124. Mukhopadhyay A, Plummer ER, Elattar A, Soohoo S, Uzir B, Quinn JE, McCluggage WG, Maxwell P, Aneke H, Curtin NJ, Edmondson RJ. Clinicopathological features of homologous recombination-deficient epithelial ovarian cancers: Sensitivity to PARP inhibitors, platinum, and survival. Cancer Res. American Association for Cancer Research; 2012; 72: 5675–82. doi: 10.1158/0008-5472.CAN-12-0324.
125. Daza-Martin M, Starowicz K, Jamshad M, Tye S, Ronson GE, Mackay HL, Singh Chauhan A, Walker AK, Stone HR, Beesley JFJ, Coles JL, Garvin AJ, Stewart GS, et al. Isomerization of BRCA1-BARD1 promotes replication fork protection Phosphorylation of BRCA1 S114 promotes fork protection. Nature. doi: 10.1038/s41586-019-1363-4.
126. McCabe N, Turner NC, Lord CJ, Kluzek K, Białkowska A, Swift S, Giavara S, O'Connor MJ, Tutt AN, Zdzienicka MZ, Smith GCM, Ashworth A. Deficiency in the Repair of DNA Damage by Homologous Recombination and Sensitivity to Poly(ADP-Ribose) Polymerase Inhibition. Cancer Res. American Association for Cancer Research; 2006; 66: 8109–15. doi: 10.1158/0008-5472.CAN-06-0140.
127. Konstantinopoulos PA, Ceccaldi R, Shapiro GI, D'Andrea AD. Homologous Recombination Deficiency: Exploiting the Fundamental Vulnerability of Ovarian Cancer. Cancer Discov. American Association for Cancer Research; 2015; 5: 1137–54. doi: 10.1158/2159-8290.CD-15-0714.
128. Bajrami I, Frankum JR, Konde A, Miller RE, Rehman FL, Brough R, Campbell J, Sims D, Rafiq R, Hooper S, Chen L, Kozarewa I, Assiotis I, et al. Genome-wide Profiling of Genetic Synthetic Lethality Identifies CDK12 as a Novel Determinant of PARP1/2 Inhibitor Sensitivity. Cancer Res. American Association for Cancer Research; 2014; 74: 287–97. doi: 10.1158/0008-5472.CAN-13-2541.
129. Joshi PM, Sutor SL, Huntoon CJ, Karnitz LM. Ovarian cancer-associated mutations disable catalytic activity of CDK12, a kinase that promotes homologous recombination repair and resistance to cisplatin and poly(ADP-ribose) polymerase inhibitors. J Biol Chem. American Society for Biochemistry and Molecular Biology;

2014; 289: 9247–53. doi: 10.1074/jbc.M114.551143.

130. Lord CJ, McDonald S, Swift S, Turner NC, Ashworth A. A high-throughput RNA interference screen for DNA repair determinants of PARP inhibitor sensitivity. DNA Repair (Amst). Elsevier; 2008; 7: 2010–9. doi: 10.1016/J.DNAREP.2008.08.014.
131. Horton JK, Stefanick DF, Prasad R, Gassman NR, Kedar PS, Wilson SH. Base excision repair defects invoke hypersensitivity to PARP inhibition. Mol Cancer Res. American Association for Cancer Research; 2014; 12: 1128–39. doi: 10.1158/1541-7786.MCR-13-0502.
132. Zhang Y, Rohde LH, Wu H. Involvement of nucleotide excision and mismatch repair mechanisms in double strand break repair. Curr Genomics. Bentham Science Publishers; 2009; 10: 250–8. doi: 10.2174/138920209788488544.
133. Fleury H, Carmona E, Morin VG, Meunier L, Masson J-Y, Tonin PN, Provencher D, Mes-Masson A-M. Cumulative defects in DNA repair pathways drive the PARP inhibitor response in high-grade serous epithelial ovarian cancer cell lines. Oncotarget. Impact Journals, LLC; 2017; 8: 40152–68. doi: 10.18632/oncotarget.10308.
134. Alexandrov LB, Nik-Zainal S, Wedge DC, Aparicio SAJR, Behjati S, Biankin A V., Bignell GR, Bolli N, Borg A, Børresen-Dale A-L, Boyault S, Burkhardt B, Butler AP, et al. Signatures of mutational processes in human cancer. Nature. 2013; 500: 415–21. doi: 10.1038/nature12477.
135. Abkevich V, Timms KM, Hennessy BT, Potter J, Carey MS, Meyer LA, Smith-McCune K, Broaddus R, Lu KH, Chen J, Tran T V, Williams D, Iliev D, et al. Patterns of genomic loss of heterozygosity predict homologous recombination repair defects in epithelial ovarian cancer. Br J Cancer. Nature Publishing Group; 2012; 107: 1776–82. doi: 10.1038/bjc.2012.451.
136. myChoice® CDx - Myriad Oncology [Internet]. Available 2020 Aug 2, from https://myriad-oncology.com/mychoice-cdx/
137. Birkbak NJ, Wang ZC, Kim J-Y, Eklund AC, Li Q, Tian R, Bowman-Colin C, Li Y, Greene-Colozzi A, Iglehart JD, Tung N, Ryan PD, Garber JE, et al. Telomeric allelic imbalance indicates defective DNA repair and sensitivity to DNA-damaging

agents. Cancer Discov. NIH Public Access; 2012; 2: 366–75. doi: 10.1158/2159-8290.CD-11-0206.

138. Popova T, Manié E, Rieunier G, Caux-Moncoutier V, Tirapo C, Dubois T, Delattre O, Sigal-Zafrani B, Bollet M, Longy M, Houdayer C, Sastre-Garau X, Vincent-Salomon A, et al. Ploidy and large-scale genomic instability consistently identify basal-like breast carcinomas with BRCA1/2 inactivation. Cancer Res. American Association for Cancer Research; 2012; 72: 5454–62. doi: 10.1158/0008-5472.CAN-12-1470.
139. Mateo J, Lord CJ, Serra V, Tutt A, Balmaña J, Castroviejo-Bermejo M, Cruz C, Oaknin A, Kaye SB, Bono JS de. A decade of clinical development of PARP inhibitors in perspective. Ann Oncol. Elsevier; 2019; 30: 1437–47. doi: 10.1093/ANNONC/MDZ192.
140. Barber LJ, Sandhu S, Chen L, Campbell J, Kozarewa I, Fenwick K, Assiotis I, Rodrigues DN, Reis-Filho JS, Moreno V, Mateo J, Molife LR, De Bono J, et al. Secondary mutations in *BRCA2* associated with clinical resistance to a PARP inhibitor. J Pathol. John Wiley & Sons, Ltd; 2013; 229: 422–9. doi: 10.1002/path.4140.
141. Kondrashova O, Nguyen M, Shield-Artin K, Tinker A V., Teng NNH, Harrell MI, Kuiper MJ, Ho G-Y, Barker H, Jasin M, Prakash R, Kass EM, Sullivan MR, et al. Secondary Somatic Mutations Restoring *RAD51C* and *RAD51D* Associated with Acquired Resistance to the PARP Inhibitor Rucaparib in High-Grade Ovarian Carcinoma. Cancer Discov. American Association for Cancer Research; 2017; 7: 984–98. doi: 10.1158/2159-8290.CD-17-0419.
142. Norquist B, Wurz KA, Pennil CC, Garcia R, Gross J, Sakai W, Karlan BY, Taniguchi T, Swisher EM. Secondary somatic mutations restoring BRCA1/2 predict chemotherapy resistance in hereditary ovarian carcinomas. J Clin Oncol. American Society of Clinical Oncology; 2011; 29: 3008–15. doi: 10.1200/JCO.2010.34.2980.
143. Drost R, Dhillon KK, van der Gulden H, van der Heijden I, Brandsma I, Cruz C, Chondronasiou D, Castroviejo-Bermejo M, Boon U, Schut E, van der Burg E, Wientjens E, Pieterse M, et al. BRCA1185delAG tumors may acquire therapy

resistance through expression of RING-less BRCA1. J Clin Invest. American Society for Clinical Investigation; 2016; 126: 2903–18. doi: 10.1172/JCI70196.

144. Wang Y, Bernhardy AJ, Cruz C, Krais JJ, Nacson J, Nicolas E, Peri S, van der Gulden H, van der Heijden I, O'Brien SW, Zhang Y, Harrell MI, Johnson SF, et al. The BRCA1- 11q Alternative Splice Isoform Bypasses Germline Mutations and Promotes Therapeutic Resistance to PARP Inhibition and Cisplatin. Cancer Res. American Association for Cancer Research; 2016; 76: 2778–90. doi: 10.1158/0008-5472.CAN-16-0186.
145. Kondrashova O, Topp M, Nesic K, Lieschke E, Ho G-Y, Harrell MI, Zapparoli G V., Hadley A, Holian R, Boehm E, Heong V, Sanij E, Pearson RB, et al. Methylation of all BRCA1 copies predicts response to the PARP inhibitor rucaparib in ovarian carcinoma. Nat Commun. Nature Publishing Group; 2018; 9: 3970. doi: 10.1038/s41467-018-05564-z.
146. ter Brugge P, Kristel P, van der Burg E, Boon U, de Maaker M, Lips E, Mulder L, de Ruiter J, Moutinho C, Gevensleben H, Marangoni E, Majewski I, Jóźwiak K, et al. Mechanisms of Therapy Resistance in Patient-Derived Xenograft Models of BRCA1-Deficient Breast Cancer. J Natl Cancer Inst. Oxford Academic; 2016; 108: djw148. doi: 10.1093/jnci/djw148.
147. Nacson J, Krais JJ, Bernhardy AJ, Clausen E, Feng W, Wang Y, Nicolas E, Cai KQ, Tricarico R, Hua X, DiMarcantonio D, Martinez E, Zong D, et al. BRCA1 Mutation-Specific Responses to 53BP1 Loss-Induced Homologous Recombination and PARP Inhibitor Resistance. Cell Rep. Cell Press; 2018; 24: 3513-3527.e7. doi: 10.1016/J.CELREP.2018.08.086.
148. Dev H, Chiang T-WW, Lescale C, de Krijger I, Martin AG, Pilger D, Coates J, Sczaniecka-Clift M, Wei W, Ostermaier M, Herzog M, Lam J, Shea A, et al. Shieldin complex promotes DNA end-joining and counters homologous recombination in BRCA1-null cells. Nat Cell Biol. Nature Publishing Group; 2018; 20: 954–65. doi: 10.1038/s41556-018-0140-1.
149. Jaspers JE, Kersbergen A, Boon U, Sol W, Van Deemter L, Zander SA, Drost R, Wientjens E, Ji J, Aly A, Doroshow JH, Cranston A, Martin NMB, et al. Loss of 53BP1 causes PARP inhibitor resistance in BRCA1-mutated mouse mammary

tumors. Cancer Discov. American Association for Cancer Research; 2013; 3: 68–81. doi: 10.1158/2159-8290.CD-12-0049.

150. Xu G, Ross Chapman J, Brandsma I, Yuan J, Mistrik M, Bouwman P, Bartkova J, Gogola E, Warmerdam D, Barazas M, Jaspers JE, Watanabe K, Pieterse M, et al. REV7 counteracts DNA double-strand break resection and affects PARP inhibition. Nature. Nature Publishing Group; 2015; 521: 541–4. doi: 10.1038/nature14328.
151. Noordermeer SM, Adam S, Setiaputra D, Barazas M, Pettitt SJ, Ling AK, Olivieri M, Álvarez-Quilón A, Moatti N, Zimmermann M, Annunziato S, Krastev DB, Song F, et al. The shieldin complex mediates 53BP1-dependent DNA repair. Nature. Nature Publishing Group; 2018; 560: 117–21. doi: 10.1038/s41586-018-0340-7.
152. Liao H, Ji F, Helleday T, Ying S. Mechanisms for stalled replication fork stabilization: new targets for synthetic lethality strategies in cancer treatments. EMBO Rep. European Molecular Biology Organization; 2018; 19. doi: 10.15252/embr.201846263.
153. Ying S, Hamdy FC, Helleday T. Mre11-dependent degradation of stalled DNA replication forks is prevented by BRCA2 and PARP1. Cancer Res. American Association for Cancer Research; 2012; 72: 2814–21. doi: 10.1158/0008-5472.CAN-11-3417.
154. Ray Chaudhuri A, Callen E, Ding X, Gogola E, Duarte AA, Lee J-E, Wong N, Lafarga V, Calvo JA, Panzarino NJ, John S, Day A, Crespo AV, et al. Replication fork stability confers chemoresistance in BRCA-deficient cells. Nature. NIH Public Access; 2016; 535: 382–7. doi: 10.1038/nature18325.
155. Rondinelli B, Gogola E, Yücel H, Duarte AA, van de Ven M, van der Sluijs R, Konstantinopoulos PA, Jonkers J, Ceccaldi R, Rottenberg S, D'Andrea AD. EZH2 promotes degradation of stalled replication forks by recruiting MUS81 through histone H3 trimethylation. Nat Cell Biol. Nature Publishing Group; 2017; 19: 1371–8. doi: 10.1038/ncb3626.
156. Dungrawala H, Bhat KP, Le Meur R, Chazin WJ, Ding X, Sharan SK, Wessel SR, Sathe AA, Zhao R, Cortez D. RADX Promotes Genome Stability and Modulates Chemosensitivity by Regulating RAD51 at Replication Forks. Mol Cell. NIH Public

Access; 2017; 67: 374-386.e5. doi: 10.1016/j.molcel.2017.06.023.

157. Zellweger R, Dalcher D, Mutreja K, Berti M, Schmid JA, Herrador R, Vindigni A, Lopes M. Rad51-mediated replication fork reversal is a global response to genotoxic treatments in human cells. J Cell Biol. The Rockefeller University Press; 2015; 208: 563–79. doi: 10.1083/jcb.201406099.
158. Taglialatela A, Alvarez S, Leuzzi G, Sannino V, Ranjha L, Huang J-W, Madubata C, Anand R, Levy B, Rabadan R, Cejka P, Costanzo V, Ciccia A. Restoration of Replication Fork Stability in BRCA1- and BRCA2-Deficient Cells by Inactivation of SNF2-Family Fork Remodelers. Mol Cell. Cell Press; 2017; 68: 414-430.e8. doi: 10.1016/J.MOLCEL.2017.09.036.
159. Pettitt SJ, Krastev DB, Brandsma I, Dréan A, Song F, Aleksandrov R, Harrell MI, Menon M, Brough R, Campbell J, Frankum J, Ranes M, Pemberton HN, et al. Genome-wide and high-density CRISPR-Cas9 screens identify point mutations in PARP1 causing PARP inhibitor resistance. Nat Commun. Nature Publishing Group; 2018; 9: 1849. doi: 10.1038/s41467-018-03917-2.
160. Gogola E, Duarte AA, de Ruiter JR, Wiegant WW, Schmid JA, de Bruijn R, James DI, Guerrero Llobet S, Vis DJ, Annunziato S, van den Broek B, Barazas M, Kersbergen A, et al. Selective Loss of PARG Restores PARylation and Counteracts PARP Inhibitor-Mediated Synthetic Lethality. Cancer Cell. Cell Press; 2018; 33: 1078-1093.e12. doi: 10.1016/J.CCELL.2018.05.008.
161. Shoemaker RH. The NCI60 human tumour cell line anticancer drug screen. Nat Rev Cancer. Nature Publishing Group; 2006; 6: 813–23. doi: 10.1038/nrc1951.
162. Shankavaram UT, Varma S, Kane D, Sunshine M, Chary KK, Reinhold WC, Pommier Y, Weinstein JN. CellMiner: a relational database and query tool for the NCI-60 cancer cell lines. BMC Genomics. BioMed Central; 2009; 10: 277. doi: 10.1186/1471-2164-10-277.
163. Fojo T, Farrell N, Ortuzar W, Tanimura H, Weinstein J, Myers TG. Identification of non-cross-resistant platinum compounds with novel cytotoxicity profiles using the NCI anticancer drug screen and clustered image map visualizations. Critical Reviews in Oncology/Hematology. Elsevier Ireland Ltd; 2005. p. 25–34. doi: 10.1016/j.critrevonc.2004.09.008.

164. Bai R, Paull KD, Herald CL, Malspeis L, Pettit GR, Hamel E. Halichondrin B and Homohalichondrin B, Marine Natural Products Binding in the Vinca Domain of Tubulin DISCOVERY OF TUBULIN-BASED MECHANISM OF ACTION BY ANALYSIS OF DIFFERENTIAL CYTOTOXICITY DATA*. 1991.
165. Holbeck SL, Sausville EA. The Proteasome and the COMPARE Algorithm. Proteasome Inhibitors in Cancer Therapy. Humana Press; 2004. p. 99–107. doi: 10.1007/978-1-59259-794-9_8.
166. Yang W, Soares J, Greninger P, Edelman EJ, Lightfoot H, Forbes S, Bindal N, Beare D, Smith JA, Thompson IR, Ramaswamy S, Futreal PA, Haber DA, et al. Genomics of Drug Sensitivity in Cancer (GDSC): a resource for therapeutic biomarker discovery in cancer cells. Nucleic Acids Res. Oxford University Press; 2012; 41: D955–61. doi: 10.1093/nar/gks1111.
167. Barretina J, Caponigro G, Stransky N, Venkatesan K, Margolin AA, Kim S, Wilson CJ, Lehár J, Kryukov G V, Sonkin D, Reddy A, Liu M, Murray L, et al. The Cancer Cell Line Encyclopedia enables predictive modelling of anticancer drug sensitivity. Nature. 2012; 483. doi: 10.1038/nature11003.
168. Murai J, Feng Y, Yu GK, Ru Y, Tang S-W, Shen Y, Pommier Y, Murai J, Feng Y, Yu GK, Ru Y, Tang S-W, Shen Y, et al. Resistance to PARP inhibitors by SLFN11 inactivation can be overcome by ATR inhibition. Oncotarget. Impact Journals; 2016; 7: 76534–50. doi: 10.18632/oncotarget.12266.
169. Lheureux S, Oaknin A, Garg S, Bruce JP, Madariaga A, Dhani NC, Bowering V, White J, Accardi S, Tan Q, Braunstein M, Karakasis K, Cirlan I, et al. EVOLVE: A Multicenter Open-Label Single-Arm Clinical and Translational Phase II Trial of Cediranib Plus Olaparib for Ovarian Cancer after PARP Inhibition Progression. Clin Cancer Res. 2020; . doi: 10.1158/1078-0432.ccr-19-4121.
170. Cancer Genome Atlas Research Network JN, Weinstein JN, Collisson EA, Mills GB, Shaw KRM, Ozenberger BA, Ellrott K, Shmulevich I, Sander C, Stuart JM. The Cancer Genome Atlas Pan-Cancer analysis project. Nat Genet. NIH Public Access; 2013; 45: 1113–20. doi: 10.1038/ng.2764.
171. Lounis H, Provencher D, Godbout C, Fink D, Milot M-J, Mes-Masson A-M. Primary Cultures of Normal and Tumoral Human Ovarian Epithelium: A Powerful

Tool for Basic Molecular Studies. Exp Cell Res. 1994; 215: 303–9. doi: 10.1006/excr.1994.1346.

172. Ouellet V, Zietarska M, Portelance L, Lafontaine J, Madore J, Puiffe M-L, Arcand SL, Shen Z, Hébert J, Tonin PN, Provencher DM, Mes-Masson A-M. Characterization of three new serous epithelial ovarian cancer cell lines. BMC Cancer. BioMed Central; 2008; 8: 152. doi: 10.1186/1471-2407-8-152.
173. Fleury H, Communal L, Carmona E, Portelance L, Arcand SL, Rahimi K, Tonin PN, Provencher D, Mes-Masson A-M. Novel high-grade serous epithelial ovarian cancer cell lines that reflect the molecular diversity of both the sporadic and hereditary disease. Genes Cancer. 2015; 6: 378–98. doi: 10.18632/genesandcancer.76.
174. Létourneau IJ, Quinn MCJ, Wang LL, Portelance L, Caceres KY, Cyr L, Delvoye N, Meunier L, de Ladurantaye M, Shen Z, Arcand SL, Tonin PN, Provencher DM, et al. Derivation and characterization of matched cell lines from primary and recurrent serous ovarian cancer. BMC Cancer. BioMed Central; 2012; 12: 379. doi: 10.1186/1471-2407-12-379.
175. Ouellet V, Zietarska M, Portelance L, Lafontaine J, Madore J, Puiffe M, Arcand SL, Shen Z, Hébert J, Tonin PN, Provencher DM. Characterization of three new serous epithelial ovarian cancer cell lines. BMC Cancer. 2008; 8: 1–18. doi: 10.1186/1471-2407-8-152.
176. Provencher DM, Lounis H, Champoux L, Tétrault M, Manderson EN, Wang JC, Eydoux P, Savoie R, Tonin PN, Mes-Masson A-M. Characterization of four novel epithelial ovarian cancer cell lines. Vitr Cell Dev Biol - Anim. Springer-Verlag; 2000; 36: 357–61. doi: 10.1290/1071-2690(2000)036<0357:cofneo>2.0.co;2.
177. Bolger AM, Lohse M, Usadel B. Trimmomatic: a flexible trimmer for Illumina sequence data. Bioinformatics. Oxford University Press; 2014; 30: 2114–20. doi: 10.1093/bioinformatics/btu170.
178. Li H, Durbin R. Fast and accurate short read alignment with Burrows-Wheeler transform. Bioinformatics. Oxford University Press; 2009; 25: 1754–60. doi: 10.1093/bioinformatics/btp324.
179. Broad Institute. Picard Tools [Internet]. Broad Institute, GitHub repository. 2017.

Available from https://broadinstitute.github.io/picard/

180. McKenna A, Hanna M, Banks E, Sivachenko A, Cibulskis K, Kernytsky A, Garimella K, Altshuler D, Gabriel S, Daly M, DePristo MA. The Genome Analysis Toolkit: a MapReduce framework for analyzing next-generation DNA sequencing data. Genome Res. 2010; 20: 1297–303. doi: 10.1101/gr.107524.110.
181. Li H, Handsaker B, Wysoker A, Fennell T, Ruan J, Homer N, Marth G, Abecasis G, Durbin R. The Sequence Alignment/Map format and SAMtools. Bioinformatics. 2009; 25: 2078–9. doi: 10.1093/bioinformatics/btp352.
182. Cingolani P, Platts A, Wang LL, Coon M, Nguyen T, Wang L, Land SJ, Lu X, Ruden DM. A program for annotating and predicting the effects of single nucleotide polymorphisms, SnpEff: SNPs in the genome of Drosophila melanogaster strain w1118; iso-2; iso-3. Fly (Austin). Taylor & Francis; 2012; 6: 80–92. doi: 10.4161/fly.19695.
183. Sherry ST, Ward MH, Kholodov M, Baker J, Phan L, Smigielski EM, Sirotkin K. dbSNP: the NCBI database of genetic variation. Nucleic Acids Res. Oxford University Press; 2001; 29: 308–11. doi: 10.1093/nar/29.1.308.
184. Forbes SA, Beare D, Boutselakis H, Bamford S, Bindal N, Tate J, Cole CG, Ward S, Dawson E, Ponting L, Stefancsik R, Harsha B, Yin Kok C, et al. COSMIC: somatic cancer genetics at high-resolution. Nucleic Acids Res. 2017; 45. doi: 10.1093/nar/gkw1121.
185. Cingolani P, Patel VM, Coon M, Nguyen T, Land SJ, Ruden DM, Lu X. Using Drosophila melanogaster as a Model for Genotoxic Chemical Mutational Studies with a New Program, SnpSift. Front Genet. Frontiers Media SA; 2012; 3: 35. doi: 10.3389/fgene.2012.00035.
186. Liu X, Wu C, Li C, Boerwinkle E. dbNSFP v3.0: A One-Stop Database of Functional Predictions and Annotations for Human Nonsynonymous and Splice-Site SNVs. Hum Mutat. 2016; 37: 235–41. doi: 10.1002/humu.22932.
187. Jian X, Boerwinkle E, Liu X. In silico prediction of splice-altering single nucleotide variants in the human genome. Nucleic Acids Res. Oxford University Press; 2014; 42: 13534–44. doi: 10.1093/nar/gku1206.
188. R Core Team. R: A Language and Environment for Statistical Computing

[Internet]. Vienna, Austria; 2016. Available from https://www.r-project.org/

189. Kanehisa M, Goto S. KEGG: kyoto encyclopedia of genes and genomes. Nucleic Acids Res. Oxford University Press; 2000; 28: 27–30. Available from http://www.ncbi.nlm.nih.gov/pubmed/10592173

190. Arikawa E, Quellhorst G, Han Y, Pan H, Yang J. RT2 Profiler PCR Arrays: Pathway-focused gene expression profiling with qRT-PCR [Internet]. 2015. Available from https://www.qiagen.com/ca/resources/download.aspx?id=67a0be21-6869-4053-a2f9-ee98258a04a2&lang=en

191. Kumar P, Henikoff S, Ng PC. Predicting the effects of coding non-synonymous variants on protein function using the SIFT algorithm. Nat Protoc. Nature Publishing Group; 2009; 4: 1073–81. doi: 10.1038/nprot.2009.86.

192. Maathuis M, Colombo D, Kalisch M, Bühlmann P. A method and server for predicting damaging missense mutations. Nat Publ Gr. 2010; 7: 3133–64. doi: 10.1038/nmeth0410-248.

193. Shihab HA, Rogers MF, Gough J, Mort M, Cooper DN, Day INM, Gaunt TR, Campbell C. An integrative approach to predicting the functional effects of non-coding and coding sequence variation. Bioinformatics. Oxford University Press; 2015; 31: 1536–43. doi: 10.1093/bioinformatics/btv009.

194. Reva B, Antipin Y, Sander C. Predicting the functional impact of protein mutations: application to cancer genomics. Nucleic Acids Res. Oxford University Press; 2011; 39: e118. doi: 10.1093/nar/gkr407.

195. Schwarz JM, Cooper DN, Schuelke M, Seelow D. MutationTaster2: mutation prediction for the deep-sequencing age. Nat Methods. 2014; 11: 361–2. doi: 10.1038/nmeth.2890.

196. Ioannidis NM, Rothstein JH, Pejaver V, Middha S, McDonnell SK, Baheti S, Musolf A, Li Q, Holzinger E, Karyadi D, Cannon-Albright LA, Teerlink CC, Stanford JL, et al. REVEL: An Ensemble Method for Predicting the Pathogenicity of Rare Missense Variants. Am J Hum Genet. Elsevier; 2016; 99: 877–85. doi: 10.1016/j.ajhg.2016.08.016.

197. Dong C, Wei P, Jian X, Gibbs R, Boerwinkle E, Wang K, Liu X. Comparison and

integration of deleteriousness prediction methods for nonsynonymous SNVs in whole exome sequencing studies. Hum Mol Genet. Oxford University Press; 2015; 24: 2125–37. doi: 10.1093/hmg/ddu733.

198. Karczewski KJ, Francioli LC, Tiao G, Cummings BB, Alföldi J, Wang Q, Collins RL, Laricchia KM, Ganna A, Birnbaum DP, Gauthier LD, Brand H, Solomonson M, et al. Variation across 141,456 human exomes and genomes reveals the spectrum of loss-of-function intolerance across human protein-coding genes. bioRxiv. Cold Spring Harbor Laboratory; 2019; : 531210. doi: 10.1101/531210.
199. Smit AF. Interspersed repeats and other mementos of transposable elements in mammalian genomes. Curr Opin Genet Dev. 1999; 9: 657–63. Available from http://www.ncbi.nlm.nih.gov/pubmed/10607616
200. Lawrence M, Gentleman R, Carey V. rtracklayer: an R package for interfacing with genome browsers. Bioinformatics. Oxford University Press; 2009; 25: 1841–2. doi: 10.1093/bioinformatics/btp328.
201. Thorvaldsdóttir H, Robinson JT, Mesirov JP. Integrative Genomics Viewer (IGV): high-performance genomics data visualization and exploration. Brief Bioinform. Oxford University Press; 2013; 14: 178–92. doi: 10.1093/bib/bbs017.
202. Alexandrov LB, Nik-Zainal S, Wedge DC, Campbell PJ, Stratton MR. Deciphering Signatures of Mutational Processes Operative in Human Cancer. CellReports. 2013; 3: 246–59. doi: 10.1016/j.celrep.2012.12.008.
203. Rosenthal R, McGranahan N, Herrero J, Taylor BS, Swanton C, Kumar S. deconstructSigs: delineating mutational processes in single tumors distinguishes DNA repair deficiencies and patterns of carcinoma evolution. Genome Biol. BioMed Central; 2016; 17: 31. doi: 10.18637/jss.v021.i12.
204. Talevich E, Shain AH, Botton T, Bastian BC, Carlson M, Gentleman R. CNVkit: Genome-Wide Copy Number Detection and Visualization from Targeted DNA Sequencing. PLOS Comput Biol. Public Library of Science; 2016; 12: e1004873. doi: 10.1371/journal.pcbi.1004873.
205. Ritchie ME, Phipson B, Wu D, Hu Y, Law CW, Shi W, Smyth GK. limma powers differential expression analyses for RNA-sequencing and microarray studies. Nucleic Acids Res. Oxford University Press; 2015; 43: e47–e47. doi:

10.1093/nar/gkv007.

206. Barretina J, Caponigro G, Stransky N, Venkatesan K, Margolin AA, Kim S, Wilson CJ, Lehár J, Kryukov G V, Sonkin D, Reddy A, Liu M, Murray L, et al. The Cancer Cell Line Encyclopedia enables predictive modeling of anticancer drug sensitivity. Nature. NIH Public Access; 2012; 483: 603–7. doi: 10.1038/nature11003.
207. Klijn C, Durinck S, Stawiski EW, Haverty PM, Jiang Z, Liu H, Degenhardt J, Mayba O, Gnad F, Liu J, Pau G, Reeder J, Cao Y, et al. A comprehensive transcriptional portrait of human cancer cell lines. Nat Biotechnol. Nature Publishing Group; 2015; 33: 306–12. doi: 10.1038/nbt.3080.
208. Garcia-Alonso L, Iorio F, Matchan A, Fonseca N, Jaaks P, Peat G, Pignatelli M, Falcone F, Benes CH, Dunham I, Bignell G, Mcdade SS, Garnett MJ, et al. Transcription Factor Activities Enhance Markers of Drug Sensitivity in Cancer. 2018; . doi: 10.1158/0008-5472.CAN-17-1679.
209. Kuhn M. Building predictive models in R using the caret package. J Stat Softw. 2008; 28: 1–26. doi: 10.18637/jss.v028.i05.
210. Polak P, Kim J, Braunstein LZ, Karlic R, Haradhavala NJ, Tiao G, Rosebrock D, Livitz D, Kübler K, Mouw KW, Kamburov A, Maruvka YE, Leshchiner I, et al. A mutational signature reveals alterations underlying deficient homologous recombination repair in breast cancer. Nat Genet. Nature Publishing Group; 2017; 49: 1476–86. doi: 10.1038/ng.3934.
211. Alanazi M, Pathan AAK, Arifeen Z, Shaik JP, Alabdulkarim HA, Semlali A, Bazzi MD, Parine NR. Association between PARP-1 V762A Polymorphism and Breast Cancer Susceptibility in Saudi Population. Schönbach C, editor. PLoS One. Public Library of Science; 2013; 8: e85541. doi: 10.1371/journal.pone.0085541.
212. Li Y, Li S, Wu Z, Hu F, Zhu L, Zhao X, Cui B, Dong X, Tian S, Wang F, Zhao Y. Polymorphisms in genes of APE1, PARP1, and XRCC1: risk and prognosis of colorectal cancer in a Northeast Chinese population. Med Oncol. Springer US; 2013; 30: 505. doi: 10.1007/s12032-013-0505-z.
213. Wang X-G, Wang Z-Q, Tong W-M, Shen Y. PARP1 Val762Ala polymorphism reduces enzymatic activity. Biochem Biophys Res Commun. Academic Press; 2007; 354: 122–6. doi: 10.1016/J.BBRC.2006.12.162.

214. Farmer H, McCabe N, Lord CJ, Tutt ANJ, Johnson DA, Richardson TB, Santarosa M, Dillon KJ, Hickson I, Knights C, Martin NMB, Jackson SP, Smith GCM, et al. Targeting the DNA repair defect in BRCA mutant cells as a therapeutic strategy. Nature. Nature Publishing Group; 2005; 434: 917–21. doi: 10.1038/nature03445.
215. Landrum MJ, Lee JM, Riley GR, Jang W, Rubinstein WS, Church DM, Maglott DR. ClinVar: public archive of relationships among sequence variation and human phenotype. Nucleic Acids Res. Oxford University Press; 2014; 42: D980-5. doi: 10.1093/nar/gkt1113.
216. Cerami E, Gao J, Dogrusoz U, Gross BE, Sumer SO, Aksoy BA, Jacobsen A, Byrne CJ, Heuer ML, Larsson E, Antipin Y, Reva B, Goldberg AP, et al. The cBio Cancer Genomics Portal: An Open Platform for Exploring Multidimensional Cancer Genomics Data: Figure 1. Cancer Discov. 2012; 2: 401–4. doi: 10.1158/2159-8290.CD-12-0095.
217. Gao J, Aksoy BA, Dogrusoz U, Dresdner G, Gross B, Sumer SO, Sun Y, Jacobsen A, Sinha R, Larsson E, Cerami E, Sander C, Schultz N. Integrative Analysis of Complex Cancer Genomics and Clinical Profiles Using the cBioPortal. Sci Signal. 2013; 6: pl1–pl1. doi: 10.1126/scisignal.2004088.
218. Gu Y, Rosenblatt J, Morgan DO. Cell cycle regulation of CDK2 activity by phosphorylation of Thr160 and Tyr15. EMBO J. European Molecular Biology Organization; 1992; 11: 3995–4005. doi: 10.1002/j.1460-2075.1992.tb05493.x.
219. Welburn JPI, Tucker JA, Johnson T, Lindert L, Morgan M, Willis A, Noble MEM, Endicott JA. How tyrosine 15 phosphorylation inhibits the activity of cyclin-dependent kinase 2-cyclin A. J Biol Chem. J Biol Chem; 2007; 282: 3173–81. doi: 10.1074/jbc.M609151200.
220. Yu X, Chen J. DNA damage-induced cell cycle checkpoint control requires CtIP, a phosphorylation-dependent binding partner of BRCA1 C-terminal domains. Mol Cell Biol. American Society for Microbiology Journals; 2004; 24: 9478–86. doi: 10.1128/MCB.24.21.9478-9486.2004.
221. Shi Y, Massagué J. Mechanisms of TGF-β Signaling from Cell Membrane to the Nucleus. Cell. Cell Press; 2003; 113: 685–700. doi: 10.1016/S0092-8674(03)00432-X.

222. Feng X-H, Derynck R. SPECIFICITY AND VERSATILITY IN TGF-β SIGNALING THROUGH SMADS. Annu Rev Cell Dev Biol. 2005; 21: 659–93. doi: 10.1146/annurev.cellbio.21.022404.142018.
223. Chapman JR, Barral P, Vannier JB, Borel V, Steger M, Tomas-Loba A, Sartori AA, Adams IR, Batista FD, Boulton SJ. RIF1 Is Essential for 53BP1-Dependent Nonhomologous End Joining and Suppression of DNA Double-Strand Break Resection. Mol Cell. Elsevier; 2013; 49: 858–71. doi: 10.1016/j.molcel.2013.01.002.
224. Meng XW, Koh BD, Zhang J-S, Flatten KS, Schneider PA, Billadeau DD, Hess AD, Smith BD, Karp JE, Kaufmann SH. Poly(ADP-ribose) Polymerase Inhibitors Sensitize Cancer Cells to Death Receptor-mediated Apoptosis by Enhancing Death Receptor Expression. J Biol Chem. American Society for Biochemistry and Molecular Biology; 2014; 289: 20543. doi: 10.1074/JBC.M114.549220.
225. Zou M, Hu X, Xu B, Tong T, Jing Y, Xi L, Zhou W, Lu J, Wang X, Yang X, Liao F. Glutathione S-transferase isozyme alpha 1 is predominantly involved in the cisplatin resistance of common types of solid cancer. Oncol Rep. Spandidos Publications; 2018; 41: 989–98. doi: 10.3892/or.2018.6861.
226. Vaidyanathan A, Sawers L, Gannon A-L, Chakravarty P, Scott AL, Bray SE, Ferguson MJ, Smith G. ABCB1 (MDR1) induction defines a common resistance mechanism in paclitaxel- and olaparib-resistant ovarian cancer cells. Br J Cancer. Nature Publishing Group; 2016; 115: 431–41. doi: 10.1038/bjc.2016.203.
227. Frankum J, Moudry P, Brough R, Hodny Z, Ashworth A, Bartek J, Lord CJ. Complementary genetic screens identify the E3 ubiquitin ligase CBLC, as a modifier of PARP inhibitor sensitivity [Internet]. 2015. Available from www.impactjournals.com/oncotarget/
228. Chang H-Y, Fan C-C, Chu P-C, Hong B-E, Lee HJ, Chang M-S. hPuf-A/KIAA0020 Modulates PARP-1 Cleavage upon Genotoxic Stress. Cancer Res. American Association for Cancer Research; 2011; 71: 1126–34. doi: 10.1158/0008-5472.CAN-10-1831.
229. Kim J-H, Lane WS, Reinberg D. Human Elongator facilitates RNA polymerase II transcription through chromatin. Proc Natl Acad Sci. 2002; : 1241–6. Available

from www.pnas.orgcgidoi10.1073pnas.251672198

230. Huang B, Johansson MJO, Byström AS. An early step in wobble uridine tRNA modification requires the Elongator complex. RNA. Cold Spring Harbor Laboratory Press; 2005; 11: 424–36. doi: 10.1261/rna.7247705.

231. Sherill-Rofe D, Rahat D, Findlay S, Mellul A, Guberman I, Braun M, Bloch I, Lalezari A, Samiei A, Sadreyev R, Goldberg M, Orthwein A, Zick A, et al. Mapping global and local coevolution across 600 species to identify novel homologous recombination repair genes. Genome Res. Cold Spring Harbor Laboratory Press; 2019; 29: 439–48. doi: 10.1101/gr.241414.118.

232. Browne GJ, Proud CG. Regulation of peptide-chain elongation in mammalian cells [Internet]. European Journal of Biochemistry. John Wiley & Sons, Ltd; 2002. p. 5360–8. doi: 10.1046/j.1432-1033.2002.03290.x.

233. Maruyama T, Nara K, Yoshikawa H, Suzuki N. Txk, a member of the non-receptor tyrosine kinase of the Tec family, forms a complex with poly(ADP-ribose) polymerase 1 and elongation factor 1α and regulates interferon-γ gene transcription in Th1 cells. Clin Exp Immunol. Wiley-Blackwell; 2007; 147: 164–75. doi: 10.1111/j.1365-2249.2006.03249.x.

234. Duttaroy A, Bourbeau D, Wang XL, Wang E. Apoptosis rate can be accelerated or decelerated by overexpression or reduction of the level of elongation factor-1α. Exp Cell Res. Academic Press Inc.; 1998; 238: 168–76. doi: 10.1006/excr.1997.3819.

235. Yang F, Demma M, Warren V, Dharmawardhane S, Condeelis J. Identification of an actin-binding protein from Dictyostelium as elongation factor 1a. Nature. Nature Publishing Group; 1990; 347: 494–6. doi: 10.1038/347494a0.

236. Gross SR, Kinzy TG. Translation elongation factor 1A is essential for regulation of the actin cytoskeleton and cell morphology. Nat Struct Mol Biol. Nature Publishing Group; 2005; 12: 772–8. doi: 10.1038/nsmb979.

237. Glatt S, Létoquart J, Faux C, Taylor NMI, Séraphin B, Müller CW. The Elongator subcomplex Elp456 is a hexameric RecA-like ATPase. Nat Struct Mol Biol. Nature Publishing Group; 2012; 19: 314–20. doi: 10.1038/nsmb.2234.

238. Lin Z, Zhao W, Diao W, Xie X, Wang Z, Zhang J, Shen Y, Long J. Crystal

structure of elongator subcomplex Elp4-6. J Biol Chem. American Society for Biochemistry and Molecular Biology; 2012; 287: 21501–8. doi: 10.1074/jbc.M112.341560.

239. Virág L, Robaszkiewicz A, Rodriguez-Vargas JM, Oliver FJ. Poly(ADP-ribose) signaling in cell death. Mol Aspects Med. Pergamon; 2013; 34: 1153–67. doi: 10.1016/J.MAM.2013.01.007.
240. Pettitt SJ, Krastev DB, Brandsma I, Dréan A, Song F, Aleksandrov R, Harrell MI, Menon M, Brough R, Campbell J, Frankum J, Ranes M, Pemberton HN, et al. Genome-wide and high-density CRISPR-Cas9 screens identify point mutations in PARP1 causing PARP inhibitor resistance. Nat Commun. Nature Publishing Group; 2018; 9: 1849. doi: 10.1038/s41467-018-03917-2.
241. Kim Y-J, Wilson DM. Overview of base excision repair biochemistry. Curr Mol Pharmacol. NIH Public Access; 2012; 5: 3–13. doi: 10.2174/1874467211205010003.
242. Paik J, Duncan T, Lindahl T, Sedgwick B. Sensitization of human carcinoma cells to alkylating agents by small interfering RNA suppression of 3-alkyladenine-DNA glycosylase. Cancer Res. American Association for Cancer Research; 2005; 65: 10472–7. doi: 10.1158/0008-5472.CAN-05-1495.
243. Batenburg NL, Walker JR, Noordermeer SM, Moatti N, Durocher D, Zhu XD. ATM and CDK2 control chromatin remodeler CSB to inhibit RIF1 in DSB repair pathway choice. Nat Commun. Nature Publishing Group; 2017; 8: 1–17. doi: 10.1038/s41467-017-02114-x.
244. Wang J, Ding Q, Fujimori H, Motegi A, Miki Y, Masutani M. Loss of CtIP disturbs homologous recombination repair and sensitizes breast cancer cells to PARP inhibitors. Oncotarget. Impact Journals LLC; 2016; 7: 7701–14. doi: 10.18632/oncotarget.6715.
245. Mukherjee C, Tripathi V, Manolika EM, Heijink AM, Ricci G, Merzouk S, de Boer HR, Demmers J, van Vugt MATM, Ray Chaudhuri A. RIF1 promotes replication fork protection and efficient restart to maintain genome stability. Nat Commun. Nature Publishing Group; 2019; 10: 1–16. doi: 10.1038/s41467-019-11246-1.
246. Schlacher K, Christ N, Siaud N, Egashira A, Wu H, Jasin M. Double-strand break

repair-independent role for BRCA2 in blocking stalled replication fork degradation by MRE11. Cell. Elsevier; 2011; 145: 529–42. doi: 10.1016/j.cell.2011.03.041.

247. Bockstaele L, Kooken H, Libert F, Paternot S, Dumont JE, de Launoit Y, Roger PP, Coulonval K. Regulated Activating Thr172 Phosphorylation of Cyclin-Dependent Kinase 4(CDK4): Its Relationship with Cyclins and CDK Inhibitors. Mol Cell Biol. 2006; 26: 5070–85. doi: 10.1128/MCB.02006-05.
248. Okamoto A, Demetrick DJ, Spillare EA, Hagiwara K, Hussain SP, Bennett WP, Forrester K, Gerwin B, Serrano M, Beach DH. Mutations and altered expression of p16INK4 in human cancer. Proc Natl Acad Sci U S A. 1994; 91: 11045–9. Available from http://www.ncbi.nlm.nih.gov/pubmed/7972006
249. Crow J, Atay S, Banskota S, Artale B, Schmitt S, Godwin AK. Exosomes as mediators of platinum resistance in ovarian cancer. Oncotarget. Impact Journals LLC; 2017; 8: 11917–36. doi: 10.18632/oncotarget.14440.
250. Wickens M, Bernstein DS, Kimble J, Parker R. A PUF family portrait: 3′UTR regulation as a way of life. Trends in Genetics. Elsevier Current Trends; 2002. p. 150–7. doi: 10.1016/S0168-9525(01)02616-6.
251. Miller MA, Olivas WM. Roles of Puf proteins in mRNA degradation and translation. Wiley Interdiscip Rev RNA. 2011; 2: 471–92. doi: 10.1002/wrna.69.
252. Subramaniam K, Seydoux G. Dedifferentiation of primary spermatocytes into germ cell tumors in C. elegans Lacking the pumilio-like protein PUF-8. Curr Biol. Elsevier; 2003; 13: 134–9. doi: 10.1016/S0960-9822(03)00005-8.
253. Kuo M-W, Wang S-H, Chang J-C, Chang C-H, Huang L-J, Lin H-H, Yu AL-T, Li W-H, Yu J. A Novel puf-A Gene Predicted from Evolutionary Analysis Is Involved in the Development of Eyes and Primordial Germ-Cells. Volff J-N, editor. PLoS One. Public Library of Science; 2009; 4: e4980. doi: 10.1371/journal.pone.0004980.
254. Fan C-C, Lee L-Y, Yu M-Y, Tzen C-Y, Chou C, Chang M-S. Upregulated hPuf-A promotes breast cancer tumorigenesis. Tumor Biol. 2013; 34: 2557–64. doi: 10.1007/s13277-013-0801-4.
255. Strumberg D, Pilon AA, Smith M, Hickey R, Malkas L, Pommier Y. Conversion of Topoisomerase I Cleavage Complexes on the Leading Strand of Ribosomal DNA

into 5′-Phosphorylated DNA Double-Strand Breaks by Replication Runoff. Mol Cell Biol. American Society for Microbiology; 2000; 20: 3977–87. doi: 10.1128/mcb.20.11.3977-3987.2000.

256. Hsiang Y-H, Hertzberg R, Hecht S, Liu LF. Camptothecin Induces Protein-linked DNA Breaks via Mammalian DNA Topoisomerase I*. J Biol Chem. 1985; 260: 14873–8.

257. Sordet O, Larochelle S, Nicolas E, Stevens E V., Zhang C, Shokat KM, Fisher RP, Pommier Y. Hyperphosphorylation of RNA Polymerase II in Response to Topoisomerase I Cleavage Complexes and Its Association with Transcription- and BRCA1-dependent Degradation of Topoisomerase I. J Mol Biol. Academic Press; 2008; 381: 540–9. doi: 10.1016/j.jmb.2008.06.028.

258. Subramanian D, Rosenstein BS, Muller MT. Ultraviolet-induced DNA Damage Stimulates Topoisomerase I-DNA Complex Formation in Vivo: Possible Relationship with DNA Repair. Cancer Res. 1998; 58.

259. Chan GL, Doetsch PW, Haseltine WA. Cyclobutane Pyrimidine Dimers and (6-4) Photoproducts Block Polymerization by DNA Polymerase I†. Biochemistry. Wieslander, L; 1985; 24: 5723–8. doi: 10.1021/bi00342a006.

260. Karachaliou N, Gonzalez-Cao M, Crespo G, Drozdowskyj A, Aldeguer E, Gimenez-Capitan A, Teixido C, Molina-Vila MA, Viteri S, Gil MDLL, Algarra SM, Perez-Ruiz E, Marquez-Rodas I, et al. Interferon gamma, an important marker of response to immune checkpoint blockade in non-small cell lung cancer and melanoma patients. Ther Adv Med Oncol. SAGE Publications Inc.; 2018; 10. doi: 10.1177/1758834017749748.

261. Park H, Uronis H, Kang Y-K, Ng MCH, Enzinger P, Lee KW, Rutella S, Church SE, Nordstrom J, Knutson K, Erskine C, Wu T, Yen J, et al. Phase II study of olaparib + durvalumab (MEDIOLA): Updated results in germline BRCA-mutated platinum-sensitive relapsed (PSR) ovarian cancer (OC). Abstr B 44th ESMO Congr (ESMO 2019) 27 Sept – 1 Oct 2019, Barcelona, Spain. 2019; 30: v485–6. doi: 10.1093/annonc/mdz253.

262. Strickland KC, Howitt BE, Shukla SA, Rodig S, Ritterhouse LL, Liu JF, Garber JE, Chowdhury D, Wu CJ, D'Andrea AD, Matulonis UA, Konstantinopoulos PA.

Association and prognostic significance of BRCA1/2-mutation status with neoantigen load, number of tumor-infiltrating lymphocytes and expression of PD-1/PD-L1 in high grade serous ovarian cancer. Oncotarget. Impact Journals LLC; 2016; 7: 13587–98. doi: 10.18632/oncotarget.7277.

263. Hawkes NA, Otero G, Sebastiaan Winkler G, Marshall N, Dahmus ME, Krappmann D, Scheidereit C, Thomas CL, Schiavo G, Erdjument-Bromage H, Svejstrup JQ. Purification and characterization of the human elongator complex. J Biol Chem. American Society for Biochemistry and Molecular Biology; 2002; 277: 3047–52. doi: 10.1074/jbc.M110445200.

264. Lemmens BBLG, Johnson NM, Tijsterman M. COM-1 Promotes Homologous Recombination during Caenorhabditis elegans Meiosis by Antagonizing Ku-Mediated Non-Homologous End Joining. PLoS Genet. 2013; 9. doi: 10.1371/journal.pgen.1003276.

Appendices

Appendix A: Permission to include manuscript in Chapter 1

From: Cécile Le Page, PhD
Centre de recherche du CHUM
Montreal, CANADA
August 17, 2020

To whom it may concern,

PERMISSION TO INCLUDE MANUSCRIPT IN THESIS

I am writing to confirm that Setor Amuzu (PhD candidate, Department of Human Genetics, McGill University) and I are co-first authors of the manuscript titled LESSONS LEARNED FROM UNDERSTANDING CHEMOTHERAPY RESISTANCE IN TUBO-OVARIAN HIGH-GRADE SEROUS CARCINOMA FROM *BRCA1* AND *BRCA2* MUTATION CARRIERS which has been accepted for publication in the journal *Seminars in Cancer Biology*. This review article includes work that is relevant to the Introduction of Setor's PhD thesis. He duly requested my permission to include this work in his thesis. I have accordingly granted him my full permission to include this work in his thesis.

Sincerely,

.....
Cécile Le Page, PhD

Appendix B: Permission to reuse published figure in Chapter 1

Annual Reviews, Inc. - License Terms and Conditions

This is a License Agreement between Setor Amuzu ("You") and Annual Reviews, Inc. ("Publisher") provided by Copyright Clearance Center ("CCC"). The license consists of your order details, the terms and conditions provided by Annual Reviews, Inc., and the CCC terms and conditions.

All payments must be made in full to CCC.

Order Date	21-Jul-2020	Type of Use	Republish in a thesis/dissertation
Order license ID	1049934-1		
ISSN	2472-3428	Publisher	Annual Reviews
		Portion	Chart/graph/table/figure

LICENSED CONTENT

Publication Title	Annual review of cancer biology	Rightsholder	Annual Reviews, Inc.
		Publication Type	e-Journal
Date	01/01/2017	URL	http://www.annualreviews.org/journal/cancerbio
Language	English		
Country	United States of America		

REQUEST DETAILS

Portion Type	Chart/graph/table/figure	Distribution	Worldwide
Number of charts / graphs / tables / figures requested	1	Translation	Original language of publication
		Copies for the disabled?	No
Format (select all that apply)	Print, Electronic	Minor editing privileges?	No
Who will republish the content?	Academic institution	Incidental promotional use?	No
Duration of Use	Life of current and all future editions	Currency	CAD
Lifetime Unit Quantity	Up to 499		
Rights Requested	Main product		

NEW WORK DETAILS

Title	Candidate markers of olaparib sensitivity and resistance from genomic data analyses of human cancer cell lines	Institution name	McGill University
		Expected presentation date	2020-08-31
Instructor name	Dr. Ioannis Ragoussis		

ADDITIONAL DETAILS

Order reference number	N/A

The requesting person / organization to appear on the license	Setor Amuzu

REUSE CONTENT DETAILS

Title, description or numeric reference of the portion(s)	Figure 1c	Title of the article/chapter the portion is from	PARP Trapping Beyond Homologous Recombination and Platinum Sensitivity in Cancers
Editor of portion(s)	N/A	Author of portion(s)	Junko Murai , Yves Pommier
Volume of serial or monograph	3	Issue, if republishing an article from a serial	N/A
Page or page range of portion	131-150	Publication date of portion	2019-03-01

CCC Republication Terms and Conditions

1. Description of Service; Defined Terms. This Republication License enables the User to obtain licenses for republication of one or more copyrighted works as described in detail on the relevant Order Confirmation (the "Work(s)"). Copyright Clearance Center, Inc. ("CCC") grants licenses through the Service on behalf of the rightsholder identified on the Order Confirmation (the "Rightsholder"). "Republication", as used herein, generally means the inclusion of a Work, in whole or in part, in a new work or works, also as described on the Order Confirmation. "User", as used herein, means the person or entity making such republication.

2. The terms set forth in the relevant Order Confirmation, and any terms set by the Rightsholder with respect to a particular Work, govern the terms of use of Works in connection with the Service. By using the Service, the person transacting for a republication license on behalf of the User represents and warrants that he/she/it (a) has been duly authorized by the User to accept, and hereby does accept, all such terms and conditions on behalf of User, and (b) shall inform User of all such terms and conditions. In the event such person is a "freelancer" or other third party independent of User and CCC, such party shall be deemed jointly a "User" for purposes of these terms and conditions. In any event, User shall be deemed to have accepted and agreed to all such terms and conditions if User republishes the Work in any fashion.

3. Scope of License; Limitations and Obligations.

    3.1. All Works and all rights therein, including copyright rights, remain the sole and exclusive property of the Rightsholder. The license created by the exchange of an Order Confirmation (and/or any invoice) and payment by User of the full amount set forth on that document includes only those rights expressly set forth in the Order Confirmation and in these terms and conditions, and conveys no other rights in the Work(s) to User. All rights not expressly granted are hereby reserved.

    3.2. General Payment Terms: You may pay by credit card or through an account with us payable at the end of the month. If you and we agree that you may establish a standing account with CCC, then the following terms apply: Remit Payment to: Copyright Clearance Center, 29118 Network Place, Chicago, IL 60673-1291. Payments Due: Invoices are payable upon their delivery to you (or upon our notice to you that they are available to you for downloading). After 30 days, outstanding amounts will be subject to a service charge of 1-1/2% per month or, if less, the maximum rate allowed by applicable law. Unless otherwise specifically set forth in the Order Confirmation or in a separate written agreement signed by CCC, invoices are due and payable on "net 30" terms. While User may exercise the rights licensed immediately upon issuance of the Order Confirmation, the license is automatically revoked and is null and void, as if it had never been issued, if complete payment for the license is not received on a timely basis either from User directly or through a payment agent, such as a credit card company.

3.3. Unless otherwise provided in the Order Confirmation, any grant of rights to User (i) is "one-time" (including the editions and product family specified in the license), (ii) is non-exclusive and non-transferable and (iii) is subject to any and all limitations and restrictions (such as, but not limited to, limitations on duration of use or circulation) included in the Order Confirmation or invoice and/or in these terms and conditions. Upon completion of the licensed use, User shall either secure a new permission for further use of the Work(s) or immediately cease any new use of the Work(s) and shall render inaccessible (such as by deleting or by removing or severing links or other locators) any further copies of the Work (except for copies printed on paper in accordance with this license and still in User's stock at the end of such period).

3.4. In the event that the material for which a republication license is sought includes third party materials (such as photographs, illustrations, graphs, inserts and similar materials) which are identified in such material as having been used by permission, User is responsible for identifying, and seeking separate licenses (under this Service or otherwise) for, any of such third party materials; without a separate license, such third party materials may not be used.

3.5. Use of proper copyright notice for a Work is required as a condition of any license granted under the Service. Unless otherwise provided in the Order Confirmation, a proper copyright notice will read substantially as follows: "Republished with permission of [Rightsholder's name], from [Work's title, author, volume, edition number and year of copyright]; permission conveyed through Copyright Clearance Center, Inc. " Such notice must be provided in a reasonably legible font size and must be placed either immediately adjacent to the Work as used (for example, as part of a by-line or footnote but not as a separate electronic link) or in the place where substantially all other credits or notices for the new work containing the republished Work are located. Failure to include the required notice results in loss to the Rightsholder and CCC, and the User shall be liable to pay liquidated damages for each such failure equal to twice the use fee specified in the Order Confirmation, in addition to the use fee itself and any other fees and charges specified.

3.6. User may only make alterations to the Work if and as expressly set forth in the Order Confirmation. No Work may be used in any way that is defamatory, violates the rights of third parties (including such third parties' rights of copyright, privacy, publicity, or other tangible or intangible property), or is otherwise illegal, sexually explicit or obscene. In addition, User may not conjoin a Work with any other material that may result in damage to the reputation of the Rightsholder. User agrees to inform CCC if it becomes aware of any infringement of any rights in a Work and to cooperate with any reasonable request of CCC or the Rightsholder in connection therewith.

4. Indemnity. User hereby indemnifies and agrees to defend the Rightsholder and CCC, and their respective employees and directors, against all claims, liability, damages, costs and expenses, including legal fees and expenses, arising out of any use of a Work beyond the scope of the rights granted herein, or any use of a Work which has been altered in any unauthorized way by User, including claims of defamation or infringement of rights of copyright, publicity, privacy or other tangible or intangible property.

5. Limitation of Liability. UNDER NO CIRCUMSTANCES WILL CCC OR THE RIGHTSHOLDER BE LIABLE FOR ANY DIRECT, INDIRECT, CONSEQUENTIAL OR INCIDENTAL DAMAGES (INCLUDING WITHOUT LIMITATION DAMAGES FOR LOSS OF BUSINESS PROFITS OR INFORMATION, OR FOR BUSINESS INTERRUPTION) ARISING OUT OF THE USE OR INABILITY TO USE A WORK, EVEN IF ONE OF THEM HAS BEEN ADVISED OF THE POSSIBILITY OF SUCH DAMAGES. In any event, the total liability of the Rightsholder and CCC (including their respective employees and directors) shall not exceed the total amount actually paid by User for this license. User assumes full liability for the actions and omissions of its principals, employees, agents, affiliates, successors and assigns.

6. Limited Warranties. THE WORK(S) AND RIGHT(S) ARE PROVIDED "AS IS". CCC HAS THE RIGHT TO GRANT TO USER THE RIGHTS GRANTED IN THE ORDER CONFIRMATION DOCUMENT. CCC AND THE RIGHTSHOLDER DISCLAIM ALL OTHER WARRANTIES RELATING TO THE WORK(S) AND RIGHT(S), EITHER EXPRESS OR IMPLIED, INCLUDING WITHOUT LIMITATION IMPLIED WARRANTIES OF MERCHANTABILITY OR FITNESS FOR A PARTICULAR PURPOSE. ADDITIONAL RIGHTS MAY BE REQUIRED TO USE ILLUSTRATIONS, GRAPHS, PHOTOGRAPHS, ABSTRACTS, INSERTS OR OTHER PORTIONS OF THE WORK (AS OPPOSED TO THE ENTIRE WORK) IN A MANNER CONTEMPLATED BY USER;

USER UNDERSTANDS AND AGREES THAT NEITHER CCC NOR THE RIGHTSHOLDER MAY HAVE SUCH ADDITIONAL RIGHTS TO GRANT.

7. Effect of Breach. Any failure by User to pay any amount when due, or any use by User of a Work beyond the scope of the license set forth in the Order Confirmation and/or these terms and conditions, shall be a material breach of the license created by the Order Confirmation and these terms and conditions. Any breach not cured within 30 days of written notice thereof shall result in immediate termination of such license without further notice. Any unauthorized (but licensable) use of a Work that is terminated immediately upon notice thereof may be liquidated by payment of the Rightsholder's ordinary license price therefor; any unauthorized (and unlicensable) use that is not terminated immediately for any reason (including, for example, because materials containing the Work cannot reasonably be recalled) will be subject to all remedies available at law or in equity, but in no event to a payment of less than three times the Rightsholder's ordinary license price for the most closely analogous licensable use plus Rightsholder's and/or CCC's costs and expenses incurred in collecting such payment.

8. Miscellaneous.

    8.1. User acknowledges that CCC may, from time to time, make changes or additions to the Service or to these terms and conditions, and CCC reserves the right to send notice to the User by electronic mail or otherwise for the purposes of notifying User of such changes or additions; provided that any such changes or additions shall not apply to permissions already secured and paid for.

    8.2. Use of User-related information collected through the Service is governed by CCC's privacy policy, available online here:https://marketplace.copyright.com/rs-ui-web/mp/privacy-policy

    8.3. The licensing transaction described in the Order Confirmation is personal to User. Therefore, User may not assign or transfer to any other person (whether a natural person or an organization of any kind) the license created by the Order Confirmation and these terms and conditions or any rights granted hereunder; provided, however, that User may assign such license in its entirety on written notice to CCC in the event of a transfer of all or substantially all of User's rights in the new material which includes the Work(s) licensed under this Service.

    8.4. No amendment or waiver of any terms is binding unless set forth in writing and signed by the parties. The Rightsholder and CCC hereby object to any terms contained in any writing prepared by the User or its principals, employees, agents or affiliates and purporting to govern or otherwise relate to the licensing transaction described in the Order Confirmation, which terms are in any way inconsistent with any terms set forth in the Order Confirmation and/or in these terms and conditions or CCC's standard operating procedures, whether such writing is prepared prior to, simultaneously with or subsequent to the Order Confirmation, and whether such writing appears on a copy of the Order Confirmation or in a separate instrument.

    8.5. The licensing transaction described in the Order Confirmation document shall be governed by and construed under the law of the State of New York, USA, without regard to the principles thereof of conflicts of law. Any case, controversy, suit, action, or proceeding arising out of, in connection with, or related to such licensing transaction shall be brought, at CCC's sole discretion, in any federal or state court located in the County of New York, State of New York, USA, or in any federal or state court whose geographical jurisdiction covers the location of the Rightsholder set forth in the Order Confirmation. The parties expressly submit to the personal jurisdiction and venue of each such federal or state court.If you have any comments or questions about the Service or Copyright Clearance Center, please contact us at 978-750-8400 or send an e-mail to support@copyright.com.

v 1.1

Appendix C: List of DNA repair and cell cycle control genes investigated for genomic variations in HGSOC cell lines

ABL1	*CENPF*	*HES1*	*PAICS*	*SCARA3*
ACAT2	*CENPH*	*HEY1*	*PALB2*	*SETMAR*
AEN	*CENPK*	*HIST2H3C*	*PARG*	*SFN*
ALKBH1	*CENPM*	*HJURP*	*PARP1*	*SFRP1*
ANAPC1	*CENPN*	*HLTF*	*PARP2*	*SKP1*
ANAPC10	*CEP55*	*HMGA2*	*PARP3*	*SKP2*
ANAPC11	*CETN1*	*HMGB1*	*PARP4*	*SLC25A5*
ANAPC13	*CETN2*	*HMGB2*	*PARPBP*	*SLC38A2*
ANAPC2	*CETN3*	*HMGN2*	*PAXIP1*	*SLIRP*
ANAPC4	*CFL1*	*HMMR*	*PBK*	*SLX1A*
ANAPC5	*CFL2*	*HPRT1*	*PCNA*	*SLX1B*
ANAPC7	*CHAF1A*	*HSPD1*	*PER1*	*SMAD2*
ANLN	*CHAF1B*	*HUS1*	*PFN1*	*SMAD3*
ANP32E	*CHEK1*	*ID1*	*PFN2*	*SMAD4*
APC2	*CHEK2*	*IDH1*	*PKMYT1*	*SMARCA4*
APEX1	*CHFR*	*INCENP*	*PLK1*	*SMARCC1*
APEX2	*CIT*	*INF2*	*PLK3*	*SMC1A*
APTX	*CKAP2*	*IPO7*	*PMS1*	*SMC1B*
ASCC3	*CKAP5*	*ITGA6*	*PMS2*	*SMC2*
ASPM	*CKS1B*	*KAT5*	*PNKP*	*SMC3*
ATAD2	*CKS2*	*KIAA0101*	*POLA1*	*SMC5*
ATM	*CLK2*	*KIAA1524*	*POLB*	*SMC6*
ATR	*CREBBP*	*KIF11*	*POLD1*	*SMUG1*
ATRIP	*CSE1L*	*KIF15*	*POLD2*	*SNRPA1*
ATRX	*CTNNAL1*	*KIF18A*	*POLD3*	*SNRPD1*
AURKA	*CUL1*	*KIF20A*	*POLD4*	*SNRPD3*
AURKB	*CUL3*	*KIF22*	*POLE*	*SNRPG*
BABAM1	*CUL4A*	*KIF23*	*POLE2*	*SOX4*
BARD1	*CUL5*	*KIF3B*	*POLE3*	*SPAG5*
BCAS2	*DBF4*	*KIF4A*	*POLG*	*SPC24*
BCCIP	*DBI*	*KIFC1*	*POLH*	*SPC25*
BIRC5	*DCLRE1A*	*KNTC1*	*POLI*	*SPO11*
BLM	*DCLRE1B*	*KRT18*	*POLL*	*SSBP1*
BORA	*DCLRE1C*	*LIG1*	*POLM*	*STAG1*
BRCA1	*DCUN1D1*	*LIG3*	*POLQ*	*STAG2*
BRCA2	*DDB1*	*LIG4*	*PPP1CC*	*STK38L*
BRCC3	*DDB2*	*LIMK1*	*PPP1R12A*	*STK4*
BRIP1	*DERA*	*LLGL1*	*PPP2R1B*	*SYNE1*
BUB1	*DMC1*	*LLGL2*	*PPP2R2B*	*SYNE2*
BUB1B	*DNA2*	*MAD1L1*	*PPP2R5D*	*TCEA1*
BUB3	*DNTT*	*MAD2L1*	*PPP4C*	*TDG*
C17orf70	*DTL*	*MAD2L2*	*PPP4R1*	*TDP1*
C19orf40	*DTYMK*	*MAPK14*	*PPP4R4*	*TDP2*
C1orf86	*DUT*	*MAPRE1*	*PRDX4*	*TELO2*
CALM1	*E2F1*	*MAPRE2*	*PRDX6*	*TFDP1*
CCDC86	*E2F2*	*MASTL*	*PRIM1*	*TFDP2*
CCNA1	*E2F3*	*MBD4*	*PRKCA*	*TGFB1*
CCNA2	*E2F4*	*MCM2*	*PRKDC*	*TGFB2*
CCNB1	*E2F5*	*MCM3*	*PRPF19*	*TGFB3*
CCNB2	*E2F8*	*MCM4*	*PSMB3*	*TIPIN*
CCNB3	*EBP*	*MCM5*	*PSMB6*	*TK1*
CCNC	*ECT2*	*MCM6*	*PSMC3IP*	*TKT*

CCND1	*EEF1E1*	*MCM7*	*PTEN*	*TOP2A*
CCND2	*ENO1*	*MDC1*	*PTTG1*	*TOP3A*
CCND3	*EP300*	*MDM2*	*PTTG2*	*TOP3B*
CCNE1	*ERC1*	*MELK*	*RAB6A*	*TOPBP1*
CCNE2	*ERCC1*	*MGMT*	*RAB6C*	*TP53*
CCNF	*ERCC2*	*MKI67*	*RACGAP1*	*TP53BP1*
CCNG1	*ERCC3*	*MLH1*	*RAD1*	*TP73*
CCNG2	*ERCC4*	*MLH3*	*RAD17*	*TREX1*
CCNH	*ERCC5*	*MMS19*	*RAD21*	*TREX2*
CCNK	*ERCC6*	*MNAT1*	*RAD23A*	*TRIP13*
CCNL1	*ERCC8*	*MND1*	*RAD23B*	*TTK*
CCNL2	*ESPL1*	*MORF4L1*	*RAD50*	*TUBA1C*
CCNT1	*EXO1*	*MPG*	*RAD51*	*TUBA4A*
CCNT2	*EXO5*	*MRPL23*	*RAD51AP1*	*TUBG2*
CCT5	*EZH2*	*MRPL35*	*RAD51B*	*TUBGCP2*
CD320	*FAM64A*	*MRPL40*	*RAD51C*	*TUBGCP3*
CD9	*FAN1*	*MRPS17*	*RAD51D*	*TYMS*
CDC14A	*FANCA*	*MRPS28*	*RAD52*	*UBE2A*
CDC14B	*FANCC*	*MRTO4*	*RAD54B*	*UBE2B*
CDC16	*FANCE*	*MSH2*	*RAD54L*	*UBE2C*
CDC20	*FANCF*	*MSH3*	*RAD9A*	*UBE2N*
CDC20B	*FANCG*	*MSH6*	*RASSF1*	*UBE2S*
CDC23	*FANCI*	*MTHFD1*	*RB1*	*UBE2T*
CDC25A	*FANCL*	*MUS81*	*RBBP4*	*UBE2V2*
CDC25B	*FBL*	*MUTYH*	*RBBP8*	*UCK2*
CDC25C	*FBXO5*	*MYC*	*RBL1*	*UIMC1*
CDC26	*FDPS*	*MYH10*	*RBL2*	*UNG*
CDC27	*FEN1*	*MYH9*	*RBX1*	*UQCRH*
CDC45	*FLNA*	*MYL6*	*RECQL*	*USP1*
CDC5L	*FLNB*	*MYL7*	*RECQL4*	*VAMP8*
CDC6	*FMN1*	*MYLK*	*RECQL5*	*WDHD1*
CDC7	*FMN2*	*NABP2*	*REV1*	*WDR48*
CDCA5	*FOXN3*	*NBN*	*REV3L*	*WEE1*
CDCA8	*FXYD5*	*NCAPG*	*RFC1*	*WEE2*
CDH1	*FZR1*	*NDC80*	*RFC2*	*WRN*
CDK1	*GADD45A*	*NEIL1*	*RFC3*	*XAB2*
CDK10	*GADD45B*	*NEIL3*	*RFC4*	*XPA*
CDK2	*GADD45G*	*NEK2*	*RFC5*	*XPC*
CDK3	*GAPDH*	*NFATC2IP*	*RHOA*	*XRCC1*
CDK4	*GINS2*	*NHEJ1*	*RIF1*	*XRCC2*
CDK5	*GMNN*	*NSMCE4A*	*RIT1*	*XRCC3*
CDK6	*GSK3B*	*NTHL1*	*RMI1*	*XRCC4*
CDK7	*GSTO1*	*NUDT1*	*RNF4*	*XRCC5*
CDK8	*GTF2H1*	*NUDT15*	*RNF8*	*XRCC6*
CDK9	*GTF2H2*	*NUDT18*	*RNMT*	*YWHAB*
CDKL1	*GTF2H3*	*NUDT4*	*ROCK1*	*YWHAE*
CDKN1A	*GTF2H4*	*NUF2*	*ROCK2*	*YWHAG*
CDKN1B	*GTF2H5*	*OGG1*	*RPA1*	*YWHAH*
CDKN1C	*GTSE1*	*ORC1*	*RPA2*	*YWHAQ*
CDKN2A	*H2AFV*	*ORC2*	*RPA3*	*YWHAZ*
CDKN2B	*H2AFX*	*ORC3*	*RPA4*	*ZBTB17*
CDKN2C	*H2AFZ*	*ORC4*	*RRM1*	*ZRANB2*
CDKN2D	*HDAC1*	*ORC5*	*RRM2*	*ZW10*
CDKN3	*HDAC2*	*ORC6*	*RTEL1*	*ZWINT*
CENPE	*HERC2*	*PA2G4*		

Appendix D: List of Candidate olaparib sensitivity and resistance genes derived from multivariate analysis of GDSC cell lines

Ensembl ID	Coefficient	Gene	Association
ENSG00000172716	-0.11139	*SLFN11*	Sensitivity
ENSG00000143995	-0.06547	*MEIS1*	Sensitivity
ENSG00000120889	-0.05056	*TNFRSF10B*	Sensitivity
ENSG00000080608	-0.03497	*PUM3*	Sensitivity
ENSG00000157657	-0.03443	*ZNF618*	Sensitivity
ENSG00000105072	-0.03340	*C19orf44*	Sensitivity
ENSG00000135387	-0.03311	*CAPRIN1*	Sensitivity
ENSG00000184985	-0.03261	*SORCS2*	Sensitivity
ENSG00000099821	-0.03261	*POLRMT*	Sensitivity
ENSG00000132005	-0.02891	*RFX1*	Sensitivity
ENSG00000108953	-0.02658	*YWHAE*	Sensitivity
ENSG00000124496	-0.02635	*TRERF1*	Sensitivity
ENSG00000145982	-0.02624	*FARS2*	Sensitivity
ENSG00000140931	-0.02529	*CMTM3*	Sensitivity
ENSG00000163584	-0.02387	*RPL22L1*	Sensitivity
ENSG00000163359	-0.02261	*COL6A3*	Sensitivity
ENSG00000196565	-0.02233	*HBG2*	Sensitivity
ENSG00000091592	-0.02141	*NLRP1*	Sensitivity
ENSG00000107341	-0.02079	*UBE2R2*	Sensitivity
ENSG00000137074	-0.02040	*APTX*	Sensitivity
ENSG00000179094	-0.01953	*PER1*	Sensitivity
ENSG00000128713	-0.01757	*HOXD11*	Sensitivity
ENSG00000123977	-0.01631	*DAW1*	Sensitivity
ENSG00000112039	-0.01448	*FANCE*	Sensitivity
ENSG00000164736	-0.01415	*SOX17*	Sensitivity
ENSG00000101115	-0.01394	*SALL4*	Sensitivity
ENSG00000117154	-0.01259	*IGSF21*	Sensitivity
ENSG00000187961	-0.01177	*KLHL17*	Sensitivity
ENSG00000001167	-0.01104	*NFYA*	Sensitivity
ENSG00000164362	-0.00994	*TERT*	Sensitivity
ENSG00000171988	-0.00887	*JMJD1C*	Sensitivity
ENSG00000114439	-0.00874	*BBX*	Sensitivity
ENSG00000165115	-0.00836	*KIF27*	Sensitivity
ENSG00000100731	-0.00712	*PCNX1*	Sensitivity
ENSG00000183020	-0.00697	*AP2A2*	Sensitivity
ENSG00000258315	-0.00650	*C17orf49*	Sensitivity
ENSG00000196072	-0.00622	*BLOC1S2*	Sensitivity
ENSG00000170222	-0.00521	*ADPRM*	Sensitivity
ENSG00000203883	-0.00507	*SOX18*	Sensitivity
ENSG00000130176	-0.00255	*CNN1*	Sensitivity
ENSG00000172530	-0.00241	*BANP*	Sensitivity
ENSG00000120254	-0.00147	*MTHFD1L*	Sensitivity
ENSG00000183638	-0.00112	*RP1L1*	Sensitivity
ENSG00000215114	-0.00065	*UBXN2B*	Sensitivity
ENSG00000183837	-0.00058	*PNMA3*	Sensitivity

Ensembl ID	Coefficient	Gene	Association
ENSG00000122012	-0.00021	*SV2C*	Sensitivity
ENSG00000165671	-0.00003	*NSD1*	Sensitivity
ENSG00000006831	0.00004	*ADIPOR2*	Resistance
ENSG00000141279	0.00023	*NPEPPS*	Resistance
ENSG00000239305	0.00029	*RNF103*	Resistance
ENSG00000175556	0.00040	*LONRF3*	Resistance
ENSG00000105983	0.00067	*LMBR1*	Resistance
ENSG00000242802	0.00075	*AP5Z1*	Resistance
ENSG00000137491	0.00100	*SLCO2B1*	Resistance
ENSG00000171766	0.00104	*GATM*	Resistance
ENSG00000145354	0.00109	*CISD2*	Resistance
ENSG00000168763	0.00135	*CNNM3*	Resistance
ENSG00000198898	0.00135	*CAPZA2*	Resistance
ENSG00000089558	0.00139	*KCNH4*	Resistance
ENSG00000179889	0.00161	*PDXDC1*	Resistance
ENSG00000179889	0.00161	*PDXDC1*	Resistance
ENSG00000048462	0.00165	*TNFRSF17*	Resistance
ENSG00000183597	0.00170	*TANGO2*	Resistance
ENSG00000189157	0.00197	*FAM47E*	Resistance
ENSG00000105879	0.00209	*CBLL1*	Resistance
ENSG00000086232	0.00225	*EIF2AK1*	Resistance
ENSG00000168743	0.00228	*NPNT*	Resistance
ENSG00000147883	0.00238	*CDKN2B*	Resistance
ENSG00000141404	0.00281	*GNAL*	Resistance
ENSG00000137727	0.00403	*ARHGAP20*	Resistance
ENSG00000103316	0.00407	*CRYM*	Resistance
ENSG00000101417	0.00506	*PXMP4*	Resistance
ENSG00000124299	0.00565	*PEPD*	Resistance
ENSG00000188613	0.00585	*NANOS1*	Resistance
ENSG00000101412	0.00661	*E2F1*	Resistance
ENSG00000125995	0.00708	*ROMO1*	Resistance
ENSG00000144567	0.00746	*RETREG2*	Resistance
ENSG00000005471	0.00748	*ABCB4*	Resistance
ENSG00000126803	0.00769	*HSPA2*	Resistance
ENSG00000012504	0.00790	*NR1H4*	Resistance
ENSG00000109270	0.00842	*LAMTOR3*	Resistance
ENSG00000204019	0.00855	*CT83*	Resistance
ENSG00000265491	0.00947	*RNF115*	Resistance
ENSG00000106327	0.00965	*TFR2*	Resistance
ENSG00000086666	0.00971	*ZFAND6*	Resistance
ENSG00000021645	0.00980	*NRXN3*	Resistance
ENSG00000160439	0.01010	*RDH13*	Resistance
ENSG00000081665	0.01079	*ZNF506*	Resistance
ENSG00000135211	0.01085	*TMEM60*	Resistance
ENSG00000127993	0.01094	*RBM48*	Resistance
ENSG00000005249	0.01195	*PRKAR2B*	Resistance
ENSG00000141576	0.01205	*RNF157*	Resistance
ENSG00000018610	0.01254	*CXorf56*	Resistance

Ensembl ID	Coefficient	Gene	Association
ENSG00000185808	0.01332	*PIGP*	Resistance
ENSG00000158716	0.01361	*DUSP23*	Resistance
ENSG00000145022	0.01373	*TCTA*	Resistance
ENSG00000154975	0.01413	*CA10*	Resistance
ENSG00000188868	0.01422	*ZNF563*	Resistance
ENSG00000222011	0.01590	*FAM185A*	Resistance
ENSG00000170502	0.01686	*NUDT9*	Resistance
ENSG00000167074	0.01891	*TEF*	Resistance
ENSG00000133424	0.01920	*LARGE1*	Resistance
ENSG00000125356	0.01933	*NDUFA1*	Resistance
ENSG00000105835	0.01947	*NAMPT*	Resistance
ENSG00000180596	0.02040	*H2BC4*	Resistance
ENSG00000144407	0.02102	*PTH2R*	Resistance
ENSG00000108439	0.02129	*PNPO*	Resistance
ENSG00000166387	0.02191	*PPFIBP2*	Resistance
ENSG00000099974	0.02220	*DDTL*	Resistance
ENSG00000151882	0.02237	*CCL28*	Resistance
ENSG00000136052	0.02262	*SLC41A2*	Resistance
ENSG00000160856	0.02377	*FCRL3*	Resistance
ENSG00000183150	0.02833	*GPR19*	Resistance
ENSG00000168273	0.02967	*SMIM4*	Resistance
ENSG00000175874	0.03242	*CREG2*	Resistance
ENSG00000145685	0.03336	*LHFPL2*	Resistance
ENSG00000136710	0.03444	*CCDC115*	Resistance
ENSG00000101400	0.03806	*SNTA1*	Resistance
ENSG00000124257	0.04122	*NEURL2*	Resistance
ENSG00000063322	0.04475	*MED29*	Resistance
ENSG00000179833	0.04720	*SERTAD2*	Resistance
ENSG00000243955	0.08401	*GSTA1*	Resistance

Appendix E: List of Candidate olaparib sensitivity and resistance genes derived from univariate analysis of GDSC cell lines

Gene	Ensembl ID	FDR-adjusted p-value	Coefficient	Association	95% confidence interval
GPX8	ENSG00000164294	0.000628	-0.321	sensitive	-0.45 - -0.192
ITGA5	ENSG00000161638	0.0003415	-0.284	sensitive	-0.392 - -0.175
DSE	ENSG00000111817	1.85E-05	-0.258	sensitive	-0.344 - -0.173
SYDE1	ENSG00000105137	0.009849	-0.256	sensitive	-0.392 - -0.121
MRC2	ENSG00000011028	0.0008042	-0.251	sensitive	-0.354 - -0.148
HTR7	ENSG00000148680	1.961E-05	-0.248	sensitive	-0.331 - -0.165
EXT1	ENSG00000182197	0.001391	-0.245	sensitive	-0.352 - -0.139
PTPN14	ENSG00000152104	0.001684	-0.244	sensitive	-0.352 - -0.137
HNRNPC	ENSG00000092199	0.0001019	-0.241	sensitive	-0.328 - -0.154
CCDC80	ENSG00000091986	0.003295	-0.238	sensitive	-0.35 - -0.127
BNC1	ENSG00000169594	0.0003928	-0.235	sensitive	-0.326 - -0.144
HNRNPA1	ENSG00000135486	0.0004935	-0.234	sensitive	-0.327 - -0.142
PDLIM7	ENSG00000196923	0.0008375	-0.234	sensitive	-0.331 - -0.138
OSMR	ENSG00000145623	0.007547	-0.231	sensitive	-0.348 - -0.113
ITPRIP	ENSG00000148841	2.648E-05	-0.23	sensitive	-0.308 - -0.152
MMP14	ENSG00000157227	0.001128	-0.23	sensitive	-0.328 - -0.132
FSTL1	ENSG00000163430	0.005845	-0.229	sensitive	-0.343 - -0.116
CLMP	ENSG00000166250	0.0004761	-0.229	sensitive	-0.319 - -0.14
SLFN11	ENSG00000172716	1.85E-05	-0.229	sensitive	-0.305 - -0.153
RBMS2	ENSG00000076067	0.003295	-0.227	sensitive	-0.334 - -0.121
IER3	ENSG00000137331	0.003028	-0.227	sensitive	-0.333 - -0.122
AXL	ENSG00000167601	0.006954	-0.226	sensitive	-0.34 - -0.112
PLAU	ENSG00000122861	0.001332	-0.224	sensitive	-0.321 - -0.127
RPL22L1	ENSG00000163584	1.85E-05	-0.223	sensitive	-0.296 - -0.15
LOXL2	ENSG00000134013	0.003417	-0.22	sensitive	-0.324 - -0.116
FLI1	ENSG00000151702	0.001332	-0.22	sensitive	-0.314 - -0.125
ANXA2	ENSG00000182718	0.01644	-0.219	sensitive	-0.343 - -0.095
ACTN1	ENSG00000072110	0.00743	-0.217	sensitive	-0.327 - -0.106
IGF2BP2	ENSG00000073792	0.0005753	-0.217	sensitive	-0.304 - -0.13
SH3PXD2B	ENSG00000174705	0.000628	-0.217	sensitive	-0.304 - -0.129
FMNL1	ENSG00000184922	0.0008042	-0.217	sensitive	-0.305 - -0.128
ANXA1	ENSG00000135046	0.002818	-0.216	sensitive	-0.315 - -0.117
RIOK1	ENSG00000124784	0.0002731	-0.214	sensitive	-0.295 - -0.133
ANTXR1	ENSG00000169604	0.007881	-0.214	sensitive	-0.324 - -0.104
TNFRSF12A	ENSG00000006327	0.0414	-0.213	sensitive	-0.352 - -0.074
GSDME	ENSG00000105928	0.001128	-0.213	sensitive	-0.304 - -0.123
DBN1	ENSG00000113758	0.001128	-0.213	sensitive	-0.304 - -0.122
CKAP4	ENSG00000136026	0.003822	-0.212	sensitive	-0.313 - -0.111
IL31RA	ENSG00000164509	0.0006059	-0.211	sensitive	-0.296 - -0.126
PFAS	ENSG00000178921	0.0003928	-0.211	sensitive	-0.293 - -0.13
PLAUR	ENSG00000011422	0.001666	-0.209	sensitive	-0.301 - -0.117
COL4A2	ENSG00000134871	0.002461	-0.209	sensitive	-0.304 - -0.114
SRPK1	ENSG00000096063	0.0004935	-0.207	sensitive	-0.288 - -0.125

Gene	Ensembl ID	FDR-adjusted p-value	Coefficient	Association	95% confidence interval
TMEM92	ENSG00000167105	0.005082	-0.205	sensitive	-0.305 - -0.105
TUBB6	ENSG00000176014	0.002807	-0.205	sensitive	-0.3 - -0.111
LAMB3	ENSG00000196878	0.02062	-0.205	sensitive	-0.325 - -0.085
MOCOS	ENSG00000075643	0.003474	-0.204	sensitive	-0.3 - -0.107
BCAT1	ENSG00000060982	0.0006579	-0.199	sensitive	-0.28 - -0.119
RPL10A	ENSG00000198755	0.002025	-0.199	sensitive	-0.288 - -0.11
CMTM3	ENSG00000140931	0.001816	-0.197	sensitive	-0.284 - -0.11
AMOTL2	ENSG00000114019	0.03475	-0.195	sensitive	-0.319 - -0.071
FERMT1	ENSG00000101311	0.007979	-0.194	sensitive	-0.293 - -0.094
COL4A1	ENSG00000187498	0.005937	-0.194	sensitive	-0.29 - -0.098
SERPINE1	ENSG00000106366	0.01938	-0.193	sensitive	-0.305 - -0.081
CLIC4	ENSG00000169504	0.002205	-0.193	sensitive	-0.279 - -0.106
SOCS3	ENSG00000184557	0.004856	-0.193	sensitive	-0.287 - -0.099
DAW1	ENSG00000123977	0.0008611	-0.192	sensitive	-0.272 - -0.113
IL6	ENSG00000136244	0.01151	-0.19	sensitive	-0.292 - -0.088
FGFBP1	ENSG00000137440	0.01987	-0.19	sensitive	-0.3 - -0.079
PDCD1LG2	ENSG00000197646	0.007583	-0.19	sensitive	-0.287 - -0.093
TAX1BP3	ENSG00000213977	0.01428	-0.19	sensitive	-0.295 - -0.085
PXDN	ENSG00000130508	0.002858	-0.187	sensitive	-0.273 - -0.1
PAPPA	ENSG00000182752	0.00463	-0.187	sensitive	-0.277 - -0.096
S100A2	ENSG00000196754	0.01842	-0.187	sensitive	-0.294 - -0.079
KIFC3	ENSG00000140859	0.02153	-0.186	sensitive	-0.296 - -0.076
FOSL1	ENSG00000175592	0.01444	-0.186	sensitive	-0.29 - -0.083
POLR1E	ENSG00000137054	0.000502	-0.185	sensitive	-0.259 - -0.112
FANCE	ENSG00000112039	0.001128	-0.184	sensitive	-0.263 - -0.106
PIK3CD	ENSG00000171608	0.004167	-0.184	sensitive	-0.273 - -0.096
ZCCHC7	ENSG00000147905	0.001391	-0.183	sensitive	-0.262 - -0.103
PROSER2	ENSG00000148426	0.008661	-0.183	sensitive	-0.278 - -0.088
EXT2	ENSG00000151348	0.0146	-0.183	sensitive	-0.285 - -0.081
PEAR1	ENSG00000187800	0.004588	-0.183	sensitive	-0.271 - -0.094
SPEG	ENSG00000072195	0.01515	-0.182	sensitive	-0.284 - -0.08
TRIML2	ENSG00000179046	0.0009425	-0.182	sensitive	-0.257 - -0.106
AGRN	ENSG00000188157	0.0414	-0.182	sensitive	-0.3 - -0.063
PUM3	ENSG00000080608	0.000166	-0.18	sensitive	-0.247 - -0.114
ELK3	ENSG00000111145	0.003005	-0.18	sensitive	-0.264 - -0.097
NEXN	ENSG00000162614	0.006954	-0.18	sensitive	-0.27 - -0.089
TPM4	ENSG00000167460	0.003417	-0.18	sensitive	-0.265 - -0.095
FAM83G	ENSG00000188522	0.004563	-0.18	sensitive	-0.267 - -0.093
HMGA1	ENSG00000137309	0.0009764	-0.179	sensitive	-0.254 - -0.105
SERBP1	ENSG00000142864	0.001128	-0.179	sensitive	-0.254 - -0.103
DHX33	ENSG00000005100	0.001	-0.178	sensitive	-0.253 - -0.104
NLRP1	ENSG00000091592	0.001816	-0.178	sensitive	-0.257 - -0.1
RPS9	ENSG00000170889	0.004082	-0.178	sensitive	-0.263 - -0.093
COL27A1	ENSG00000196739	0.00325	-0.178	sensitive	-0.262 - -0.095
SRPX	ENSG00000101955	0.02384	-0.177	sensitive	-0.283 - -0.071
ITGB1	ENSG00000150093	0.03683	-0.177	sensitive	-0.291 - -0.064

Gene	Ensembl ID	FDR-adjusted p-value	Coefficient	Association	95% confidence interval
KIRREL1	ENSG00000183853	0.04708	-0.177	sensitive	-0.296 - -0.059
C10orf55	ENSG00000222047	0.009255	-0.177	sensitive	-0.27 - -0.084
AFAP1L1	ENSG00000157510	0.0116	-0.176	sensitive	-0.272 - -0.081
C1QBP	ENSG00000108561	0.0012	-0.175	sensitive	-0.25 - -0.1
PDGFRB	ENSG00000113721	0.007576	-0.175	sensitive	-0.265 - -0.086
FAM20C	ENSG00000177706	0.01134	-0.175	sensitive	-0.269 - -0.081
SMARCD1	ENSG00000066117	0.007225	-0.174	sensitive	-0.263 - -0.086
PLS3	ENSG00000102024	0.02154	-0.174	sensitive	-0.277 - -0.071
MTHFD1L	ENSG00000120254	0.0008375	-0.174	sensitive	-0.245 - -0.102
KHDRBS1	ENSG00000121774	0.007947	-0.174	sensitive	-0.263 - -0.084
SNRPA	ENSG00000077312	0.0097	-0.173	sensitive	-0.265 - -0.082
TLN1	ENSG00000137076	0.005885	-0.173	sensitive	-0.259 - -0.087
CCDC138	ENSG00000163006	0.00743	-0.173	sensitive	-0.261 - -0.085
RIN1	ENSG00000174791	0.0097	-0.173	sensitive	-0.265 - -0.082
GEMIN4	ENSG00000179409	0.0008611	-0.173	sensitive	-0.244 - -0.101
HMGA2	ENSG00000149948	0.006084	-0.172	sensitive	-0.257 - -0.086
FERMT2	ENSG00000073712	0.02488	-0.171	sensitive	-0.274 - -0.068
CXCL2	ENSG00000081041	0.01938	-0.171	sensitive	-0.27 - -0.072
LY6K	ENSG00000160886	0.008701	-0.171	sensitive	-0.26 - -0.082
COX10	ENSG00000006695	0.0007742	-0.17	sensitive	-0.24 - -0.101
RAB34	ENSG00000109113	0.007841	-0.17	sensitive	-0.257 - -0.083
MMP2	ENSG00000087245	0.02293	-0.169	sensitive	-0.269 - -0.068
RPL18A	ENSG00000105640	0.003354	-0.169	sensitive	-0.249 - -0.09
YARS1	ENSG00000134684	0.001366	-0.169	sensitive	-0.243 - -0.096
PPP1R18	ENSG00000146112	0.006954	-0.169	sensitive	-0.255 - -0.084
KCNG1	ENSG00000026559	0.003295	-0.168	sensitive	-0.247 - -0.089
ITGA2	ENSG00000164171	0.04485	-0.168	sensitive	-0.279 - -0.056
SAAL1	ENSG00000166788	0.003028	-0.168	sensitive	-0.246 - -0.09
CCDC69	ENSG00000198624	0.01151	-0.168	sensitive	-0.258 - -0.077
ETV5	ENSG00000244405	0.003069	-0.168	sensitive	-0.247 - -0.09
ANXA8	ENSG00000265190	0.02695	-0.168	sensitive	-0.271 - -0.066
EXOSC3	ENSG00000107371	0.001128	-0.167	sensitive	-0.238 - -0.096
RPL26	ENSG00000161970	0.00148	-0.167	sensitive	-0.24 - -0.094
IL7R	ENSG00000168685	0.009594	-0.167	sensitive	-0.255 - -0.079
ADPRM	ENSG00000170222	0.001128	-0.167	sensitive	-0.238 - -0.096
LRRC8E	ENSG00000171017	0.03561	-0.167	sensitive	-0.274 - -0.061
ILF3	ENSG00000129351	0.02105	-0.166	sensitive	-0.264 - -0.069
WLS	ENSG00000116729	0.01408	-0.165	sensitive	-0.257 - -0.074
RAB11FIP5	ENSG00000135631	0.04552	-0.165	sensitive	-0.276 - -0.055
GLIPR1	ENSG00000139278	0.01259	-0.165	sensitive	-0.255 - -0.075
NOB1	ENSG00000141101	0.00759	-0.165	sensitive	-0.249 - -0.08
PLEKHN1	ENSG00000187583	0.04549	-0.165	sensitive	-0.275 - -0.055
VCL	ENSG00000035403	0.02695	-0.164	sensitive	-0.265 - -0.064
MICALL1	ENSG00000100139	0.008256	-0.164	sensitive	-0.249 - -0.079
WASF1	ENSG00000112290	0.01833	-0.164	sensitive	-0.258 - -0.069
KIF21B	ENSG00000116852	0.01079	-0.164	sensitive	-0.251 - -0.076

Gene	Ensembl ID	FDR-adjusted p-value	Coefficient	Association	95% confidence interval
FOXF2	ENSG00000137273	0.009956	-0.164	sensitive	-0.251 - -0.077
CDC42EP2	ENSG00000149798	0.01786	-0.164	sensitive	-0.259 - -0.07
PACSIN3	ENSG00000165912	0.02108	-0.164	sensitive	-0.26 - -0.067
USP43	ENSG00000154914	0.03923	-0.163	sensitive	-0.269 - -0.058
LARP6	ENSG00000166173	0.04807	-0.163	sensitive	-0.273 - -0.054
SMOX	ENSG00000088826	0.008356	-0.162	sensitive	-0.246 - -0.078
TWNK	ENSG00000107815	0.01063	-0.162	sensitive	-0.249 - -0.076
SPART	ENSG00000133104	0.02019	-0.162	sensitive	-0.256 - -0.067
CDA	ENSG00000158825	0.02779	-0.162	sensitive	-0.262 - -0.063
IGFBP6	ENSG00000167779	0.03678	-0.162	sensitive	-0.265 - -0.058
IL1A	ENSG00000115008	0.01291	-0.161	sensitive	-0.249 - -0.073
TNFRSF10B	ENSG00000120889	0.005047	-0.161	sensitive	-0.239 - -0.082
TUT4	ENSG00000134744	0.01747	-0.161	sensitive	-0.253 - -0.069
DDX21	ENSG00000165732	0.004082	-0.161	sensitive	-0.238 - -0.084
EFEMP2	ENSG00000172638	0.01877	-0.161	sensitive	-0.254 - -0.068
YWHAE	ENSG00000108953	0.001073	-0.16	sensitive	-0.227 - -0.093
BYSL	ENSG00000112578	0.002205	-0.16	sensitive	-0.232 - -0.088
IFITM3	ENSG00000142089	0.02102	-0.16	sensitive	-0.254 - -0.066
STOML2	ENSG00000165283	0.00202	-0.16	sensitive	-0.231 - -0.089
GPR176	ENSG00000166073	0.03974	-0.16	sensitive	-0.263 - -0.056
TPM2	ENSG00000198467	0.009255	-0.16	sensitive	-0.244 - -0.076
TWIST2	ENSG00000233608	0.008256	-0.16	sensitive	-0.242 - -0.077
NPM3	ENSG00000107833	0.005558	-0.159	sensitive	-0.238 - -0.081
TNFAIP3	ENSG00000118503	0.01128	-0.159	sensitive	-0.244 - -0.073
FXR2	ENSG00000129245	0.00202	-0.159	sensitive	-0.23 - -0.088
ALDH1L2	ENSG00000136010	0.003028	-0.159	sensitive	-0.233 - -0.085
HAUS6	ENSG00000147874	0.003295	-0.159	sensitive	-0.233 - -0.084
COL13A1	ENSG00000197467	0.01245	-0.159	sensitive	-0.245 - -0.072
MAP4K4	ENSG00000071054	0.003693	-0.158	sensitive	-0.233 - -0.083
FXYD5	ENSG00000089327	0.01463	-0.158	sensitive	-0.246 - -0.07
KIAA0753	ENSG00000198920	0.001332	-0.158	sensitive	-0.226 - -0.09
NCL	ENSG00000115053	0.007125	-0.157	sensitive	-0.237 - -0.078
SINHCAF	ENSG00000139146	0.02133	-0.157	sensitive	-0.25 - -0.065
EIF3M	ENSG00000149100	0.004082	-0.157	sensitive	-0.232 - -0.082
C16orf74	ENSG00000154102	0.006749	-0.157	sensitive	-0.235 - -0.078
OSCAR	ENSG00000170909	0.003844	-0.157	sensitive	-0.232 - -0.082
MOB3A	ENSG00000172081	0.009393	-0.157	sensitive	-0.24 - -0.075
MYBBP1A	ENSG00000132382	0.00202	-0.156	sensitive	-0.225 - -0.086
NAT10	ENSG00000135372	0.01065	-0.156	sensitive	-0.24 - -0.073
RSL24D1	ENSG00000137876	0.01199	-0.156	sensitive	-0.24 - -0.071
CEP170	ENSG00000143702	0.03792	-0.156	sensitive	-0.256 - -0.055
NOC3L	ENSG00000173145	0.003423	-0.156	sensitive	-0.23 - -0.082
CARS1	ENSG00000110619	0.002205	-0.155	sensitive	-0.224 - -0.085
SLFN5	ENSG00000166750	0.0193	-0.155	sensitive	-0.244 - -0.065
TBXA2R	ENSG00000006638	0.00743	-0.154	sensitive	-0.232 - -0.076
PHF23	ENSG00000040633	0.002807	-0.154	sensitive	-0.225 - -0.083

Gene	Ensembl ID	FDR-adjusted p-value	Coefficient	Association	95% confidence interval
POLRMT	ENSG00000099821	0.005452	-0.154	sensitive	-0.231 - -0.078
RPS6	ENSG00000137154	0.01091	-0.154	sensitive	-0.237 - -0.072
FBN2	ENSG00000138829	0.00666	-0.154	sensitive	-0.231 - -0.077
PTX3	ENSG00000163661	0.01734	-0.154	sensitive	-0.242 - -0.066
ELAC2	ENSG00000006744	0.002205	-0.153	sensitive	-0.222 - -0.084
YBX3	ENSG00000060138	0.006648	-0.153	sensitive	-0.23 - -0.076
HOXD11	ENSG00000128713	0.01482	-0.153	sensitive	-0.238 - -0.068
NT5E	ENSG00000135318	0.0436	-0.153	sensitive	-0.253 - -0.052
SAA1	ENSG00000173432	0.03225	-0.153	sensitive	-0.249 - -0.057
UPP1	ENSG00000183696	0.04665	-0.153	sensitive	-0.256 - -0.051
MMP17	ENSG00000198598	0.0163	-0.153	sensitive	-0.24 - -0.067
DKK1	ENSG00000107984	0.03475	-0.152	sensitive	-0.248 - -0.055
NMI	ENSG00000123609	0.02823	-0.152	sensitive	-0.245 - -0.058
TTLL4	ENSG00000135912	0.009956	-0.152	sensitive	-0.233 - -0.072
FMNL2	ENSG00000157827	0.01065	-0.152	sensitive	-0.233 - -0.071
GART	ENSG00000159131	0.004082	-0.152	sensitive	-0.225 - -0.079
CTDNEP1	ENSG00000175826	0.00148	-0.152	sensitive	-0.218 - -0.086
LGALS1	ENSG00000100097	0.04759	-0.151	sensitive	-0.253 - -0.05
PAPOLG	ENSG00000115421	0.01189	-0.151	sensitive	-0.233 - -0.069
SCO1	ENSG00000133028	0.002807	-0.151	sensitive	-0.221 - -0.082
XDH	ENSG00000158125	0.03678	-0.151	sensitive	-0.247 - -0.054
RUVBL1	ENSG00000175792	0.004082	-0.151	sensitive	-0.224 - -0.079
APCDD1L	ENSG00000198768	0.0257	-0.151	sensitive	-0.242 - -0.059
RCL1	ENSG00000120158	0.006864	-0.15	sensitive	-0.226 - -0.075
CARM1	ENSG00000142453	0.006084	-0.15	sensitive	-0.225 - -0.075
RBMX	ENSG00000147274	0.04549	-0.15	sensitive	-0.25 - -0.05
ANKRD33B	ENSG00000164236	0.008661	-0.15	sensitive	-0.228 - -0.072
DNMBP	ENSG00000107554	0.008701	-0.149	sensitive	-0.226 - -0.071
SIX1	ENSG00000126778	0.01734	-0.149	sensitive	-0.234 - -0.064
EIF5A	ENSG00000132507	0.002818	-0.149	sensitive	-0.218 - -0.081
PNPT1	ENSG00000138035	0.006431	-0.149	sensitive	-0.223 - -0.074
EDNRA	ENSG00000151617	0.01482	-0.149	sensitive	-0.232 - -0.066
TGM2	ENSG00000198959	0.04428	-0.149	sensitive	-0.247 - -0.05
MRPS31	ENSG00000102738	0.01852	-0.148	sensitive	-0.234 - -0.063
NUP88	ENSG00000108559	0.004588	-0.148	sensitive	-0.22 - -0.076
RGS10	ENSG00000148908	0.006084	-0.148	sensitive	-0.221 - -0.074
PUS1	ENSG00000177192	0.01656	-0.148	sensitive	-0.231 - -0.064
RPL12	ENSG00000197958	0.01055	-0.148	sensitive	-0.227 - -0.069
LIMA1	ENSG00000050405	0.04054	-0.147	sensitive	-0.243 - -0.051
TFAM	ENSG00000108064	0.01488	-0.147	sensitive	-0.23 - -0.065
RAB23	ENSG00000112210	0.02823	-0.147	sensitive	-0.237 - -0.057
LLGL1	ENSG00000131899	0.0146	-0.147	sensitive	-0.23 - -0.065
HERC4	ENSG00000148634	0.01595	-0.147	sensitive	-0.229 - -0.064
TAF5	ENSG00000148835	0.04228	-0.147	sensitive	-0.244 - -0.051
SSRP1	ENSG00000149136	0.006954	-0.147	sensitive	-0.221 - -0.073
NKX6-1	ENSG00000163623	0.01412	-0.147	sensitive	-0.228 - -0.066

Gene	Ensembl ID	FDR-adjusted p-value	Coefficient	Association	95% confidence interval
ARNTL2	ENSG00000029153	0.01938	-0.146	sensitive	-0.23 - -0.061
WDR75	ENSG00000115368	0.007288	-0.146	sensitive	-0.219 - -0.072
SFPQ	ENSG00000116560	0.03466	-0.146	sensitive	-0.239 - -0.053
TRA2B	ENSG00000136527	0.02496	-0.146	sensitive	-0.234 - -0.058
ANP32B	ENSG00000136938	0.02035	-0.146	sensitive	-0.232 - -0.061
SHISAL1	ENSG00000138944	0.02557	-0.146	sensitive	-0.235 - -0.058
RPS27A	ENSG00000143947	0.01868	-0.146	sensitive	-0.23 - -0.062
NAF1	ENSG00000145414	0.01656	-0.146	sensitive	-0.228 - -0.063
EIF4A1	ENSG00000161960	0.005213	-0.146	sensitive	-0.217 - -0.074
TUBA1C	ENSG00000167553	0.02129	-0.146	sensitive	-0.232 - -0.06
TLCD3A	ENSG00000167695	0.01754	-0.146	sensitive	-0.23 - -0.063
SLC35G2	ENSG00000168917	0.0172	-0.146	sensitive	-0.229 - -0.063
IL20RB	ENSG00000174564	0.01173	-0.146	sensitive	-0.225 - -0.067
RNF217	ENSG00000146373	0.02645	-0.145	sensitive	-0.233 - -0.057
SYCP2L	ENSG00000153157	0.006954	-0.145	sensitive	-0.218 - -0.072
IGFBP7	ENSG00000163453	0.04498	-0.145	sensitive	-0.241 - -0.049
CXCL1	ENSG00000163739	0.04164	-0.145	sensitive	-0.24 - -0.05
PSIP1	ENSG00000164985	0.03173	-0.145	sensitive	-0.235 - -0.054
MTHFD2	ENSG00000065911	0.0101	-0.144	sensitive	-0.221 - -0.068
NUP37	ENSG00000075188	0.01173	-0.144	sensitive	-0.222 - -0.066
DIMT1	ENSG00000086189	0.009255	-0.144	sensitive	-0.219 - -0.069
RPL6	ENSG00000089009	0.01868	-0.144	sensitive	-0.227 - -0.061
MRPL19	ENSG00000115364	0.005896	-0.144	sensitive	-0.216 - -0.073
HOXD10	ENSG00000128710	0.02351	-0.144	sensitive	-0.231 - -0.058
GFPT2	ENSG00000131459	0.04677	-0.144	sensitive	-0.24 - -0.048
LRFN4	ENSG00000173621	0.005082	-0.144	sensitive	-0.215 - -0.074
TEAD4	ENSG00000197905	0.01796	-0.144	sensitive	-0.226 - -0.061
NAV3	ENSG00000067798	0.02584	-0.143	sensitive	-0.23 - -0.056
HEATR1	ENSG00000119285	0.00759	-0.143	sensitive	-0.216 - -0.07
CD274	ENSG00000120217	0.02105	-0.143	sensitive	-0.227 - -0.059
COL5A1	ENSG00000130635	0.04122	-0.143	sensitive	-0.237 - -0.05
LRRIQ1	ENSG00000133640	0.01508	-0.143	sensitive	-0.223 - -0.063
CAPRIN1	ENSG00000135387	0.003354	-0.143	sensitive	-0.21 - -0.076
ZNF697	ENSG00000143067	0.04177	-0.143	sensitive	-0.236 - -0.049
PLEKHO1	ENSG00000023902	0.04335	-0.142	sensitive	-0.235 - -0.048
GLT8D2	ENSG00000120820	0.02861	-0.142	sensitive	-0.23 - -0.055
TRIP10	ENSG00000125733	0.04677	-0.142	sensitive	-0.237 - -0.047
YARS2	ENSG00000139131	0.00904	-0.142	sensitive	-0.216 - -0.068
LSM6	ENSG00000164167	0.01622	-0.142	sensitive	-0.222 - -0.062
SEMA6B	ENSG00000167680	0.01821	-0.142	sensitive	-0.224 - -0.06
TSR1	ENSG00000167721	0.003334	-0.142	sensitive	-0.209 - -0.075
HASPIN	ENSG00000177602	0.01455	-0.142	sensitive	-0.221 - -0.063
XRCC5	ENSG00000079246	0.009162	-0.141	sensitive	-0.214 - -0.067
NAV1	ENSG00000134369	0.03454	-0.141	sensitive	-0.23 - -0.052
CTPS1	ENSG00000171793	0.01022	-0.141	sensitive	-0.216 - -0.066
ZBED2	ENSG00000177494	0.04247	-0.141	sensitive	-0.234 - -0.049

Gene	Ensembl ID	FDR-adjusted p-value	Coefficient	Association	95% confidence interval
NPM1	ENSG00000181163	0.008661	-0.141	sensitive	-0.215 - -0.068
MAT2B	ENSG00000038274	0.01151	-0.14	sensitive	-0.216 - -0.065
EIF4B	ENSG00000063046	0.02389	-0.14	sensitive	-0.223 - -0.056
COL16A1	ENSG00000084636	0.03602	-0.14	sensitive	-0.23 - -0.051
RPL3	ENSG00000100316	0.02907	-0.14	sensitive	-0.226 - -0.053
BAG2	ENSG00000112208	0.007225	-0.14	sensitive	-0.211 - -0.069
TAF1B	ENSG00000115750	0.005709	-0.14	sensitive	-0.209 - -0.071
DYRK3	ENSG00000143479	0.03113	-0.14	sensitive	-0.227 - -0.053
RPL27A	ENSG00000166441	0.02048	-0.14	sensitive	-0.221 - -0.058
KIF7	ENSG00000166813	0.02941	-0.14	sensitive	-0.226 - -0.053
B3GNT5	ENSG00000176597	0.03174	-0.14	sensitive	-0.227 - -0.052
POLR2A	ENSG00000181222	0.005845	-0.14	sensitive	-0.209 - -0.07
RFLNB	ENSG00000183688	0.027	-0.14	sensitive	-0.225 - -0.054
SLC39A10	ENSG00000196950	0.007914	-0.14	sensitive	-0.212 - -0.068
PHB2	ENSG00000215021	0.01729	-0.14	sensitive	-0.22 - -0.06
MSANTD3	ENSG00000066697	0.04482	-0.139	sensitive	-0.232 - -0.047
RPL24	ENSG00000114391	0.01572	-0.139	sensitive	-0.218 - -0.061
MMP19	ENSG00000123342	0.03602	-0.139	sensitive	-0.228 - -0.05
EIF3G	ENSG00000130811	0.009195	-0.139	sensitive	-0.211 - -0.066
CCNA1	ENSG00000133101	0.01799	-0.139	sensitive	-0.22 - -0.059
SENP3	ENSG00000161956	0.004966	-0.139	sensitive	-0.206 - -0.071
POLR1C	ENSG00000171453	0.01164	-0.139	sensitive	-0.214 - -0.064
TMA16	ENSG00000198498	0.01549	-0.139	sensitive	-0.217 - -0.061
METAP2	ENSG00000111142	0.01008	-0.138	sensitive	-0.212 - -0.065
CCT4	ENSG00000115484	0.00912	-0.138	sensitive	-0.21 - -0.066
SACS	ENSG00000151835	0.04372	-0.138	sensitive	-0.23 - -0.047
TERT	ENSG00000164362	0.0146	-0.138	sensitive	-0.215 - -0.061
ADAMTS6	ENSG00000049192	0.01757	-0.137	sensitive	-0.215 - -0.058
PFKP	ENSG00000067057	0.01023	-0.137	sensitive	-0.21 - -0.064
USP34	ENSG00000115464	0.01429	-0.137	sensitive	-0.213 - -0.061
GBP1	ENSG00000117228	0.03466	-0.137	sensitive	-0.223 - -0.05
PHF3	ENSG00000118482	0.01199	-0.137	sensitive	-0.211 - -0.063
XPO5	ENSG00000124571	0.01173	-0.137	sensitive	-0.211 - -0.063
RPS2	ENSG00000140988	0.01723	-0.137	sensitive	-0.216 - -0.059
MRM3	ENSG00000171861	0.008661	-0.137	sensitive	-0.209 - -0.066
FOXL1	ENSG00000176678	0.02458	-0.137	sensitive	-0.219 - -0.055
PTBP1	ENSG00000011304	0.01424	-0.136	sensitive	-0.211 - -0.061
RIC1	ENSG00000107036	0.0172	-0.136	sensitive	-0.214 - -0.059
CCL20	ENSG00000115009	0.02796	-0.136	sensitive	-0.219 - -0.052
HSD11B1	ENSG00000117594	0.01987	-0.136	sensitive	-0.215 - -0.057
CDC123	ENSG00000151465	0.01099	-0.136	sensitive	-0.209 - -0.063
ZNF143	ENSG00000166478	0.01091	-0.136	sensitive	-0.209 - -0.063
EGFL7	ENSG00000172889	0.01738	-0.136	sensitive	-0.214 - -0.058
WT1	ENSG00000184937	0.01023	-0.136	sensitive	-0.208 - -0.064
NFYA	ENSG00000001167	0.01729	-0.135	sensitive	-0.213 - -0.058
AASS	ENSG00000008311	0.0182	-0.135	sensitive	-0.213 - -0.057

Gene	Ensembl ID	FDR-adjusted p-value	Coefficient	Association	95% confidence interval
GNA15	ENSG00000060558	0.04569	-0.135	sensitive	-0.225 - -0.045
ZNRD1	ENSG00000066379	0.03111	-0.135	sensitive	-0.219 - -0.051
KIF14	ENSG00000118193	0.01091	-0.135	sensitive	-0.208 - -0.063
DYSF	ENSG00000135636	0.03111	-0.135	sensitive	-0.219 - -0.051
WRAP53	ENSG00000141499	0.009255	-0.135	sensitive	-0.206 - -0.064
MCFD2	ENSG00000180398	0.03754	-0.135	sensitive	-0.222 - -0.048
THOC1	ENSG00000079134	0.03233	-0.134	sensitive	-0.218 - -0.05
SCLY	ENSG00000132330	0.04121	-0.134	sensitive	-0.221 - -0.046
MPRIP	ENSG00000133030	0.0146	-0.134	sensitive	-0.209 - -0.059
GID4	ENSG00000141034	0.009505	-0.134	sensitive	-0.205 - -0.064
WDR43	ENSG00000163811	0.0243	-0.134	sensitive	-0.215 - -0.054
SERPINB8	ENSG00000166401	0.0229	-0.134	sensitive	-0.214 - -0.054
LUZP1	ENSG00000169641	0.03541	-0.134	sensitive	-0.22 - -0.049
PLRG1	ENSG00000171566	0.01002	-0.134	sensitive	-0.205 - -0.063
ADAT2	ENSG00000189007	0.04808	-0.134	sensitive	-0.224 - -0.044
PMS1	ENSG00000064933	0.02927	-0.133	sensitive	-0.215 - -0.051
GSDMD	ENSG00000104518	0.02254	-0.133	sensitive	-0.212 - -0.054
STAG1	ENSG00000118007	0.008515	-0.133	sensitive	-0.201 - -0.064
UBE2G1	ENSG00000132388	0.01188	-0.133	sensitive	-0.205 - -0.061
USP24	ENSG00000162402	0.01003	-0.133	sensitive	-0.203 - -0.062
LY6D	ENSG00000167656	0.04863	-0.133	sensitive	-0.223 - -0.043
RPL4	ENSG00000174444	0.03213	-0.133	sensitive	-0.217 - -0.05
YES1	ENSG00000176105	0.04526	-0.133	sensitive	-0.222 - -0.045
FOXL2	ENSG00000183770	0.01769	-0.133	sensitive	-0.209 - -0.057
SF3A2	ENSG00000104897	0.0391	-0.132	sensitive	-0.217 - -0.046
STC2	ENSG00000113739	0.02622	-0.132	sensitive	-0.212 - -0.052
RPF1	ENSG00000117133	0.01189	-0.132	sensitive	-0.203 - -0.06
KRI1	ENSG00000129347	0.04017	-0.132	sensitive	-0.217 - -0.046
RRAS2	ENSG00000133818	0.0495	-0.132	sensitive	-0.221 - -0.043
EEF1A1	ENSG00000156508	0.02108	-0.132	sensitive	-0.21 - -0.054
MLKL	ENSG00000168404	0.04245	-0.132	sensitive	-0.219 - -0.045
DNAJC24	ENSG00000170946	0.007638	-0.132	sensitive	-0.2 - -0.065
AURKB	ENSG00000178999	0.01455	-0.132	sensitive	-0.205 - -0.058
ZMYM1	ENSG00000197056	0.02019	-0.132	sensitive	-0.21 - -0.055
TTC4	ENSG00000243725	0.009255	-0.132	sensitive	-0.201 - -0.063
DVL2	ENSG00000004975	0.01198	-0.131	sensitive	-0.202 - -0.06
CCAR1	ENSG00000060339	0.04236	-0.131	sensitive	-0.217 - -0.045
IL11	ENSG00000095752	0.04665	-0.131	sensitive	-0.219 - -0.044
DDX58	ENSG00000107201	0.02444	-0.131	sensitive	-0.209 - -0.052
PFN1	ENSG00000108518	0.01621	-0.131	sensitive	-0.205 - -0.057
DCAF15	ENSG00000132017	0.02906	-0.131	sensitive	-0.211 - -0.05
ELP5	ENSG00000170291	0.009251	-0.131	sensitive	-0.2 - -0.063
PLK3	ENSG00000173846	0.02163	-0.131	sensitive	-0.208 - -0.054
CKAP5	ENSG00000175216	0.01384	-0.131	sensitive	-0.203 - -0.059
FZD2	ENSG00000180340	0.04799	-0.131	sensitive	-0.218 - -0.043
SUPT3H	ENSG00000196284	0.009594	-0.131	sensitive	-0.2 - -0.062

Gene	Ensembl ID	FDR-adjusted p-value	Coefficient	Association	95% confidence interval
VGLL3	ENSG00000206538	0.03884	-0.131	sensitive	-0.216 - -0.046
POLR3B	ENSG00000013503	0.01151	-0.13	sensitive	-0.2 - -0.06
SNAPC1	ENSG00000023608	0.02508	-0.13	sensitive	-0.209 - -0.052
ZNF280C	ENSG00000056277	0.02642	-0.13	sensitive	-0.209 - -0.051
TCOF1	ENSG00000070814	0.01325	-0.13	sensitive	-0.202 - -0.059
CAD	ENSG00000084774	0.02409	-0.13	sensitive	-0.208 - -0.052
NID2	ENSG00000087303	0.02622	-0.13	sensitive	-0.209 - -0.051
PABPC4	ENSG00000090621	0.01189	-0.13	sensitive	-0.2 - -0.059
HNRNPH3	ENSG00000096746	0.02571	-0.13	sensitive	-0.209 - -0.051
SNW1	ENSG00000100603	0.01292	-0.13	sensitive	-0.201 - -0.059
ADGRE1	ENSG00000174837	0.02564	-0.13	sensitive	-0.209 - -0.051
CRLF3	ENSG00000176390	0.02907	-0.13	sensitive	-0.21 - -0.05
SLC7A5	ENSG00000103257	0.01754	-0.129	sensitive	-0.203 - -0.055
C19orf44	ENSG00000105072	0.01821	-0.129	sensitive	-0.204 - -0.055
LYAR	ENSG00000145220	0.02645	-0.129	sensitive	-0.208 - -0.051
QTRT2	ENSG00000151576	0.02105	-0.129	sensitive	-0.205 - -0.053
PTPN2	ENSG00000175354	0.03117	-0.129	sensitive	-0.21 - -0.049
XPOT	ENSG00000184575	0.01164	-0.129	sensitive	-0.199 - -0.059
TNIP3	ENSG00000050730	0.02455	-0.128	sensitive	-0.205 - -0.051
WDR3	ENSG00000065183	0.0199	-0.128	sensitive	-0.203 - -0.054
SSR3	ENSG00000114850	0.0182	-0.128	sensitive	-0.202 - -0.054
CFAP58	ENSG00000120051	0.01723	-0.128	sensitive	-0.2 - -0.055
LARS1	ENSG00000133706	0.01763	-0.128	sensitive	-0.201 - -0.055
UPF2	ENSG00000151461	0.03273	-0.128	sensitive	-0.208 - -0.047
MARS1	ENSG00000166986	0.01402	-0.128	sensitive	-0.198 - -0.057
ARMC4	ENSG00000169126	0.03286	-0.128	sensitive	-0.208 - -0.047
OAF	ENSG00000184232	0.0391	-0.128	sensitive	-0.211 - -0.045
MME	ENSG00000196549	0.02373	-0.128	sensitive	-0.205 - -0.052
CSNK2A3	ENSG00000254598	0.00912	-0.128	sensitive	-0.194 - -0.061
TTC27	ENSG00000018699	0.01375	-0.127	sensitive	-0.197 - -0.057
RPS13	ENSG00000110700	0.03735	-0.127	sensitive	-0.209 - -0.046
ADAM19	ENSG00000135074	0.02855	-0.127	sensitive	-0.205 - -0.049
CCDC58	ENSG00000160124	0.03139	-0.127	sensitive	-0.206 - -0.048
LPAR3	ENSG00000171517	0.02663	-0.127	sensitive	-0.204 - -0.049
RASA3	ENSG00000185989	0.03085	-0.127	sensitive	-0.206 - -0.048
RPF2	ENSG00000197498	0.01329	-0.127	sensitive	-0.196 - -0.057
SLC4A7	ENSG00000033867	0.02504	-0.126	sensitive	-0.202 - -0.05
SALL4	ENSG00000101115	0.0243	-0.126	sensitive	-0.201 - -0.05
EIF3E	ENSG00000104408	0.03113	-0.126	sensitive	-0.205 - -0.047
TARS1	ENSG00000113407	0.01151	-0.126	sensitive	-0.194 - -0.058
GNB4	ENSG00000114450	0.04182	-0.126	sensitive	-0.209 - -0.044
KIF18A	ENSG00000121621	0.0112	-0.126	sensitive	-0.193 - -0.058
ZSWIM4	ENSG00000132003	0.01595	-0.126	sensitive	-0.197 - -0.055
SLC25A37	ENSG00000147454	0.01821	-0.126	sensitive	-0.199 - -0.053
UBLCP1	ENSG00000164332	0.01719	-0.126	sensitive	-0.197 - -0.054
BMS1	ENSG00000165733	0.0146	-0.126	sensitive	-0.196 - -0.056

Gene	Ensembl ID	FDR-adjusted p-value	Coefficient	Association	95% confidence interval
PARP14	ENSG00000173193	0.03939	-0.126	sensitive	-0.208 - -0.045
LMNB2	ENSG00000176619	0.0146	-0.126	sensitive	-0.196 - -0.056
PBX2	ENSG00000204304	0.02191	-0.126	sensitive	-0.201 - -0.052
RPS18	ENSG00000231500	0.04046	-0.126	sensitive	-0.208 - -0.044
MNAT1	ENSG00000020426	0.02018	-0.125	sensitive	-0.198 - -0.052
SLC35F2	ENSG00000110660	0.01938	-0.125	sensitive	-0.198 - -0.053
TRIM5	ENSG00000132256	0.03398	-0.125	sensitive	-0.203 - -0.046
ACTR2	ENSG00000138071	0.0362	-0.125	sensitive	-0.205 - -0.045
RPS3	ENSG00000149273	0.04363	-0.125	sensitive	-0.208 - -0.043
SAV1	ENSG00000151748	0.03017	-0.125	sensitive	-0.203 - -0.047
CWC22	ENSG00000163510	0.02329	-0.125	sensitive	-0.2 - -0.051
FARSA	ENSG00000179115	0.0182	-0.125	sensitive	-0.197 - -0.053
NAP1L1	ENSG00000187109	0.03109	-0.125	sensitive	-0.203 - -0.047
CPS1	ENSG00000021826	0.01877	-0.124	sensitive	-0.196 - -0.052
HOXA9	ENSG00000078399	0.0412	-0.124	sensitive	-0.206 - -0.043
NRDC	ENSG00000078618	0.01821	-0.124	sensitive	-0.195 - -0.053
PHGDH	ENSG00000092621	0.01766	-0.124	sensitive	-0.196 - -0.053
GCDH	ENSG00000105607	0.03398	-0.124	sensitive	-0.203 - -0.046
PLAA	ENSG00000137055	0.0146	-0.124	sensitive	-0.193 - -0.055
ASAP1	ENSG00000153317	0.04576	-0.124	sensitive	-0.206 - -0.041
FAM167A	ENSG00000154319	0.02733	-0.124	sensitive	-0.199 - -0.048
CHST11	ENSG00000171310	0.04105	-0.124	sensitive	-0.204 - -0.043
MAK16	ENSG00000198042	0.02213	-0.124	sensitive	-0.198 - -0.051
SOX18	ENSG00000203883	0.02508	-0.124	sensitive	-0.2 - -0.049
CARD16	ENSG00000204397	0.04939	-0.124	sensitive	-0.208 - -0.04
SMG6	ENSG00000070366	0.02338	-0.123	sensitive	-0.196 - -0.05
MAP3K20	ENSG00000091436	0.03339	-0.123	sensitive	-0.201 - -0.046
BBX	ENSG00000114439	0.0164	-0.123	sensitive	-0.193 - -0.053
RFX1	ENSG00000132005	0.01367	-0.123	sensitive	-0.191 - -0.055
UHRF2	ENSG00000147854	0.03113	-0.123	sensitive	-0.199 - -0.046
FHL3	ENSG00000183386	0.04682	-0.123	sensitive	-0.206 - -0.041
SORCS2	ENSG00000184985	0.04102	-0.123	sensitive	-0.204 - -0.043
PRMT3	ENSG00000185238	0.02427	-0.123	sensitive	-0.197 - -0.049
CCNB1IP1	ENSG00000100814	0.042	-0.122	sensitive	-0.201 - -0.042
NOP2	ENSG00000111641	0.03541	-0.122	sensitive	-0.199 - -0.044
TTI2	ENSG00000129696	0.04394	-0.122	sensitive	-0.203 - -0.041
PSAT1	ENSG00000135069	0.01291	-0.122	sensitive	-0.189 - -0.055
ALKBH8	ENSG00000137760	0.01723	-0.122	sensitive	-0.192 - -0.053
PELP1	ENSG00000141456	0.02444	-0.122	sensitive	-0.195 - -0.049
RPP30	ENSG00000148688	0.01463	-0.122	sensitive	-0.191 - -0.054
VAX1	ENSG00000148704	0.03265	-0.122	sensitive	-0.198 - -0.045
ADAM17	ENSG00000151694	0.0243	-0.122	sensitive	-0.195 - -0.049
UBASH3B	ENSG00000154127	0.0353	-0.122	sensitive	-0.199 - -0.044
SHANK1	ENSG00000161681	0.03884	-0.122	sensitive	-0.201 - -0.043
NAA15	ENSG00000164134	0.02114	-0.122	sensitive	-0.193 - -0.05
SH3RF3	ENSG00000172985	0.02456	-0.122	sensitive	-0.195 - -0.049

Gene	Ensembl ID	FDR-adjusted p-value	Coefficient	Association	95% confidence interval
OLR1	ENSG00000173391	0.04335	-0.122	sensitive	-0.202 - -0.041
CSTF3	ENSG00000176102	0.02488	-0.122	sensitive	-0.195 - -0.048
VARS1	ENSG00000204394	0.01952	-0.122	sensitive	-0.192 - -0.051
PCNX1	ENSG00000100731	0.02632	-0.121	sensitive	-0.194 - -0.047
RAN	ENSG00000132341	0.03923	-0.121	sensitive	-0.199 - -0.043
BUD13	ENSG00000137656	0.04432	-0.121	sensitive	-0.201 - -0.041
RPS8	ENSG00000142937	0.04902	-0.121	sensitive	-0.202 - -0.039
IMPDH2	ENSG00000178035	0.03157	-0.121	sensitive	-0.197 - -0.045
RRS1	ENSG00000179041	0.02042	-0.121	sensitive	-0.192 - -0.05
C11orf98	ENSG00000278615	0.02105	-0.121	sensitive	-0.193 - -0.05
WDR18	ENSG00000065268	0.02823	-0.12	sensitive	-0.194 - -0.046
STEAP1B	ENSG00000105889	0.03984	-0.12	sensitive	-0.197 - -0.042
COPS7B	ENSG00000144524	0.03931	-0.12	sensitive	-0.198 - -0.042
PDCD11	ENSG00000148843	0.04408	-0.12	sensitive	-0.199 - -0.041
MITD1	ENSG00000158411	0.03683	-0.12	sensitive	-0.197 - -0.043
HBE1	ENSG00000213931	0.01789	-0.12	sensitive	-0.189 - -0.051
ORC2	ENSG00000115942	0.03972	-0.119	sensitive	-0.196 - -0.042
TRIM25	ENSG00000121060	0.04554	-0.119	sensitive	-0.198 - -0.04
ADGRE2	ENSG00000127507	0.04927	-0.119	sensitive	-0.2 - -0.039
RABGGTB	ENSG00000137955	0.02105	-0.119	sensitive	-0.189 - -0.049
TMEM256	ENSG00000205544	0.01569	-0.119	sensitive	-0.186 - -0.052
SLC25A3	ENSG00000075415	0.02885	-0.118	sensitive	-0.19 - -0.045
SEH1L	ENSG00000085415	0.03926	-0.118	sensitive	-0.194 - -0.042
ELP4	ENSG00000109911	0.03113	-0.118	sensitive	-0.191 - -0.044
THG1L	ENSG00000113272	0.03017	-0.118	sensitive	-0.19 - -0.045
NUDCD1	ENSG00000120526	0.0172	-0.118	sensitive	-0.186 - -0.051
MRPS2	ENSG00000122140	0.03535	-0.118	sensitive	-0.193 - -0.043
SYMPK	ENSG00000125755	0.04677	-0.118	sensitive	-0.196 - -0.039
APTX	ENSG00000137074	0.02032	-0.118	sensitive	-0.188 - -0.049
BRD4	ENSG00000141867	0.0429	-0.118	sensitive	-0.195 - -0.04
DUSP11	ENSG00000144048	0.04807	-0.118	sensitive	-0.197 - -0.039
PIGO	ENSG00000165282	0.02473	-0.118	sensitive	-0.19 - -0.047
MCRS1	ENSG00000187778	0.02615	-0.118	sensitive	-0.19 - -0.047
RACK1	ENSG00000204628	0.03017	-0.118	sensitive	-0.192 - -0.045
ZFP64	ENSG00000020256	0.02994	-0.117	sensitive	-0.189 - -0.044
TRMT11	ENSG00000066651	0.03213	-0.117	sensitive	-0.191 - -0.044
SLC1A3	ENSG00000079215	0.04467	-0.117	sensitive	-0.194 - -0.039
USP10	ENSG00000103194	0.03792	-0.117	sensitive	-0.193 - -0.042
SMU1	ENSG00000122692	0.02618	-0.117	sensitive	-0.188 - -0.046
ALDH1B1	ENSG00000137124	0.02508	-0.117	sensitive	-0.188 - -0.046
TAF1A	ENSG00000143498	0.02568	-0.117	sensitive	-0.187 - -0.046
DUSP7	ENSG00000164086	0.03074	-0.117	sensitive	-0.19 - -0.044
RPL35A	ENSG00000182899	0.0469	-0.117	sensitive	-0.196 - -0.039
IL27RA	ENSG00000104998	0.03383	-0.116	sensitive	-0.189 - -0.043
CAMTA2	ENSG00000108509	0.02444	-0.116	sensitive	-0.185 - -0.046
PGF	ENSG00000119630	0.0425	-0.116	sensitive	-0.192 - -0.04

Gene	Ensembl ID	FDR-adjusted p-value	Coefficient	Association	95% confidence interval
ODF2L	ENSG00000122417	0.02898	-0.116	sensitive	-0.187 - -0.044
CCT7	ENSG00000135624	0.03111	-0.116	sensitive	-0.189 - -0.044
RABEPK	ENSG00000136933	0.01924	-0.116	sensitive	-0.183 - -0.049
TATDN1	ENSG00000147687	0.03152	-0.116	sensitive	-0.188 - -0.043
OTUB1	ENSG00000167770	0.03111	-0.116	sensitive	-0.189 - -0.044
ADARB1	ENSG00000197381	0.03857	-0.116	sensitive	-0.191 - -0.041
NCBP3	ENSG00000074356	0.02645	-0.115	sensitive	-0.186 - -0.045
MRPL2	ENSG00000112651	0.02695	-0.115	sensitive	-0.184 - -0.045
C17orf49	ENSG00000258315	0.03453	-0.115	sensitive	-0.187 - -0.042
TIGAR	ENSG00000078237	0.04408	-0.114	sensitive	-0.19 - -0.039
MED31	ENSG00000108590	0.02427	-0.114	sensitive	-0.183 - -0.046
TP53	ENSG00000141510	0.02048	-0.114	sensitive	-0.181 - -0.047
PFDN2	ENSG00000143256	0.02105	-0.114	sensitive	-0.182 - -0.047
NSD1	ENSG00000165671	0.03262	-0.114	sensitive	-0.186 - -0.042
CLP1	ENSG00000172409	0.03066	-0.114	sensitive	-0.186 - -0.043
RFXANK	ENSG00000064490	0.03932	-0.113	sensitive	-0.187 - -0.04
PDCD2	ENSG00000071994	0.04996	-0.113	sensitive	-0.189 - -0.037
GTPBP4	ENSG00000107937	0.03303	-0.113	sensitive	-0.184 - -0.042
CDC20	ENSG00000117399	0.02907	-0.113	sensitive	-0.183 - -0.043
TRERF1	ENSG00000124496	0.04372	-0.113	sensitive	-0.188 - -0.038
FRS3	ENSG00000137218	0.03815	-0.113	sensitive	-0.186 - -0.04
NTMT1	ENSG00000148335	0.02539	-0.113	sensitive	-0.182 - -0.045
SPATA5L1	ENSG00000171763	0.04408	-0.113	sensitive	-0.187 - -0.038
TVP23C	ENSG00000175106	0.04677	-0.113	sensitive	-0.188 - -0.037
RP1L1	ENSG00000183638	0.03265	-0.113	sensitive	-0.184 - -0.042
UBE2D1	ENSG00000072401	0.03466	-0.112	sensitive	-0.183 - -0.041
SPAG7	ENSG00000091640	0.02496	-0.112	sensitive	-0.179 - -0.044
C9orf40	ENSG00000135045	0.04677	-0.112	sensitive	-0.187 - -0.037
TAF1D	ENSG00000166012	0.0429	-0.112	sensitive	-0.186 - -0.038
HBG2	ENSG00000196565	0.02455	-0.112	sensitive	-0.18 - -0.045
RBM7	ENSG00000076053	0.0353	-0.111	sensitive	-0.182 - -0.041
DARS1	ENSG00000115866	0.0499	-0.111	sensitive	-0.186 - -0.036
TOP1MT	ENSG00000184428	0.04996	-0.111	sensitive	-0.187 - -0.036
IPO7	ENSG00000205339	0.02907	-0.111	sensitive	-0.179 - -0.042
UBE2R2	ENSG00000107341	0.03383	-0.11	sensitive	-0.18 - -0.041
ZPR1	ENSG00000109917	0.03163	-0.11	sensitive	-0.179 - -0.041
MIS12	ENSG00000167842	0.03541	-0.11	sensitive	-0.179 - -0.04
STX8	ENSG00000170310	0.0353	-0.11	sensitive	-0.179 - -0.04
CYB5D1	ENSG00000182224	0.03111	-0.11	sensitive	-0.179 - -0.041
FXR1	ENSG00000114416	0.03287	-0.109	sensitive	-0.177 - -0.04
RPP40	ENSG00000124787	0.0283	-0.109	sensitive	-0.177 - -0.042
TYW3	ENSG00000162623	0.04216	-0.109	sensitive	-0.18 - -0.037
UBTD2	ENSG00000168246	0.04755	-0.109	sensitive	-0.181 - -0.036
SMIM13	ENSG00000224531	0.0496	-0.109	sensitive	-0.182 - -0.035
LARP4	ENSG00000161813	0.04759	-0.108	sensitive	-0.18 - -0.036
GTPBP8	ENSG00000163607	0.0342	-0.108	sensitive	-0.176 - -0.04

Gene	Ensembl ID	FDR-adjusted p-value	Coefficient	Association	95% confidence interval
DHX36	ENSG00000174953	0.04601	-0.108	sensitive	-0.179 - -0.036
EBNA1BP2	ENSG00000117395	0.03857	-0.107	sensitive	-0.176 - -0.038
CDC37L1	ENSG00000106993	0.04028	-0.106	sensitive	-0.174 - -0.037
DRG2	ENSG00000108591	0.03974	-0.106	sensitive	-0.174 - -0.037
PSMA1	ENSG00000129084	0.03542	-0.106	sensitive	-0.173 - -0.038
MELK	ENSG00000165304	0.0407	-0.106	sensitive	-0.175 - -0.037
EIF4EBP1	ENSG00000187840	0.04394	-0.106	sensitive	-0.177 - -0.036
MED17	ENSG00000042429	0.03066	-0.105	sensitive	-0.171 - -0.04
CDC37	ENSG00000105401	0.04173	-0.105	sensitive	-0.173 - -0.036
UBA5	ENSG00000081307	0.04308	-0.104	sensitive	-0.173 - -0.036
WARS2	ENSG00000116874	0.04426	-0.104	sensitive	-0.173 - -0.035
PCNP	ENSG00000081154	0.03988	-0.103	sensitive	-0.17 - -0.036
HSP90AB1	ENSG00000096384	0.04772	-0.103	sensitive	-0.173 - -0.034
G3BP1	ENSG00000145907	0.04351	-0.103	sensitive	-0.171 - -0.035
MRPL52	ENSG00000172590	0.04534	-0.103	sensitive	-0.171 - -0.034
EMC6	ENSG00000127774	0.04238	-0.102	sensitive	-0.17 - -0.035
PSMB6	ENSG00000142507	0.04787	-0.101	sensitive	-0.17 - -0.033
PIGX	ENSG00000163964	0.04668	0.102	resistance	0.034 - 0.17
CDKN2A	ENSG00000147889	0.0451	0.103	resistance	0.035 - 0.172
PPP1R27	ENSG00000182676	0.04433	0.103	resistance	0.035 - 0.171
NDUFA2	ENSG00000131495	0.04784	0.104	resistance	0.034 - 0.174
SLC25A44	ENSG00000160785	0.04928	0.104	resistance	0.034 - 0.175
ATP5MF	ENSG00000241468	0.04807	0.104	resistance	0.034 - 0.174
SARAF	ENSG00000133872	0.04105	0.105	resistance	0.036 - 0.173
UBR3	ENSG00000144357	0.0425	0.105	resistance	0.036 - 0.174
RAMAC	ENSG00000169612	0.04569	0.105	resistance	0.035 - 0.174
UQCR10	ENSG00000184076	0.04433	0.105	resistance	0.035 - 0.174
MAOB	ENSG00000069535	0.04914	0.106	resistance	0.035 - 0.178
TYW1	ENSG00000198874	0.04362	0.106	resistance	0.036 - 0.176
PPP1R12B	ENSG00000077157	0.04352	0.107	resistance	0.036 - 0.178
CBX7	ENSG00000100307	0.04408	0.107	resistance	0.036 - 0.178
CDIPT	ENSG00000103502	0.04677	0.107	resistance	0.036 - 0.179
NAPB	ENSG00000125814	0.04102	0.107	resistance	0.037 - 0.177
ROMO1	ENSG00000125995	0.03802	0.107	resistance	0.038 - 0.177
CKMT2	ENSG00000131730	0.03732	0.107	resistance	0.038 - 0.175
PDE6A	ENSG00000132915	0.03323	0.107	resistance	0.039 - 0.174
CALM3	ENSG00000160014	0.042	0.107	resistance	0.037 - 0.177
AP5Z1	ENSG00000242802	0.04522	0.107	resistance	0.036 - 0.178
WFDC1	ENSG00000103175	0.03676	0.108	resistance	0.039 - 0.178
EPHX2	ENSG00000120915	0.04772	0.108	resistance	0.035 - 0.18
USP6	ENSG00000129204	0.04677	0.108	resistance	0.036 - 0.18
PRKRIP1	ENSG00000128563	0.04245	0.109	resistance	0.037 - 0.18
AHCYL2	ENSG00000158467	0.04075	0.109	resistance	0.038 - 0.18
H2BC15	ENSG00000233822	0.02648	0.109	resistance	0.043 - 0.175
FRY	ENSG00000073910	0.04159	0.11	resistance	0.038 - 0.181
ABCB1	ENSG00000085563	0.04729	0.11	resistance	0.036 - 0.183

Gene	Ensembl ID	FDR-adjusted p-value	Coefficient	Association	95% confidence interval
BMX	ENSG00000102010	0.04394	0.11	resistance	0.037 - 0.182
NENF	ENSG00000117691	0.03157	0.11	resistance	0.041 - 0.179
PEPD	ENSG00000124299	0.0494	0.11	resistance	0.036 - 0.184
SERF2	ENSG00000140264	0.03884	0.11	resistance	0.039 - 0.182
CA10	ENSG00000154975	0.03698	0.11	resistance	0.039 - 0.18
VSIG10L	ENSG00000186806	0.0389	0.11	resistance	0.039 - 0.181
CA11	ENSG00000063180	0.03841	0.111	resistance	0.039 - 0.183
MAPK1	ENSG00000100030	0.029	0.111	resistance	0.042 - 0.179
ATP6V1A	ENSG00000114573	0.0396	0.111	resistance	0.039 - 0.184
NR1D1	ENSG00000126368	0.04772	0.111	resistance	0.037 - 0.186
NDUFB11	ENSG00000147123	0.04086	0.111	resistance	0.039 - 0.184
FBXO25	ENSG00000147364	0.03989	0.111	resistance	0.039 - 0.183
GRIK4	ENSG00000149403	0.04236	0.111	resistance	0.038 - 0.183
ADRA2A	ENSG00000150594	0.04604	0.111	resistance	0.037 - 0.185
CTNND2	ENSG00000169862	0.0407	0.111	resistance	0.039 - 0.184
ARL6IP1	ENSG00000170540	0.03683	0.111	resistance	0.04 - 0.182
PCDHB9	ENSG00000177839	0.04999	0.111	resistance	0.036 - 0.186
SLC2A11	ENSG00000133460	0.03017	0.112	resistance	0.042 - 0.182
ALKBH4	ENSG00000160993	0.02648	0.112	resistance	0.044 - 0.179
ATP5ME	ENSG00000169020	0.02473	0.112	resistance	0.045 - 0.18
GATM	ENSG00000171766	0.03566	0.112	resistance	0.041 - 0.184
ZNF442	ENSG00000198342	0.0325	0.112	resistance	0.042 - 0.182
SMIM5	ENSG00000204323	0.04486	0.112	resistance	0.038 - 0.187
STAG3	ENSG00000066923	0.02907	0.113	resistance	0.043 - 0.183
ROGDI	ENSG00000067836	0.0482	0.113	resistance	0.037 - 0.19
EPHA8	ENSG00000070886	0.0418	0.113	resistance	0.039 - 0.187
FAM3A	ENSG00000071889	0.03614	0.113	resistance	0.041 - 0.185
YPEL3	ENSG00000090238	0.03841	0.113	resistance	0.04 - 0.186
UPB1	ENSG00000100024	0.03383	0.113	resistance	0.042 - 0.184
MLYCD	ENSG00000103150	0.03017	0.113	resistance	0.043 - 0.184
DYRK1B	ENSG00000105204	0.04255	0.113	resistance	0.039 - 0.187
ZNF141	ENSG00000131127	0.03213	0.113	resistance	0.042 - 0.183
KCNJ3	ENSG00000162989	0.03678	0.113	resistance	0.041 - 0.185
DNALI1	ENSG00000163879	0.04255	0.113	resistance	0.039 - 0.188
PARM1	ENSG00000169116	0.04121	0.113	resistance	0.039 - 0.187
NCMAP	ENSG00000184454	0.04862	0.113	resistance	0.037 - 0.19
LAMTOR4	ENSG00000188186	0.03732	0.113	resistance	0.04 - 0.185
DNM3	ENSG00000197959	0.03911	0.113	resistance	0.04 - 0.186
CYP51A1	ENSG00000001630	0.02125	0.114	resistance	0.047 - 0.182
ABCC8	ENSG00000006071	0.04532	0.114	resistance	0.038 - 0.19
ELN	ENSG00000049540	0.0439	0.114	resistance	0.039 - 0.19
MFSD11	ENSG00000092931	0.02088	0.114	resistance	0.047 - 0.181
ENPP5	ENSG00000112796	0.04859	0.114	resistance	0.037 - 0.191
RPN2	ENSG00000118705	0.04755	0.114	resistance	0.038 - 0.191
HMGCS2	ENSG00000134240	0.03939	0.114	resistance	0.04 - 0.188
RAD9B	ENSG00000151164	0.02941	0.114	resistance	0.043 - 0.184

Gene	Ensembl ID	FDR-adjusted p-value	Coefficient	Association	95% confidence interval
SST	ENSG00000157005	0.02504	0.114	resistance	0.045 - 0.183
CFAP410	ENSG00000160226	0.03857	0.114	resistance	0.041 - 0.188
SLC45A2	ENSG00000164175	0.04554	0.114	resistance	0.038 - 0.19
FAM174B	ENSG00000185442	0.042	0.114	resistance	0.039 - 0.188
FOXRED2	ENSG00000100350	0.04743	0.115	resistance	0.038 - 0.191
DHRS7	ENSG00000100612	0.04122	0.115	resistance	0.04 - 0.191
ATG4A	ENSG00000101844	0.04283	0.115	resistance	0.039 - 0.191
CBLL1	ENSG00000105879	0.04352	0.115	resistance	0.039 - 0.191
GRPR	ENSG00000126010	0.0353	0.115	resistance	0.042 - 0.189
ATP6V1E1	ENSG00000131100	0.04522	0.115	resistance	0.039 - 0.192
TMCO1	ENSG00000143183	0.0203	0.115	resistance	0.048 - 0.182
GTF2IRD2	ENSG00000196275	0.02085	0.115	resistance	0.048 - 0.183
ATP2A1	ENSG00000196296	0.02907	0.115	resistance	0.044 - 0.187
ZNF28	ENSG00000198538	0.02695	0.115	resistance	0.045 - 0.185
DHFR	ENSG00000228716	0.0433	0.115	resistance	0.039 - 0.191
MROH8	ENSG00000101353	0.04665	0.116	resistance	0.038 - 0.193
SEM1	ENSG00000127922	0.0189	0.116	resistance	0.049 - 0.183
DGCR6L	ENSG00000128185	0.02133	0.116	resistance	0.048 - 0.185
TAOK2	ENSG00000149930	0.02455	0.116	resistance	0.046 - 0.185
SENP8	ENSG00000166192	0.01931	0.116	resistance	0.049 - 0.183
ATP5PD	ENSG00000167863	0.02564	0.116	resistance	0.046 - 0.187
ZFP3	ENSG00000180787	0.03571	0.116	resistance	0.042 - 0.19
SLC44A4	ENSG00000204385	0.03841	0.116	resistance	0.041 - 0.191
SDHAF1	ENSG00000205138	0.03718	0.116	resistance	0.042 - 0.191
IGLL5	ENSG00000254709	0.03939	0.116	resistance	0.041 - 0.191
DDTL	ENSG00000099974	0.01515	0.117	resistance	0.051 - 0.182
CHD6	ENSG00000124177	0.03553	0.117	resistance	0.042 - 0.192
AKAP9	ENSG00000127914	0.02369	0.117	resistance	0.047 - 0.186
GARNL3	ENSG00000136895	0.04485	0.117	resistance	0.04 - 0.195
HUNK	ENSG00000142149	0.03731	0.117	resistance	0.042 - 0.191
ST6GAL2	ENSG00000144057	0.04428	0.117	resistance	0.04 - 0.195
NYAP2	ENSG00000144460	0.02733	0.117	resistance	0.045 - 0.189
RETREG2	ENSG00000144567	0.02458	0.117	resistance	0.047 - 0.187
ACSL6	ENSG00000164398	0.0339	0.117	resistance	0.043 - 0.191
C15orf40	ENSG00000169609	0.04303	0.117	resistance	0.04 - 0.195
MBLAC1	ENSG00000214309	0.02	0.117	resistance	0.049 - 0.185
CASTOR2	ENSG00000274070	0.0353	0.117	resistance	0.043 - 0.191
SLC4A1	ENSG00000004939	0.02885	0.118	resistance	0.045 - 0.19
PER3	ENSG00000049246	0.03377	0.118	resistance	0.043 - 0.192
PDK3	ENSG00000067992	0.02885	0.118	resistance	0.045 - 0.192
GDPD3	ENSG00000102886	0.02819	0.118	resistance	0.045 - 0.19
KISS1R	ENSG00000116014	0.02728	0.118	resistance	0.046 - 0.191
NDUFA1	ENSG00000125356	0.01755	0.118	resistance	0.051 - 0.186
POMT1	ENSG00000130714	0.0243	0.118	resistance	0.047 - 0.189
CCT6B	ENSG00000132141	0.02395	0.118	resistance	0.047 - 0.189
DISP2	ENSG00000140323	0.02959	0.118	resistance	0.045 - 0.19

Gene	Ensembl ID	FDR-adjusted p-value	Coefficient	Association	95% confidence interval
FN3KRP	ENSG00000141560	0.01572	0.118	resistance	0.051 - 0.184
PTPRR	ENSG00000153233	0.04527	0.118	resistance	0.04 - 0.197
TCN2	ENSG00000185339	0.04105	0.118	resistance	0.041 - 0.195
PEX26	ENSG00000215193	0.02629	0.118	resistance	0.046 - 0.19
RPS6KA6	ENSG00000072133	0.04569	0.119	resistance	0.04 - 0.199
ELOB	ENSG00000103363	0.01581	0.119	resistance	0.052 - 0.186
LRRC29	ENSG00000125122	0.04121	0.119	resistance	0.041 - 0.196
ITFG1	ENSG00000129636	0.0482	0.119	resistance	0.039 - 0.2
FMO5	ENSG00000131781	0.01929	0.119	resistance	0.05 - 0.189
ETFA	ENSG00000140374	0.04332	0.119	resistance	0.041 - 0.198
FCRL5	ENSG00000143297	0.04054	0.119	resistance	0.042 - 0.197
CACFD1	ENSG00000160325	0.04433	0.119	resistance	0.04 - 0.198
LRRN2	ENSG00000170382	0.03877	0.119	resistance	0.042 - 0.195
NKPD1	ENSG00000179846	0.02526	0.119	resistance	0.047 - 0.191
MYL5	ENSG00000215375	0.02153	0.119	resistance	0.049 - 0.189
PDK4	ENSG00000004799	0.04772	0.12	resistance	0.04 - 0.201
DYNLRB1	ENSG00000125971	0.02455	0.12	resistance	0.048 - 0.192
THEM6	ENSG00000130193	0.04815	0.12	resistance	0.039 - 0.201
HERC3	ENSG00000138641	0.03383	0.12	resistance	0.044 - 0.196
CREG1	ENSG00000143162	0.04244	0.12	resistance	0.041 - 0.199
LIX1	ENSG00000145721	0.02779	0.12	resistance	0.046 - 0.193
SMIM4	ENSG00000168273	0.02171	0.12	resistance	0.049 - 0.191
SLC25A20	ENSG00000178537	0.04522	0.12	resistance	0.04 - 0.2
INKA2	ENSG00000197852	0.0336	0.12	resistance	0.044 - 0.195
SLC18A1	ENSG00000036565	0.04255	0.121	resistance	0.041 - 0.2
BMF	ENSG00000104081	0.0286	0.121	resistance	0.047 - 0.195
CLMN	ENSG00000165959	0.0391	0.121	resistance	0.043 - 0.199
COQ7	ENSG00000167186	0.01987	0.121	resistance	0.051 - 0.192
TTYH1	ENSG00000167614	0.0189	0.121	resistance	0.051 - 0.191
TCAP	ENSG00000173991	0.01736	0.121	resistance	0.052 - 0.191
CLN3	ENSG00000188603	0.0222	0.121	resistance	0.049 - 0.193
ZNF682	ENSG00000197124	0.04144	0.121	resistance	0.042 - 0.2
MAN2B2	ENSG00000013288	0.04868	0.122	resistance	0.04 - 0.203
CLN5	ENSG00000102805	0.02941	0.122	resistance	0.046 - 0.197
DBP	ENSG00000105516	0.02153	0.122	resistance	0.05 - 0.195
SLCO2B1	ENSG00000137491	0.02199	0.122	resistance	0.05 - 0.194
ATP7A	ENSG00000165240	0.02108	0.122	resistance	0.05 - 0.194
MACROD2	ENSG00000172264	0.0182	0.122	resistance	0.052 - 0.193
NANOS1	ENSG00000188613	0.02648	0.122	resistance	0.048 - 0.196
ZNF782	ENSG00000196597	0.031	0.122	resistance	0.046 - 0.198
TMEM185A	ENSG00000269556	0.01675	0.122	resistance	0.053 - 0.191
UBE2D4	ENSG00000078967	0.01291	0.123	resistance	0.056 - 0.191
ACOT8	ENSG00000101473	0.01543	0.123	resistance	0.054 - 0.191
SHD	ENSG00000105251	0.04082	0.123	resistance	0.043 - 0.203
CISH	ENSG00000114737	0.03579	0.123	resistance	0.044 - 0.201
NDUFA5	ENSG00000128609	0.02751	0.123	resistance	0.048 - 0.198

Gene	Ensembl ID	FDR-adjusted p-value	Coefficient	Association	95% confidence interval
SFTPB	ENSG00000168878	0.01747	0.123	resistance	0.053 - 0.194
TAPT1	ENSG00000169762	0.03425	0.123	resistance	0.045 - 0.201
DNAJC30	ENSG00000176410	0.01486	0.123	resistance	0.054 - 0.192
PPFIA3	ENSG00000177380	0.03377	0.123	resistance	0.045 - 0.201
PIPOX	ENSG00000179761	0.02329	0.123	resistance	0.05 - 0.197
TTC3	ENSG00000182670	0.03972	0.123	resistance	0.043 - 0.203
CCDC180	ENSG00000197816	0.0225	0.123	resistance	0.05 - 0.196
NRXN3	ENSG00000021645	0.02405	0.124	resistance	0.05 - 0.198
CCL22	ENSG00000102962	0.04808	0.124	resistance	0.041 - 0.208
CPEB3	ENSG00000107864	0.04106	0.124	resistance	0.043 - 0.204
CNTFR	ENSG00000122756	0.04121	0.124	resistance	0.043 - 0.205
PIGT	ENSG00000124155	0.04808	0.124	resistance	0.041 - 0.208
WDR45B	ENSG00000141580	0.03213	0.124	resistance	0.046 - 0.202
TLCD4	ENSG00000152078	0.04604	0.124	resistance	0.041 - 0.206
BMT2	ENSG00000164603	0.03174	0.124	resistance	0.046 - 0.201
STARD5	ENSG00000172345	0.03017	0.124	resistance	0.047 - 0.2
ZNF774	ENSG00000196391	0.03017	0.124	resistance	0.047 - 0.202
SIRT2	ENSG00000068903	0.01569	0.125	resistance	0.055 - 0.195
ARHGAP5	ENSG00000100852	0.04677	0.125	resistance	0.041 - 0.208
APBA1	ENSG00000107282	0.02779	0.125	resistance	0.048 - 0.202
SLC25A16	ENSG00000122912	0.01345	0.125	resistance	0.056 - 0.193
CALML4	ENSG00000129007	0.03262	0.125	resistance	0.047 - 0.204
STXBP5L	ENSG00000145087	0.02703	0.125	resistance	0.049 - 0.202
CYP2U1	ENSG00000155016	0.03273	0.125	resistance	0.046 - 0.203
GOLGA7B	ENSG00000155265	0.04373	0.125	resistance	0.042 - 0.207
TMED4	ENSG00000158604	0.01621	0.125	resistance	0.054 - 0.195
C4orf3	ENSG00000164096	0.01821	0.125	resistance	0.053 - 0.197
EPB42	ENSG00000166947	0.0358	0.125	resistance	0.045 - 0.204
COL22A1	ENSG00000169436	0.0182	0.125	resistance	0.053 - 0.197
DCXR	ENSG00000169738	0.01428	0.125	resistance	0.056 - 0.195
MACO1	ENSG00000204178	0.03311	0.125	resistance	0.046 - 0.204
AC244197.3	ENSG00000241489	0.01227	0.125	resistance	0.057 - 0.192
SARM1	ENSG00000004139	0.04486	0.126	resistance	0.043 - 0.21
RGS11	ENSG00000076344	0.02828	0.126	resistance	0.048 - 0.203
NIPAL2	ENSG00000104361	0.03683	0.126	resistance	0.045 - 0.207
RGS9	ENSG00000108370	0.02108	0.126	resistance	0.052 - 0.2
CDKN2C	ENSG00000123080	0.0433	0.126	resistance	0.043 - 0.209
SRMS	ENSG00000125508	0.04987	0.126	resistance	0.041 - 0.211
MCCC2	ENSG00000131844	0.04807	0.126	resistance	0.041 - 0.211
DNAH3	ENSG00000158486	0.03353	0.126	resistance	0.046 - 0.205
TSHR	ENSG00000165409	0.0286	0.126	resistance	0.049 - 0.204
FAM102A	ENSG00000167106	0.02458	0.126	resistance	0.05 - 0.201
TSHZ1	ENSG00000179981	0.03113	0.126	resistance	0.047 - 0.205
ZNF652	ENSG00000198740	0.02192	0.126	resistance	0.051 - 0.201
DNASE1	ENSG00000213918	0.01833	0.126	resistance	0.053 - 0.198
ZNF688	ENSG00000229809	0.01099	0.126	resistance	0.059 - 0.194

Gene	Ensembl ID	FDR-adjusted p-value	Coefficient	Association	95% confidence interval
SYPL1	ENSG00000008282	0.03555	0.127	resistance	0.046 - 0.208
NR1H4	ENSG00000012504	0.01482	0.127	resistance	0.056 - 0.199
PPP1R37	ENSG00000104866	0.02898	0.127	resistance	0.049 - 0.205
ATP1A3	ENSG00000105409	0.04046	0.127	resistance	0.044 - 0.21
STON2	ENSG00000140022	0.03553	0.127	resistance	0.046 - 0.209
NPEPPS	ENSG00000141279	0.01557	0.127	resistance	0.056 - 0.198
EBP	ENSG00000147155	0.0157	0.127	resistance	0.055 - 0.198
GUCY1A2	ENSG00000152402	0.04054	0.127	resistance	0.044 - 0.21
KCNJ6	ENSG00000157542	0.02213	0.127	resistance	0.052 - 0.202
ACE	ENSG00000159640	0.02648	0.127	resistance	0.05 - 0.205
RSPH1	ENSG00000160188	0.03884	0.127	resistance	0.045 - 0.21
ACOX1	ENSG00000161533	0.01786	0.127	resistance	0.054 - 0.2
GJB1	ENSG00000169562	0.04433	0.127	resistance	0.043 - 0.21
PRSS36	ENSG00000178226	0.02897	0.127	resistance	0.049 - 0.205
VPS50	ENSG00000004766	0.00759	0.128	resistance	0.063 - 0.194
CACNG4	ENSG00000075461	0.04807	0.128	resistance	0.042 - 0.214
ACHE	ENSG00000087085	0.02155	0.128	resistance	0.052 - 0.203
SCP2	ENSG00000116171	0.01842	0.128	resistance	0.054 - 0.201
GPR89A	ENSG00000117262	0.01092	0.128	resistance	0.059 - 0.196
FAM155B	ENSG00000130054	0.02907	0.128	resistance	0.049 - 0.206
WDR61	ENSG00000140395	0.01605	0.128	resistance	0.056 - 0.201
LEFTY2	ENSG00000143768	0.01429	0.128	resistance	0.057 - 0.199
WHAMM	ENSG00000156232	0.02512	0.128	resistance	0.051 - 0.206
SMIM14	ENSG00000163683	0.02133	0.128	resistance	0.052 - 0.203
KCNMB3	ENSG00000171121	0.01334	0.128	resistance	0.057 - 0.198
KSR2	ENSG00000171435	0.0243	0.128	resistance	0.051 - 0.206
EFCAB12	ENSG00000172771	0.03262	0.128	resistance	0.048 - 0.208
MTHFR	ENSG00000177000	0.01675	0.128	resistance	0.055 - 0.2
TRIM52	ENSG00000183718	0.01546	0.128	resistance	0.056 - 0.199
FHIT	ENSG00000189283	0.02173	0.128	resistance	0.052 - 0.203
C1orf226	ENSG00000239887	0.04746	0.128	resistance	0.042 - 0.213
RNF115	ENSG00000265491	0.01569	0.128	resistance	0.056 - 0.2
PPP2R5A	ENSG00000066027	0.04486	0.129	resistance	0.044 - 0.215
SNAP29	ENSG00000099940	0.009162	0.129	resistance	0.061 - 0.196
CTSH	ENSG00000103811	0.03972	0.129	resistance	0.045 - 0.213
SLC9A3R1	ENSG00000109062	0.03538	0.129	resistance	0.047 - 0.21
VTN	ENSG00000109072	0.02133	0.129	resistance	0.053 - 0.206
CHKA	ENSG00000110721	0.02389	0.129	resistance	0.052 - 0.207
CNPPD1	ENSG00000115649	0.0172	0.129	resistance	0.055 - 0.202
TPRG1L	ENSG00000158109	0.04075	0.129	resistance	0.045 - 0.213
NAPEPLD	ENSG00000161048	0.01124	0.129	resistance	0.06 - 0.198
ZG16B	ENSG00000162078	0.04677	0.129	resistance	0.043 - 0.215
POLR2J3	ENSG00000168255	0.01294	0.129	resistance	0.058 - 0.2
ZSWIM1	ENSG00000168612	0.00961	0.129	resistance	0.061 - 0.197
ZNRF2	ENSG00000180233	0.02504	0.129	resistance	0.051 - 0.207
METTL7A	ENSG00000185432	0.02444	0.129	resistance	0.052 - 0.207

Gene	Ensembl ID	FDR-adjusted p-value	Coefficient	Association	95% confidence interval
SH3BGR	ENSG00000185437	0.01582	0.129	resistance	0.057 - 0.202
ABCB4	ENSG00000005471	0.01189	0.13	resistance	0.059 - 0.2
ACTL6B	ENSG00000077080	0.02904	0.13	resistance	0.05 - 0.211
DHRS12	ENSG00000102796	0.007852	0.13	resistance	0.063 - 0.196
ZNHIT1	ENSG00000106400	0.01307	0.13	resistance	0.059 - 0.202
SCAPER	ENSG00000140386	0.01784	0.13	resistance	0.056 - 0.205
OAZ3	ENSG00000143450	0.01223	0.13	resistance	0.059 - 0.2
SAR1B	ENSG00000152700	0.0173	0.13	resistance	0.056 - 0.204
BLCAP	ENSG00000166619	0.03015	0.13	resistance	0.049 - 0.211
CXXC4	ENSG00000168772	0.02481	0.13	resistance	0.052 - 0.209
PCLO	ENSG00000186472	0.0323	0.13	resistance	0.048 - 0.211
MAGEH1	ENSG00000187601	0.03974	0.13	resistance	0.046 - 0.214
SYCP2	ENSG00000196074	0.01685	0.13	resistance	0.056 - 0.204
MASP2	ENSG00000009724	0.02048	0.131	resistance	0.054 - 0.207
HERC1	ENSG00000103657	0.03563	0.131	resistance	0.048 - 0.215
AP3B2	ENSG00000103723	0.02703	0.131	resistance	0.051 - 0.212
ZSWIM3	ENSG00000132801	0.01581	0.131	resistance	0.057 - 0.205
SLC2A8	ENSG00000136856	0.0362	0.131	resistance	0.047 - 0.215
PPP1R14D	ENSG00000166143	0.03017	0.131	resistance	0.05 - 0.212
H2BC4	ENSG00000180596	0.01173	0.131	resistance	0.06 - 0.202
DUSP8	ENSG00000184545	0.02508	0.131	resistance	0.052 - 0.21
NEU1	ENSG00000204386	0.02108	0.131	resistance	0.054 - 0.208
SELENOP	ENSG00000250722	0.01164	0.131	resistance	0.06 - 0.202
KMT2C	ENSG00000055609	0.02454	0.132	resistance	0.053 - 0.212
PLPP1	ENSG00000067113	0.02568	0.132	resistance	0.052 - 0.212
KCNC3	ENSG00000131398	0.01329	0.132	resistance	0.059 - 0.205
PIGM	ENSG00000143315	0.01388	0.132	resistance	0.059 - 0.204
TLCD3B	ENSG00000149926	0.04932	0.132	resistance	0.043 - 0.22
FCRL3	ENSG00000160856	0.01559	0.132	resistance	0.058 - 0.206
TMED3	ENSG00000166557	0.02504	0.132	resistance	0.052 - 0.211
TMEM129	ENSG00000168936	0.006749	0.132	resistance	0.066 - 0.198
SPDYE5	ENSG00000170092	0.01199	0.132	resistance	0.06 - 0.204
CXXC5	ENSG00000171604	0.01518	0.132	resistance	0.058 - 0.205
P4HTM	ENSG00000178467	0.02108	0.132	resistance	0.054 - 0.21
NOS1AP	ENSG00000198929	0.03466	0.132	resistance	0.048 - 0.216
CYP46A1	ENSG00000036530	0.02199	0.133	resistance	0.054 - 0.212
FMO4	ENSG00000076258	0.01595	0.133	resistance	0.058 - 0.208
CRYM	ENSG00000103316	0.008977	0.133	resistance	0.064 - 0.202
SBDS	ENSG00000126524	0.03174	0.133	resistance	0.05 - 0.216
VIL1	ENSG00000127831	0.02648	0.133	resistance	0.052 - 0.213
CCDC115	ENSG00000136710	0.01181	0.133	resistance	0.061 - 0.205
ARHGAP20	ENSG00000137727	0.02302	0.133	resistance	0.054 - 0.212
TMEM50B	ENSG00000142188	0.008276	0.133	resistance	0.065 - 0.202
MFSD6	ENSG00000151690	0.02615	0.133	resistance	0.052 - 0.213
CELF3	ENSG00000159409	0.03062	0.133	resistance	0.05 - 0.216
CPLX1	ENSG00000168993	0.03377	0.133	resistance	0.049 - 0.217

Gene	Ensembl ID	FDR-adjusted p-value	Coefficient	Association	95% confidence interval
ST8SIA3	ENSG00000177511	0.02027	0.133	resistance	0.055 - 0.211
ENTPD8	ENSG00000188833	0.0391	0.133	resistance	0.047 - 0.22
H4-16	ENSG00000197837	0.0146	0.133	resistance	0.059 - 0.207
ICA1	ENSG00000003147	0.04237	0.134	resistance	0.046 - 0.222
TMEM159	ENSG00000011638	0.04868	0.134	resistance	0.044 - 0.224
DGCR2	ENSG00000070413	0.01151	0.134	resistance	0.062 - 0.206
RALY	ENSG00000125970	0.006954	0.134	resistance	0.066 - 0.202
FBXL16	ENSG00000127585	0.01569	0.134	resistance	0.059 - 0.209
NCAN	ENSG00000130287	0.02022	0.134	resistance	0.056 - 0.213
DEPTOR	ENSG00000155792	0.01013	0.134	resistance	0.063 - 0.205
SLC25A42	ENSG00000181035	0.02446	0.134	resistance	0.053 - 0.214
GET1	ENSG00000182093	0.01262	0.134	resistance	0.061 - 0.207
HEPACAM2	ENSG00000188175	0.01325	0.134	resistance	0.06 - 0.207
ZNF468	ENSG00000204604	0.01151	0.134	resistance	0.062 - 0.206
MCF2L	ENSG00000126217	0.02329	0.135	resistance	0.055 - 0.216
CASK	ENSG00000147044	0.0178	0.135	resistance	0.057 - 0.212
MSI2	ENSG00000153944	0.02703	0.135	resistance	0.052 - 0.217
CYB5A	ENSG00000166347	0.01003	0.135	resistance	0.064 - 0.207
ATCAY	ENSG00000167654	0.02649	0.135	resistance	0.053 - 0.217
TMEM208	ENSG00000168701	0.01297	0.135	resistance	0.061 - 0.209
GTF2IRD2B	ENSG00000174428	0.006132	0.135	resistance	0.068 - 0.202
IRX5	ENSG00000176842	0.01173	0.135	resistance	0.062 - 0.208
FITM2	ENSG00000197296	0.02155	0.135	resistance	0.055 - 0.215
ADAMTSL2	ENSG00000197859	0.01438	0.135	resistance	0.06 - 0.21
COBLL1	ENSG00000082438	0.01557	0.136	resistance	0.059 - 0.212
ABLIM1	ENSG00000099204	0.0274	0.136	resistance	0.053 - 0.219
SLA2	ENSG00000101082	0.02453	0.136	resistance	0.054 - 0.217
SNTA1	ENSG00000101400	0.02437	0.136	resistance	0.054 - 0.217
RBM48	ENSG00000127993	0.006954	0.136	resistance	0.067 - 0.204
PRADC1	ENSG00000135617	0.008701	0.136	resistance	0.065 - 0.207
SLC40A1	ENSG00000138449	0.01656	0.136	resistance	0.059 - 0.213
KCNH1	ENSG00000143473	0.04433	0.136	resistance	0.046 - 0.225
EPHX1	ENSG00000143819	0.03111	0.136	resistance	0.051 - 0.221
ZNF394	ENSG00000160908	0.01938	0.136	resistance	0.057 - 0.215
ZSWIM5	ENSG00000162415	0.01538	0.136	resistance	0.06 - 0.212
DEGS2	ENSG00000168350	0.01987	0.136	resistance	0.057 - 0.216
GLB1	ENSG00000170266	0.02434	0.136	resistance	0.055 - 0.218
DSCAML1	ENSG00000177103	0.01904	0.136	resistance	0.057 - 0.214
MAP7D2	ENSG00000184368	0.009096	0.136	resistance	0.065 - 0.208
TMEM198	ENSG00000188760	0.01685	0.136	resistance	0.059 - 0.214
STKLD1	ENSG00000198870	0.01685	0.136	resistance	0.059 - 0.213
MED29	ENSG00000063322	0.005452	0.137	resistance	0.07 - 0.205
RAB9B	ENSG00000123570	0.03553	0.137	resistance	0.05 - 0.224
SORT1	ENSG00000134243	0.01621	0.137	resistance	0.06 - 0.214
IFNAR1	ENSG00000142166	0.009956	0.137	resistance	0.065 - 0.21
NRSN1	ENSG00000152954	0.02191	0.137	resistance	0.056 - 0.217

Gene	Ensembl ID	FDR-adjusted p-value	Coefficient	Association	95% confidence interval
DUSP23	ENSG00000158716	0.03507	0.137	resistance	0.05 - 0.224
CADPS	ENSG00000163618	0.03017	0.137	resistance	0.052 - 0.222
CARMIL3	ENSG00000186648	0.03325	0.137	resistance	0.051 - 0.223
ZSCAN25	ENSG00000197037	0.01123	0.137	resistance	0.064 - 0.211
KMT2E	ENSG00000005483	0.01134	0.138	resistance	0.064 - 0.213
STOML1	ENSG00000067221	0.0142	0.138	resistance	0.062 - 0.214
PAG1	ENSG00000076641	0.01325	0.138	resistance	0.062 - 0.213
MAPRE3	ENSG00000084764	0.03017	0.138	resistance	0.052 - 0.224
KIAA1257	ENSG00000114656	0.01586	0.138	resistance	0.06 - 0.216
C5AR2	ENSG00000134830	0.01004	0.138	resistance	0.065 - 0.212
SOGA1	ENSG00000149639	0.03041	0.138	resistance	0.052 - 0.225
DIRAS2	ENSG00000165023	0.01335	0.138	resistance	0.062 - 0.214
SCAMP5	ENSG00000198794	0.01291	0.138	resistance	0.062 - 0.213
LILRA2	ENSG00000239998	0.02508	0.138	resistance	0.055 - 0.222
ARHGAP33	ENSG00000004777	0.04808	0.139	resistance	0.046 - 0.233
DAPK2	ENSG00000035664	0.00961	0.139	resistance	0.066 - 0.213
PCDHB4	ENSG00000081818	0.02733	0.139	resistance	0.054 - 0.224
FAM189A2	ENSG00000135063	0.0225	0.139	resistance	0.056 - 0.221
THRB	ENSG00000151090	0.04996	0.139	resistance	0.045 - 0.234
ORMDL3	ENSG00000172057	0.008661	0.139	resistance	0.067 - 0.211
COX14	ENSG00000178449	0.01173	0.139	resistance	0.064 - 0.214
MTURN	ENSG00000180354	0.01325	0.139	resistance	0.063 - 0.215
HEXA	ENSG00000213614	0.01998	0.139	resistance	0.058 - 0.22
E2F1	ENSG00000101412	0.0132	0.14	resistance	0.063 - 0.217
GGA2	ENSG00000103365	0.02397	0.14	resistance	0.056 - 0.223
CERT1	ENSG00000113163	0.008256	0.14	resistance	0.068 - 0.213
ARFGEF2	ENSG00000124198	0.01189	0.14	resistance	0.064 - 0.215
PHYHIPL	ENSG00000165443	0.01766	0.14	resistance	0.06 - 0.221
NHLRC3	ENSG00000188811	0.009251	0.14	resistance	0.067 - 0.213
ZNF736	ENSG00000234444	0.01914	0.14	resistance	0.059 - 0.221
PDK2	ENSG00000005882	0.005213	0.141	resistance	0.072 - 0.209
ASIC4	ENSG00000072182	0.007576	0.141	resistance	0.069 - 0.212
PEX1	ENSG00000127980	0.008356	0.141	resistance	0.068 - 0.215
FN3K	ENSG00000167363	0.009956	0.141	resistance	0.066 - 0.215
CXorf40A	ENSG00000197620	0.005213	0.141	resistance	0.072 - 0.21
BLVRB	ENSG00000090013	0.02989	0.142	resistance	0.054 - 0.23
MAP3K1	ENSG00000095015	0.01798	0.142	resistance	0.061 - 0.224
MAN1C1	ENSG00000117643	0.0146	0.142	resistance	0.063 - 0.221
GUCD1	ENSG00000138867	0.01199	0.142	resistance	0.065 - 0.218
FLVCR1	ENSG00000162769	0.02397	0.142	resistance	0.057 - 0.228
NFASC	ENSG00000163531	0.02948	0.142	resistance	0.054 - 0.23
GPR137C	ENSG00000180998	0.03398	0.142	resistance	0.052 - 0.231
CNTN2	ENSG00000184144	0.01151	0.142	resistance	0.065 - 0.218
MPC1	ENSG00000060762	0.009255	0.143	resistance	0.068 - 0.217
MMP15	ENSG00000102996	0.04104	0.143	resistance	0.05 - 0.236
RTN2	ENSG00000125744	0.006954	0.143	resistance	0.071 - 0.215

Gene	Ensembl ID	FDR-adjusted p-value	Coefficient	Association	95% confidence interval
OS9	ENSG00000135506	0.009753	0.143	resistance	0.067 - 0.218
SPATA25	ENSG00000149634	0.004351	0.143	resistance	0.074 - 0.212
HID1	ENSG00000167861	0.04772	0.143	resistance	0.047 - 0.24
CREG2	ENSG00000175874	0.02101	0.143	resistance	0.059 - 0.226
GPR19	ENSG00000183150	0.01065	0.143	resistance	0.067 - 0.219
DUSP28	ENSG00000188542	0.01685	0.143	resistance	0.062 - 0.225
C2orf72	ENSG00000204128	0.01833	0.143	resistance	0.061 - 0.226
CYB5RL	ENSG00000215883	0.01789	0.143	resistance	0.061 - 0.226
PPP1R3E	ENSG00000235194	0.02171	0.143	resistance	0.058 - 0.227
FAM13B	ENSG00000031003	0.006749	0.144	resistance	0.071 - 0.216
FAM214A	ENSG00000047346	0.009255	0.144	resistance	0.069 - 0.22
SCGN	ENSG00000079689	0.007852	0.144	resistance	0.07 - 0.218
PCDHB10	ENSG00000120324	0.02483	0.144	resistance	0.057 - 0.23
TUBA4A	ENSG00000127824	0.02108	0.144	resistance	0.059 - 0.229
CASD1	ENSG00000127995	0.00961	0.144	resistance	0.068 - 0.219
SPTBN4	ENSG00000160460	0.01482	0.144	resistance	0.064 - 0.224
AKAP5	ENSG00000179841	0.01429	0.144	resistance	0.064 - 0.224
TANGO2	ENSG00000183597	0.009594	0.144	resistance	0.068 - 0.22
TMPRSS2	ENSG00000184012	0.02062	0.144	resistance	0.06 - 0.229
MB	ENSG00000198125	0.01789	0.144	resistance	0.061 - 0.226
DYNLL2	ENSG00000264364	0.005049	0.144	resistance	0.074 - 0.214
LMCD1	ENSG00000071282	0.01605	0.145	resistance	0.063 - 0.227
ADCY2	ENSG00000078295	0.007011	0.145	resistance	0.072 - 0.219
ZCWPW1	ENSG00000078487	0.003295	0.145	resistance	0.077 - 0.213
ZFAND6	ENSG00000086666	0.006387	0.145	resistance	0.072 - 0.217
PLD3	ENSG00000105223	0.009594	0.145	resistance	0.069 - 0.221
TMEM248	ENSG00000106609	0.006308	0.145	resistance	0.073 - 0.218
ACAP3	ENSG00000131584	0.00743	0.145	resistance	0.071 - 0.218
HADH	ENSG00000138796	0.02779	0.145	resistance	0.056 - 0.234
TEF	ENSG00000167074	0.005445	0.145	resistance	0.074 - 0.216
STK32A	ENSG00000169302	0.01582	0.145	resistance	0.063 - 0.227
KCNJ11	ENSG00000187486	0.02907	0.145	resistance	0.055 - 0.234
CBFA2T2	ENSG00000078699	0.006024	0.146	resistance	0.074 - 0.219
CDR2L	ENSG00000109089	0.04604	0.146	resistance	0.049 - 0.244
FRK	ENSG00000111816	0.03542	0.146	resistance	0.053 - 0.238
OSBPL2	ENSG00000130703	0.01134	0.146	resistance	0.067 - 0.224
RAB37	ENSG00000172794	0.01298	0.146	resistance	0.066 - 0.226
ZNF429	ENSG00000197013	0.01291	0.146	resistance	0.066 - 0.226
CORO7	ENSG00000262246	0.03273	0.146	resistance	0.054 - 0.238
IYD	ENSG00000009765	0.007381	0.147	resistance	0.072 - 0.222
TCEANC	ENSG00000176896	0.01729	0.147	resistance	0.063 - 0.231
MUC20	ENSG00000176945	0.01345	0.147	resistance	0.066 - 0.229
ATP6AP2	ENSG00000182220	0.01685	0.147	resistance	0.064 - 0.231
CCDC183	ENSG00000213213	0.005256	0.147	resistance	0.075 - 0.219
ABCC11	ENSG00000121270	0.003829	0.148	resistance	0.077 - 0.218
BICDL1	ENSG00000135127	0.01732	0.148	resistance	0.063 - 0.232

Gene	Ensembl ID	FDR-adjusted p-value	Coefficient	Association	95% confidence interval
SORL1	ENSG00000137642	0.008256	0.148	resistance	0.072 - 0.224
PDPK1	ENSG00000140992	0.004121	0.148	resistance	0.077 - 0.219
GPR89B	ENSG00000188092	0.008256	0.148	resistance	0.072 - 0.224
ZNF138	ENSG00000197008	0.02389	0.148	resistance	0.06 - 0.237
SEC14L5	ENSG00000103184	0.01091	0.149	resistance	0.07 - 0.229
AGFG2	ENSG00000106351	0.005049	0.149	resistance	0.076 - 0.222
CGN	ENSG00000143375	0.03884	0.149	resistance	0.053 - 0.246
LGALS4	ENSG00000171747	0.005449	0.149	resistance	0.076 - 0.222
UMODL1	ENSG00000177398	0.01131	0.149	resistance	0.069 - 0.229
FNIP2	ENSG00000052795	0.004511	0.15	resistance	0.078 - 0.223
SLC35A2	ENSG00000102100	0.01482	0.15	resistance	0.066 - 0.234
MANBA	ENSG00000109323	0.00766	0.15	resistance	0.073 - 0.226
CISD2	ENSG00000145354	0.003414	0.15	resistance	0.079 - 0.221
LRRC26	ENSG00000184709	0.01164	0.15	resistance	0.069 - 0.232
PIK3IP1	ENSG00000100100	0.00961	0.151	resistance	0.072 - 0.231
SC5D	ENSG00000109929	0.002858	0.151	resistance	0.081 - 0.221
GADD45G	ENSG00000130222	0.01227	0.151	resistance	0.069 - 0.234
DNAJB2	ENSG00000135924	0.007381	0.151	resistance	0.074 - 0.227
PARP6	ENSG00000137817	0.002858	0.151	resistance	0.082 - 0.221
MPC2	ENSG00000143158	0.008661	0.151	resistance	0.073 - 0.229
NUDT9	ENSG00000170502	0.002845	0.151	resistance	0.081 - 0.22
DAAM1	ENSG00000100592	0.007852	0.152	resistance	0.074 - 0.23
TBC1D30	ENSG00000111490	0.01929	0.152	resistance	0.064 - 0.241
ARFGEF3	ENSG00000112379	0.01931	0.152	resistance	0.064 - 0.24
CHMP3	ENSG00000115561	0.02605	0.152	resistance	0.06 - 0.245
WNT4	ENSG00000162552	0.01291	0.152	resistance	0.069 - 0.235
HYKK	ENSG00000188266	0.006954	0.152	resistance	0.075 - 0.228
FBLL1	ENSG00000188573	0.00613	0.152	resistance	0.076 - 0.228
BLOC1S3	ENSG00000189114	0.004966	0.152	resistance	0.078 - 0.225
NSF	ENSG00000073969	0.003005	0.153	resistance	0.082 - 0.224
PPARGC1A	ENSG00000109819	0.004082	0.153	resistance	0.08 - 0.227
PLA2G12A	ENSG00000123739	0.003565	0.153	resistance	0.081 - 0.225
VAPB	ENSG00000124164	0.005733	0.153	resistance	0.077 - 0.229
LNX2	ENSG00000139517	0.01063	0.153	resistance	0.072 - 0.235
UNC80	ENSG00000144406	0.01621	0.153	resistance	0.066 - 0.239
MAGIX	ENSG00000269313	0.00351	0.153	resistance	0.081 - 0.226
LOC102724788	ENSG00000277196	0.007914	0.153	resistance	0.074 - 0.231
YPEL1	ENSG00000100027	0.01656	0.154	resistance	0.067 - 0.241
PRODH	ENSG00000100033	0.006253	0.154	resistance	0.077 - 0.23
PHOSPHO2	ENSG00000144362	0.007015	0.154	resistance	0.076 - 0.232
KALRN	ENSG00000160145	0.01153	0.154	resistance	0.071 - 0.237
LDLRAD4	ENSG00000168675	0.01189	0.154	resistance	0.071 - 0.238
EIF2AK3	ENSG00000172071	0.003354	0.154	resistance	0.082 - 0.227
SLC26A11	ENSG00000181045	0.01518	0.154	resistance	0.068 - 0.241
DDC	ENSG00000132437	0.01066	0.155	resistance	0.072 - 0.237
ZDHHC9	ENSG00000188706	0.01557	0.155	resistance	0.068 - 0.242

Gene	Ensembl ID	FDR-adjusted p-value	Coefficient	Association	95% confidence interval
CAPZA2	ENSG00000198898	0.003295	0.155	resistance	0.083 - 0.228
SYNGR2	ENSG00000108639	0.04058	0.156	resistance	0.054 - 0.257
TTLL7	ENSG00000137941	0.02194	0.156	resistance	0.064 - 0.249
PTH2R	ENSG00000144407	0.002498	0.156	resistance	0.085 - 0.227
PGAP3	ENSG00000161395	0.002553	0.156	resistance	0.085 - 0.228
CATSPERG	ENSG00000099338	0.00202	0.157	resistance	0.087 - 0.226
PODXL2	ENSG00000114631	0.01003	0.157	resistance	0.074 - 0.24
HCN3	ENSG00000143630	0.006409	0.157	resistance	0.079 - 0.236
AKR7A3	ENSG00000162482	0.002259	0.157	resistance	0.086 - 0.229
HDAC11	ENSG00000163517	0.02154	0.157	resistance	0.064 - 0.25
CIART	ENSG00000159208	0.003183	0.158	resistance	0.084 - 0.232
DCTN5	ENSG00000166847	0.001096	0.158	resistance	0.091 - 0.224
RNF103	ENSG00000239305	0.002553	0.158	resistance	0.086 - 0.23
GRN	ENSG00000030582	0.01189	0.159	resistance	0.073 - 0.245
CDH26	ENSG00000124215	0.002615	0.159	resistance	0.086 - 0.231
RALGPS1	ENSG00000136828	0.00961	0.159	resistance	0.075 - 0.243
RDH13	ENSG00000160439	0.009426	0.159	resistance	0.076 - 0.243
PLA2G4F	ENSG00000168907	0.01842	0.159	resistance	0.067 - 0.251
TRAPPC2	ENSG00000196459	0.008356	0.159	resistance	0.077 - 0.242
ARHGEF10L	ENSG00000074964	0.01258	0.16	resistance	0.073 - 0.247
PPM1H	ENSG00000111110	0.003005	0.16	resistance	0.086 - 0.235
NEURL2	ENSG00000124257	0.001128	0.16	resistance	0.092 - 0.228
TMEM60	ENSG00000135211	0.001073	0.16	resistance	0.093 - 0.227
NPTN	ENSG00000156642	0.01549	0.16	resistance	0.07 - 0.25
REPS2	ENSG00000169891	0.005765	0.16	resistance	0.081 - 0.239
FAM47E	ENSG00000189157	0.004223	0.161	resistance	0.083 - 0.238
SLC1A2	ENSG00000110436	0.004198	0.162	resistance	0.084 - 0.24
ZNF253	ENSG00000256771	0.007547	0.162	resistance	0.079 - 0.244
ATP6V0A1	ENSG00000033627	0.003005	0.163	resistance	0.088 - 0.239
LMBRD2	ENSG00000164187	0.001825	0.163	resistance	0.091 - 0.235
CKMT1A	ENSG00000223572	0.01842	0.163	resistance	0.069 - 0.257
SLC25A40	ENSG00000075303	0.003295	0.164	resistance	0.087 - 0.24
KCNH4	ENSG00000089558	0.003423	0.164	resistance	0.087 - 0.242
LIPH	ENSG00000163898	0.03719	0.164	resistance	0.059 - 0.27
FAM174A	ENSG00000174132	0.006954	0.164	resistance	0.081 - 0.247
SCUBE2	ENSG00000175356	0.009956	0.164	resistance	0.077 - 0.251
ARHGEF38	ENSG00000236699	0.008327	0.164	resistance	0.079 - 0.249
ZNF506	ENSG00000081665	0.001336	0.165	resistance	0.094 - 0.237
ITM2B	ENSG00000136156	0.004966	0.165	resistance	0.085 - 0.245
SELENBP1	ENSG00000143416	0.003581	0.165	resistance	0.087 - 0.243
CROT	ENSG00000005469	0.002705	0.166	resistance	0.09 - 0.243
GNPTG	ENSG00000090581	0.002034	0.166	resistance	0.092 - 0.24
CTSV	ENSG00000136943	0.01418	0.166	resistance	0.074 - 0.258
EPHA10	ENSG00000183317	0.007854	0.166	resistance	0.081 - 0.251
ST6GALNAC2	ENSG00000070731	0.0146	0.167	resistance	0.074 - 0.259
HRH3	ENSG00000101180	0.003028	0.167	resistance	0.09 - 0.245

Gene	Ensembl ID	FDR-adjusted p-value	Coefficient	Association	95% confidence interval
TBC1D9	ENSG00000109436	0.00961	0.167	resistance	0.079 - 0.254
RAB40B	ENSG00000141542	0.00148	0.167	resistance	0.094 - 0.24
PCDH1	ENSG00000156453	0.04408	0.167	resistance	0.056 - 0.277
SYNJ1	ENSG00000159082	0.004324	0.167	resistance	0.086 - 0.247
ANKS1B	ENSG00000185046	0.006954	0.167	resistance	0.083 - 0.251
TRIM67	ENSG00000119283	0.002807	0.168	resistance	0.091 - 0.245
RAI2	ENSG00000131831	0.004588	0.168	resistance	0.086 - 0.249
PDXDC1	ENSG00000179889	0.001155	0.168	resistance	0.097 - 0.24
HLF	ENSG00000108924	0.001787	0.169	resistance	0.095 - 0.244
MANSC1	ENSG00000111261	0.01325	0.169	resistance	0.076 - 0.262
ITGA9	ENSG00000144668	0.00333	0.169	resistance	0.09 - 0.249
AKAP6	ENSG00000151320	0.00202	0.169	resistance	0.094 - 0.245
H2BC21	ENSG00000184678	0.001128	0.169	resistance	0.097 - 0.24
XKR7	ENSG00000260903	0.003965	0.169	resistance	0.088 - 0.249
ABHD12	ENSG00000100997	0.002914	0.17	resistance	0.091 - 0.249
SCG3	ENSG00000104112	0.003414	0.17	resistance	0.09 - 0.25
TMEM59	ENSG00000116209	0.002084	0.17	resistance	0.094 - 0.246
SMIM22	ENSG00000267795	0.01747	0.17	resistance	0.073 - 0.267
TMEM63C	ENSG00000165548	0.002159	0.171	resistance	0.094 - 0.249
PI4KA	ENSG00000241973	0.002025	0.172	resistance	0.095 - 0.248
TMEM175	ENSG00000127419	0.0008042	0.173	resistance	0.102 - 0.244
GDE1	ENSG00000006007	0.00142	0.174	resistance	0.099 - 0.25
TXNDC16	ENSG00000087301	0.004998	0.174	resistance	0.089 - 0.258
ZNF540	ENSG00000171817	0.001642	0.174	resistance	0.098 - 0.25
WASL	ENSG00000106299	0.007547	0.176	resistance	0.086 - 0.266
LARGE1	ENSG00000133424	0.001332	0.176	resistance	0.1 - 0.253
CKMT1B	ENSG00000237289	0.01081	0.176	resistance	0.082 - 0.27
ATP6AP1	ENSG00000071553	0.001065	0.177	resistance	0.103 - 0.252
CHMP4B	ENSG00000101421	0.003295	0.177	resistance	0.094 - 0.259
SCAMP2	ENSG00000140497	0.003354	0.177	resistance	0.094 - 0.26
SVOP	ENSG00000166111	0.002807	0.177	resistance	0.096 - 0.259
PPFIBP2	ENSG00000166387	0.002763	0.177	resistance	0.096 - 0.258
RASA4B	ENSG00000170667	0.001128	0.177	resistance	0.102 - 0.251
SSBP2	ENSG00000145687	0.005885	0.178	resistance	0.09 - 0.267
TRAPPC6A	ENSG00000007255	0.002132	0.18	resistance	0.099 - 0.26
NPNT	ENSG00000168743	0.003035	0.18	resistance	0.096 - 0.264
CBLN1	ENSG00000102924	0.001269	0.181	resistance	0.103 - 0.259
LAMTOR3	ENSG00000109270	0.0003858	0.181	resistance	0.111 - 0.251
SYP	ENSG00000102003	0.002511	0.182	resistance	0.099 - 0.265
ABHD11	ENSG00000106077	0.006954	0.182	resistance	0.09 - 0.274
CTSD	ENSG00000117984	0.01929	0.182	resistance	0.077 - 0.288
CD63	ENSG00000135404	0.02397	0.182	resistance	0.073 - 0.292
TCTA	ENSG00000145022	0.0005407	0.182	resistance	0.109 - 0.254
TMEM45B	ENSG00000151715	0.01675	0.182	resistance	0.079 - 0.285
TSPAN15	ENSG00000099282	0.0146	0.184	resistance	0.082 - 0.287
DLGAP3	ENSG00000116544	0.0009477	0.184	resistance	0.107 - 0.26

Gene	Ensembl ID	FDR-adjusted p-value	Coefficient	Association	95% confidence interval
MMP24	ENSG00000125966	0.006749	0.184	resistance	0.092 - 0.277
SCARB2	ENSG00000138760	0.004082	0.184	resistance	0.096 - 0.272
KCNH6	ENSG00000173826	0.001128	0.185	resistance	0.106 - 0.263
PLEKHA6	ENSG00000143850	0.009446	0.186	resistance	0.088 - 0.284
ZNF789	ENSG00000198556	0.0004935	0.186	resistance	0.113 - 0.259
LGALS3	ENSG00000131981	0.02154	0.187	resistance	0.077 - 0.298
SYTL2	ENSG00000137501	0.002039	0.187	resistance	0.104 - 0.271
RASEF	ENSG00000165105	0.008356	0.187	resistance	0.09 - 0.283
SCRT1	ENSG00000261678	0.0008544	0.187	resistance	0.11 - 0.264
GSTA1	ENSG00000243955	0.0001557	0.188	resistance	0.119 - 0.257
CTSA	ENSG00000064601	0.009287	0.189	resistance	0.09 - 0.288
RUNDC3A	ENSG00000108309	0.0005753	0.189	resistance	0.114 - 0.265
FAM185A	ENSG00000222011	8.561E-05	0.19	resistance	0.123 - 0.258
TRIM24	ENSG00000122779	0.00177	0.191	resistance	0.107 - 0.275
SMDT1	ENSG00000183172	0.001332	0.192	resistance	0.109 - 0.274
ASAH1	ENSG00000104763	0.0004935	0.193	resistance	0.117 - 0.268
TTC39A	ENSG00000085831	0.002084	0.194	resistance	0.107 - 0.281
RASA4	ENSG00000105808	0.0004935	0.195	resistance	0.118 - 0.271
KCNB1	ENSG00000158445	0.002858	0.195	resistance	0.105 - 0.285
NAPA	ENSG00000105402	0.0001019	0.196	resistance	0.125 - 0.266
EPB41L1	ENSG00000088367	0.005258	0.198	resistance	0.101 - 0.295
RNF157	ENSG00000141576	0.001	0.201	resistance	0.117 - 0.285
IFITM10	ENSG00000244242	0.001128	0.206	resistance	0.119 - 0.294
DGCR6	ENSG00000183628	5.494E-05	0.208	resistance	0.135 - 0.281
VAMP8	ENSG00000118640	0.01605	0.211	resistance	0.092 - 0.331
RIMKLA	ENSG00000177181	0.0001724	0.218	resistance	0.137 - 0.298
PXMP4	ENSG00000101417	1.504E-06	0.227	resistance	0.159 - 0.295
PDZRN3	ENSG00000121440	0.0005213	0.229	resistance	0.138 - 0.319
FAM222A	ENSG00000139438	0.0001557	0.234	resistance	0.148 - 0.32